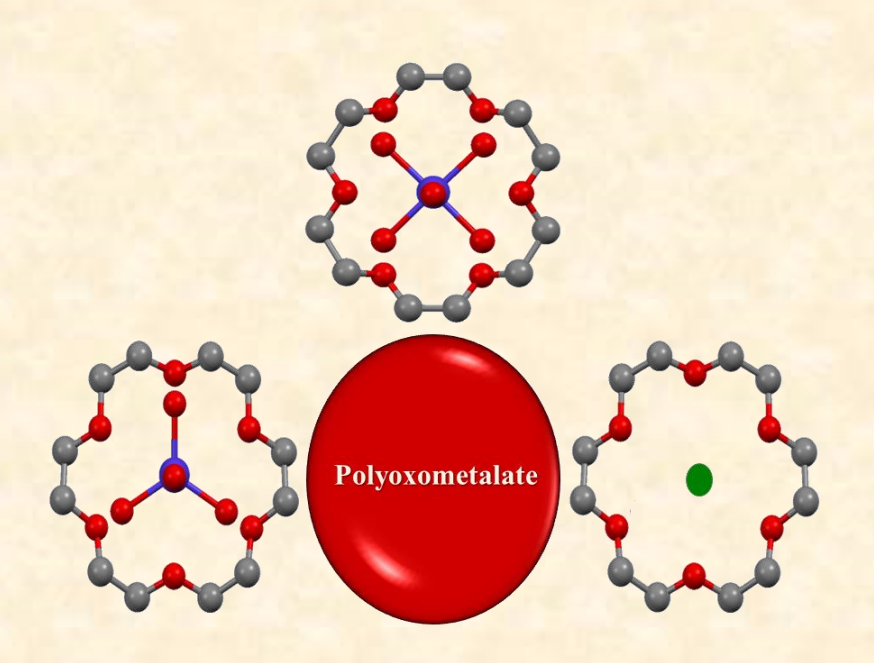


Supramolecular Chemistry of Polyoxometalates: Molecular Recognition, Inorganic Rearrangement and Electrocatalysis

A Thesis Submitted for the Degree of Doctor of Philosophy

By

N. TANMAYA KUMAR



October, 2020 School of Chemistry University of Hyderabad Hyderabad-500 046, India

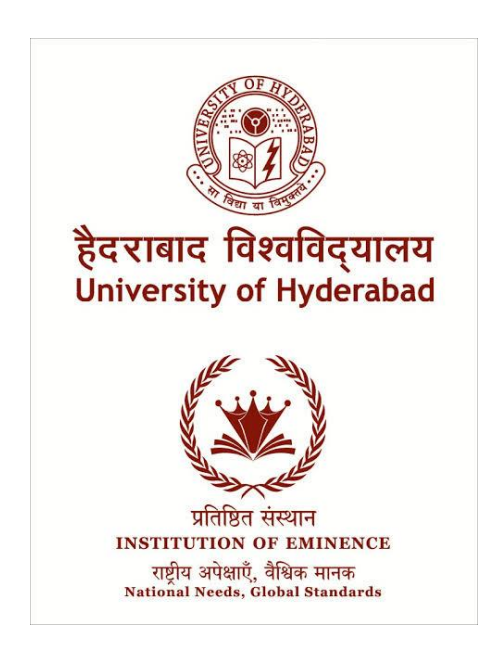
Supramolecular Chemistry of Polyoxometalates:

Molecular Recognition, Inorganic Rearrangement and Electrocatalysis

A Thesis Submitted for the Degree of DOCTOR OF PHILOSOPHY

By

N. Tanmaya Kumar



School of Chemistry, University of Hyderabad, Hyderabad-500 046, India.

October, 2020

Dedicated to

My Gord and Saviour Jesus Christ

and

My Grandparents

Late Raghab Nayak

Late Sobhabati Mallick

CONTENTS

	Page No.
Declaration	i
Certificate	ii
Acknowledgements	iii
Synopsis	vi
Chapter 1. A General Overview on Supramolecular Aspects Motivation of the Present Work	of Polyoxometalates and
1.1 Polyoxometalates	
1.1.1 Overview	1
1.1.2 History	3
1.2 Structure of Polyoxometalates	3
1.3 Synthesis of Polyoxometalates	4
1.4 Properties of Polyoxometalates	
1.4.1 Thermal Stability	5
1.4.2 Adsorption and Absorption Properties	6
1.4.3 Acidic Properties	6
1.4.4 Redox Properties	8
1.5 Supramolecular Chemistry of Polyoxometalates	8
1.6 Polyoxometalate- Crown-Ether Based Supramolecular	9
Assemblies for Molecular Recognition	
1.7 Polyoxometalates for Electrocatalysts	10
1.8 Motivation of the Present Work	11
1.9 References	13

Chai	oter 2.	. Transit	ion Me	etal-Ag	ua-Com	plexes:	Six or	Five F	old (Coordination	or I	Cogether

2.1. Introduction	20	
2.2. Results and Discussion		
2.2.1. Synthesis	22	
2.2.2. Crystallography	22	
2.2.3. A Comparative Discussion on the Crystal Structures of 1-3	26	
2.2.4. Spectral Characterization	32	
2.2.5. Thermogravimetric Analysis (TGA) and PXRD Analysis	35	
2.2.6. Electrochemistry	36	
2.3. Conclusion	39	
2.4. Experimental		
2.4.1. Synthesis	40	
2.5. References	41	
Chapter 3. Polyoxometalates Stabilized Ammonium Cation and Ur		n
Inclusion Crown Ether Complexes: Synthesis, Characterization and C	rystallography)n
Inclusion Crown Ether Complexes: Synthesis, Characterization and Com		n
Inclusion Crown Ether Complexes: Synthesis, Characterization and C3.1. Introduction3.2. Results and Discussion	Crystallography 44)n
Inclusion Crown Ether Complexes: Synthesis, Characterization and Complexes: Synthesis and Discussion 3.2.1. Synthesis	Crystallography 44 45)n
Inclusion Crown Ether Complexes: Synthesis, Characterization and Com	44 45 46	on
Inclusion Crown Ether Complexes: Synthesis, Characterization and Cha	44 45 46 52	on
Inclusion Crown Ether Complexes: Synthesis, Characterization and Complexes: Synthesis, Characterization and Complexes: Synthesis, Characterization 3.2. Results and Discussion 3.2.1. Synthesis 3.2.2. Crystallography 3.2.3. Spectral Characterization 3.2.4. Thermogravimetric Analysis (TGA) and PXRD	44 45 46 52 54	on
Inclusion Crown Ether Complexes: Synthesis, Characterization and C 3.1. Introduction 3.2. Results and Discussion 3.2.1. Synthesis 3.2.2. Crystallography 3.2.3. Spectral Characterization 3.2.4. Thermogravimetric Analysis (TGA) and PXRD 3.2.5 EDAX Studies	44 45 46 52 54 56	on
Inclusion Crown Ether Complexes: Synthesis, Characterization and C 3.1. Introduction 3.2. Results and Discussion 3.2.1. Synthesis 3.2.2. Crystallography 3.2.3. Spectral Characterization 3.2.4. Thermogravimetric Analysis (TGA) and PXRD 3.2.5 EDAX Studies 3.2.6 Discussion on the Type of Guest Molecule Encapsulated	44 45 46 52 54 56 56	on
Inclusion Crown Ether Complexes: Synthesis, Characterization and Complexes: Synthesis, Characterization and Complexes: Synthesis, Characterization 3.2.1. Synthesis 3.2.2. Crystallography 3.2.3. Spectral Characterization 3.2.4. Thermogravimetric Analysis (TGA) and PXRD 3.2.5 EDAX Studies 3.2.6 Discussion on the Type of Guest Molecule Encapsulated 3.3. Conclusion	44 45 46 52 54 56	on
Inclusion Crown Ether Complexes: Synthesis, Characterization and C 3.1. Introduction 3.2. Results and Discussion 3.2.1. Synthesis 3.2.2. Crystallography 3.2.3. Spectral Characterization 3.2.4. Thermogravimetric Analysis (TGA) and PXRD 3.2.5 EDAX Studies 3.2.6 Discussion on the Type of Guest Molecule Encapsulated	44 45 46 52 54 56 56	on

58

3.5. References

Chapter	4 .	A	New	Rearrangement	Reaction	Resulting	in	Ammonium	Ion	at	Room
Tempera	tur	e									

4.1. Introduction	60
4.2. Results and Discussion	
4.2.1. Synthesis: Emergence of a Rearrangement Reaction	61
4.2.2. Serendipitous Observation: Crystal Structure Analysis	64
4.2.3. Spectroscopy	68
4.2.4. Thermogravimetric Analysis and Powder X-Ray diffraction	Analysis 72
4.2.4 EXAFS and CHN Analysis	72
4.3. Conclusion	74
4.4. Experimental	
4.4.1. Synthesis	75
4.5. References	75
Chapter 5. A Polyoxometalate Supported Copper Dimeric Complex:	Synthesis, Structure and
Electrocatalysis	
5.1. Introduction	80
5.2. Results and Discussion	
5.2.1. Synthesis	82
5.2.2. Crystallography	82
5.2.3. Spectroscopy	87
5.2.4. Electrochemical Studies	90
5.2.5. Electrocatalytic Water Oxidation	93
5.2.6. Electrocatalytic Proton Reduction	94
5.2.7. Electrocatalytic H ₂ O ₂ Reduction	96
5.3. Conclusion	97
5.4. Experimental	
5.4.1. Synthesis	97
5.5. References	98

Summary	101
Future Scope	103
Appendix	105
List of Publications	167
Posters and Presentations	168

DECLARATION

I, N. Tanmaya Kumar hereby declare that the matter embodied in the thesis "Supramolecular Chemistry of Polyoxometalates: Molecular Recognition, Inorganic Rearrangement and Electrocatalysis" is the result of my investigation carried out in School of Chemistry, University of Hyderabad, Hyderabad, India, under the supervision of Prof. Samar K. Das.

In keeping with the general practice of reporting scientific observations, due acknowledgements have been made wherever the work described is based on the findings of other investigators. Any omission, which might have occurred by oversight or error, is regretted. This research work is free from plagiarism. I hereby agree that my thesis can be deposited in Shodhganga/INFLIBNET. A report on plagiarism statistics from the University Library is enclosed.

Prof. Samar K. Das

(Supervisor)

Prof. Samar K. Das School of Chemistry University of Hyderabad Hyderabad-500 046., INDIA. (15CHPH20)

N. Tanmaya Kumar



CERTIFICATE

This is to certify that the thesis entitled "Supramolecular Chemistry of Polyoxometalates: Molecular Recognition, Inorganic Rearrangement and Electrocatalysis" submitted by Mr. N. Tanmaya Kumar bearing registration number 15CHPH20 in partial fulfillment of the requirements for award of Doctor of Philosophy in the School of Chemistry is a bonafide work carried out by him under my supervision and guidance.

This thesis is free from plagiarism and has not been submitted previously in part or in full to this or any other University or Institution for award of any degree or diploma.

Parts of this thesis have been published in the following publications:

- 1. A polyoxometalate supported copper dimeric complex: Synthesis, structure and electrocatalysis N. Tanmaya Kumar, Umashis Bhoi, Pragya Naulakha, Samar K. Das* Inorg. Chim. Acta. 2020, 506, 119554. (Chapter 5)
- 2. Supramolecular sandwiches stabilized by a polyoxometalate: synthesis, structure and electrocatalytic water oxidation N. Tanmaya Kumar, and Samar K. Das* (Manuscript under preparation) (Chapter 2)
- Gas-liquid interfacial reaction of triethylamine vapour and polyoxometalate solution leading to the generation of ammonium ion N. Tanmaya Kumar, Samar K. Das* (Manuscript under preparation) (Chapter 4)

He has also participated in oral/poster presentations in the following conferences:

- 1. Poster presentation in CHEMFEST-2017, SoC, UoH, Hyderabad, India.
- 2. Poster presentation in MTIC-XVIII, IIT-Guwahati, India.
- 3. Oral presentation in CHEMFEST-2020, SoC, UoH, Hyderabad, India.

Further the student has passed the following courses towards fulfilment of coursework requirement for Ph. D.:

	Course	Title	Credits	Pass/Fail
1.	CY-801	Research Proposal	3	Pass
2.	CY-806	Instrumental Methods B	3	Pass
3.	CY-401	Basic Concepts in Coordination Chemistry	3	Pass
4.	CY-505	Main Group and Inner Transition Elements	3	Pass

Prof. Samar K. Das 20

20/10/2020

Prof. Santar K. Das School of Chemistry University of Hyderabad Hyderabad-500 046., INDIA. Dean School of Chemistry

> Dean SCHOOL OF CHEMISTRY University of Hyderapad Hyderabad-500 046

I

Acknowledgements

It is a great pleasure to take this opportunity to express my gratitude towards all the people who rendered their help and support during my research work.

It is with high regards and profound respect I wish to express my deep sense of gratitude to Prof. Samar K. Das, my supervisor. I owe it to him for his inspiring guidance, keen interest and encouragement being a fatherly figure throughout my thesis work. He has always been approachable, helpful and extremely patient. It has been a great privilege to obtain the opportunity to associate with him.

I acknowledge my sincere regards to Prof. Anunay Samanta, Dean, School of Chemistry, for providing the facilities need for research. I extend my sincere thanks to former Deans Prof. T. P. Radhakrishnan and Prof. M. Durga Prasad and all the faculty members, School of Chemistry for co-operation on various aspects. I am thankful to Prof. Pradeepta K. Panda and Prof. V. Baskar for their guidance as my Doctoral Committee members. I am also thankful to Dr. Manju Sharma for her support and the collaborative work.

At this time, I recall with deep respect to my teachers Dr. Purnendu Parhi, Dr. K. S. K. Varadwaj, Dr. A. K. Sutar, Dr. Smruti Prava Das, Dr. Bairagi Ch. Mallick, Prof. N. Dastagiri Reddy, Prof. Bala Manimaran, Prof. Binoy Krishna Saha, Mr. Gopinath Das, Mr. D. Vasudev Rao, Mr. Rabindranath Mallick for their perpetual inspiration and it was their encouragement, which paved me as a researcher. Also, I like to pay my respectful regards to all my teachers at various stages of my academic life.

I consider myself prized enough to have polite and well-mannered lab seniors Dr. Paulami Manna, Dr. I. Krishna Naik, Dr. B. Ramakrishna, Dr. B. Suresh, Dr. Subhabrata Mukhopadhyay, Dr. K. Prathap, Dr. Y. Sridevi, Dr. Girijesh, Dr. Joyashish Debgupta, Dr. Suranjana Bose, Dr. Veera Reddy, Dr. M. Pradeep, Dr. K. Sathish, Dr. N. Rajendar, Dr. Pinky Saha, Mrs. Olivia Neogi, Mrs. Ramathulasamma and Mr. M. Sateesh. I wish to thank my friends Ms. Chandani Singh and Ms. Joycy N. Haokip and my dear juniors Ms. Olivia Basu, Mr. Debu Jana, Ms. Athira Ravi and Ms. K. Hema Kumari for their love and support. A special token of thank to Mr. Umashis Bhoi, Ms. Ankita Kumari, Mr. Krushna Mohan Das, Mr. Atanu Haldar, Mr. Gourav Dey, Mrs. Ayesha, Ms. Shalini and Mr. Jay Patel for their help in my different projects.

I am also lucky enough to have the support of many School of Chemistry seniors, specially, Dr. Chandrasekhar, Dr. Rajendra Mallick, Dr. Koushik Ghosh, Dr. AnilKumar Gunnam, Dr. Junaid Ali, Dr. Navendu Mondal, Dr. Suman Ghosh, Dr. Sudipta Seth, Dr. Sneha Paul, Dr. Sabari Ghosh, Dr. Rudraditya Sarkar, Dr. Sugata Goswami, Dr. Srujana, Dr. Divya

Madhuri, Dr. E. Ramesh, Dr. Mohan, Dr. Arijit for their help and guidance at different stages of the journey. I thank my friends Ms. Sameeta, Ms. Sipra, Mrs. Mou, Mr. Ankit, Mr. Apurba, Mr. Senthilnathan, Ms. Tasnim, Mr. Sinivas V., Mr. Ramesh G., Mr. Anif Pasha, Mr. Saddam, Mr. Arun Kanakati, Mr. Venkatesh, Mr. Joy, Mr. Anupam and Mr. Nithun. I am thankful to my juniors Shyam, Irfan, Shuvam Debnath, Mojahid, Saiprasanna, Vinod, Vinay for their help and encouragement during these years.

I also thank Dr. Siddhartha Satapathay, Prof. Debasish acharya, Dr. Prajna Mishra, Dr. Alok Mishra, Dr. Meera Padhy for showering their love as a family member during my stay in Hyderabad.

I also thank all the non-teaching staff/instrument operators, especially Dr. Durgaprasad, Mr. Sunil, Mr. Venkat Ramanna, Mr. Mahesh Rathod, Mr. Shyam, of the School of Chemistry for their assistance on various occasions. I thank DST funded National Single Crystal X-ray Diffraction Facility, UGC/ UPE for providing the basic requirements and CSIR for the financial support and RRCAT, Indore for providing facilities for EXAFS studies.

I am indeed fortunate to have friends in my life over the years like Dr. Sourav Mete, Souvik, Samyabadi, Saikat, Sayan, Bappaditya, Animesh, Kushal, Yogajivan, Satyam, Dibyajyoti, Sritama, Vineet, Sobhan, Alok, Anubhab, Smrutisikha, Suchi di, Anup, Tapas, Shuvam, Abinash, Uday, Subhashish Panda, Gopinath, Goutam, Subhasish bhai, Gourav bhai for their encouragement during these five years. I am greatly thankful to Tapan bhai, Dr. Chakradhar Sahoo, Dillip, Dhruv Da, Dhiren bhai, Kali bhai, Ranjit bhai, Jitu bhai, Hemadri bhai, Golak, Dinesh, Sambit Dasmohapatra, Lipan, Ruturaj, Atasi, Rekha Di, Sonali Di, Rashmi Di, Goura bhai, Subhashree, Abhay bhai and my whole family of OCC for making my life beautiful at University of Hyderabad. My days at University of Hyderabad would have been stressful unless I had my Family@UoH. They were the people, who heard me when I needed someone, who were with me at all the times of sharing happiness or despair. I thank Raju bhai, Sameeta, Sipra, Jayakrushna, Mamina, Soutrick, Pradipta, Shailendra, Suman, Uma, Satya, Bisworanjan, Chiranjit, Baikuntha, Saritha, Priya, Teju, Santanu, Umesh, Sadanand, Gorachand, Shuvam, Smruti Pragyan, Sachi, Abhipsa, Gopendra, Jagannath, Biswamohan, Omprakash, Atulya, Rajkishore, Dipu, Smrutilipi, Soumya Srimayee and Jyoti. I also thank Satyabrata, Swayamsikha, Sambit, Sachidananda, Nilakantha, Subhashish, Chinmaya, Chittabrata, Jagannath Dash, Bandita, Itishree, for making the last one year of my Ph.D. even more memorable. This family really was my stress-reliever and I will be always indebted to them. I express my heartfelt thanks to Anku for his unconditional love, those intellectual discussions and his care during the last five years. I also thank Sunil, Gouttam, Abhishek, Prakash for being wonderful juniors.

The evening walks with Chandani and Rajendar bhaiyya, the outings and deep conversations with Soutrick, Jayakrushna, Shailendra, Pradipta, Satyabrata and

Swayamsikha and every act done by various individuals just to make me happy are highly acknowledged, that boosted me day in and day out.

Looking back finally I kneel to my parents, Mr. Prasanta Kumar Panda and Dr. N. Leena Chand; whom I adore most for their love, blessing and confidence on me in building the very platform of my life. Also, I express my love to my sister, Er. N. Smruti Chhanda, for her immeasurable affection. I feel blessed for my family members, Mr. Prabhudutt, Mrs. Sunita, Mr. Sanjeeb, Mrs. Smita Rekha, Mr. Debasish, Mrs. Pranjyan, and I am thankful for their prayers and blessings. I am thankful to my cousins Sarthak, Samikshya, Sourav, Sudipta and Aradhya for their support. I am grateful to my grandparents for their encouragement towards my higher studies and giving me the required lessons as and when required. I also thank my uncles Dr. Girish Ch. Mallick and Mr. Naresh Ch. Mallick for their encouragement at each step of mine. I am thankful to Rev. T. K. Samantaroy, Rev. Sweetborn Nayak and Rev. Prasanta Bag and their families for praying for me. I thank Mr. Sunit Singh for his help and support at every now and then. I thank my extended families, who always prayed for me and helped me to achieve this.

I am grateful to PUCF family for always remembering me in their prayers, especially Dr. Victor Anandkumar and Delcy akka. I am also thankful to HCU EU ministry for enabling me to face the odds fearlessly. I am greatly thankful to Bethel family for making me spiritually strong, which gave me the strength to face all uncertain days, special thanks to Pastor Peter Samuel and Nirupama akka. I also thank my mother church Phulbani Odia Baptist Church for its prayers for me. I thank Mr. Ashish Joseph and Mary bhabi for their encouragement and care during these days.

And at last but not the least, those who are distant but close to my soul, accompanying me time to time when I am facing the odd, make me laugh, sharing my grief and cherishing my joy, will always be remembered by me.

Tanmaya

University of Hyderabad

October, 2020.

SYNOPSIS

The thesis work entitled as "Supramolecular Chemistry of Polyoxometalates: Molecular Recognition, Inorganic Rearrangement and Electrocatalysis" consists of five chapters followed by concluding remarks and future scope: (1) A general overview on supramolecular aspects of polyoxometalates and motivation of the present work, (2) Transition metal-aqua-complexes: six or five fold coordination or together, (3) Polyoxometalates stabilized ammonium cation and unusual chloride anion inclusion crown ether complexes: synthesis, characterization and crystallography, (4) A new rearrangement reaction resulting in ammonium ion at room temperature, (5) A polyoxometalate supported copper dimeric complex: Synthesis, structure and electrocatalysis.

Each chapter is sub-divided into four parts. The first chapter *i.e.*, Introduction, consists of an overview of polyoxometalates, followed by their structure, properties, supramolecular aspects and motivation of the present work. All other chapters (Chapters 2–5) consist of (a) Introduction, (a) Results and Discussion, (c) Conclusion, and (d) Experimental Section. The compounds, presented in this thesis work, are generally characterized by powder X-ray diffraction (PXRD) studies, IR spectral studies, CHNS analyses, thermogravimetric analysis (TGA) and solid-state UV-visible spectroscopy (UV-DRS), and ofcourse unambiguously characterized by single crystal X-ray diffraction (SCXRD) studies.

Chapter 1

A General Overview on Supramolecular Aspects of Polyoxometalates and Motivation of the Present Work

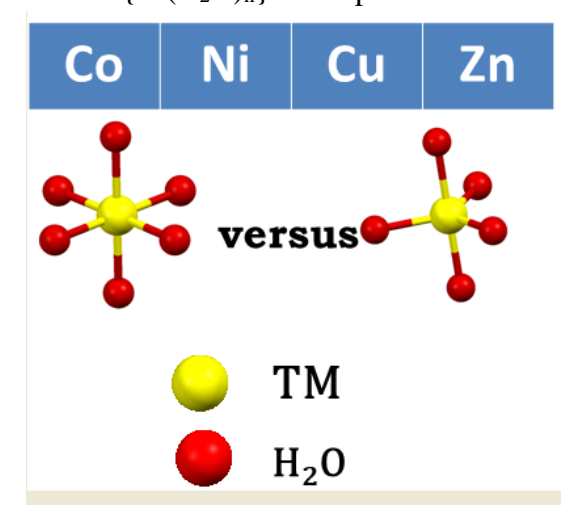
This chapter starts with more basic knowledge about the polyoxometalates and the research progress has been discussed mainly under three sections: (1) a brief introduction, followed by history, structure, synthesis and properties of polyoxometalates, (2) the supramolecular aspects of polyoxometalates and (3) finally, the motivation to study the supramolecular aspects and applications of these polyoxometalates. The chapter intends to introduce the fascinating world of polyoxometalates and throws light on the recent developments of polyoxometalate based supramolecular chemistry. The main objectives of the thesis work are conversed shortly.

Chapter 2

Transition Metal-Aqua-Complexes: Six or Five Fold Coordination or Together

The coordination number around a 3d transition metal ion M^{2+} in water is not just six, as believed for many years. For instance, the Cu^{2+} ion, dissolved in water, has convincingly been established to be $\{Cu^{II}(H_2O)_5\}^{2+}$ instead of $\{Cu^{II}(H_2O)_6\}^{2+}$, the later one was generally believed. On the other hand, Ni^{2+} in water is found to be octahedral $\{Ni^{II}(H_2O)_6\}^{2+}$. We have attempted to isolate M^{2+} -aqua-coordination complex cations (M = Co, Ni, and Zn) in a polyoxometalate

(POM) matrix anion using a crown-ether to stabilize these metal-aqua-species (through the formation of supramolecular sandwiches) as single crystals and characterized unambiguously by their crystal structure determinations. We have synthesized cobalt(II)-, nickel(II)- and zinc(II)-aqua-complex-associated compounds [{Co(H₂O)₅([18]-crown-6)₂}{Co(H₂O)₆([18]-crown-6)₂}][Mo₆O₁₉]₂ (1), [Ni(H₂O)₆([18]-crown-6)₂][Mo₆O₁₉] (2) and [Zn(H₂O)₅([18]-crown-6)₂][Mo₆O₁₉] (3). Compound 1 includes an interesting simultaneous co-existence of both Co(II)-penta-aqua-coordination complex {Co(H₂O)₅}²⁺ and Co(II)-hexa-aqua-coordination complex {Co(H₂O)₆}²⁺ in 1:1 ratio, whereas compounds 2 and 3 contain Ni(II)-hexa-aqua-coordination complex {Ni(H₂O)₆}²⁺ and Zn(II)-penta-aqua-coordination complex {Zn(H₂O)₅}²⁺, respectively. These results not only help us to understand the choice of coordination number (n) of 3d transition metal-aqua coordination complexes {M(H₂O)_n}²⁺ (M = Co, Ni, and Zn; n = 5, 6) but also offer an understanding to the dynamic equilibrium between coordination numbers 5 and 6 of {M(H₂O)_n}²⁺ of a particular metal ion.



Chapter 3

Polyoxometalates Stabilized Ammonium Cation and Unusual Chloride Anion Inclusion Crown Ether Complexes: Synthesis, Characterization and Crystallography

Two supramolecular compounds exhibiting encapsulation of guest molecules in the cavities of two different crown-ether host entities with varying cavity size are reported. In the compounds, two different Keggin anions, $[PMo_{12}O_{40}]^{3-}$ and $[SiMo_{12}O_{40}]^{4-}$, act as the stabilizing anions. Whereas, a chloride anion is encapsulated in the crown ether with small cavity size, 18-crown-6, two ammonium ions and two acetonitrile molecules are encapsulated in the cavity of the larger crown ether, dibenzo-24-crown-8. The encapsulation of chloride anion in the cavity of the crown ether is very unusual, in terms of hard-soft acid-base (HSAB) principle, but here the polyoxometalate anion plays a role in stabilizing the overall molecule. Both the compounds have been characterized using routine characterization techniques and their structures have been elucidated using single crystal X-ray diffraction technique. Further, silver nitrate test and the Nessler's reagent test have been performed on both the compounds, to ensure the presence of

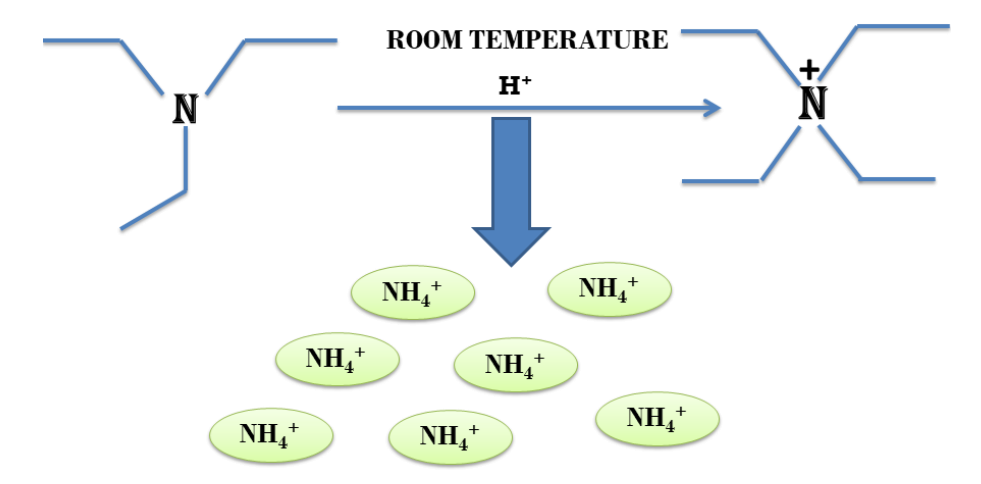
chloride anion and the ammonium cation, respectively. The two compounds of study are $[H_3PMo_{12}O_{40}\{HCl(18\text{-crown-6})\}_3]\cdot 4CH_3CN$ (compound 1) and $[SiMo_{12}O_{40}\{(NH_4)_2(dibenzo-24\text{-crown-8})\}_2\{(CH_3CN)_2(dibenzo-24\text{-crown-8})\}]\cdot 2CH_3CN$ (compound 2).



Chapter 4

A New Rearrangement Reaction Resulting in Ammonium Ion at Room Temperature

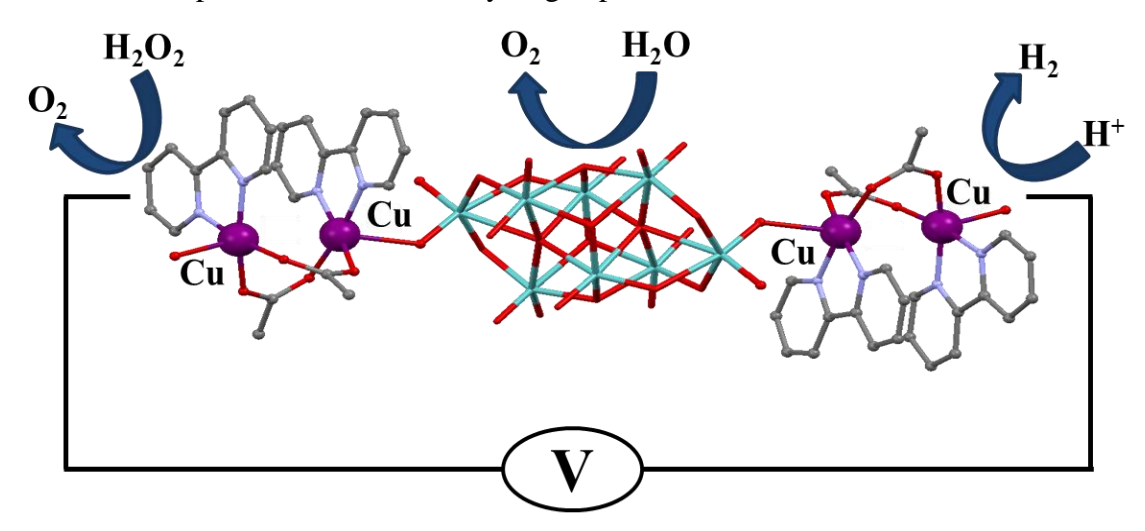
Triethylamine is a volatile liquid and exists in the atmosphere in the gas phase. It is a hazardous air pollutant and identified as a toxic air contaminant. Thus, producing ammonia (a vital chemical for fertilizer production) from the vapour state of this toxic substance is a challenging task. Diffusion of the vapour of triethylamine, (C₂H₅)₃N into an acidified aqueous solution of sodium molybdate results in the formation of single crystals of compound $[(C_2H_5)_3NH]_2[(C_2H_5)_4N][NaMo_8O_{26}]$ (1). Notably, compound 1 includes a $[(C_2H_5)_4N]^+$ cation, even though the concerned reaction mixture was not treated with any tetraethylammonium salt. The formation of the $[(C_2H_5)_4N]^+$ cation from $(C_2H_5)_3N$ in an acidic aqueous medium is logically possible when an ammonium cation (NH₄⁺) is formed in the overall reaction: $4(C_2H_5)_3N + 4H^+ \rightarrow 3[(C_2H_5)_4N]^+ + [NH_4]^+$. We have thus demonstrated the room temperature ammonia synthesis from a polyoxometalate solution, to which $(C_2H_5)_3N$ vapour is diffused a gas-liquid interfacial reaction. Although the resulting NH₄⁺ cation (identified by Nessler's reagent test) is not included in the crystals of compound 1, it can be made associated with a crown ether in the isolation of single crystals of compound [NH₄⊂B15C5]₃[PMo₁₂O₄₀]⋅B15C5 (2), (B15C5 = benzo-15-crown-5). ¹H NMR studies on compound 2 have established the presence of H-bonded NH₄⁺ ion in 2.



Chapter 5

A Polyoxometalate Supported Copper Dimeric Complex: Synthesis, Structure and Electrocatalysis

A polyoxometalate (POM) supported copper dimeric complex, [Mo₈O₂₆{Cu₂(2,2'-bpy)₂ (CH₃COO)₂H₂O}₂]·H₄Mo₈O₂₆·16H₂O (1) has been synthesized using conventional wet synthesis. The compound has been characterized using routine spectral techniques and its molecular structure has been elucidated using single crystal X-ray crystallography. The two copper(II) ions are bridged by acetate ions and each copper ion is also coordinated to 2,2'-bipyridine molecule. In each dimer, one of the copper ions is bonded to the POM anion from one side, whereas the other copper ion is bonded to a water molecule, hence acquiring a pentacoordinated square pyramidal structure around each copper center. The lattice water molecules play an important role to stabilize the system, by forming a water pentamer, which binds both the polyoxometalate supported transition metal complex and the other POM anion [Mo₈O₂₆]⁴. Interestingly, compound 1 is found to function as a versatile heterogeneous electro-catalyst for water oxidation, proton reduction and hydrogen peroxide reduction.



Concluding Remarks and Future Scope

The last section of this thesis describes the summary and future scope of this thesis work. This thesis has discussed on the supramolecular aspects of polyoxometalates. Utilization of supramolecular interactions between the polyoxometalates and the crown ether for molecular recognition is described in chapters 2 and 3. Chapter 4 establishes a rearrangement reaction, where in a triethylamine rearranges to ammonium cation at room temperature and through supramolecular interactions, the ammonium cation hence generated is associated in the crown ether cavity, where polyoxometalate stabilizes the supramolecular entity. The synthesis, characterization and use as an electrocatalyst of a polyoxometalate supported transition metal dimeric complex is explained in Chapter 5.

The future scope of this work includes mainly application aspects. We can use the supramolecular crown-ether-polyoxometalate moieties for sensing applications. We have demonstrated in chapter 5, that M–OH₂ functionality can act as electrocatalyst for water oxidation. We would like to explore this strategy for designing of photo-/electro-chemical water oxidation catalysts.

CHAPTER

1

A General Overview on Supramolecular Aspects of Polyoxometalates and Motivation of the Present Work

1.1 Polyoxometalates

1.1.1 Overview

Polyoxometalates (POMs) are a unique class of transition metal oxides, which have been enormously studied in recent years for their diverse applications in a variety of fields ranging from biology, magnetism, medical sciences to materials sciences. Although the chemistry is not new, as it was first discovered more than two hundred years ago, but still this specific family of compounds fascinates the present-day scientists. Polyoxometalates, as the name suggests, are anionic clusters of transition metal oxides, where the oxygen atoms are in the oxo *i.e.*, O^{2-} state and the transition metals are generally from Group V or VI of the periodic table, usually V, Mo and W and rarely Nb, Ta, etc., in their highest oxidation states (usually V or VI). The transition metal is called the addenda atom. These addenda atoms have bridging oxygen atoms, μ_2 –O, which bind to other addenda atom that also contains a μ_2 –O, which again binds another addenda atom and so on, forming the polyoxometalate structure. Depending on the type of the polyoxometalate, μ_3 , μ_4 or higher oxygen bridges are also present.^{1,2}

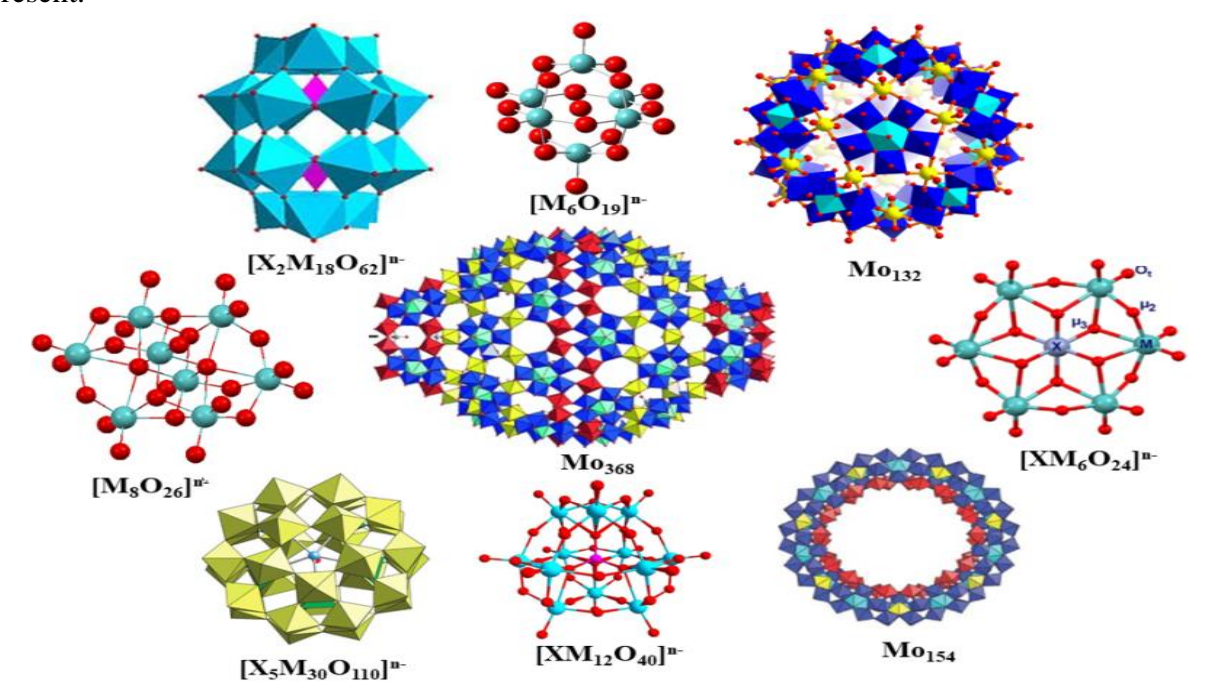


Figure 1.1. Different types of polyoxometalates.

In the recent few years, polyoxometalates have gained enormous attention from contemporary scientists working in diverse areas of research. The reasons for this are as follows:³⁻⁵

- a. Chemical properties of polyoxometalates, like solubilities, acidities and redox potentials in several media (aqueous as well as organic) can be modified by picking different constituent elements and various counter cations.
- b. Polyoxometalates exhibit thermal and oxidative stability in comparison to common organometallic complexes and various enzymes.
- c. Transition metal-substituted POMs with "controlled active sites" can easily be produced.

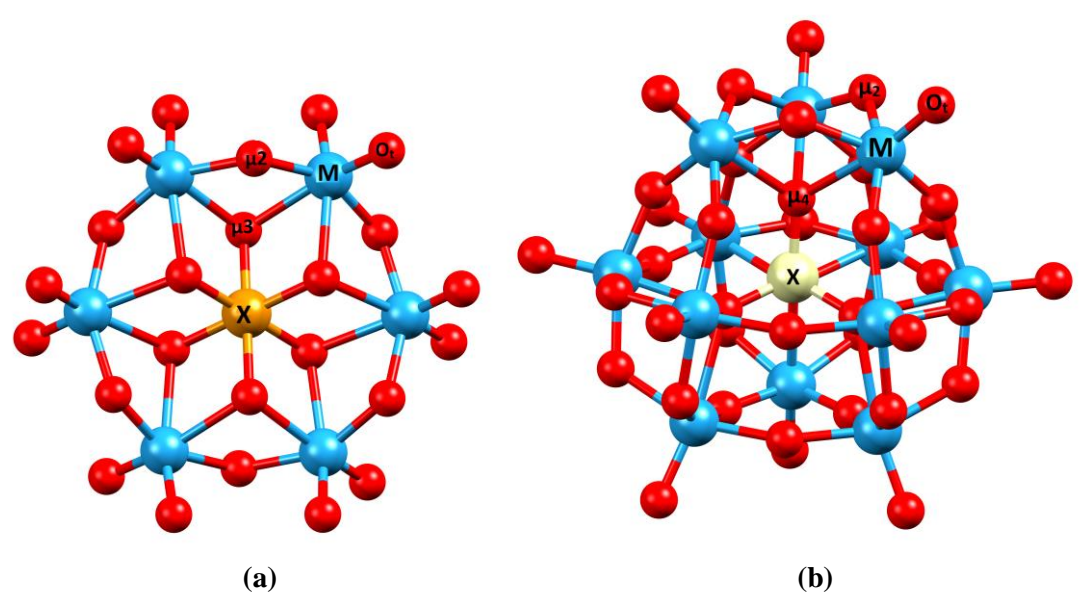


Figure 1.2. (a) Anderson-Evans type POM with two bridging (μ_2 and μ_3) and terminal oxygen (O_t) labeled (red), the addenda atoms (M) (blue) and the heteroatom (X) (orange). (b) Keggin type POM with two bridging oxygen (μ_2 and μ_4) and terminal oxygen (O_t) labeled (red), the addenda atoms (M) (blue) and the heteroatom (X) in (light-yellow).

The polyoxometalates can be categorised as isopolyanions (IPA) and heteropolyanions (HPA), which can be easily distinguished depending upon their composition and their structures. Isopolyanions are polyoxometalates which only have addenda atoms coordinated to the oxygen atoms. Heteropolyanions, like isopolyanions, contain the addenda atoms, but also have another element present: the heteroatom. The general formula for the isopolyanions is $[M_m O_y]^p$ and that of HPAs is $[X_x M_m O_y]^{q_-}$ where $x \le m.^{1,7-12}$ M is called the addenda atom which usually is a transition metal from group 5 or 6 in its higher/highest oxidation state having an electron configuration of d^1 or $d^0.^{1,6,13}$ Usually, molybdenum(VI) or tungsten(VI) are used as the addenda atom, because of the suitable environment shaped due to their ionic radius, charge and available (empty) d orbitals to form the essential metal-oxygen π bond. Apart from Mo and W, V(V), Nb(V) and Ta(V) also have been efficaciously used as the addenda atoms. $^{14-18}$

1.1.2 History

Polyoxometalate history run ahead to the days when the enigmatic 'blue water' was found in the Valley of the Ten Thousand Smokes, Katamai national park of southern Alaska, during the stretches of the early Native Americans. But, the field gained congregated scientific attention only in the nineteenth century, when Berzelius in 1826 described the formation of a yellow precipitate when ammonium molybdate is added to an excess of phosphoric acid, which is now known commonly as the phosphomolybdic acid $[PMo_{12}O_{40}]^{3-}$ having a canary yellow color. having a canary yellow color.

As the days passed by, the field gained the lure of the then-contemporary scientists and more than seven hundred heteropolyanions were reported by the early twentieth century, with the 12:1 composition of 12-tungstosilic acid.²¹ Till then, the actual structure of these compounds was still under question. Werner in 1907, for the first time, attempted to determine the structure of polyoxometalates,²² followed by Miolati and Pizzighelli.²³ Later improvements in these directions were contributed by Rosenheim.²⁴ According to Miolati and Rosenheim the building blocks in polyoxometalates are based on six-coordinate units of MO_4^{2-} or $M_2O_7^{2-}$, here M represents the addenda atom. But, this postulate as well as the structure hence proposed are not in agreement with the structures that are obtained via modern chemistry methods. Based on the theory of the measure of element radii, however, Pauling challenged the Miolati and Rosenheim postulate and postulated that the basic units hence formed, were octahedral in structure.²⁵ The greatest breakthrough in this direction came, when the crystal structure of the polyoxometalate series was solved by Keggin successfully using X-ray diffraction, which supported the Pauling's theory, based on 18-tungstophosphoric acid, $(H_5O_2)_3[PW_{12}O_{40}]$.²⁶

Twentieth century witnessed the major improvements in polyoxometalate chemistry, as the physical and chemical properties along with the structures of many polyoxometalates were elucidated and reported.²⁷ Till then there was limited knowledge on the formation, degradation, and interconversion of polyoxometalates. In 1963, the condensation reactions that are involved in the formation of polyoxometalates were studied by Souchay.¹³ In 1960s, M. T. Pope used NMR technique to determine the polyoxometalate structure.^{28,29} Following this, he published hundreds of reports on this field, and developed methods of synthesis and characterization of vanadium, niobium, tantalum based substituted heteropolyanions and their organic derivatives as well.^{30, 31} Later on many other researchers like Kozhevnikov,^{7,32-36} Hill,^{11,37-40} Muller,⁴¹⁻⁴⁶, Tsigdinos,^{14,47-50} Neumann⁵¹⁻⁵⁶ have contributed immeasurably to this field. At present Kortz,⁵⁷⁻⁶¹ Cronin,⁶²⁻⁶⁶ Proust,⁶⁷⁻⁷¹ Tianbo Liu,⁷²⁻⁷⁶ S. Roy,⁷⁷⁻⁸¹ Patzke⁸²⁻⁸⁶ and our group⁸⁷⁻⁹¹ have made remarkable advances to this field by introducing new frontiers, ideas and applications of polyoxometalates hence making this field a more interesting one.

1.2 Structure of Polyoxometalates

Polyoxometalate compounds, within the solid-state, have polyoxoanions, cations like protons, metals, and water of crystallization. Sometimes additionally, they also contain some neutral organic molecules. From the catalysis point of view based on polyoxometalates, it's

very vital to differentiate between the primary, secondary and tertiary structures. ⁹²⁻⁹⁶ It has also been understood that other than these structures, tertiary and higher-order structures affect the catalytic activity. ⁹⁵ The various varieties of structures for the polyoxoanion are represented in Figure 1.3.

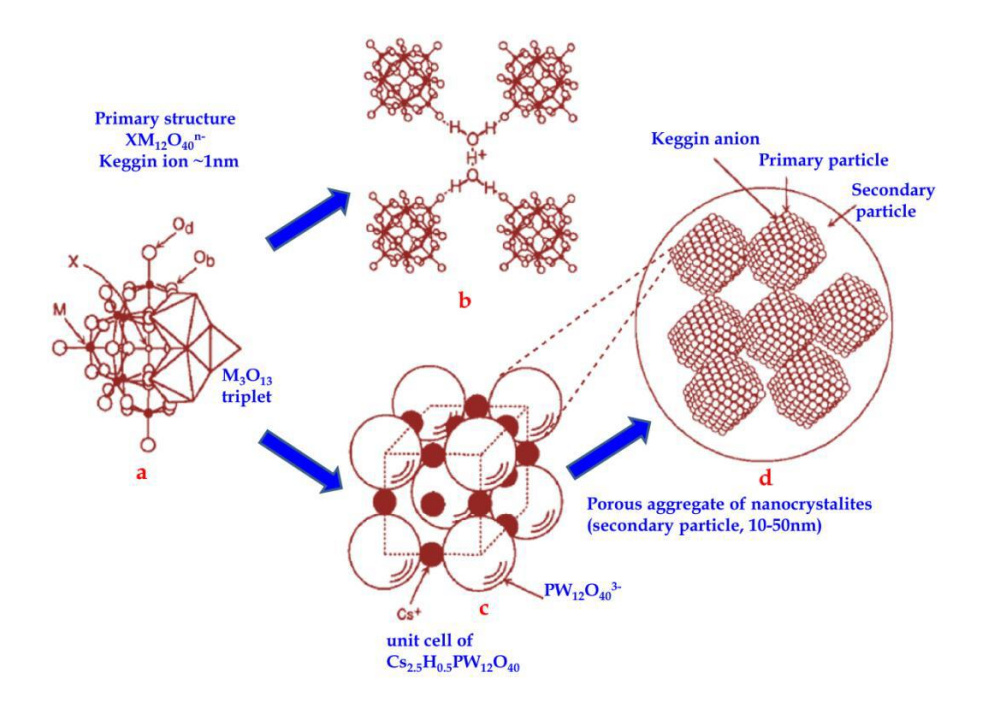


Figure 1.3. Various structures of Keggin type polyoxometalates (a) Primary structure (b) Secondary structure of $H_nXM_{12}O_{40} \cdot 6H_2O$. (c) Secondary structure of the $Cs_3PW_{12}O_{40}$ unit cell. (d) Tertiary structure having porous aggregates. ⁹⁶

The elementary structure of a polyoxoanion molecule is named a "primary structure", which is formed when oxonions condense (Figure 1.3a). Secondary structure of solid polyoxometalates form, when polyoxoanions coordinate with acidic protons, other cations and/or water molecules of hydration (Figure 1.3b). The structure containing six water molecules of hydration each for one Keggin ion, is considered to be stable, therefore, establishing a body-centered cubic (bcc) structure where the Keggin ions are present at the lattice points and H_5O^{2+} bridges along the faces. The terminal oxygen atoms are bound to a H atom of an H_5O^{2+} bridge. The acidic protons, in these structures, are present between the lattice points, within the H_5O^{2+} bridges. If the number of water molecules present is less than six, acidic protons could be present in the remaining H_5O^{2+} bridges, in H_3O^+ or could also be coordinated to the oxygen atoms of the Keggin unit directly. The tertiary structure of solid polyoxometalates is assembled. (Figure 1.3c).

1.3 Synthesis of Polyoxometalates

Transition metal cations, in aqueous solutions, are generally coordinated to aqua (H_2O) , oxo (O^{2-}) or hydroxo (OH^-) ligands. The acidity of these coordinated ligands is proportional to the charge on the metal cation. Greater the positive charge of the metal, the more easily the protons dissociate from the ligands. In this perspective, the metals of group 5 and 6 of the periodic table of elements, in their highest oxidation state, like V^{5+} , Mo^{6+} , W^{6+} ,

form stable complexes with oxo (O^{2-}) ligands in aqueous alkaline solutions, forming VO_4^{3-} , MoO_4^{2-} , WO_4^{2-} . When acidified, *olation*, *i.e.*, a condensation reaction takes place, giving rise to M–O–M bonds. These process repeats to make the polyoxometalates.⁵

Additionally, there is also an expansion of coordination number, resulting in the condensed structures. The polyoxometalates, hence formed, are therefore regulated by a set of conditions, like pH, temperature, counterions, solvent, stoichiometry, concentration, etc. Thus, a small variation in any of these conditions can lead to numerous compounds. A point here to note is that the formation of the coordination bonds is reversible. Hence, the oxobridges in these polyoxometalates can be sliced as a result of the addition of bases, and controlled degradation may lead to many more new compounds, which are called lacunary polyoxometalates, in contrast to plenary or saturated polyoxometalates. The derivatization of preformed polyoxometalates is now fairly understood and rational syntheses of regio-specifically substituted Keggin and Dawson polyoxometalates are developed.⁶

1.4 Properties of Polyoxometalates

Polyoxometalates generally have low surface area (1-10 m²/g) and hence have high solubility in water. The polyoxometalates have inter-particle pores, and not intra-crystalline.

1.4.1 Thermal Stability

Stabilities of any substance can be defined in various dimension, like thermal and hydrolytic stability in solution, and these are dependent on the polyoxometalate type. 92-94 Solid polyoxometalates in the acidic form are stable thermally and are applicable to high temperature vapour phase reactions. The variation in their thermal stability with polyatom, heteroatom and polyanion structure is:

$$[PW_{12}O_{40}]^{3\text{-}} > [PMo_{12}O_{40}]^{3\text{-}} > [SiMo_{12}O_{40}]^{4\text{-}}$$

The mixed addenda HPAs usually exhibit lower thermal stability. Thermal stability of polyoxometalates is studied extensively by thermogravimetric analysis (TGA), differential thermal analysis (DTA), X-ray diffraction (XRD), etc. techniques.

Heteropolyacids	Endotherm (K)	Exotherm (K)
H ₃ PW ₁₂ O ₄₀	448-569	853-868
H4SiW ₁₂ O ₄₀	413-551	743-773
H ₃ PMo ₁₂ O ₄₀	336-432	663-681
H4SiM012O40	337-453	609-628

Table 1.1. DTA results of various Heteropolyacids⁹⁷

The DTA outcomes corresponding to various polyoxometalates at lower temperatures show an endotherm, and at elevated temperatures, an exotherm (Table 1.1). The elimination of water can be reasoned for the low-temperature endotherm. The decomposition of the cagelike structure of the HPAs yielding a compact crystalline product constituted of large oxides of Mo(VI) and W(VI) leads to the observed high-temperature endotherm.

Herve *et al.* investigated the thermal changes of structures employing XRD, TGA, and DTA for Keggin type polyoxoanions e.g., H₃PW₁₂O₄₀·29H₂O, H₃PMo₁₂O₄₀·29H₂O, and H₄PMo₁₁O₄₀·29H₂O.⁹⁸

From TGA and DTA studies, it is shown that there are two types of water molecules in polyoxometalates, namely, the water of crystallization and constitutional water molecules. Molecules of water of crystallization are lost usually at a temperature below 473K. The constitutional water molecules (i.e., acidic protons that are coordinated to the oxygen atoms of the POMs) of $H_3PMo_{12}O_{40}$ and $H_3PW_{12}O_{40}$ are lost at 623K and 543K respectively.

In situ X-ray Diffraction, ³¹P Nuclear Magnetic Resonance spectroscopy and thermoanalysis studies inferred that H₃PMo₁₂O₄₀ undergoes a two-step thermolysis, as shown below:

$$H_{3}PMo_{12}O_{40}.nH_{2}O \xrightarrow[nH_{2}O]{473-623\,K} H_{3}PMo_{12}O_{40} \xrightarrow[-1.5H_{2}O]{658\,K} H_{x}PMo_{12}O_{38.5+\frac{x}{2}(x=0.01)}$$

The MoO₃ phase is seen only at a temperature more than 573 K.

According to Hodnett and Moffat, the identical decomposition process goes via $H_3PW_{12}O_{40}$. 99 TGA of $H_3PW_{12}O_{40}$ and $Cs_{2.5}H_{0.5}PW_{12}O_{40}$ displays that, at a temperature as low as 573K, all molecules of water of crystallization are lost, and as water is formed as a result of reaction between H^+ and lattice oxygens at temperatures above 623 K, acidic groups are removed. The no. of H^+ lost, n, in $Cs_{2.5}H_{0.5-n}PW_{12}O_{40-n}$ were 0.24, 0.31 and 0.32 after reactions at 623K, 673K and 773K respectively. A similar proton loss of $K_{2.5}H_{0.5}PMo_{12}O_{40}$ initiates at around 500K.

1.4.2 Adsorption and Absorption Properties

A notable characteristic property of few solid polyoxometalates is their capability to absorb. They absorb a good amount of polar or basic molecules, like alcohols and nitrogen bases easily into the solid bulk. 100-102 The process rest on the basicity as well as the size of the absorbate and also the rigidity of the secondary structure. While in the case of desorption, alcohol desorption is easy, but pyridine and ammonia desorption occurs only at high temperature.

1.4.3 Acidic Properties¹⁰³

It was proved that acidic forms of polyoxometalates, like, $H_3PX_{12}O_{40}$ (X= Mo/W) are Bronsted acids in the solid-state. They also exhibit strong acidic properties as compared to standard solid acids like H_3PO_4/SiO_2 , $SiO_2-Al_2O_3$, HX, and HY zeolites. ^{101,104} The acidity of

heteropolyacids is much stronger as compared to the respective oxoacids of the constituent elements as well as common mineral acids (Table 1.2). The higher strength in acidity can be attributed to:

- 1. Negative charge dispersion over the atoms of the polyanion and
- 2. Less dispersed negative charge over the outer surface of the POM due to the double-bond character of the M=O bond, resulting in the polarization of the negative charge of M to O_t .

Table 1.2. Various acids and	l acidic form of Polyoxometalates and their D	Dissociation Constants. 103

Sl. No.	Acids	pK1	pK2	pK3
1	H ₃ PW ₁₂ O ₄₀	1.6	3.0	4.0
2	$H_4PW_{11}VO_{40}$	1.8	3.2	4.4
3	H ₃ PMo ₁₂ O ₄₀	2.0	3.6	5.9
4	H ₄ SiMo ₁₂ O ₄₀	2.1	3.9	5.9
5	H_2SO_4	6.6	-	-
6	HCl	4.3	-	-
7	HNO ₃	9.4	-	-

The reason for the efficiency of polyoxoanions as catalysts is the associated high Bronsted acidity. This high Bronsted acidity is because of the large polarization of negative charge on the polyoxoanionic species. They are complex Bronsted acids, with very strong Brønsted acidity, nearing the superacid region. Varying the chemical composition of the POMs would vary the acid-base character of polyoxoanions. This displays enormously high proton mobility, although HPAs are able to stabilize organic as well as inorganic cationic intermediates. Apart from this, polyoxometalates in the solid-state are thermally stable than other known acids of higher strength.

In aqueous solution, acidic forms of polyoxometalates *i.e.* heteropolyacids are strong, and fully dissociated. Even if $[SiW_{12}O_{40}]^{4-}$ and $[PW_{12}O_{40}]^{3-}$ anions accept two and three electrons respectively, they continue to be deprotonated. When in solutions, polyoxometalates are observed to be stronger than mineral acids such as HCl, H₂SO₄, HNO₃. The acid strength is highly dependent on the central atom in these Keggin anions; their acidity depends on the total anionic charge than to the kind of metal atom present in the heteropoly acids. The acidity is found to follow the order:

$$H_3PW_{12}O_{40} > H_4SiW_{12}O_{40} > H_3AsW_{12}O_{40} > H_4GeW_{12}O_{40}.$$

1.4.4 Redox Properties

In most polyoxometalates, as described above, the addenda metal atoms are highly oxidised (d^0) and hence, they have the ability to act as oxidizing agents.⁴ Certain polyoxoanions are easily reducible forming blue species, more commonly known as "heteropoly blues" or "molybdenum blues". In most of the polyoxometalates structures, the addenda atoms dwell in "octahedral" sites having one or two terminal oxygen (O_t) atoms. As a result, they undertake reversible reduction forming moieties of the type {MOL₅} in which one or more of the metal centers has a reduced *i.e.* d^1 configuration.

The reductions in polyoxmetalates involve single or multi-electron steps following protonation. It depends on the type of solvent used, the charge of the POM as well as the acidity of the resulting solution. Addenda atoms have a great influence on the oxidation potential, but central heteroatom(s) has/have negligible influence. The polyanions having Mo and V as addenda atoms have high oxidation potentials, because these ions have a tendency to reduce easily. The oxidative ability follows the trend $V^- > Mo^- > W^-$ containing HPA.

Redox properties of dodecapolyoxoanions depend both on the elements constituting the polyoxometalates as well as counter cations. The oxidizing ability (or reducibility) is valued from the reduction of polyoxometalates compounds by H_2 , CO, and organic compounds.

As the reducing agent is activated, the rate at which the reduction of polyoxoanions occurs almost matches the oxidation potential in solution. As in heteropolyanions mixed with Pd/C powders, the reduction by H₂ follows the order:

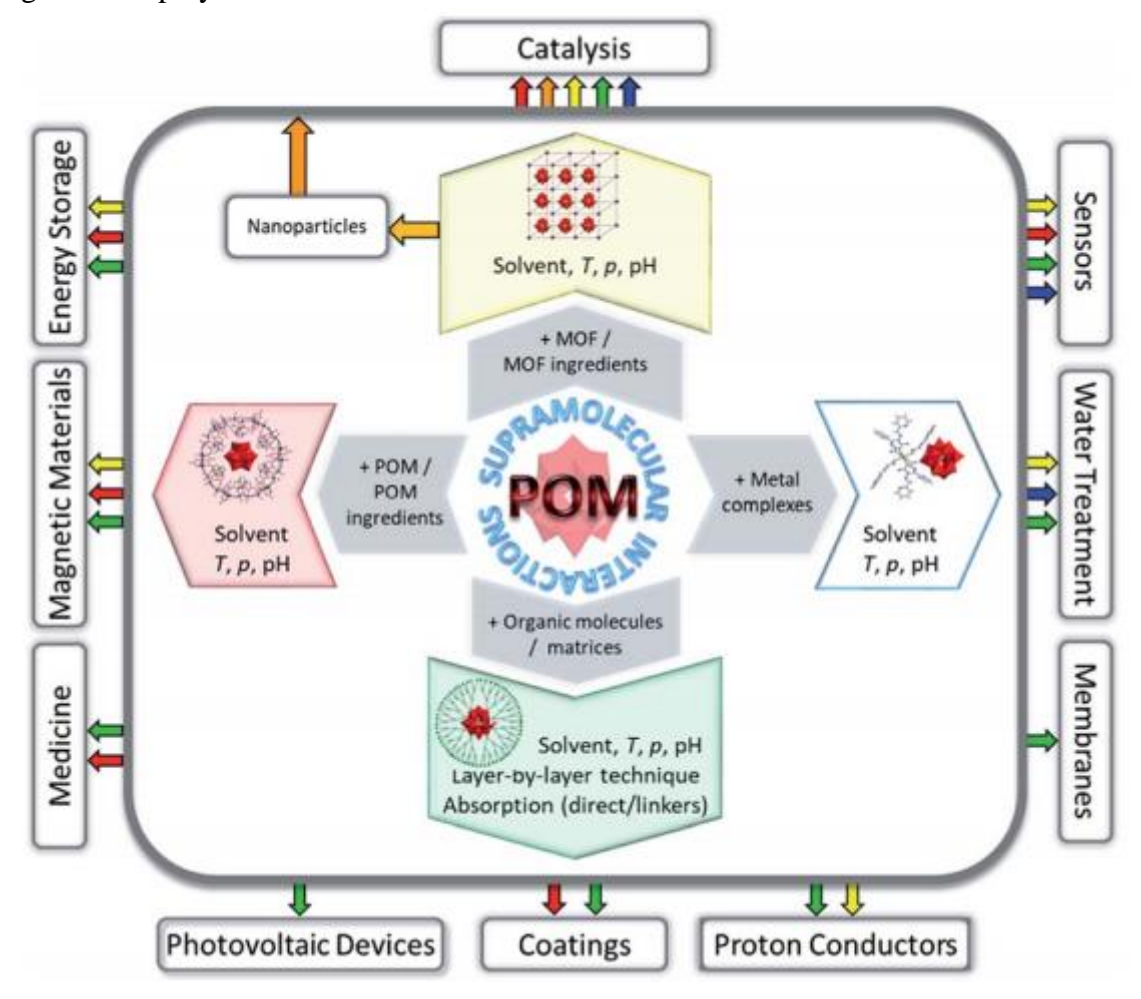
$$PMo_{12} > SiMo_{12} > PW_{12} > SiW_{12}$$
.

1.5 Supramolecular Chemistry of Polyoxometalates

Polyoxometalates have been widely used in the field of supramolecular chemistry. The ionic and the various non-covalent interactions (*viz.*, van der Waals' force, hydrogen bonding, *etc.*) between the polyoxometalates themselves, or other molecular systems can be attributed to the negatively charged polyoxometalates, having negatively charged surface oxygen atoms, which provide an immense platform for the study of the electrostatic interactions between them. One of the most noteworthy facts essential to polyoxometalate based supramolecular assemblies is that, the primary formation has no pointed impact on the structural features of polyoxometalates, thus retaining the resulting polyoxometalates remaining analogous to the situation, before the supramolecular interactions. Moreover, flexibility in physicochemical properties of polyoxometalates and other entities of the supramolecular assemblies is possible to improve synergistically, leading to their enhanced effectiveness in catalytic reactions, ¹⁰⁶ dye adsorption etc. ^{107,108}

Supramolecular interactions and the resulting network between polyoxometalates and different supramolecular entities have till now allowed an expedient isolation of formerly subtle polyoxometalates in crystalline form, ^{109,110} stabilization of magnetic polyoxometalates, that are hypersensitive; ¹¹¹ polyoxometalates surface area increase, having an influence on

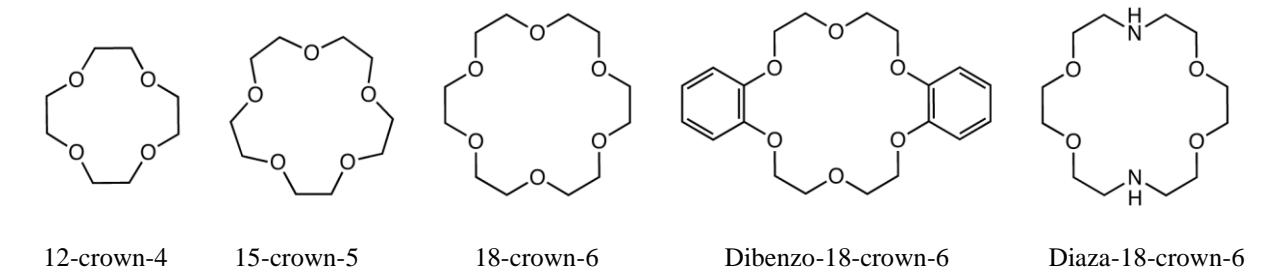
catalysis, ¹¹² optimizations of the biocompatibility of polyoxoanions ¹¹³⁻¹¹⁵ and uniform arrangement of polyoxometalates on surfaces. ^{116,117}



Scheme 1.1. Possible applications of various types of POM-containing supramolecular assemblies. 118

1.6 Polyoxometalate- Crown-ether Based Supramolecular Assemblies for Molecular Recognition

They are hosts for a variety of cations as well as neutral molecules. They are made up of ether oxygen atoms arranged in a cyclic pattern connected by organic moieties, usually – CH₂CH₂- groups. Metal-binding ability of unidentate ethers such as the common solvent, diethyl ether, is very poor, but, crown ethers have metal binding ability due to the chelate and macrocyclic effects. Apart from O, they may also have N or S as the heteroatoms. Crown ethers have excellent ability of molecular recognition, transportation and catalysis. Some common crown ethers are represented in Scheme 1.2.



Scheme 1.2. Common crown ethers.

Polyoxometalate based crown-ether molecular assemblies, connected through supramolecular assemblies have been used widely for *molecular recognition*, which can be defined as definite interaction that are observed between two or more molecules with the help of non-covalent bonding such as hydrogen-bonding (H-bonding), metal coordination, halogen bonding (X-bonding), van der Waals forces, hydrophobic forces, π – π interactions, electrostatic and/or electromagnetic effects. ^{121,122}

As discussed earlier, polyoxometalates have negatively charged oxygen atoms, which can form H-bonds with various donor atoms. So, the crown ether-cation supramolecular complex cation can be associated to a polyoxometalate anion through Coulombic interactions and H-bonds, provided that the polyoxometalate is placed at an appropriate accepting site in the lattice of the crystal. Crown ethers can stabilize water of crystallization in the polyoxometalates to yield better quality crystals. ^{123,124} These complexes have attracted very special interest in the field of polyoxometalate chemistry and has also opened a broad research area in the field of inorganic-organic hybrids. This class of compounds is found to be very useful, as far as the separation of various metal ions like Ca²⁺, Sr²⁺, Ba²⁺, Pb²⁺, and, also rare earth metals like Pr³⁺ and Eu³⁺ from acidic solutions, using precipitation methods is concerned. ¹²⁵⁻¹²⁷

1.7 Polyoxometalates for Electrocatalysts

A wide variety of polyoxometalates have been used as catalysts for a wide variety of reactions. These days, polyoxometalates have been also extensively used for electrocatalysis. Electrocatalysis can be defined as 'the relative capability of various moieties, to increase the rate of any electrochemical process, when used as the electrode surfaces or at the electrode surfaces, under the same environments'. 128

Polyoxometalates exhibit unique electrochemical redox behaviour because just by a slight change in their structure or composition, we can fine tune them for various purposes. The oxidation/reduction states of polyoxometalates are quite stable and they can participate in fast reversible electron transfer reactions. However, there are very few reports where polyoxometalates have been proven to be stable because they easily degrade to respective metal oxides, which under the electrocatalytic conditions, act as active catalysts, for electrocatalytic water oxidation (i.e., at high anodic potential). As far as coordination complexes are concerned, metal oxides formations as well as oxidative degradation of organic ligands are the major concerns, requiring additional attention. To solve the issue of stability, grafting of the coordination complex, at the molecular level on polyoxometalate

surface can be deliberated as an operative substitute since the coordinate-covalent bond, linked with the polyoxometalate augments the mechanical rigidity of the coordinated coordination complex that increases the electron transfer rate. These two matters are vital concerning deficiency of electrochemical stability of metal complexes, that are not supported over any other species. In these hybrid compounds, we can use the catalytic properties of both polyoxometalates as well as metal coordination complexes. These countenances probable cooperative interaction between purely inorganic polyoxometalates and involved complex(es), resulting in enhanced functionality. This augments their possible use in water splitting catalysis as well as in other fields such as, materials sciences, biological sciences, and pharmaceutical sciences. 140-145

Compounds containing polyoxometalate coordinated to polyoxometalates, ¹³⁴ are common to chemists. Various reports show these complexes as robust electrocatalysts for various reactions.

1.8 Motivation of the Thesis

The polyoxometalate chemistry is a known field since ages, and a lot of work has been done on this and using this. Many research groups across the world have contributed to this interesting field. Our group since the last two decades is actively involved in the synthesis, characterization, and application of diverse polyoxometalates and polyoxometalate based supramolecular complexes.

In 2006,¹⁴⁶ our group reported a copper pentahydrate complex that was sandwiched between two crown-ether moieties. The supramolecular entity was stabilized by a hexamolybdate anion (Figure 1.4). This was the first crystal structural evidence to the claim by Pasquarello *et al.*,¹⁴⁷ where they claimed based on neutron diffraction and first-principle molecular dynamics, that Cu(II) ion prefers a penta-aqua coordination, which was contradicting the generally accepted picture that *3d* metals in their +2 oxidation state prefer hexa-aqua coordination. Keeping this result in mind, we thought of studying the coordination behavior of other 3d metals like Co²⁺, Ni²⁺ and Zn²⁺ where water binds them as ligands. We used the same strategy that we used in the previous report¹⁴⁶ and the same polyoxometalate and the same crown ether. The results are discussed in *Chapter 2* of the thesis.

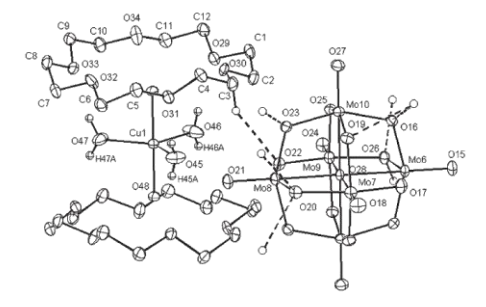


Figure 1.4. Supramolecular sandwich of trigonal bipyramidal $Cu^{II}(H_2O)_5$. ¹⁴⁶

Supramolecular chemistry-based polyoxometalates have been also studied by our group earlier, where we have used different crown ethers and were successful in the inclusion of ammonium ions in the crown ether cavity and these supramolecular entities were stabilized

by different polyoxometalates (Figure 1.5).¹⁴⁸ In those cases, ammonium thiocyanate (NH₄SCN) and ammonium heptamolybdate were used as the ammonium source. To study the same effects, we performed the experiments with ammonium chloride as the source of ammonium ions, and two different crown ethers and two different polyoxometalates were used. The results hence obtained are discussed in *Chapter 3* of the thesis.

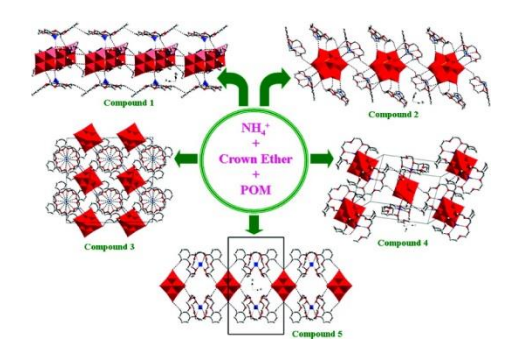


Figure 1.5. Ammonium ion inclusion in crown ether cavities stabilized by polyoxometalates. 148

A gas-liquid interfacial reaction, where volatile organic amines, namely piperidine and piperazine were allowed to diffuse into an acidified aqueous solution of sodium molybdate, at room temperature was reported recently by our group. In both cases, the protonated piperidine and piperazine molecules were arrested in the rooms formed between the octamolybdate clusters formed *in situ*, and bound through hydrogen bonding interactions. This gave an idea of the absorption of volatile organic amines found in the atmosphere using polyoxometalates (Figure 1.6). The same idea has been put into exercise using trimethylamine as the volatile organic amine, keeping all other reaction conditions identical. It exhibits the capture of protonated triethylamine molecules in the polyoxometalate framework through hydrogen bonding interactions along with a unique rearrangement reaction where triethylamine breaks down to form a tetraethyammonium ion and ammonium ion. The detailed discussion is described in *Chapter 4* of the thesis.

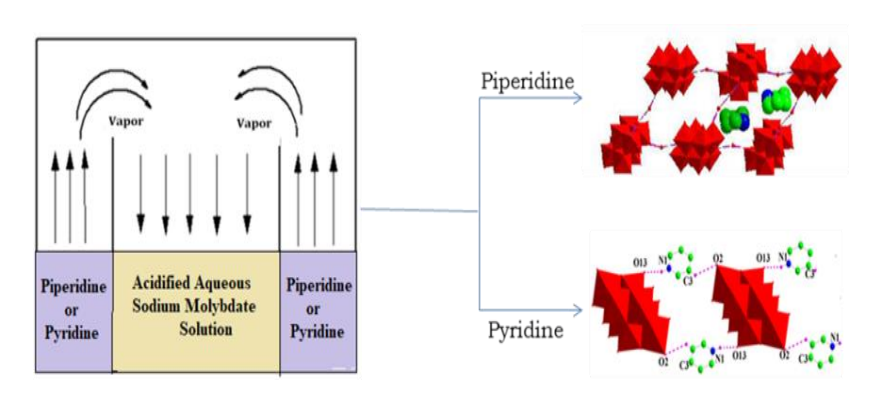


Figure 1.6 Gas-liquid interfacial reaction leading to the arrest of volatile organic amines in supramolecular networks of polyoxometalates. 149

We have reported various polyoxometalate supported transition metal complexes, i.e., transition metal complexes connected to polyoxometalates, through its one or more terminal oxygen atoms, where these oxygen atoms, and hence the whole of the polyoxometalate acts as a ligand. Recently, we have reported these polyoxometalate supported transition metal

complexes as potential candidates as catalysts for electrocatalytic reactions like water oxidation and water reduction. Apart from these reports, many other groups have given various reports where these polyoxometalate supported transition metal complexes have served as electrocatalysts for various other reactions. Keeping these reports in mind, we have synthesized and characterized a copper dimeric complex, that is supported on a polyoxometalate, $[Mo_8O_{26}]^{4-}$, and we have used the complex as an electrocatalyst for water oxidation, water reduction, and hydrogen peroxide reduction. Chapter 5 of the thesis describes the detailed synthesis, characterization, single-crystal X-ray diffraction crystal structure analysis and the utilization of this copper dimeric complex supported on a polyoxometalate as electrocatalysis.

1.9 References

- 1. Pope, M. T. Heteropoly and Isopoly Oxometalates, Springer-Verlag: Berlin, 1983.
- 2. Carraro, M.; Gross, S. Materials, 2014, 7(5):3956–3989.
- 3. Pope, M. T.; Muller, A. *Polyoxometalate Chemistry: From Topology via Self-Assembly to Applications*, Kluwer, Dordrecht, **2001**.
- 4. Pope, M. T.; Muller, A. *Polyoxometalate Molecular Science* Kluwer Academic Publishers, **2003**.
- 5. Pope, M. T. *Inorganic Chemistry Concepts Vol.* 8: Heteropoly and Isopoly Oxometalates, Springer, Berlin, 1983.
- 6. Cock, J. D. Interaction of polyoxometalates and model proteins: structural and luminescence investigation Ph.D. Thesis, **2016.**
- 7. Kozhevnikov, I. *Catalysis by Polyoxometalates*; Catalysis for Fine Chemical Synthesis; Wiley & Sons, LTD, **2002**; Vol. 2.
- 8. Misono, M. Mat. Chem. Phy. 1987, 17, 103-120.
- 9. Okuhara, T.; Mizuno, N.; Misono, M. Adv. Cat. 1996, 41, 1-140.
- 10. Mizuno, N.; Misono, M. J. Mol. Cat. 1994, 86, 319-342.
- 11. Hill, C. L. Chem. Rev. 1998, 98, 1-2.
- 12. Maksimov, G. Russ. Chem. Rev. 1995, 64, 445-461.
- 13. Souchay, P. *Polyanions et polycations*; Monographies de chimie mineerale; Gaithier-Villars, Paris, **1963**.
- 14. Tsigdinos, G.; Hallada, C. Inorg. Chem. 1968, 7, 437 441.
- 15. Grate, J. H. J. Mol. Cat. A: Chem. 1996, 114, 93-101.
- 16. Odyakov, V. F.; Zhizhina, E. G.; Maksimovskaya, R. I. *Appl. Cat. A: Gen.* **2008**, *342*, 126-130.
- 17. Nyman, M. Dalton Trans. 2011, 40, 8049 8058.
- 18. Li, S.; Liu, S.; Liu, S.; Liu, Y.; Tang, Q.; Shi, Z.; Ouyang, S.; Ye, J. J. Am. Chem. Soc. **2012**, 134, 19716-19721.
- 19. Müller, A.; Serain, C. Acc. Chem. Res. 2000, 33, 2-10.
- 20. Berzelius, J. Annalen der Physik 1826, 82, 369-392.
- 21. de Marignac, G. Le fond d'un portefeuille; Annales de Chimie et de Physique, **1864**; Vol. 3, p. 1.
- 22. Werner, A. Ber Deutschen Chem. Ges. 1907, 40, 40.

- 23. Miolati, A.; Turin, R.; Pizzighelli, R. J. Prak. Chemie 1907, 77, 417-456.
- 24. Baker, L. C.; Glick, D. C. Chem. Rev. 1998, 98, 3-49.
- 25. Pauling, L. J. Am. Chem. Soc. 1929, 51, 4, 1010-1026.
- 26. Keggin, J. F. Proc. Royal Soc. A: Math., Phys. Engg. Sci. 1934, 144, 75-100.
- 27. Varga, G.; Papaconstantinou, E.; Pope, M. *Inorg. Chem.* **1970**, *9*, 662-667.
- 28. Pope, M.; Varga, G. Chem. Commun. 1966, 653-654.
- 29. So, H.; Pope, M. Inorg. Chem. 1972, 11, 1441 1443.
- 30. Leparulo-Loftus, M.; Pope, M. *Inorg. Chem.* **1987**, *26*, 2112 2120.
- 31. Mbomekalle, I.; Keita, B.; Lu, Y. W.; Nadjo, L.; Contant, R.; Belai, N.; Pope, M. *Eur. J. Inorg. Chem.* **2004**, 2004, 4132 4139.
- 32. Kozhevnikov, I.; Matveev, K. Russ. Chem. Rev. 1982, 51, 1075-1088.
- 33. Kozhevnikov, I.; Matveev, K. Appl. Catal. 1983, 5, 135-150.
- 34. Kozhevnikov, I. Russ. Chem. Rev. 1987, 56, 811-825.
- 35. Kozhevnikov, I. Catal. Rev. 1995, 37, 311-352.
- 36. Kozhevnikov, I. J. Mol. Catal. A: Chem. 2007, 262, 86-92.
- 37. Hill, C.; Prosser-McCartha, C. Coord. Chem. Rev. 1995, 143, 407-455.
- 38. Grigoriev, V. A.; Hill, C. L.; Weinstock, I. A. J. Am. Chem. Soc. **2000**, 122, 3544 3545.
- 39. Geletii; Atalla; Bailey; Delannoy; Hill, C. L.; Weinstock, I. A. J. Am. Chem. Soc. 2004, 126, 1-2.
- 40. Hill, C. J. Mol. Cat. A: Chem. 2007, 262, 2-6.
- 41. Pope, M.; Muller, Angew. Chem. Int. Ed. 1991, 30, 34-48.
- 42. Pope, M.; Müller, A. *Polyoxometalate chemistry: from topology via self- assembly to applications*; Kluwer Academic Publishers, **2001**
- 43. Müller, A.; Roy, S. Coord. Chem. Rev. 2003, 245, 153 166.
- 44. Nicoara, A.; Patrut, A.; Margineanu, D.; Müller, A. *Electrochem. Comm.* **2003**, *5*, 511-518.
- 45. Gouzerh, P.; Che, M. l'actualité chimique 2006, 298, 1 14.
- 46. Weinstock, I. A.; Müller, A. Isr. J. Chem. 2011, 51, 176-178.
- 47. Hallada, C. J.; Tsigdinos, G.; Hudson, B. S. J. Phys. Chem. A 1968, 72, 4304-4307.
- 48. Tsigdinos, G.; Hallada, C. Inorg. Chem. 1970, 9, 2488 2492.
- 49. Tsigdinos, G.; Hallada, C. J. Less Com. Metals 1974, 36, 79 93.
- 50. Tsigdinos, G. Topics in Current Chemistry 1978, 76, 1-64.
- 51. Neumann, R.; Dahan, M. J. Am. Chem. Soc. 1998, 120, 11969-11976.
- 52. Khenkin, A. M.; Weiner, L.; Wang, Y.; Neumann, R. J. Am. Chem. Soc. **2001**, 123, 8531-8542.
- 53. Hirao, H.; Kumar, D.; Chen, H.; Neumann, R.; Shaik, S. J. Phys. Chem. C 2007, 111, 7711-7719.
- 54. Khenkin, A. M.; Leitus, G.; Neumann, R. J. Am. Chem. Soc. 2010, 132, 11446-11448.
- 55. Efremenko, I.; Neumann, R. J. Phys. Chem. A 2011, 115, 4811 4826.
- 56. Efremenko, I.; Neumann, R. J. Am. Chem. Soc. 2012, 134, 20669-20680.
- 57. Haider, A.; Ibrahim, M.; Bassil, B. S.; Carey, A.M.; Nguyen Viet, A.; Xing, X.; Ayass, W. W.; Miñambres, J. F.; Liu, R.; Zhang, G.; Keita, B.; Mereacre, V.; Powell,

- A. K.; Balinski, K.; N'Diaye, A. T.; Kuepper, K.; Chen, H.-Y.; Stimming, U.; Kortz, U. *Inorg. Chem.* **2016**, *55*, 2755-2764.
- 58. Wang, K.-Y.; Bassil, B. S.; Carey, A. M.; Mougharbel, A. S.; Kortz, U. *Eur. J. Inorg. Chem.* **2017**, 4210–4213.
- 59. Bassil, B. S.; Haider, A.; Ibrahim, M.; Mougharbel, A. S.; Bhattacharya, S.; Christian, J. H.; Bindra, J. K.; Dalal, N. S.; Wang, M.; Zhang, G.; Keita, B.; Rutkowska, I. A.; Kulesza, P. J.; Kortz, U. *Dalton Trans.* **2018**, *47*, 12439–12448.
- Douvas, A. M.; Tsikrizis, D.; Tselios, C.; Kennou, S.; Haider, A.; Mougharbel, A. S.;
 Kortz, U.; Palilis, L. C.; Hiskia, A.; Coutsolelos, A. G.; Vasilopoulou, M.; Argitis, P.
 Phys. Chem. Chem. Phys. 2019, 21, 427-437.
- 61. Ma, T.; Yang, P.; Dammann, I.; Lin, Z.; Mougharbel, A. S.; Li, M.-X.; Adăscăliței, F.; Mitea, R.; Silvestru, C.; Thorstenson, C.; Ullrich, M. S.; Cseh, K.; Jakupec, M. A.; Keppler, B. K.; Donalisio, M.; Cavalli, R.; Lembo, D.; Kortz, U. *Inorg. Chem.* **2020**, *59*, 2978-2987.
- 62. Zhan, C.; Zheng, Q.; Long, D. -L.; Vilà-Nadal, L.; Cronin, L. *Angew. Chem. Int. Ed.*, **2019**, *131*, 17442-17446.
- 63. Chen, J.-J.; Symes, M. D.; Cronin, L. Nature Chem., 2018, 10, 1042-1047.
- 64. Duros, V.; Grizou, J.; Xuan, W.; Hosni, Z.; Long, D. -L.; Miras, H. N.; Cronin, L. *Angew. Chem. Int. Ed.*, **2017**, *56*, 10815-10820.
- 65. Zang, H. -Y.; Chen, J. -J.; Long, D. -L.; Cronin, L.; Miras, H. N. *Chem. Sci.*, **2016**, *7*, 3798-3804.
- 66. Sartzi, C.; Miras, H. N.; Vilà-Nadal, L.; Long, D. -L.; Cronin, L. *Angew. Chem. Int. Ed.*, **2015**, *54*, 15488-15492.
- 67. Girardi, M.; Platzer, D.; Griveau, S.; Bedioui, F.; Alves, S.; Proust, A.; Blanchard, S. *Eur. J. Inorg. Chem.* **2019**, *3-4*, 387-393.
- 68. Makrygenni, O.; Brouri, D.; Proust, A.; Launay, F.; Villanneau, R. *Micro. Meso. Mat.* **2019**, 278, 314-321.
- 69. Volatron, F.; Noël, J.-M.; Rinfray, C.; Decorse, P.; Combellas, C.; Kanoufi, F.; Proust, A. *J. Mater. Chem. C*, **2015**, *3*, 6266-6275.
- 70. Girardi, M.; Blanchard, S.; Griveau, S.; Simon, P.; Fontecave, M.; Bedioui, F.; Proust, A. Eur. J. Inorg. Chem., 2015, 3642-3648.
- 71. Jallet, V.; Guillemot, G.; Lai, J.; Bauduin, P.; Nardello-Rataj, V.; Proust, A. *Chem. Commun.*, **2014**, 6610-6612.
- 72. Luo, J.; Zhang, B.; Yvon, C.; Hutin, M.; Gerislioglu, S.; Wesdemiotis, C.; Cronin, L.; Liu, T. *Eur. J. Inorg. Chem.* **2019**, *(3-4)*, 380-386.
- 73. Zhou, J.; Hu, J.; Li, M.; Li, H.; Wang, W.; Liu, Y.; Winans, R. E.; Li, T.; Liu, T.; Yin, P. *Mater. Chem. Front*, **2018**, *2* (*11*), 2070-2075.
- 74. Zhang, B.; Song, J.; Hu, L.; Hill, C. L.; Liu, T. *Langmuir* **2016**, *32*, 12856 12861.
- 75. Zhou, J.; Yin, P.; Chen, X.; Hu, L.; Liu, T. Chem. Comm. 2015, 51, 15982 15985.
- 76. Rachel, A.; Scullion, A.; Surman, J.; Xu, F.; Mathieson, J. S.; Long, D.-L.; Haso, F.; Liu, T.; Cronin, L. *Angew. Chem. Int. Ed.* **2014**, *126*, 10196 10201.
- 77. Barman, S.; Sreejith, S.; Garai, S.; Pochamoni, R.; Roy, S. *ChemPhotoChem* **2019**, *3*, 93.

- 78. Barman, S.; Das, S.; Sreejith, S. S.; Garai, S.; Pochamoni, R.; Roy, S. *ChemCommun* **2018**, *54*, 2369.
- 79. Das, S.; Roy, S. J. Mol. Eng. Mater. 2017, 5, 1750001.
- 80. Roy, S. CrystEngComm 2014, 16, 4667.
- 81. Roy, S. Inorg. Chem. 2011, 32, 113.
- 82. Lubin, N.; Robin, G.; Triana, C. A.; Bernhard, S.; Kim, K.; Patzke, G. R. *Dalton Trans.* **2019**, *48*(*35*),13293-13304.
- 83. Joaquín, S.-L.; Song, F.; Patzke, G. R.; Galan-Mascaros, J. R. *Front. Chem.* **2018**, *6*, 302.
- 84. Car, P.-E.; Patzke, G. R. *Inorganics* **2015**, *3*(*4*),511-515.
- 85. von Allmen, K.; Car, P.-E.; Blacque, O.; Fox, T.; Müller, R.; Patzke, G. R. Zeitschrift für Anorganische und Allgemeine Chemie, **2014** 640(5),781-789.
- 86. Lubin, N.; Bernhard, S.; Stephen, W.; Patzke, G. R. Eur. J. Inorg. Chem. S **2013**,10-11,1681-1692.
- 87. Shivaiah, V.; Narasimha Reddy, P. V.; Cronin, L.; Das, S. K. *J. Chem. Soc. Dalton Trans.*, **2002**, 3781 3782.
- 88. Shivaiah, V.; Nagaraju, M.; Das, S. K. *Inorg. Chem.*, **2003**, *42*, 6604 6606.
- 89. Shivaiah, V.; Das, S. K. Inorg. Chem., 2005, 44, 7313 7315
- 90. Arumuganathan, T.; Das, S. K. *Inorg. Chem.* **2009**, *48*,496-507.
- 91. Chatterjee, T.; Kumar, N. T.; Das, S. K. Polyhedron, 2017, 127, 68-83.
- 92. M. Misono, K. Sakata, Y. Yoneda, W. Lee, *Proc. 7th Int. Congr. Catal.*, Tokyo, p. 1047. Kodansha, Tokyo, Elsevier, Amsterdam, **1981**.
- 93. M. Misono, Catal. Rev. Sci. Eng., 1987, 29, 269-321.
- 94. M. Misono, Catal. Rev. Sci. Eng., 1988, 30, 339.
- 95. M. Misono, in Proc. 10th Int. Congr. Catal., Budapest, 1992," p. 69. Elsevier, Amsterdam, and Akademiai Kiado, Budapest, 1993.
- 96. T. Okuhara, N. Mizuno, M. Misono, *Adv. Catal.*, **1996**, *41*, 113.
- 97. Patel, K. R. Manganese Substituted Polyoxometalates and their Functionalization: Synthesis, Characterization and Oxidation of Alkenes (Ph.D. Thesis), **2012**.
- 98. Canny, J.; Tézé, A.; Thouvenot, R.; Hervé, G. Inorg. Chem., 1986, 25, 2114.
- 99. Moffat, J. B.; Twing, M. V.; Spencer, M. S. Metal-oxygen clusters: The surface and catalytic properties of heteropolyoxometalates, Kluwer Academic plenum, New York, **2001**.
- 100. M. Misono, Barry, H. F., Mitchell, P. C. H., *Proc. Climax 4th Intern. Conf. Chem. Uses Molybdenum*; Eds.; p 289, **1982**.
- 101. M. Misono, N. Mizuno, K. Katamura, A. Kasai, Y. Konishi, K. Sakata, T. Okuhara, Y. Yoneda, *Bull. Chem. Soc. Jpn.*, **1982**, *55*, 400.
- 102. T. Okuhara, S. Tatematsu, K. Y. Lee, M. Misono, *Bull. Chem. Soc. Jpn.* **1989**,62, 717.
- 103. M. Furuta, K. Sakata, M. Misono, Y. Yoneda, Chem. Lett., 1979, 31.
- 104. Kozhevnikov, I. V. Chem. Rev., 1998, 98, 171 -198.
- 105. Kozhevnikov, I. V. Russ. Chem. Rev., 1987, 56, 811-825.
- 106. Cai, L.-X.; Li, S.-C.; Yan, D.-N.; Zhou, L.-P.; Guo, F.; Sun, Q.-F. *J. Am. Chem. Soc.*, **2018**, *140*, 4869–4876.

- 107. Zou, C.; Zhang, Z.; Xu, X.; Gong, Q.; Li, J.; Wu, C.-D. *J. Am. Chem. Soc.*, **2012**, *134*, 87–90.
- 108. Sun, J.-W.; Yan, P.-F.; An, G.-H.; Sha, J.-Q.; Li, G.-M.; Yang, G.-Y. *Sci. Rep.*, **2016**, 6, 25595.
- 109. Xuan, W.; Surman, A. J.; Zheng, Q.; Long, D.-L.; Cronin, L. *Angew. Chem., Int. Ed.*, **2016**, *55*, 12703–12707.
- 110. Falaise, C.; Moussawi, M. A.; Floquet, S.; Abramov, P. A.; Sokolov, M. N.; Haouas, M.; Cadot, E. *J. Am. Chem. Soc.*, **2018**, *140*, 11198–11201. W. Salomon, Y. Lan, E. Rivi`ere, S. Yang, C. Roch-Marchal,
- 111. Salomon, W.; Lan, Y.; Rivi`ere, E.; Yang, S.; Roch-Marchal, C.; Dolbecq, A.; Simonnet-J´egat, C.; Steunou, N.; Leclerc-Laronze, N.; Ruhlmann, L.; Mallah, T.; Wernsdorfer, W.; Mialane, P. *Chem.–Eur. J.*, **2016**, 22, 6564–6574.
- 112. Paille, G.; Gomez-Mingot, M.; Roch-Marchal, C.; Lassalle-Kaiser, B.; Mialane, P.; Fontecave, M.; Mellot-Draznieks, C.; Dolbecq, A. *J. Am. Chem. Soc.*, **2018**, *140*, 3613–3618.
- 113. Gao, P.; Wu, Y.; Wu, L. Soft Matter, **2016**, 12, 8464–8479.
- 114. Gong, Y.; Hu, Q.; Wang, C.; Zang, L.; Yu, L. Langmuir, 2016, 32, 421–427.
- 115. Azizullah, N.-u. R.; Haider, A.; Kortz, U.; Afridi, S. U.; Sohail, M.; Joshi, S. A.; Iqbal, J. *Int. J. Pharm.*, **2017**, *533*, 125–137.
- 116. Shen, F.-C.; Wang, Y.-R.; Li, S.-L.; Liu, J.; Dong, L.-Z.; Wei, T.; Cui, Y.-C.; Wu, X. L.; Xu, Y.; Lan, Y.-Q. *J. Mater. Chem. A*, **2018**, *6*, 1743–1750.
- 117. Lombana, A.; Rinfray, C.; Volatron, F.; Izzet, G.; Battaglini, N.; Alves, S.; Decorse, P.; Lang, P.; Proust, A. *J. Phys. Chem. C*, **2016**, *120*, 2837–2845.
- 118. Stuckart, M.; Monakhov, K. Y. Chem. Sci., 2019, 10, 4364-4376.
- 119. Steed, J.W.; Atwood, J. L. *Supramolecular Chemistry*, John Wiley and sons Ltd., p-88
- 120. Lehn, J.M. Angew. Chem., Int. Ed., 1998, 27, 89.
- 121. Lockett, M. R.; Lange, H.; Breiten, B.; Heroux, A.; Sherman, W.; Rappoport, D.; Yau, P. O.; Snyder, P. W.; Whitesides, G. M. *Angew. Chem. Int. Ed.* **2003**, *52* (*30*), 7714–7717.
- 122. Breiten, B.; Lockett, M. R.; Sherman, W.; Fujita, S.; Al-Sayah, M.; Lange, H.; Bowers, C. M.; Heroux, A.; Krilov, G.; Whitesides, G. M. *J. Am. Chem. Soc.* **2013**, *135* (*41*), 15579–15584.
- 123. You, W.S.; Wang, E.B.; Xu, Y.; Li, Y.; Li, Xu, L.; Hu, C W., *Inorg. Chem.*, **2001**, *40*, 5468-5471.
- 124. Li, Y.G.; Wang, E. B.; Wang, S. T.; Lu Y.; Hu, C. W.; Hu, Jia, H.Q.; J. *Mol. Struct.*, **2001**, *607*, 133-141.
- 125. Svec, V.; Mikulaj, V.; Hanzel, R. J. *Radioanal. Nucl. Chem.*, **1996**, 208, 487.
- 126. Sheen, S. R.; Shiu, J. S. Analyst, 1992, 117, 1691.
- 127. Fernando, L. A.; Miles, M. L.; Boven, L. H. Anal. Chem., 1980, 52, 1115.
- 128. Barbir, F. *PEM Fuel Cells: Theory and Practice*; Academic Press Sustainable World Series, Elsevier, **2005**.
- 129. Lv, H.; Geletii, Y. V.; Zhao, C.; Vickers, J. W.; Zhu, G.; Luo, Z.; Song, J.; Lian, T.; Musaev, D. G.; Hill, C. L. *Chem. Soc. Rev.* **2012**, *41*, 7572–7589.

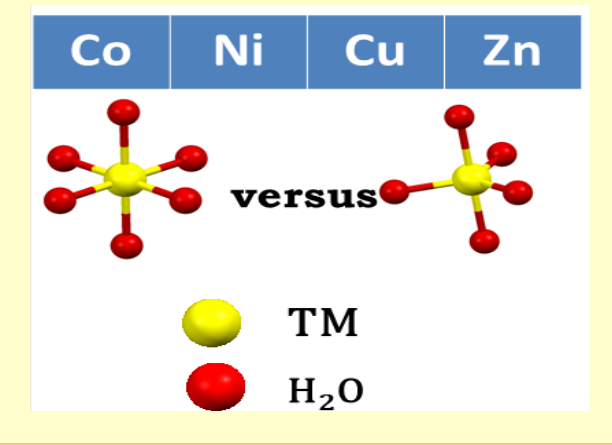
- 130. Folkman, S. J.; Finke, R. G. ACS Catal. 2017, 7, 7–16.
- 131. Stracke, J. J.; Finke, R. G. J. Am. Chem. Soc. 2011, 133, 14872–14875.
- 132. Li, J.; Güttinger, R.; Moré, R.; Song, F.; Wan, W.; Patzke, G. R. *Chem. Soc. Rev.* **2017**, *46*, 6124–6147.
- 133. Asraf, M. A.; Younus, H. A.; Yusubov, M.; Verpoort, F. *Catal. Sci. Technol.* **2015**, 5, 4901–4925.
- 134. Li, X.-M.; Chen, Y.-G.; Shi, T. Solid State Sci. 2016, 52, 112–117.
- 135. Li, M.-T.; Sha, J.-Q.; Zong, X.-M.; Sun, J.-W.; Yan, P.-F.; Li, L.; Yang, X.-N. *Cryst. Growth Des.* **2014**, *14*, 2794–2802.
- 136. Liu, C.-M.; Huang, Y.-H.; Zhang, D.-Q.; Jiang, F.-C.; Zhu, D.-B. *J. Coord. Chem.* **2003**, *56*, 953–960.
- 137. Wang, H.; Cheng, C.; Tian, Y. Chin. J. Chem. 2009, 27, 1099–1102.
- 138. Li, Y.-F.; Hubble, D. G.; Miller, R. G.; Zhao, H.-Y.; Pan, W.-P.; Parkin, S.; Yan, B. *Polyhedron* **2010**, *29*, 3324–3328.
- 139. Yi, Z.; Zhang, X.; Yu, X.; Liu, L.; Xu, X.; Cui, X.; Xu, J. J. Coord. Chem. **2013**, 66, 1876–1888.
- 140. Xu, Y.; Xu, J.-Q.; Zhang, K.-L.; Zhang, Y.; You, X.-Y. *Chem. Commun.* **2000**, *0*, 153–154.
- 141. Wang, Y.; Zou, B.; Xiao, L.-N.; Jin, N.; Peng, Y.; Wu, F.-Q.; Ding, H.; Wang, T.-G.; Gao, Z.-M.; Zheng, D.-F.; Cui, X.-B.; Xu, J.-Q. *J. Solid State Chem.* **2011**, *184*, 557–562.
- 142. Cui, J.-W.; Cui, X.-B.; Yu, H.-H.; Xu, J.-Q.; Yi, Z.-H.; Duan, W.-J. *Inorg. Chim. Acta* **2008**, *361*, 2641–2647.
- 143. Devi, R. N.; Burkholder, E.; Zubieta, J. Inorg. Chim. Acta 2003, 348, 150–156.
- 144. Dolbecq, A.; Dumas, E.; Mayer, C. R.; Mialane, P. *Chem. Rev.* 2010, **110**, 6009–6048.
- 145. Kumar, A.; Gupta, A. K.; Devi, M.; Gonsalves, K. E.; Pradeep, C. P. *Inorg. Chem.* **2017**, *56*, 10325–10336.
- 146. Shivaiah, V.; Das, S. K. Angew. Chem. Int. Ed. 2006, 45, 245-248.
- 147. Pasquarello, A. et al. *Science* **2001**, 291, 856 859.
- 148. Chatterjee, T.; Sarma, M.; Das, S. K. Cryst. Growth Des., 2010, 10, 3149-3163
- 149. Shivaiah, V.; Kumar, N. T.; Das, S. K. J. Chem. Sci., 2018, 130:37
- 150. Singh, C.; Mukhopadhyay, S.; Das, S. K. Inorg. Chem. 2018, 57 (11), 6479-6490.
- 151. Singh, C.; Das, S. K. Polyhedron, 2019, 172, 80-86.
- 152. Kumar, N. T.; Bhoi, U.; Naulakha, P.; Das, S. K. *Inorg. Chim. Acta*, **2020**, *506*, 119554.

CHAPTER

2

Transition Metal-Aqua-Complexes: Six or Five Fold Coordination or Together

Abstract. The coordination number around a 3d transition metal ion M²⁺ in water is not just six, as believed for many years. For instance, the Cu²⁺ ion, dissolved in water, has convincingly been established to be {Cu^{II}(H₂O)₅}²⁺ instead of {Cu^{II}(H₂O)₆}²⁺, the later one was generally believed. On the other hand, Ni²⁺ in water is found to be octahedral $\{Ni^{II}(H_2O)_6\}^{2+}$. We have attempted to isolate M^{2+} aqua-coordination complex cations (M = Co, Ni, and Zn) in a polyoxometalate (POM) matrix anion using a crown-ether to stabilize these metal-aqua-species (through the formation of supramolecular sandwiches) as single crystals and characterized unambiguously by their crystal structure determinations. We have synthesized cobalt(II)-, nickel(II)and zinc(II)-aqua-complex-associated compounds $[{Co(H_2O)_5([18]-crown-6)_2}{Co(H_2O)_6([18]-crown-6)_2}][Mo_6O_{19}]_2$ (1), $[Ni(H_2O)_6([18]-crown-6)_2][Mo_6O_{19}]$ **(2)** and [Zn(H₂O)₅([18]-crown-6)2][Mo₆O₁₉] (3). Compound 1 includes an interesting simultaneous co-existence of both Co(II)-penta-aqua-coordination complex $\{\text{Co}(H_2O)_5\}^{2+}$ and Co(II)-hexa-aquacoordination complex {Co(H₂O)₆}²⁺ in 1:1 ratio, whereas compounds 2 and 3 contain Ni(II)-hexa-aqua-coordination complex {Ni(H₂O)₆}²⁺ and Zn(II)-pentaaqua-coordination complex $\{Zn(H_2O)_5\}^{2+}$, respectively. These results not only help us to understand the choice of coordination number (n) of 3d transition metalaqua coordination complexes $\{M(H_2O)_n\}^{2+}$ (M = Co, Ni, and Zn; n = 5, 6) but also offer an understanding to the dynamic equilibrium between coordination numbers 5 and 6 of $\{M(H_2O)_n\}^{2+}$ of a particular metal ion.



2.1 Introduction

Transition metals are of great interest to all-time chemists, since their discoveries, as far as their various applications are concerned which may be attributed to a plethora of properties that are associated with them. Transition metals also have profound importance in biological processes. Study of these properties as well as their applications to a great extent demands for a detailed study of their chemical behaviour towards various ligands. It will also enable the chemists to design more sophisticated complexes that are mimics of the active sites of biological metalloproteins, which can be used in our day to day life for meeting the needs of the society. In general, these transition metal salts are available in respective hydrated forms, where they are coordinated to the neutral water ligands. Basic coordination chemistry says that, usually divalent 3d transition metals prefer hexa-hydrated complexes, i.e., six water molecules being coordinated to the central metal atom forming a regular octahedron in all cases except for Cr(II) and Cu(II), which have d⁴ and d⁹ outer electronic configuration, respectively thus exhibiting the more stable Jahn-Teller distorted octahedron of hexa-aqua coordination. Various techniques and theories have also proven the above facts. ²⁻¹⁰

In 2011, Williams and Jeremy gave a generalized fact on the coordination number i.e., the first hydration sphere of divalent transition metals, wherein, based on the Infrared Radiative Photodissociation (IRPD) spectroscopy, they concluded that at 215K, the average coordination number of Mn²⁺, Fe²⁺, Co²⁺, and Ni²⁺ is ~ 6.² Paola D'Angelo *et al.* did an extensive EXAFS study and molecular dynamics study of the nitrates of Co, Ni and Zn and found that the coordination number of all the three compounds with water is 6.¹¹ The study reveals that the TM–O distance (O atom of H₂O) falls in the range of 2.07–2.09 Å. The EXAFS studies were recorded at room temperature. Prior to this, Marcus, ¹² and Ohtaki and Radnai¹³ reviewed the then available data about the ionic radii of divalent cations in aqueous solutions and structure and dynamics of hydrated ions respectively, where they had shown the coordination number of Co(II), Ni(II) and Zn(II) to be 6 and the distance to be in the same region as mentioned above.

In contrary to this widely accepted fact, Pasquarello and co-workers in the year 2001 gave a combined report¹⁴ of experimental and theoretical studies, where they proved a breakthrough result that Cu(II) ion prefers a penta-aqua complex over a hexa-aqua complex, even though the similar size cation Ni(II) adopts a six-fold coordination of water molecules. The pertinent authors, in favour of their unusual results, argued that this is due to the 3d⁹ electronic structure, and by virtue of Jahn-Teller effect, it forms a distorted octahedron.¹⁴

In this line, we were successful in isolating the penta-aqua Cu(II) coordination complex in a system, the single crystal of which showed that, the *trigonal bipyramidal* (*tbp*) $[Cu(H_2O)_5]^{2+}$ complex is sandwiched between two 18-crown-6 entities and stabilized by an isopolyanion, *viz.* $[Mo_6O_{19}]^{2-}$ as the counter anion.¹⁵ This was a strong evidence to the claim

of Pasquarello and his group.¹⁴ If Jahn-Teller effect is responsible for five-fold coordination of copper-aqua complex, then it is interesting to see the fate of Co(II)-aqua complex cation in terms of the number of water coordination. Co^{2+} , a d^7 system, can have either a $t_{2g}^{6}e_g^{1}$ state (i.e., a low spin state) with an unpaired electron (S = 1/2) or a $t_{2g}^5 e_g^2$ high spin state having three unpaired electrons (S = 3/2). As far as spectrochemical series is concerned, a high spin complex is favoured (water ligand is approximately in the middle of the series). On the other hand, a low spin complex is most favoured if we consider the crystal field stabilization energy (CFSE). And a low spin Co(II)-hexa-aqua-octahedral coordination complex $(t_{2g}{}^{6}e_{g}{}^{1}$ electronic state) would exhibit Jahn-Teller effect. If it is so, then there is a probability of formation of penta-aqua Co(II) complex cation, [Co(H₂O)₅]²⁺. This fundamental issue of whether it is penta-aqua-coordination complex cation, [Co(H₂O)₅]²⁺or hexa-aqua-coordination complex cation, [Co(H₂O)₆]²⁺, is one of the major concerns of the present work. Ni(II) ion (a d⁸ system), which does not exhibit Jahn-Teller distortion, was shown to exhibit six fold water coordination (as expected) by Pasquarello and his co-workers who performed the simulation studies for Ni(II) ion in water. ¹⁴ Zn(II) also, like other divalent transition metal ions prefer hexa-aqua coordination, as believed. But, the studies by Cooper et al. follow with a new inference to this fact, reporting a five-fold water coordination for Zn(II), based on IR action spectroscopy and theoretical calculations. 16

This anomaly of penta- and hexa-coordination of water molecules around 3d bivalent transition metal ions is a fundamental problem of inorganic chemistry as far as the dynamics of water coordination to the 3d M²⁺ ion is concerned. An extreme boundary of this dynamics is the isolation of such metal-aqua coordination complexes in their crystalline forms, which is not so easy unless we combine this metal agua species with an appropriate matrix. A proper environment around the metal-aqua species in a crystal might tune the energy of the system in such a way that a particular metal-aqua coordination in a particular geometry is favoured and isolated. In this line, our previous report on serendipitous isolation and crystal structure of the trigonal bipyramidal (tbp) penta-aqua Cu(II) coordination complex, [Cu(H₂O)₅]²⁺, perfectly sandwiched by two crown ethers in a polyoxometalate matrix, 15 recent EXAFS studies of Co(II)-, Ni(II)- and Zn(II)-salts in water¹¹ and certainly, the landmark paper of Pasquarello and co-workers¹⁴ instigated us to synthesize and structurally characterize Co(II)-, Ni(II)- and Zn(II)-aqua coordination complexes so that, we understand more on this fundamental issue of 3d M(II)-aqua coordination numbers. We have chosen polyoxometalate (POM) matrix to isolate and crystallize 3d M(II)-aqua coordination complexes, because POMs are negatively charged metal oxide clusters of highly oxidised early transition metals, ¹⁷ and these can utilize their virtue of supramolecular interactions in stabilizing unusual chemical species 15,18 (e.g., metal-aqua coordination complexes in the present study) in the crystalline state.

Here in this chapter, we have synthesized and structurally characterized three compounds: $[Co(H_2O)_5([18]\text{-crown-6})_2][Co(H_2O)_6([18]\text{-crown-6})_2][Mo_6O_{19}]_2$ (1), $[Ni(H_2O)_6([18]\text{-crown-6})_2][Mo_6O_{19}]$ (2), and $[Zn(H_2O)_5([18]\text{-crown-6})_2][Mo_6O_{19}]$ (3), where, compound 1 includes octahedral $\{Co(H_2O)_6\}$ as well as trigonal bipyramidal $\{Co(H_2O)_5\}$ species in 1:1 ratio, compound 2 has only one octahedral $\{Ni(H_2O)_6\}$ complex and compound

3 contains only one trigonal bipyramidal {Zn(H₂O)₅} complex per respective formula units. We have also synthesized the copper analogue (**4**), reported earlier by our group, ¹⁵ for the comparative studies.

2.2Results and Discussion

2.2.1 Synthesis

The serendipitous synthesis of **4** and its single crystal structure analysis, showing five-fold coordination of water molecules around Cu(II) ion, ¹⁵ motivated us to come across and learn the breakthrough results of Pasquarello and co-workers¹⁴ that, on the contrary to 'six fold coordination of similar charged cations and similar sized cations like Mg²⁺ and Ni²⁺, the Cu²⁺ aqua ion adopts a fivefold coordination'. ¹⁴ This fundamental work and the recent EXAFS results of aqueous solutions of Co(II)-, Ni(II)- and Zn(II)-salts exhibiting six-fold water coordination around these M(II) ions, ¹¹ inspired us to isolate Co(II)-, Ni(II)- and Zn(II)-aqua ions (as single crystals) in the same synthesis condition, applied to the synthesis of Cu(II)-aqua-compound **4**. Thus, all three compounds **1-3** were synthesized by following the synthesis procedure of compound **4**. The relevant synthetic procedures include the reaction of 18-crown-6, [Bu₄N]₂[Mo₆O₁₉] and the corresponding metal nitrates in acetonitrile, which is already acidified with acetic acid. The formation of the title compounds in the reaction mixture can be described by the following equations (Eqn. 2.1- Eqn. 2.4).

2.2.2 Crystallography

Compound 1 crystallizes in the orthorhombic P_{mmn} space group. The asymmetric unit of compound 1 consists of half of the isopolyanion cluster $\{Mo_6O_{19}\}^{2-}$ i.e., $\{Mo_3O_{9.5}\}^{1-}$ unit (there are four molybdenum atoms having half occupancy and one molybdenum having full occupancy; similarly nine oxygen atoms having half occupancy and five oxygen atoms having full occupancy), one [18]-crown-6 molecule (in two crystallographically independent fragments), one $\{Co(H_2O)_3\}$ moiety with one-fourth occupancy of cobalt (with half occupancy of all three coordinated oxygen atoms) and another $\{Co(H_2O)_3\}$ moiety with one-fourth occupancy of cobalt (with half occupancy of two coordinated oxygen atoms and one-fourth occupancy of third coordinated oxygen atom). The asymmetric unit, observed in the crystal structure of compound 1, is shown in Figure 2.1a. Therefore, one formula unit of compound 1 consists of two $\{Mo_6O_{19}\}^{2-}$ isopolyanions, four [18]-crown-6 molecules, one

	Compound 1	Compound 2	Compound 3
Empirical formula	$C_{48}H_{118}Co_2Mo_{12}O_{73}$	C ₂₄ H ₄₈ Mo ₆ NiO ₃₇	$C_{24}O_{36}Mo_6Zn$
fw	3132.56	1562.97	1505.27
$T(K), \lambda(A)$	299(2), 0.71073	299(2), 0.71073	299(2), 0.71073
Crystal system	Orthorhombic	Triclinic	Orthorhombic
Space group	Pmmn	P-1	Pmma
a (Å)	19.323 (3)	10.4943(5)	18.527(5)
b (Å)	22.124(4)	10.8443(5)	11.318(3)
c (Å)	11.2771(16)	11.1423(5)	11.318
α (°)	90.00	91.563(2)	90
β (°)	90.00	106.976(2)	90
γ (0)	90.00	95.893(2)	90
$V(\mathring{A}^3)$	4821.1(13)	1204.18(10)	2373.3(9)
Z, d _{calcd} (g cm ³)	2, 2.158	1, 2.155	2, 2.106
$\mu \text{ (mm}^{-1}), F(000)$	1.95, 3096	2.00, 768	2.133, 1428.0
goodness-of-fit on	1.071	1.03	1.08
F2			
R1	0.044	0.059	0.0708
wR2	0.126	0.159	0.2400
Largest diff.	1.84	0.159	0.786
peak/hole (e Å ⁻³)			

Table 2.1. Crystal Structure analysis of compounds 1-3.

 $\{Co(H_2O)_5\}^{2+}$ moiety and one $\{Co(H_2O)_6\}^{2+}$ moiety (Figure 2.1b) and it is formulated as $[\{Co(H_2O)_5([18]\text{-crown-6})_2\}\{Co(H_2O)_6\ ([18]\text{-crown-6})_2][Mo_6O_{19}]_2\ (1)$. The beauty of this compound $\mathbf{1}$ is the simultaneous co-existence of hexa-aqua $Co(H_2O)_6\}^{2+}$ and penta-aqua $\{Co(H_2O)_5\}^{2+}$ coordination complex cations side by side in the same crystal structure as shown in Figure 2.1c. This unusual crystal structure clearly points out the presence of both of these hexa-aqua $Co(H_2O)_6\}^{2+}$ and penta-aqua $\{Co(H_2O)_5\}^{2+}$ coordination complex cations in the reaction mixture, from which compound $\mathbf{1}$ has been crystallized. This hints that, when a cobalt(II) salt is dissolved in water, it forms both hexa-aqua $Co(H_2O)_6\}^{2+}$ and penta-aqua $\{Co(H_2O)_5\}^{2+}$ species in the salt solution. However, this is in contrast to the EXAFS analysis of the aqueous solution of a Co(II) salt, that show the coordination number of Co(II)-aqua complex as $6.^{11}$

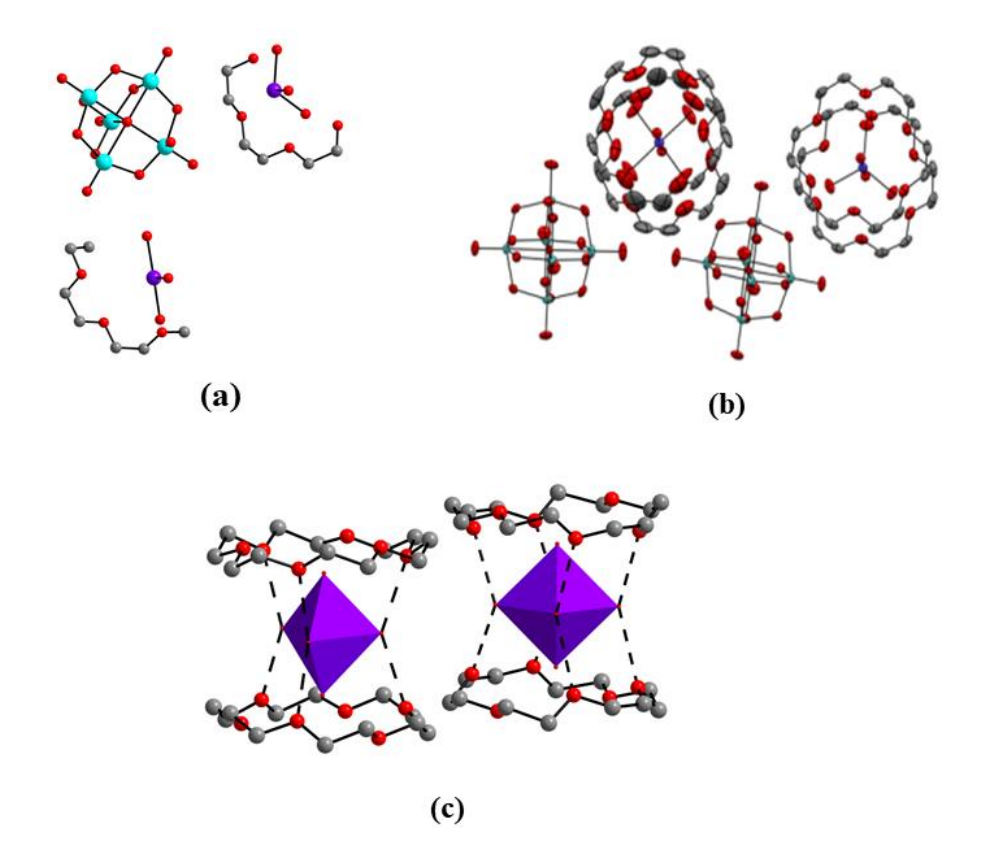


Figure 2.1. (a) Asymmetric unit in the crystal of $[\{Co(H_2O)_5([18]\text{-crown-6})_2\}\{Co(H_2O)_6([18]\text{-crown-6})_2\}][Mo_6O_{19}]_2$ (1); details are mentioned in the text. (b) Thermal ellipsoidal plot (50 % probability) of overall molecular structure of compound 1. (c) Right: hexa-aqua Co(II) complex, $\{Co(H_2O)_6\}^{2+}$ sandwiched by two crown ethers; all four water molecules in the equatorial positions (basal plane) are H-bonded to crown-ethers' oxygen atoms. Left: penta-aqua Co(II) complex, $\{Co(H_2O)_5\}^{2+}$ sandwiched by two crown ethers; all three water molecules in the equatorial positions (basal plane) are H-bonded to crown-ethers' oxygen atoms. Dotted lines represent hydrogen bonds. Both these hexa-aqua $\{Co(H_2O)_6\}^{2+}$ and penta-aqua $\{Co(H_2O)_5\}^{2+}$ coordination complex cations, shown in blue-purple polyhedral representations, co-exist side by side, in the crystal structure of compound 1.

Compound [Ni(H₂O)₆([18]-crown-6)₂][Mo₆O₁₉] (**2**) crystallizes in a triclinic *P-1* space group. Its asymmetric unit (Figure 2.2a) has half of the isopolyanion cluster $\{Mo_6O_{19}\}^{2-}$ i.e., $\{Mo_3O_{9.5}\}^{1-}$ unit (there are nine oxygen atoms having full occupancy and one oxygen atom having half occupancy), one [18]-crown-6 molecule (in four fragments) and one $\{Ni(H_2O)_3\}$ moiety with half occupancy of nickel (with full occupancies of all three coordinated oxygen atoms). Thus a full molecule of compound **2** includes one $\{Mo_6O_{19}\}^{2-}$ isopolyanion, two crown ether molecules and one $\{Ni(H_2O)_6\}^{2+}$ moiety as written in the formula $[Ni(H_2O)_6([18]\text{-crown-6})_2][Mo_6O_{19}]$ (**2**). The molecular structure of compound is presented in Figure 2.2b as a thermal ellipsoidal diagram. In the crystal structure, the nickel(II)-hexa-aqua complex is perfectly sandwiched by two crown ethers as shown in Figure 2.2c. Six fold coordination for nickel(II)-aqua complex has already been established using first principles molecular dynamics simulation studies by A. Pasquarello *et. al.*¹⁴

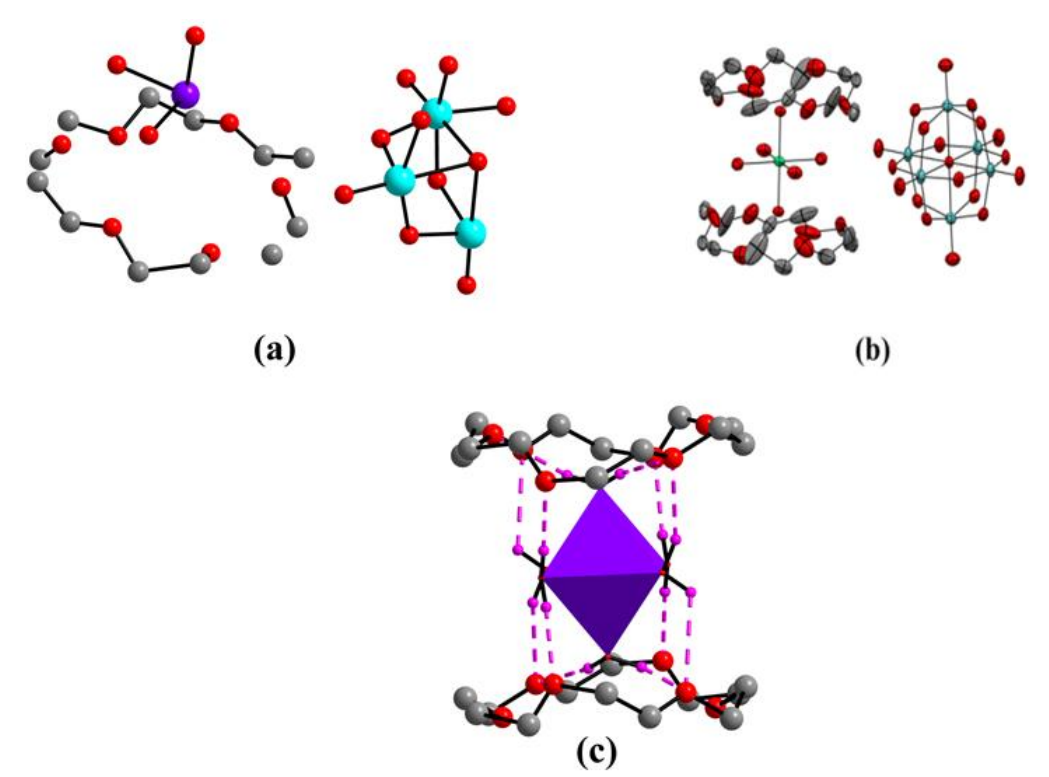


Figure 2.2. (a) Asymmetric unit in the crystal of $[Ni(H_2O)_6([18]-crown-6)_2][Mo_6O_{19}]$ (2); details are mentioned in the text. (b) Thermal ellipsoidal plot (50% probability) of overall molecular structure of compound 2. (c) Hexa-aqua Ni(II) complex, $\{Ni(H_2O)_6\}^{2+}$ sandwiched by two crown ethers; all four water molecules in the equatorial positions (basal plane) are hydrogen bonded to crown-ethers' oxygen atoms. Purple dotted lines represent hydrogen bonds. Hydrogen atoms are shown in purple colour. Hexa-aqua $\{Ni(H_2O)_6\}^{2+}$ coordination complex cation is shown as blue-purple octahedron in the crystal structure of compound 2.

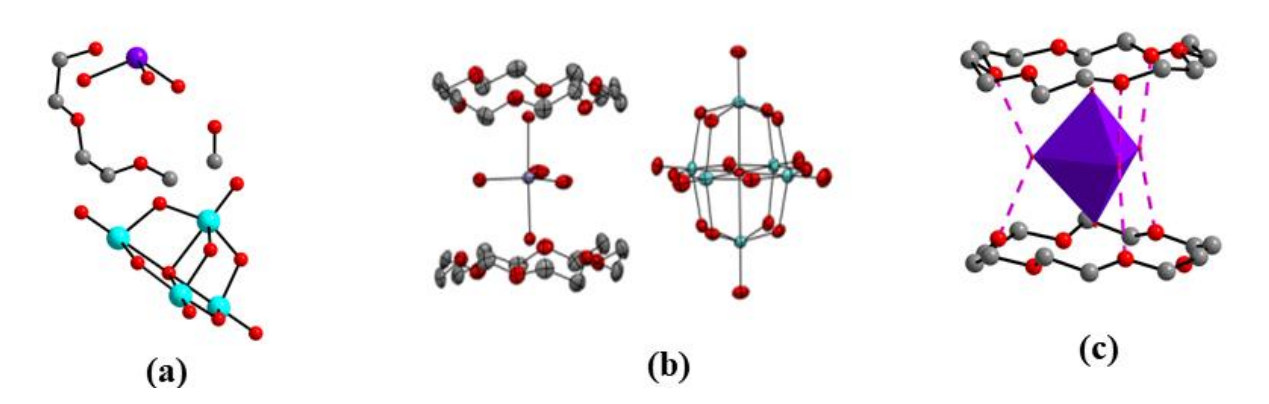


Figure 2.3. (a) Asymmetric unit in the crystal of $[Zn(H_2O)_5([18]\text{-crown-6})_2][Mo_6O_{19}]$ (3); details are mentioned in the text. (b) Thermal ellipsoidal plot (50 % probability) of overall molecular structure of compound 3. (c) Penta-aqua Zn(II) complex, $\{Zn(H_2O)_5\}^{2+}$ sandwiched by two crown ethers; all three water molecules in the equatorial positions (basal plane) are H-bonded to crown-ethers' oxygen atoms. Purple dotted lines represent hydrogen bonds. Penta-aqua $\{Zn(H_2O)_5\}^{2+}$ coordination complex cation is shown as blue-purple trigonal-bipyramid in the crystal structure of compound 3.

Compound $[Zn(H_2O)_5([18]-crown-6)_2][Mo_6O_{19}]$ (3) crystallizes in orthorhombic *Pmma* space group. The pertinent asymmetric unit (Figure 2.3a) in its crystal structure is basically one-fourth of the full molecule, i.e., $\{Mo_{1.5}O_{4.75}\}^{0.5-}$ (two molybdenum atoms with half occupancy and two molybdenum atoms with one-fourth occupancy; one oxygen atom

with full occupancy, six oxygen atoms with half occupancy and three oxygen atoms with one-fourth occupancy), $\{Zn_{0.25}(H_2O)_{1.25}\}^{0.5+}$ and half of the crown ether molecule. Thus one formula unit of compound 3 includes a penta-aqua {Zn(H₂O)₅}²⁺ coordination complex cation, a polyoxometalate cluster anion $\{Mo_6O_{19}\}^{2-}$ and two crown ether molecules as shown in Figure 2.3b (thermal ellipsoidal representation). The trigonal bipyramidal (tbp) ${\rm \{Zn(H_2O)_5\}^{2+}}$ is sandwiched by these two crown ethers as shown in Figure 2.3b and 2.3c. This is unusual fivefold water coordination around Zn²⁺ ion. This result strongly indicates that penta-aqua $\{Zn(H_2O)_5\}^{2+}$ species was definitely present in synthesis reaction mixture of compound 3, before its crystallization (nucleation) started. This also indicates the presence of {Zn(H₂O)₅}²⁺ species (along with commonly observed {Zn(H₂O)₆}²⁺ species in crystalline compounds) in the aqueous solution of a Zn(II) salt. Even though, the EXAFS analysis of a Zn(II) salt solution shows Zn(II)-aqua-coordination complex to be hexa-coordinated ${Zn(H_2O)_6}^{2+,11}$ Williams, Armentrout and their co-workers' results on IR action spectroscopy of an aqueous solution of ZnCl₂ and gas phase theoretical studies of hydrated Zn(II) complexes, providing evidences that Zn has a coordination number = 5, 16 are significant in the context of unambiguous crystallographic characterization of a tbp- ${\rm Zn(H_2O)_5}^{2+}$ complex cation in the crystal of a polyoxometalate matrix. Indeed, the present work of isolation of a penta-aqua complex $\{Zn(H_2O)_5\}^{2+}$ supports the efforts of Cooper et al.16 on primary hydration sphere of Zn(II) exhibiting fivefold coordination of water molecules.

2.2.2 A Comparative Discussion on the Crystal Structures of 1-3.

The Bond Valence Sum (BVS) calculations show that both the cobalt ions in compound 1, nickel ion in compound 2, and zinc ion in compound 3 are in their +2 oxidation states. Similarly, all Mo in the hexamolybdate anions in all the three compounds are in +6 oxidation state.

In all the three compounds 1-3, the isopolyanion, $[Mo_6O_{19}]^{2-}$ is present as the counter anion. It has six Mo(VI) atoms, each surrounded by six oxygen atoms, forming distorted octahedra, each corner or edge shared with another octahedra to form the clus-ter. Out of the six oxygen atoms, one is terminal oxygen atom (O_t), one central oxygen (O_c) and four bridging oxygen atoms (O_b). Mo–O bond lengths are: Mo–O_t, 1.673-1.688 Å; Mo–O_c, 2.300-2.333 Å and Mo–O_b, 1.920-1.943 Å. The Mo–O_b–Mo bond angles are in the range of 116.25-117.011° and Mo–O_c–Mo vary between 179.48-180.00°. These values of bond lengths and angles are in accordance to the reported $[Mo_6O_{19}]^{2-}$ anions.

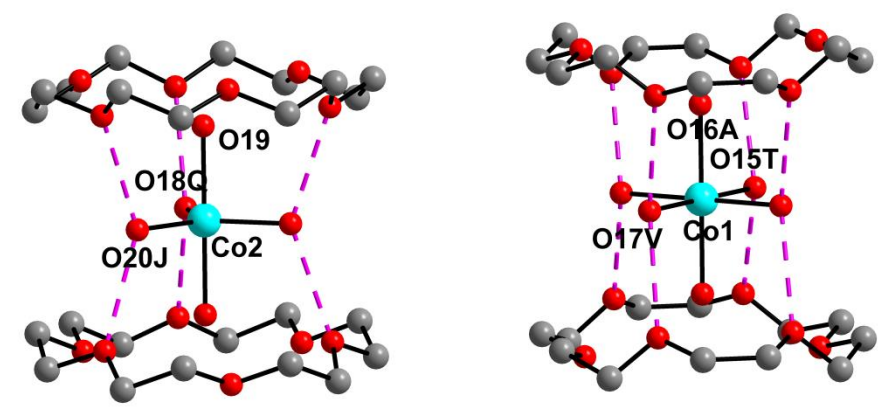


Figure 2.4. Tbp- $\{Co(H_2O)_5\}^{2+}$ and octahedral $\{Co(H_2O)_6\}^{2+}$ coordination complex cations, each sandwiched by two crown-ethers, in the crystal of $[\{Co(H_2O)_5([18]\text{-crown}6)_2\}\{Co(H_2O)_6([18]\text{-crown}-6)_2\}][Mo_6O_{19}]_2$ (1). Purple dashed lines represent the hydrogen bonds.

The difference in the three compounds is in the coordination number of the central metal atom, i.e., Co(II) in compound [{Co(H₂O)₅([18]-crown-6)₂}{Co(H₂O)₆ ([18]-crown-6)₂}][Mo₆O₁₉]₂ (1), Ni(II) in compound [Ni(H₂O)₆([18]-crown-6)₂][Mo₆O₁₉] (2) and Zn(II) in compound [Zn(H₂O)₅([18]-crown-6)₂][Mo₆O₁₉] (3). The aqua coordination number to Cu(II) in compound 4 ion has been earlier shown to be 5, ^{14,15} which is in contradiction to the generally accepted picture of hexa-aqua coordination to divalent transition metal ions. In compound 1, two Co(II) centers are present. Interestingly, the two Co(II) ions are in two different coordination environments. One of the Co(II) ions is coordinated to six water molecules, and the other one is coordinated to five water molecules (Figure 2.4, 2.5, 2.6). This 'simultaneous coexistence' of a penta- as well as a hexa-aqua Co(II) complex, is a new finding to the best of our knowledge. In contrast to the readily accepted picture of following a trend of hexa-aqua coordination always, we are successful in isolating the trigonal bipyramidal (tbp)-penta-aqua complex {Co(H₂O)₅}²⁺ co-existent with the hexa-aqua octahedral (O_h) complex {Co(H₂O)₆}²⁺ in the same formula unit. The two out-of-plane Co1-O16A (O_h) and Co2-O19 (tbp) bond lengths are 2.084 Å and 2.072 Å

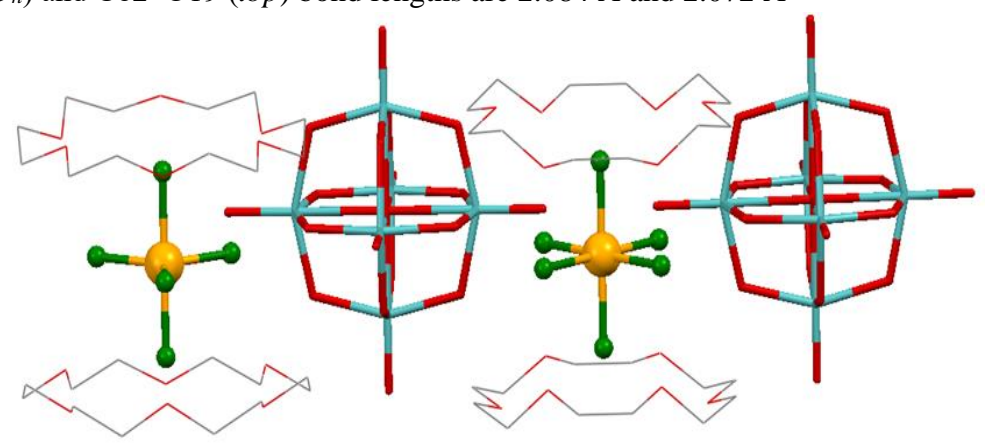


Figure 2.5. Ball and stick representation of Compound 1.

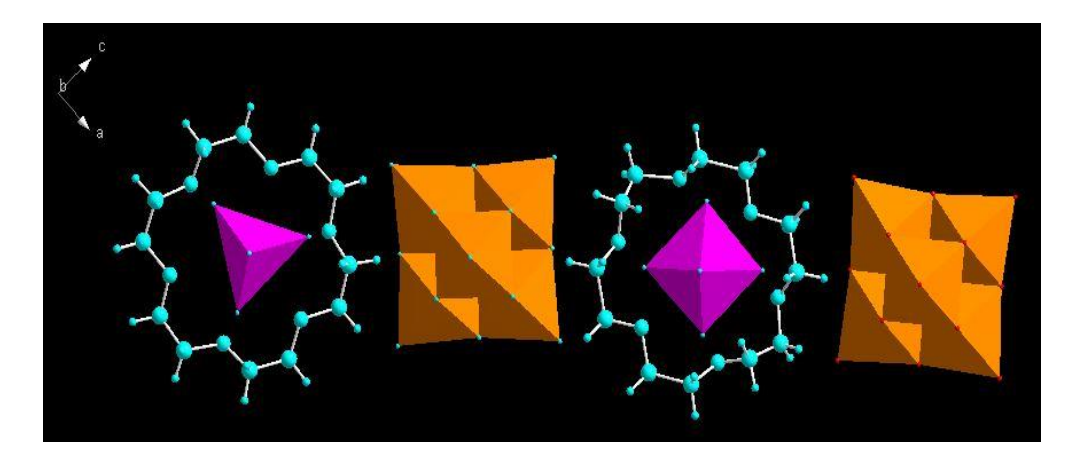


Figure 2.6. Polyhedral representation of compound 1.

respectively. The in-plane Co1–O (O15T, O17V, O15T, O17V) (O_h) and Co2–O (O18Q, O18Q, O20J) (tbp) distances are 2.065-2.066 Å and 1.987-1.994 Å respectively (Figure 2.4). The out-of-plane angles O16A–Co1–O17V (O_h) and O19–Co2–O20J (tbp) are 90.37° and 90.22°, respectively. Similarly, the in-plane O–Co1–O (O15T, O17V) (O_h) and O–Co2–O (O18Q, O20J) (tbp) angles are 89.42° and 121.10° (Figure 2.7).

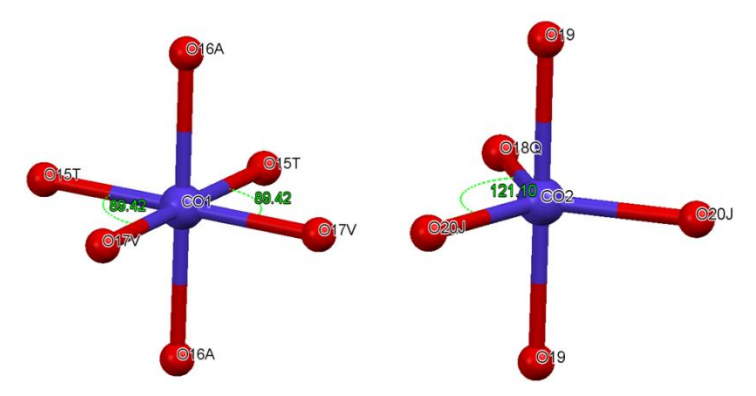


Figure 2.7 Bond angles between the basal oxygen atoms in the octahedral $\{Co(H_2O)_6\}^{2+}$ and the trigonal bipyramid $\{Co(H_2O)_5\}^{2+}$ in compound 1.

In the crystal structure of compound **2**, the Ni²⁺ cation is hexa-aqua coordination as expected (Figure 2.8; 2.9, 2.10). The out-of-plane Ni1–O17 bond length is 2.032 Å. The inplane Ni1–O18 and Ni1–O19 bond lengths respectively are 2.050 and 2.058 Å (Figure 2.8).



Figure 2.8. (a) Octahedral- $\{Ni(H_2O)_6\}^{2+}$ complex cation, sandwiched by two crown-ether moieties in the crystal of compound $[Ni(H_2O)_6([18]-crown-6)_2][Mo_6O_{19}]$ (2).

The out of plane O17–Ni1–O18 is at an angle of 89.46°. Similarly, the in-plane O18–Ni1–O19 angle is 89.56°, hence forming almost a perfect octahedron (Figures 2.2c and 2.8 and Figure 2.10b).

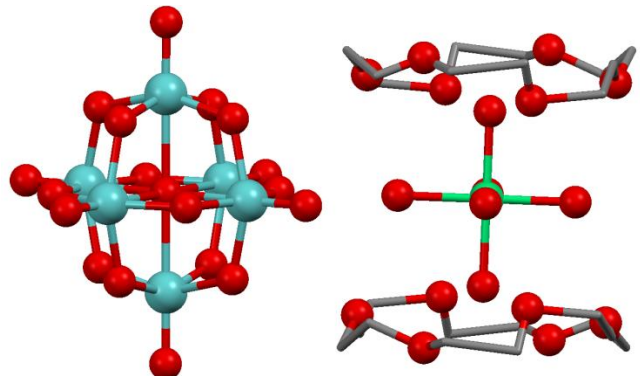


Figure 2.9. The supramolecular $Ni(H_2O)_6$ –18-crown-6 sandwich stabilized by the hexamolybdate anion.

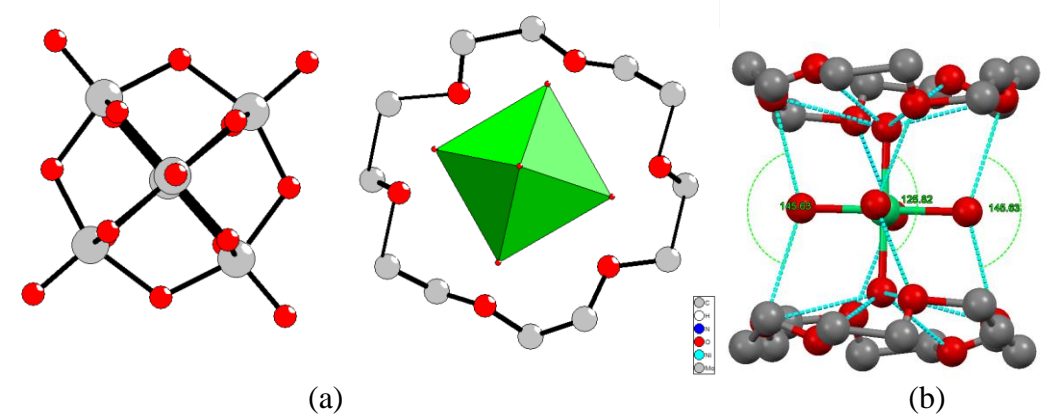


Figure 2.10 (a) Polyhedral representation of compound 2. (b) The supramolecular sandwich showing H-bonding interactions between the hydrogen atoms of the water molecules coordinated to the nickel(II) ion in compound 2 and the crown ether along with their bond angles.

In the crystal structure of compound 3, the Zn^{2+} cation is coordinated to five H_2O molecules (Figure 2.11, 2.12, 2.13), in a way very similar to that in the case of compound 4,



Figure 2.11. Tbp- $\{Zn(H_2O)_5\}^{2+}$ coordination complex cation, sandwiched between two crown ethers, in the crystal of in the crystal of compound $[Zn(H_2O)_5([18]-crown-6)_2][Mo_6O_{19}]$ (3). Purple dashed lines represent the hydrogen bonds.

reported earlier from our laboratory. As shown in Figure 2.11, the out-of-plane Zn1–O11 bond length is 2.033Å. The in-plane Zn1–O12 and Zn1–O13 bond distances are 2.028Å and 1.888Å, respectively. The out of plane O13–Zn1–O11 angle is 89.46°. Similarly, the in-plane O12–Zn1–O13 angle is 121.3°, hence forming a trigonal bipyramid as shown in Figure 2.11 and 2.13b).

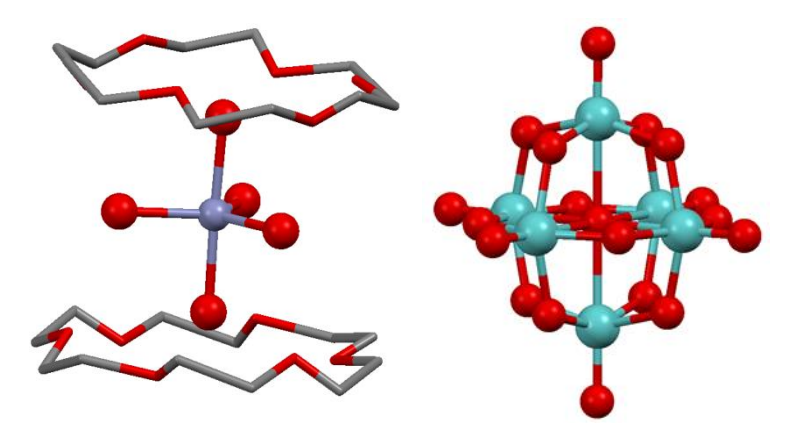


Figure 2.12. The $Zn(H_2O)_5$ moiety sandwiched between two crown ethers and the isopolyanion that stabilizes the sandwich.

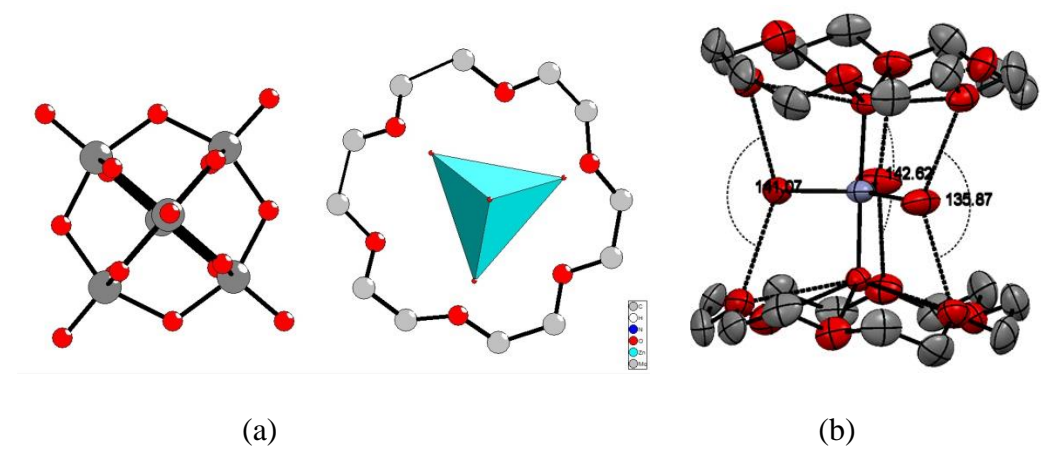


Figure 2.13 (a) Polyhedral representation of compound 3. (b) The supramolecular sandwich showing H-bonding interactions between the hydrogen atoms of the H_2O molecules coordinated to zinc(II) ion in compound 3 and the crown ether along with their bond angles.

Both the octahedral (O_h) and trigonal bipyramidal (tbp) Co-aqua complexes in compound **1**, the octahedral Ni-aqua complex in compound **2**, and the Zn-aqua tbp complex in compound **3** are immaculately sandwiched between two [18]-crown-6 molecules. The hydrogen atoms of the axial water molecules of the aqua complexes get H-bonded to the oxygen atoms in the crown ether molecules (Figures 2.4, 2.8 and 2.11). These hydrogen bonding interactions make the sandwiches stable. In the case of Co- and Zn- penta-aqua complexes, the aqua complex is expected to exhibit the 'Berry pseudo-rotation', i.e., the conversion from trigonal bipyramidal to square pyramidal geometry and vice versa, because of the negligible energy difference between these two conformations. But, the strong H-bonds between crown ether molecules and the tbp-{M(H₂O)₅}²⁺ (as shown in Figures 2.4 left and 2.11), restricts the conversion rand the complexes exhibit only tbp conformation. This observation can be reasoned by realizing the fact that the tbp conformation of {M(H₂O)₅}²⁺

can form maximum number of hydrogen bonds with the crown ethers compared to its square pyramidal conformation — thus lowering the overall energy of the *tbp*-conformation of $\{M(H_2O)_5\}^{2+}$ in the pertinent crystals. This energy consideration in the crystalline lattice has some relevance to the formation of metal-aqua complexes $\{M(H_2O)_n\}^{2+}$ at lower side of the temperature during the first-principles molecular dynamics simulation studies (vide infra) of 3d metal-aqua complexes.

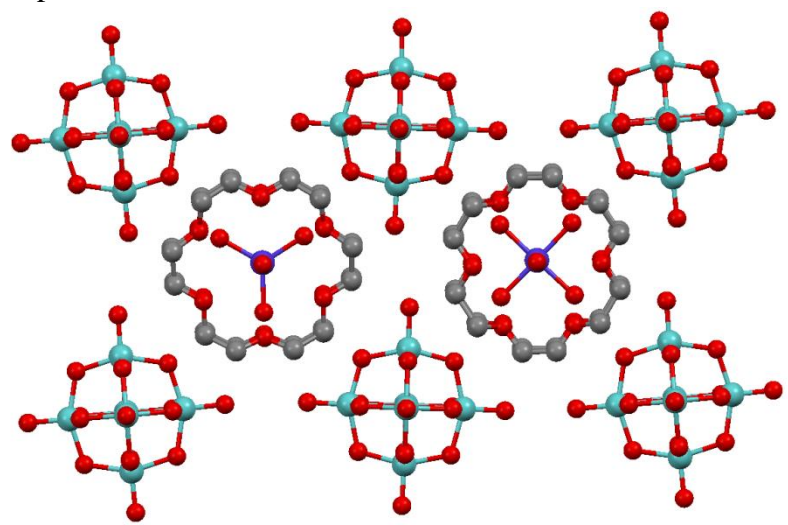


Figure 2.14. Packing in compound 1 exhibiting the penta-coordinated Co-aqua sandwich and the hexa-coordinated Co-aqua sandwich surrounded by four isoployanions each.

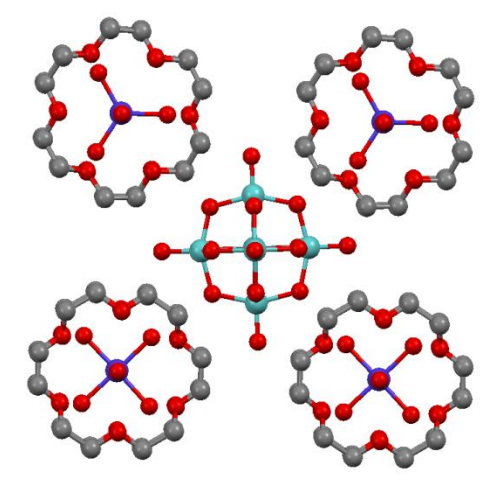


Figure 2.15. A hexamolybdate ion surrounded by four sandwich entities.

The isopolyanion, $[Mo_6O_{19}]^{2-}$, is present in the title compounds not only as a counter anion, but it also plays a role in stabilizing the supramolecular sandwiches. In the crystals, each sandwich is associated with four surrounding isopolyanions, through C–H···O hydrogen bonding interactions. Similarly, each isopolyanion is also surrounded by four sandwiches (Figures 2.14, 2.15, 2.16 and 2.17). The arrangement of the sandwiches and the isopolyanions is exactly the same as was seen for Cu(II) ion in compound $[Cu(H_2O)_5([18]-crown-6)_2]$ $[Mo_6O_{19}]$ (4).¹² The polyoxometalate anion and the sandwiches are connected to each other through H–bonds. The H atoms of the crown ether from one side bifurcate to connect with

two different bridging oxygen atoms of one of the POM anions. This same polyoxometalate is also connected from the other side with another sandwich, through three bridging oxygen atoms of the polyoxometalate. Thus, H-bonds play a very vital role in stabilizing the compounds.

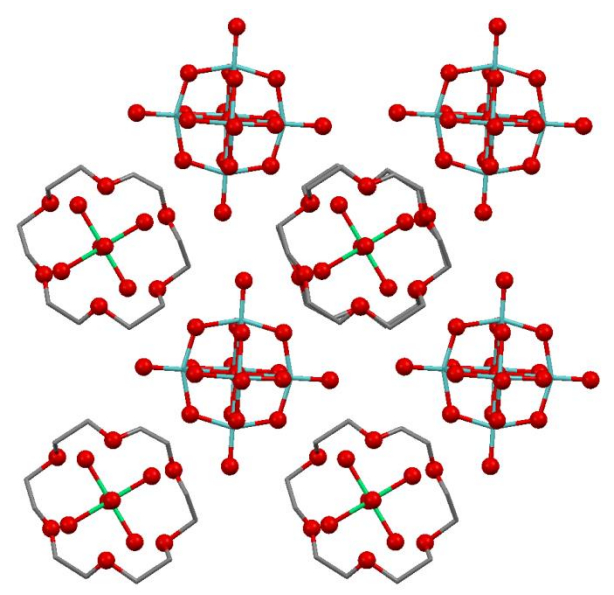


Figure 2.16. The packing in compound **2** showing that each sandwich is surrounded by four hexamolybdate anions and also each hexamolybdate anion is surrounded by four metal-aqua sandwich entities.

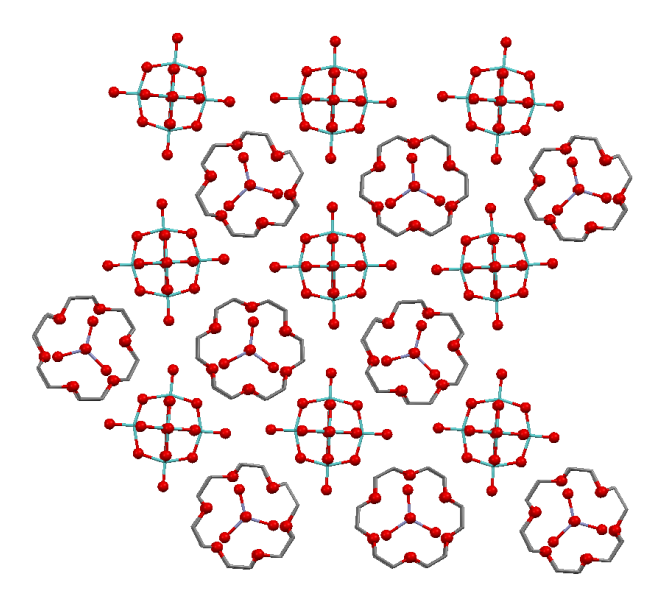


Figure 2.17. The Packing in compound 3 showing that the sandwich is surrounded by four isopolyanions and the isopolyanion is in-turn surrounded by four sandwiches.

2.2.4 Spectral Characterization.

The Fourier Transform Infrared (FTIR) spectra of all the four compounds **1-4** have been recorded and are plotted in Figure 2.18 along with the FTIR spectra of [Bu₄N]₂[Mo₆O₁₉] and 18-crown-6. Almost all the IR peaks of the 18-crown-6 are found in the FTIR spectra of compounds **1-4**, signifying presence of the crown-ether molecule. Similarly, the signature

peaks of the $[Mo_6O_{19}]^{2-}$ anion, i.e., the peaks at 800 and 950 cm⁻¹ are also retained in the spectra of the compounds, revealing the presence of $[Mo_6O_{19}]^{2-}$ anion. The other peaks at around 1475, 2875 and 2957 cm⁻¹, found in the infra-red spectrum of $[Bu_4N]_2[Mo_6O_{19}]$, are absent in the compounds because they correspond to the peaks of the $[Bu_4N]^+$ unit. The broad peak observed nearly at 3400 cm⁻¹ and the peak at 1625 cm⁻¹ in compounds **1-4** confirm that water molecules are present in all the four compounds. The peak at 800 cm⁻¹ (broad feature) for compounds **1-4** can be attributed to the TM–OH₂ bonds¹⁹ along with the characteristic peak of $[Mo_6O_{19}]^{2-}$ cluster anion.

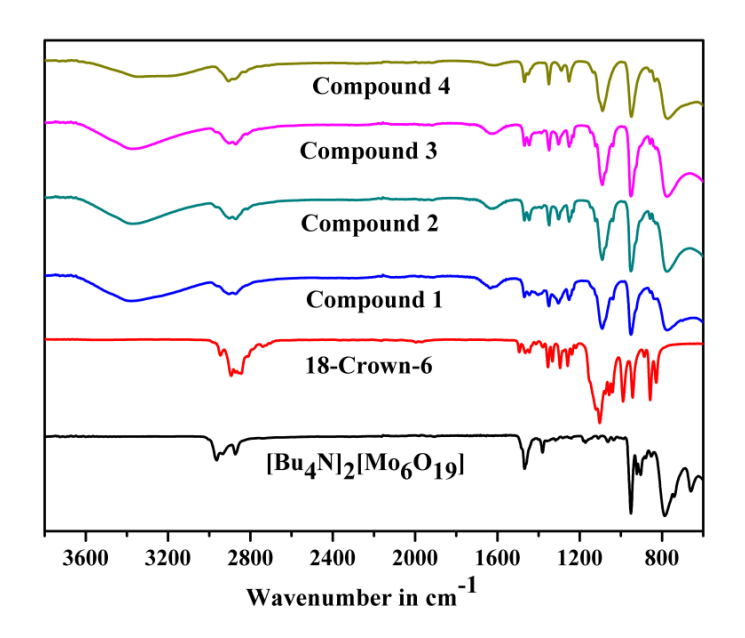


Figure 2.18. FT-IR spectra of compounds 1-4, $[Bu_4N]_2[Mo_6O_{19}]$ and 18-crown-6.

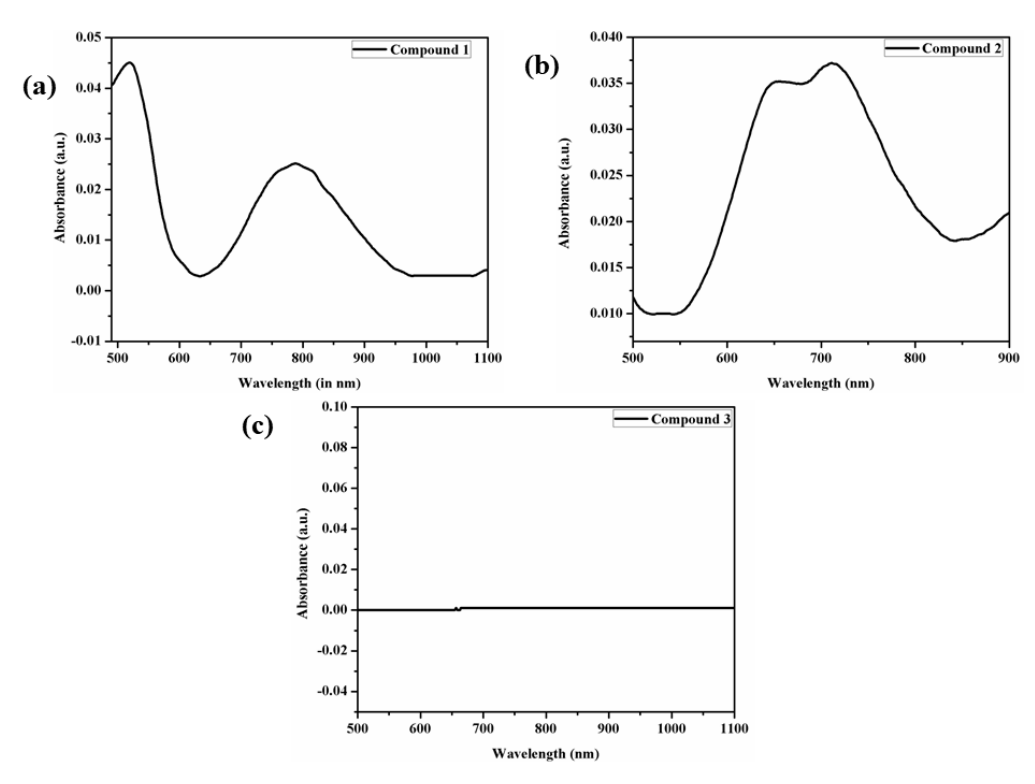


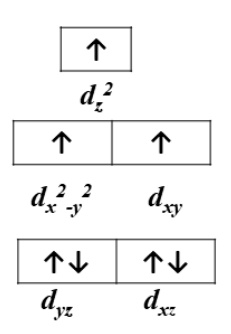
Figure 2.19. UV-visible spectra of compounds 1-3.

Co(II): d⁷ system

Octahedral system

1	1	
d_z^2	d_{x-y}^{2}	
		_
↑↓	↑↓	ተ

Trigonal bipyramidal system



Ni(II): d8 octahedral system

$$\begin{array}{c|cccc} \uparrow & \uparrow \\ \hline d_z^2 & d_{x-y}^{2-2} \\ \hline \uparrow \downarrow & \uparrow \downarrow & \uparrow \downarrow \\ \hline d_{xy} & d_{yz} & d_{xz} \\ \hline \end{array}$$

Cu(II): d⁹ tbp system

Zn(II): d¹⁰ tbp system



Figure 2.20. Crystal field splitting diagrams of Co(II), Ni(II), Cu(II) and Zn(II) in compounds 1, 2, 4 and 3 respectively.

The electronic absorption spectra of compound 1-3 are shown in Figure 2.19. Water being a weak field ligand leads to high spin complexes. The crystal field splitting diagrams of all the complexes are shown in Figure 2.20. As can be seen from this figure, two transitions are possible for compound 1. In an octahedral complex, a transition from t_{2g} to e_g orbital, and in trigonal biyramidal (tbp) complex, a transition from d_{yz} or d_{xz} to d_{x2-y2} or d_{xy} orbital is possible. The broad feature at around 760 - 820 nm (Figure 2.19a) may be attributed to these d-d transitions from O_h and as well as tbp Co(II)-aqua- complexes. The intense band around 500 nm (Figure 2.19a) may be due to ligand to metal (water to Co^{2+}) charge transfer transition. Similarly, in compound 2, since nickel is hexa-coordinated, hence leading to an octahedral geometry; thus a transition is possible from completely filled t_{2g} orbitals to partially filled e_g orbital. The splitting observed in the band can be attributed to the spin-orbit coupling, due to which ${}^3T_{1g}(F)$ state mixes with the 1E_g state, since at the Δ_0 value for Ni(II) and six water ligands, their energy difference is very low; hence making two transitions of almost equal energy possible, 20 as experimentally observed in Figure 2.19b. In case of

compound 3, as zinc is in d^{10} configuration, hence leaving no space for any transition, so there are no transitions observed in its electronic spectrum in the visible region, hence proving that no transitions take place upon UV rays irradiation.

2.2.5 Thermogravimetric Analysis (TGA) and PXRD Analysis

Thermal stability of compounds **1-3** was assessed using TGA. The respective TG plots are given is Figure 2.21. The thermal behaviour of compound **4** is already reported earlier. As expected, all the three compounds first undergo the loss of water molecules, attached to the central metal atom, followed by the decomposition of the 18-crown-6 moieties. Thereafter, the polyoxometalate cluster anion decomposes leading to metal oxides.

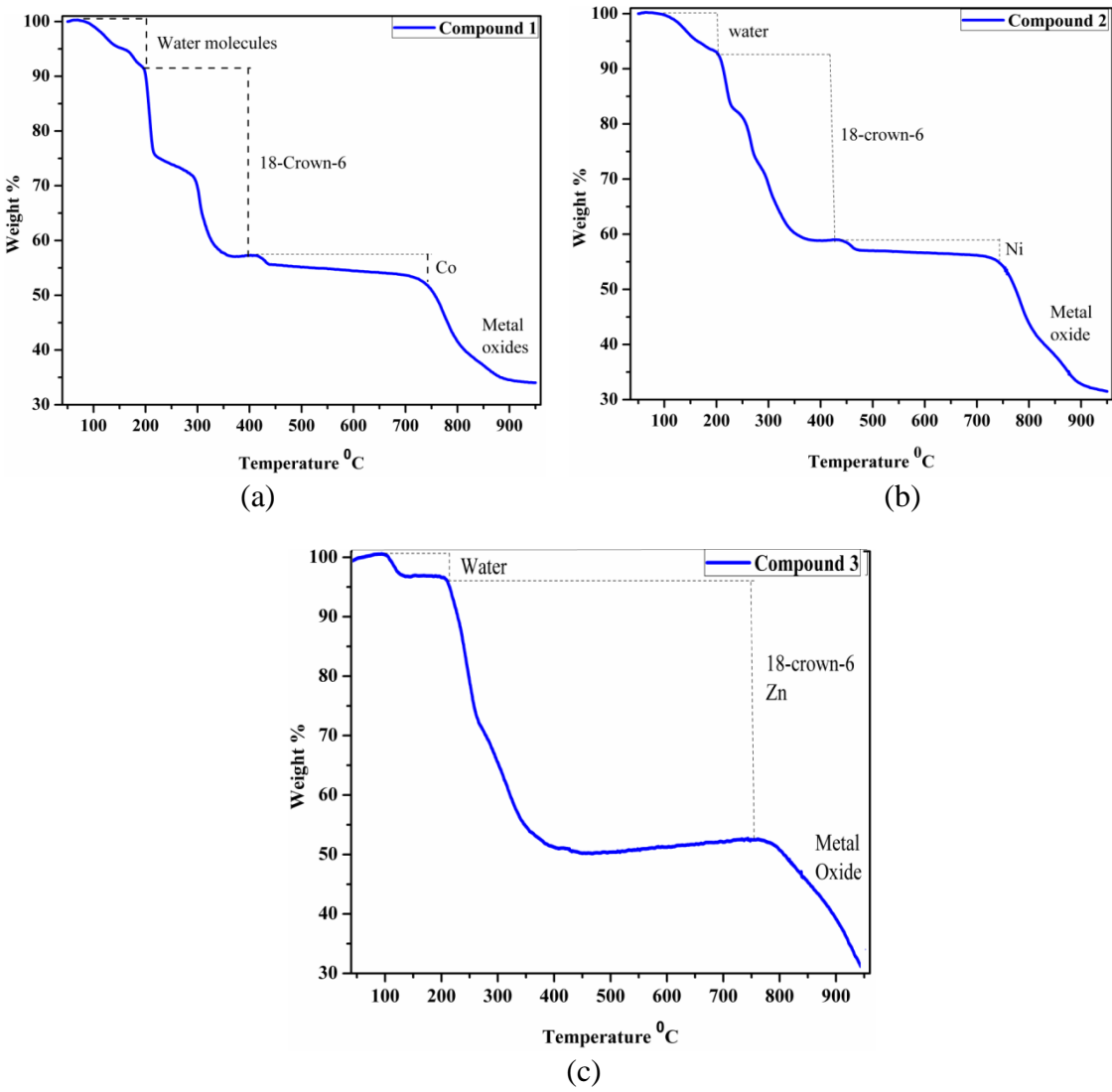


Figure 2.21. Thermogravimetric Analysis plots of compounds 1-3.

The powder X-ray diffraction (PXRD) patterns, obtained from the CIF files of the SCXRD data of compounds **1-3** (calculated PXRD patterns), match nicely with those (observed PXRD patterns), obtained from the bulk samples as shown in Figure 2.22. This approves the bulk homogeneity of the samples.

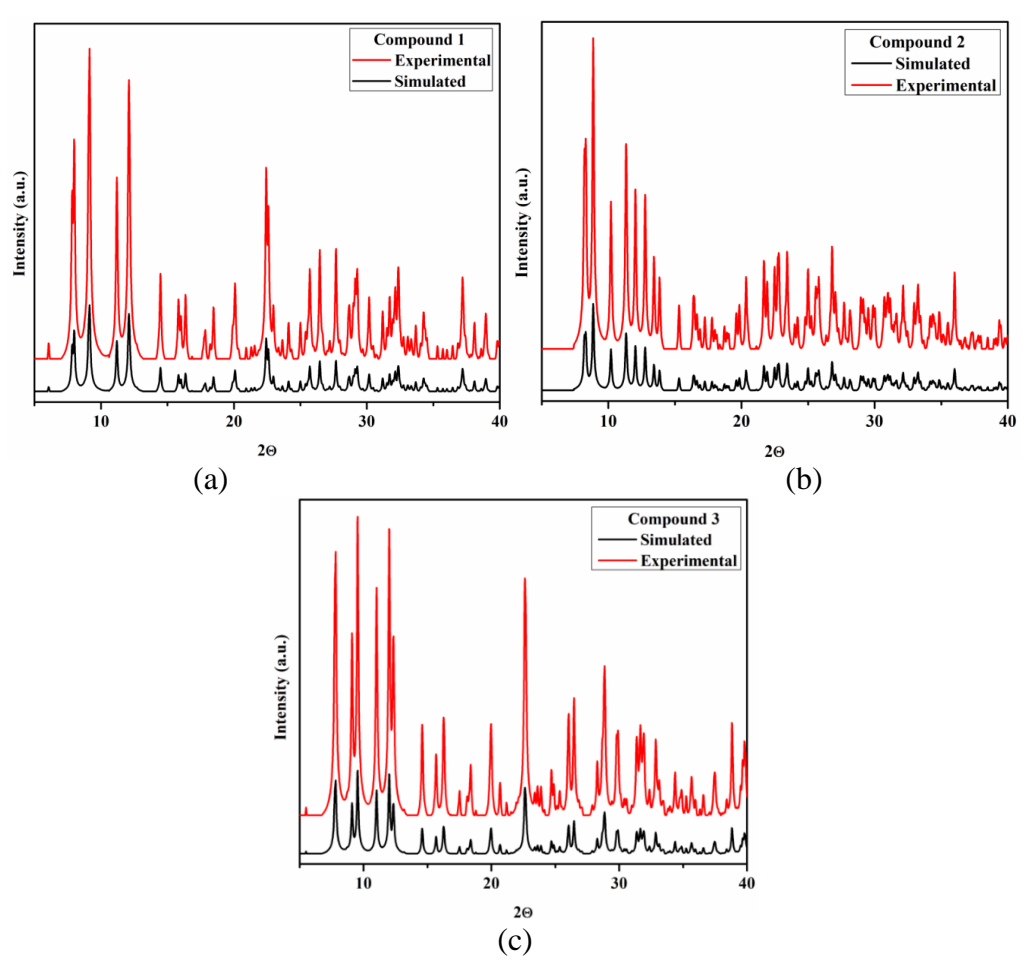


Figure 2.22. Simulated and Experimental Powder X-ray Diffraction plots of compounds 1-3.

2.2.6 Electrochemistry

We have performed electrochemical studies on compounds [{Co(H₂O)₅([18] $crown6)_2$ { $Co(H_2O)_6([18]-crown-6)_2$ }[$Mo_6O_{19}]_2$ (1), $[Ni(H_2O)_6([18]-crown-6)_2][Mo_6O_{19}]$ (2) and $[Zn(H_2O)_5([18]-crown-6)_2][Mo_6O_{19}]$ (3) to investigate the red-ox response of the metal-aqua species $\{Co(H_2O)_6\}^{2+}$: $\{Co(H_2O)_5\}^{2+}$, $\{Ni(H_2O)_6\}^{2+}$ and $\{Zn(H_2O)_5\}^{2+}$ in compounds 1, 2 and 3 respectively. Compounds 1-3 are insoluble in water and thus electrochemistry was carried in a heterogeneous manner. Compound 1 having both octahedral $Co(H_2O)_6$ ²⁺ and trigonal bipyramidal $\{Co(H_2O)_5\}^{2+}$ complexes shows four redox responses corresponding to four probable couples as shown in Figure 2.23. After examining the cyclic voltammogram (CV) plots of 18-crown-6, [Bu₄N]₂[Mo₆O₁₉], Co(NO₃)₂·6H₂O and compound 1 (Figure 2.23b), it can be argued that the redox couples, A-H, B-G, C-F and D-E (marked in Figure 2.23a) have originated from O_h -{Co^{II}(H₂O)₆}²⁺ and tbp-{CoII(H₂O)₅}²⁺ species only. Among these two species, the tbp-{Co^{II}(H₂O)₅}²⁺ complex cation should be oxidized more easily than O_h -{Co^{II}(H₂O)₆}²⁺; thus A-H response (Figure 2.23a) should correspond to tbp- $\{\text{Co}^{\text{III}}(\text{H}_2\text{O})_5\}^{3+}/\text{tbp-}\{\text{Co}^{\text{II}}(\text{H}_2\text{O})_5\}^{2+}\text{ couple and B- G redox response corresponds to }O_{h^{-1}}$ $\{\text{Co}^{\text{III}}(\text{H}_2\text{O})_6\}^{3+}/ O_h - \{\text{Co}^{\text{II}}(\text{H}_2\text{O})_6\}^{2+} \text{ couple}$ (Figure 2.23). Subsequent C-F and D-E responses (Figure 2.23a) can be assigned to $tbp-\{Co^{IV}(H_2O)_5\}^{4+}/tbp-\{Co^{III}(H_2O)_5\}^{3+}$ and O_{h-1}

 ${Co^{IV}(H_2O)_6}^{4+}/O_h-{Co^{III}(H_2O)_6}^{3+}$ couples, respectively. Logically, the species ${Co^{IV}(H_2O)_6}^{4+}$ is highly acidic and it can deprotonate to form ${O=Co^{IV}(H_2O)_5}^{2+}$ species. But in the present study, each aqua species is sandwiched by two crown-ethers that are strongly hydrogen bonded to the metal-aqua species. So, the oxo-species formation by deprotonation can be discarded. The oxidative responses of crown-ether and the isopolyanion $[Mo_6O_{19}]^{2-}$ at around +0.1~V~(vs.~NHE), as shown in Figure 2.23b, fortunately do not mix up with the redox responses of Co-aqua species.

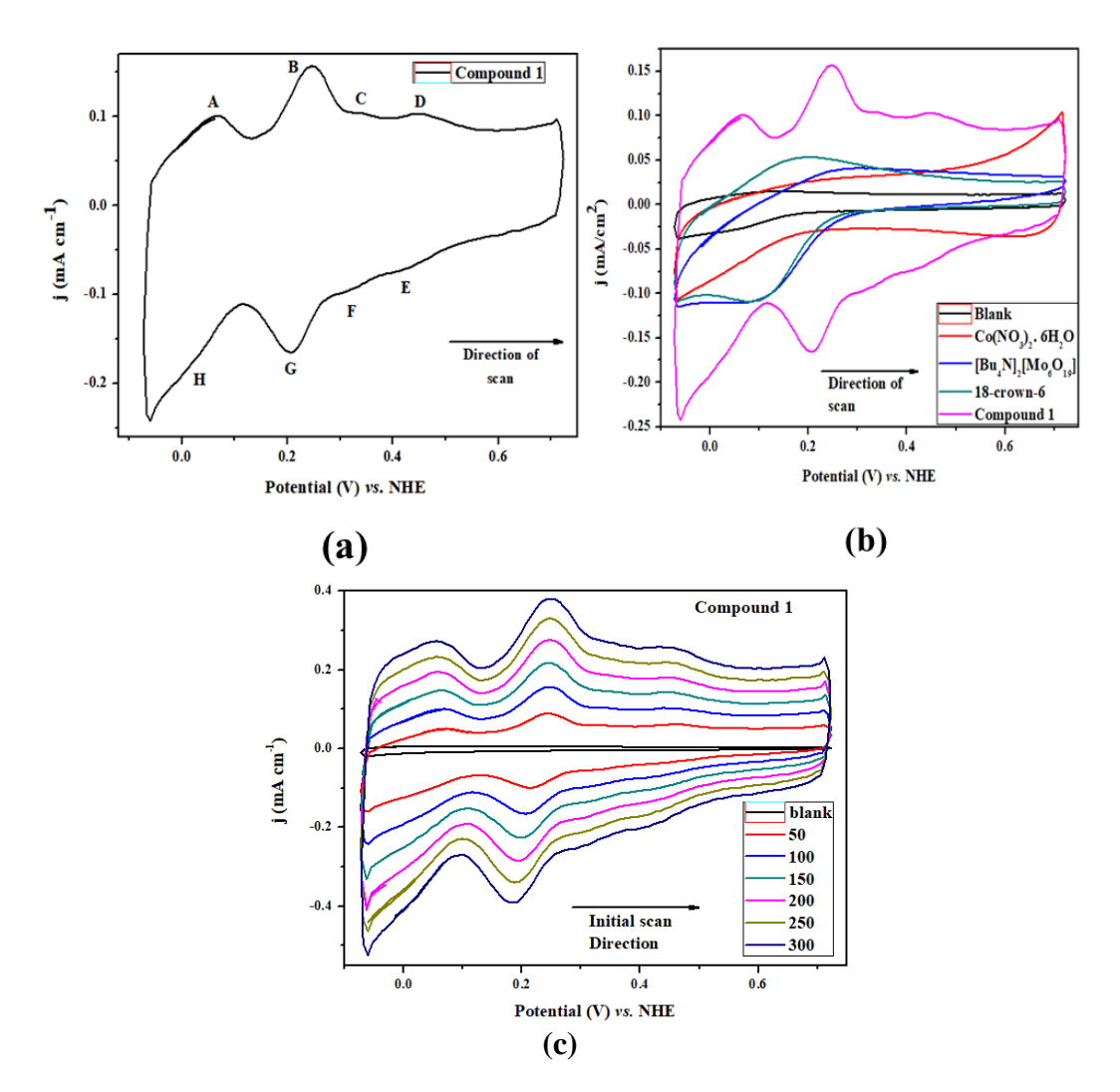


Figure 2.23. Cyclic voltammograms: (a) compound $[\{Co(H_2O)_5([18]\text{-crown6})_2\}\{Co(H_2O)_6([18]\text{-crown-6})_2\}][Mo_6O_{19}]_2$ (1); (b) compound 1 along with 18-crown-6, $[Bu_4N]_2[Mo_6O_{19}]$ and $Co(NO_3)_2\cdot 6H_2O$. (c) Scan rate variation studies of cyclic voltammograms of compound 1. The experiments were done in heterogeneous manner using glassy carbon electrode as the working electrode and Ag/AgCl as the reference electrode at room temperature. Pt flag was used as the counter electrode. The experiments were done in aqueous 0.1M KCl in neutral medium. Scan rate = 100 mV/sec.

The metal-aqua species of compounds **2** and **3** were also done and are not much redox active. The features are given in Figures 2.24 and 2.25 respectively.

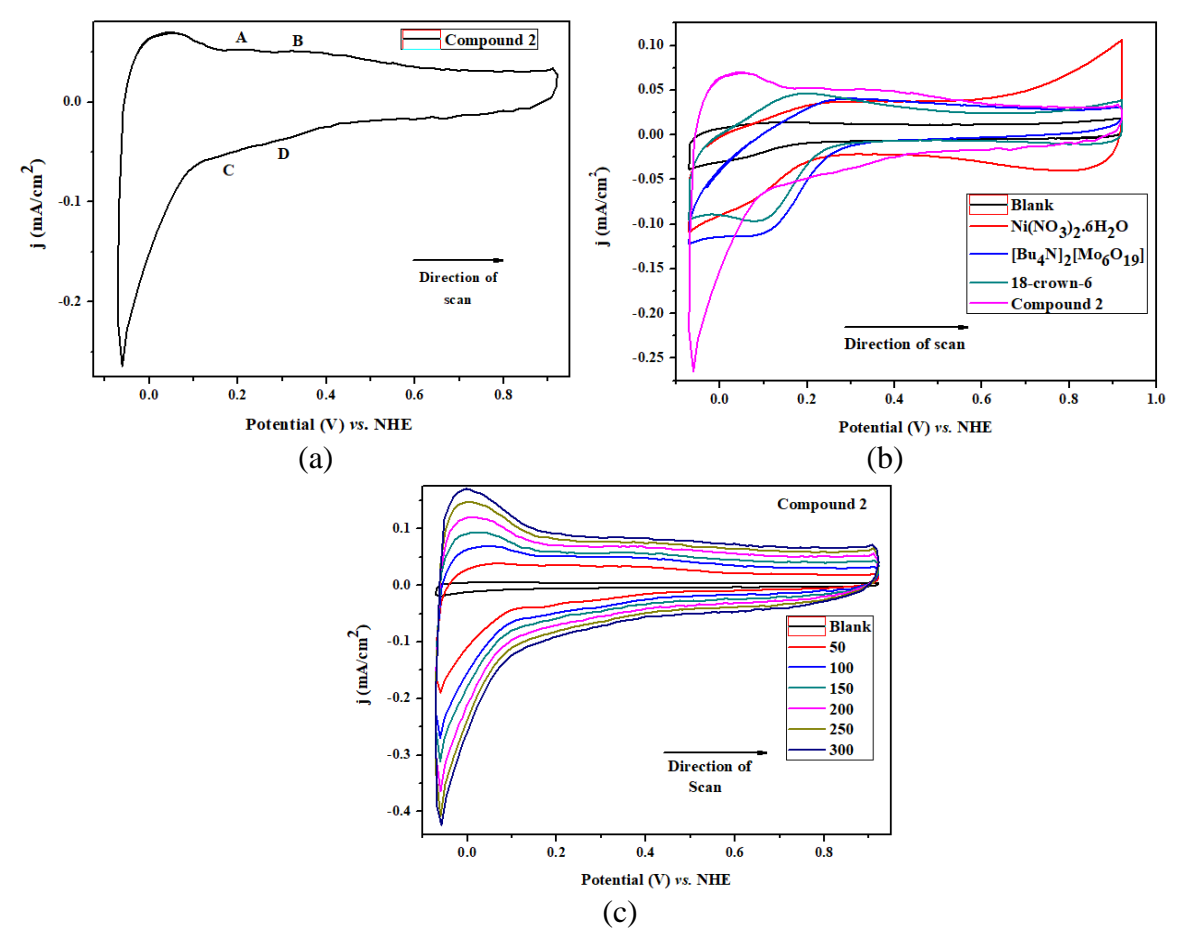


Figure 2.24. Cyclic voltammograms: (a) compound $[\{Ni(H_2O)_6 ([18]\text{-crown-}6)_2\}][Mo_6O_{19}]$ (2); (b) compound 2 along with 18-crown-6, $[Bu_4N]_2[Mo_6O_{19}]$ and $Ni(NO_3)_2\cdot 6H_2O$. (c) Scan rate variation studies of cyclic voltammograms of compound 2. The experiments were done in heterogeneous manner using glassy carbon electrode as the working electrode and Ag/AgCl as the reference electrode at room temperature. Pt flag was used as the counter electrode. The experiments were done in aqueous 0.1M KCl in neutral medium. Scan rate = 100 mV/sec.

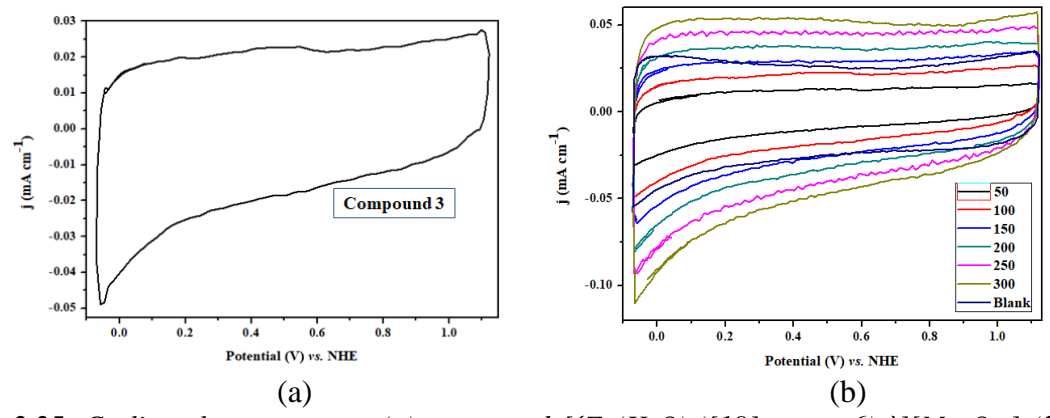


Figure 2.25. Cyclic voltammograms: (a) compound $[\{Zn(H_2O)_5([18]\text{-crown-}6)_2\}][Mo_6O_{19}]$ (3); (b) Scan rate variation studies of cyclic voltammograms of compound 3. The experiments were done in heterogeneous manner using glassy carbon electrode as the working electrode and Ag/AgCl as the reference electrode at room temperature. Pt flag was used as the counter electrode. The experiments were done in aqueous 0.1M KCl in neutral medium. Scan rate = 100 mV/sec.

Compound 2 having octahedral $\{Ni(H_2O)_6\}^{2+}$ complex shows two redox responses corresponding to two probable couples. The couples A-C and B-D correspond to $\{Ni^{III}(H_2O)_6\}^{3+}/\{Ni^{III}(H_2O)_6\}^{2+}$ and $\{Ni^{IV}(H_2O)_6\}^{4+}/\{Ni^{III}(H_2O)_6\}^{3+}$ couples, respectively.

2.3 Conclusion

The coordination number of a 3d M(II) ion in water is still a subject of fundamental research. Even though both five- and six-fold coordinated Cu(II) ions appear in crystalline compounds, it has been established by both neutron diffraction and first-principles molecular dynamics that Cu(II) aqua ion prefers a fivefold coordination in its aqueous solution. We have corroborated this fivefold coordination of Cu²⁺ ion, further, by demonstrating a particular inorganic synthesis to achieve the fivefold coordination of Cu²⁺ aqua complex cation in a polyoxometalate (POM) matrix as single crystals. Albeit the fivefold and six-fold water coordination around a Cu(II) ion is competitive (as far as the occurrence of both hexaand penta-aqua Cu(II) complex cations in crystalline compounds are concerned), our synthesis is unique in the sense that the resulting compound accommodate only the desired fivefold coordination, $\{Cu(H_2O)_5\}^{2+}$, found in aqueous solution of Cu^{2+} . We thus applied this synthetic route, in the present work, to synthesize other 3d transition metal ($M = Co^{2+}$, Ni^{2+} and Zn²⁺) aqua coordination complex cations (with the same POM anion) as single crystals. isolated and structurally characterized compounds $[{Co(H_2O)_5([18]-crown 6)_2$ {Co(H₂O)₆([18]-crown-6)₂}][Mo₆O₁₉]₂ (1), [Ni(H₂O)₆([18]-crown-6)₂][Mo₆O₁₉] (2) and $[Zn(H_2O)_5([18]-crown-6)_2][Mo_6O_{19}]$ (3). Compound 1 includes $tbp-\{Co(H_2O)_5\}^{2+}$ and O_{h-1} $\{Co(H_2O)_6\}^{2+}$ together in 1:1 ratio, whereas compounds 2 and 3 contain O_h - $\{Ni(H_2O)_6\}^{2+}$ and tbp-{Zn(H₂O)₅}²⁺, respectively. The coordination numbers of Co²⁺, Ni²⁺ and Zn²⁺ in their aqueous solutions are determined using EXAFS analysis and reported to be 6.0. This not only contradicts to our crystallographic results of cobalt(II)- and zinc(II)-aqua complexes (present work) but also disagree with the results of Williams and Armentrout for Zn(II), who performed IR action spectroscopy of Zn(II) aqueous solution and gas phase theoretical studies of hydrated Zn(II) complex and concluded that Zn(II) has a primary hydration sphere of five. The discrepancies between the EXAFS analysis results with experimentally observed findings for Co(II)- and Zn(II)-aqua complexes come partly from the fact that EXAFS analysis requires fitting data with priori assumptions about the target structure, for example, fivefold-, sixfold-aqua coordination, etc. The isolation of penta-aqua- $\{Co(H_2O)_5\}^{2+}$ species in the crystal of compound 1, even at room temperature, is favoured by the formation of a perfect supramolecular sandwich through strong hydrogen bonding interactions between equatorial water molecules of the tbp-{Co(H₂O)₅}²⁺ species and oxygen atoms of two crownether molecules. Thus, the stabilization of $tbp-\{Co(H_2O)_5\}^{2+}$ species by strong hydrogen bonding interactions in the crystal of compound 1 is equivalent to the formation of pentaaqua-{Co(H₂O)₅}²⁺ species from Co²⁺ ion and water molecules at a lower temperature. A trigonal bipyramidal (tbp) conformation over square pyramidal conformation for penta-aqua- ${\rm Co(H_2O)_5}^{2+}$ species is favoured in the crystal of compound 1 because the *tbp* conformation can exert more number of hydrogen bonds (i.e., more stabilization) than a square pyramidal conformation of $\{Co(H_2O)_5\}^{2+}$ does. Being a d⁷ system Co(II) can exhibit high spin (S = 3/2) as well as low spin (S = $\frac{1}{2}$) states, depending on the conditions around the ion. As such Co²⁺ ion, in O_h -{Co(H₂O)₆}²⁺ prefers to show high spin state with three unpaired electrons. If a particular condition applies and it goes to low spin state ($S = \frac{1}{2}$), it would show Jahn-Teller distortion and it may result in penta-aqua-tbp-{Co(H₂O)₅}²⁺ (relatively more stable than O_h - ${\rm Co(H_2O)_6}^{2+}$ due to tetragonal elongation (Z_{out}). In the case of Ni(II) system, the observations (crystal structure of compound 2) are in accordance with an O_h -{Ni(H₂O)₆}²⁺ structural arrangement. But in the case of Zn(II) system, the story is a quite different. Unlike Co²⁺, Ni²⁺ and Cu²⁺, Zn²⁺ which has a filled d shell and the electronic configuration, [Ar]3d¹⁰4s⁰, cannot apply a strong effect on the coordination number. Zn(II) generally shows a coordination number of 4, 5 or 6 in different inorganic phases. As far as Zn(II)-aqua complexes are concerned, the works (experimental as well as theoretical) of Cooper et al. are worth mentioning. They showed that infrared photodissociation (IRPD) spectrum of [Zn^{II}(H₂O)₅]²⁺ and calculated (gas phase) five coordinated MP2(full) ground-state (GS) species are largely consistent, pointing towards a fivefold coordinated $\{Zn(H_2O)_5\}^{2+}$. In the same line, there are some reports of crystal structures of inorganic compounds that have described the structure of tbp-{Zn(H₂O)₅}²⁺. However, in a recent report,²¹ Ducher et al. used a nonlocal functional which includes van der Waals (vdw-DF2) contributions and demonstrated the relative energetic stability of the Zn^{II}-aqua complexes, giving an idea in which Zn seems mostly as a hexa-aqua complex, $\{Zn^{II}(H_2O)_6\}^{2+}$. Therefore, in the present work, our crystallographic observation of a $tbp-\{Zn(H_2O)_5\}^{2+}$, sandwiched between two crown ether molecules in a polyoxometalate matrix (relevant single crystals are synthesized at room temperature) is on par with low temperature (150 K) simulation studies of ${Zn^{II}(H_2O)_n}^{2+}$ (n= 4-15).

In a nut shell, we have demonstrated a new insight of Co(II) chemistry in an aqueous solution in the sense that we have shown the co-existence of hexa-aqua- $\{Co^{II}(H_2O)_6\}^{2+}$ and penta-aqua- $\{Co^{II}(H_2O)_5\}^{2+}$ complex cations in solid state in contrast to the generally accepted picture of the existence of only hexa-aqua- $\{Co^{II}(H_2O)_6\}^{2+}$ species in Co(II)-aqueous solution. We have also shown that a penta-aqua- $\{Zn^{II}(H_2O)_5\}^{2+}$ can subsist in an aqueous Zn(II) solution, which can be trapped as $tbp-\{Zn^{II}(H_2O)_5\}^{2+}$ in between two crown ethers (formation of a perfect supramolecular sandwich) in a polyoxometalate matrix in the solid state. We have used single crystal X-ray crystallography as an experimental tool (besides routine spectral characterizations).

2.4 Experimental Section

2.4.1 Synthesis

Synthesis of [Co(H₂O)₅([18]-crown-6)₂Co(H₂O)₆([18]-crown-6)₂[[Mo₆O₁₉]₂(1)

0.06g (0.227 mmol) of 18-crown-6 was dissolved in 50 ml. acetonitrile followed by 10ml. glacial acetic acid. To the mixture 0.03g (0.022 mmol) [Bu₄N]₂[Mo₆O₁₉] was added. 0.145g (0.51 mmol) of Co(NO₃)₂·6H₂O was added to the above clear light yellow solution. The pink solution hence formed was stirred for 18 hours at ambient conditions. Then this solution was filtered and left undisturbed at room temperature for crystallization. Orange crystals of 1, suitable for X-ray diffraction studies, were obtained after 4-5 days. The crystals were

collected by filtration and washed with cold water. FT-IR (cm⁻¹) 3380, 2904, 2871, 1636, 1468, 1444, 1401, 1350, 1303, 1251, 1090, 951, 775.

Synthesis of $[Ni(H_2O)_6(18-crown-6)_2][Mo_6O_{19}]$ (2)

The synthesis of 2 was done in a similar manner as for 1, but Ni(NO₃)₂·6H₂O was used instead of Co(NO₃)₂·6H₂O. Green colour crystals were formed in this case. FT-IR (cm⁻¹) 3374, 2906, 2871, 1629, 1468, 1445, 1348, 1302, 1251, 1089, 951, 857, 775.

Synthesis of $[Zn(H_2O)_5(18-crown-6)_2][Mo_6O_{19}]$ (3)

The synthesis of 3 was done in a similar manner as for 1, but Zn(NO₃)₂·6H₂O was used instead of Co(NO₃)₂·6H₂O. Yellow colour crystals were formed in this case. FT-IR (cm⁻¹) 3344, 2906, 2871, 1618, 1468, 1350, 1289, 1251, 1089, 948, 834, 772.

Synthesis of $[Cu(H_2O)_6(18-crown-6)_2][Mo_6O_{19}]$ (4)

The synthesis of 3 was done following the reported procedure. ¹⁵ The green colour crystals hence formed were further confirmed by using the FT-IR techniques and single crystal X-ray diffraction pattern, which exactly matched with that of the reported one.

2.5 References

- 1. E. Ochiai, Bioinorganic Chemistry, An Introduction. Allen Bacon, Boston, 1977.
- 2. O'Brein, J. T.; Williams, E. R.; J. Phys. Chem. A., 2011, 115, 14612-14619.
- 3. Frank, P.; Benfatto, M.; Szilagyi, R. K.; D'Angelo, P.; Della Longa, S.; Hodgson, K. O. Inorg. Chem. 2005, 44, 1922–1933.
- 4. D'Angelo, P.; Barone, V.; Chillemi, G.; Sanna, N.; Meyer-Klaucke, W.; Pavel, N. V. J. Am. Chem. Soc. 2002, 124, 1958–1967.
- 5. Fratiello, A.; Kubo, V.; Peak, S.; Sanchez, B.; Schuster, R. E. Inorg. Chem. 1971, 10, 2552-2557.
- 6. Ohtaki, H.; Radnai, T. Chem. Rev. 1993, 93, 1157–1204.
- 7. Matwiyoff, N. A.; Darley, P. E. J. Phys. Chem. 1968, 72, 2659–2661.
- 8. Rudolph, W. W.; Pye, C. C. Phys. Chem. Chem. Phys. 1999, 1, 4583.
- 9. Schwenk, C. F.; Loeffler, H. H.; Rode, B. M. J. Am. Chem. Soc. 2003, 125, 1618-1624.
- 10. Rode, B. M.; Schwenk, C. F.; Hofer, T. S.; Randolf, B. R. Coord. Chem. Rev. 2005, 249, 2993–3006.
- 11. D'Angelo, P.; Barone, V.; Chillemi, G.; Sanna, N.; Meyer-Klaucke, W.; Pavel, N. V. J. Am. Chem. Soc. 2002, 124, 1958-1967.
- 12. Marcus, Y. Chem. Rev., 1988, 88, 1475-1498.
- 13. Ohtaki, H.; Radnai, T. Chem. Rev., 1993, 93, 1154-1204.
- 14. Pasquarello, A.; Petri, I.; Salmon, P. S.; Parisel, O.; Car, R.; Toth, E.; Powell, D. H.; Fischer, H. E.; Helm, L.; Merbach, A. E. Science, 2001, 291, 856-859
- 15. Shivaiah, V.; Das, S. K. Angew. Chem. Int. Ed. 2006, 45, 245-248.

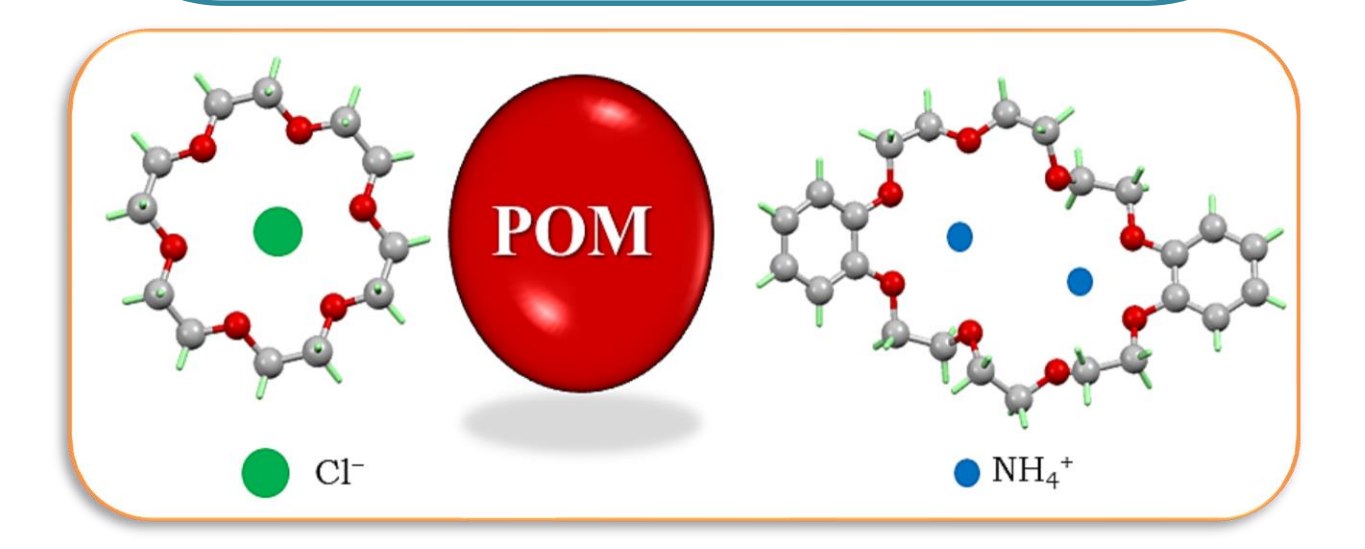
- 16. Cooper, T. E.; O'Brien, J. T.; Williams, E. R.; Armentrout, P. B. J. Phys. Chem. A **2010**, 114, 12646-12655.
- 17. Pope, M. T. Heteropoly and isopoly oxometalates, Springer-Verlag, Berlin Heidelberg, New York, Tokyo, 1983.
- 18. Stuckart, M.; Monakhov, K. Y.; Chem. Sci., 2019, 10, 4364-4376.
- 19. Cotton, F. A., The Infrared spectra of transition metal complexes in Lewis, J.; and Wilkins, R. G.; Modern Coordination Chemistry, Inter-science, 1960.
- 20. Cotton, F. A.; Wilkinson, G. Adv. Inorg. Chem. 5th ed., Wiley: New York, 1998, p-745.
- 21. Ducher, M.; Pietrucci, F.; Balan, E.; Ferlat, G.; Paulatto, L.; Blanchard, M. J. Chem. *Theory Comput.*, **2017**,][, 3340-3347.

CHAPTER

3

Polyoxometalates Stabilized Ammonium Cation and Unusual Chloride anion Inclusion Crown Ether Complexes: Synthesis, Characterization and Crystallography

Abstract. Two supramolecular compounds exhibiting encapsulation of guest molecules in the cavities of two different crown-ether host entities with varying cavity size are reported. In the compounds, two different Keggin anions, [PMo₁₂O₄₀]³⁻ and [SiMo₁₂O₄₀]⁴⁻, act as the stabilizing anions. Whereas, a chloride anion is encapsulated in the crown ether with small cavity size, 18-crown-6, two ammonium ions and two acetonitrile molecules are encapsulated in the cavity of the larger crown ether, dibenzo-24-crown-8. The encapsulation of chloride anion in the cavity of the crown ether is very unusual, in terms of hard-soft acid-base (HSAB) principle, but here the polyoxometalate anion plays a role in stabilizing the overall molecule. Both the compounds have been characterized using routine characterization techniques and their structures have been elucidated using single crystal X-ray diffraction technique. Further, silver nitrate test and the Nessler's reagent test have been performed on both the compounds, to ensure the presence of chloride anion and the ammonium cation, respectively. The two compounds of study $[H_3PMo_{12}O_{40}\{HCl(18-crown-6)\}_3]\cdot 4CH_3CN$ (compound and $[SiMo_{12}O_{40}\{(NH_4)_2(dibenzo-24-crown-8)\}_2\{(CH_3CN)_2(dibenzo-24-crown-8)\}]$ ·2CH₃CN (compound 2).



3.1Introduction

Since the serendipitous discovery of 18-crown-6 by C. J. Pedersen in 1967,¹ the family of crown-ethers, including more such compounds, have been extensively used for artificial molecular recognition. These crown-ethers are the first generation of hosts that paved the path to the concept of supramolecular chemistry.² The secondary interactions involved in the host-guest chemistry of the crown-ether moieties and the guest molecules mimic natural systems as well as leads to the construction of new functional materials as well.³ The structural forms of the hence formed supramolecular cationic species are dependent on the size of the cavity of the hosts, i.e., crown ethers. These crown-ethers contain hard ether-oxygen-bridges and show a binding preference for hard species, on the basis of hard-soft acid base principle, thus showing a binding preference for alkali metal cations, like Na⁺, K⁺, Cs⁺ etc. Apart from these cations, they also incorporate oxonium ions and ammonium ions in their cavities.⁴

There are numerous reports, where the crown ether based supramolecular host-guest entity is stabilized by various moieties, that are able to act as obligatory anions (thus complementing the cations encapsulated/ included in the crown ether cavities) and also stabilize the host-guest entity by serving supramolecular, mainly hydrogen bonding, interactions. Polyoxometalates are one such family of compounds that have been extensively used as stabilizing anions for these crown-ether guest moieties. Polyoxometalates are metal oxide anionic clusters exhibiting structural and electronic diversities. These polyoxometalates contain negatively charged surface oxygen atoms, which take part in H-bonds with various donor atoms, hence making them suitable candidates for supramolecular interactions.

Herein we report the encapsulation of a chloride anion, [H₃PMo₁₂O₄₀{HCl(18-crown-(compound 1) and ammonium cations and acetonitrile molecules, 6) $_{3}$ -4CH $_{3}$ CN $[SiMo_{12}O_{40}\{(NH_4)_2(dibenzo-24-crown-8)\}_2\{(CH_3CN)_2(dibenzo-24-crown-8)\}]\cdot 2CH_3CN$ (compound 2) in the crown-ether cavity. The encapsulation of the chloride anion in the cavity of a crown ether is very rare. It leads us to an intriguing paradigm to explore the encapsulation of unusual anionic guests in the crown ether hosts. Although this chemistry is all new, but still a similar report on this unusual oxygen-halide secondary interaction is not new. In 2013, Ripmeester and co-workers reported the occupancy of Cl₂ and Br₂ in the small cages of clatharate hydrates, revealing halogen bonds between water oxygen atoms and the dihalogen molecules.⁷ Ochoa-Resendiz et al. in 2016 also reported the halogen bonding in clatharate compounds based on energy partitioning analysis along with electronic shift studies that are associated with transitions to the main valence bands.8 In 2017, Alavi and co-workers reported the results of ab initio calculations and natural orbital molecular orbital analysis for Cl₂ and Br₂ guests in the cages of clatharate hydrates. Although clatharates and crown-ethers are two different families of hosts, still they provide similar environments to encapsulate various guest molecules (halogens in this case) in their cages or cavities. This gives a blink of possibility for the encapsulation of halogens in the crown-ether cavities. The encapsulated halogen ion in the cavity of the crown ether, is stabilized by a Keggin type polyoxometalate, i.e., PMo₁₂O₄₀³⁻, and four acetonitrile solvent molecules, thus giving the formula [HCl(18C6)]₃[H₃PMo₁₂O₄₀]·4CH₃CN (1) (18C6: 18-crown-6). The inclusion chemistry of ammonium ions in crown ether although very well documented, but only once had it been tried to associate with polyoxometlates by Tanmay et al., 10 where they successfully isolated and studied five ammonium encapsulated polyoxometalate associated crystals.

3.2Results and Discussion

3.2.1 Synthesis

Single crystal for the compound 1 and 2 are grown from the acidified organic medium. Polyoxometalates H₃[PMo₁₂O₄₀]·xH₂O and H₄[SiMo₁₂O₄₀]·xH₂O are allowed to react with respective crown ether and NH₄Cl. The polyoxoanions are quiet stable in these reaction conditions and upon their association with the [guest @ (crown ether)] {guest: Cl⁻ in compound 1 and NH4⁺ and CH₃CN in compound 2}, they crystallize to form the supramolecular cationic species.

Silver Nitrate Test

Silver nitrate test is a very fundamental method for the detection of the presence of chloride anions in any solution. When AgNO₃ is added to any solution containing Cl⁻ anions, then a white curdy precipitate of AgCl is formed. 11

$$Cl^- + Ag^+ \rightarrow AgCl \downarrow$$

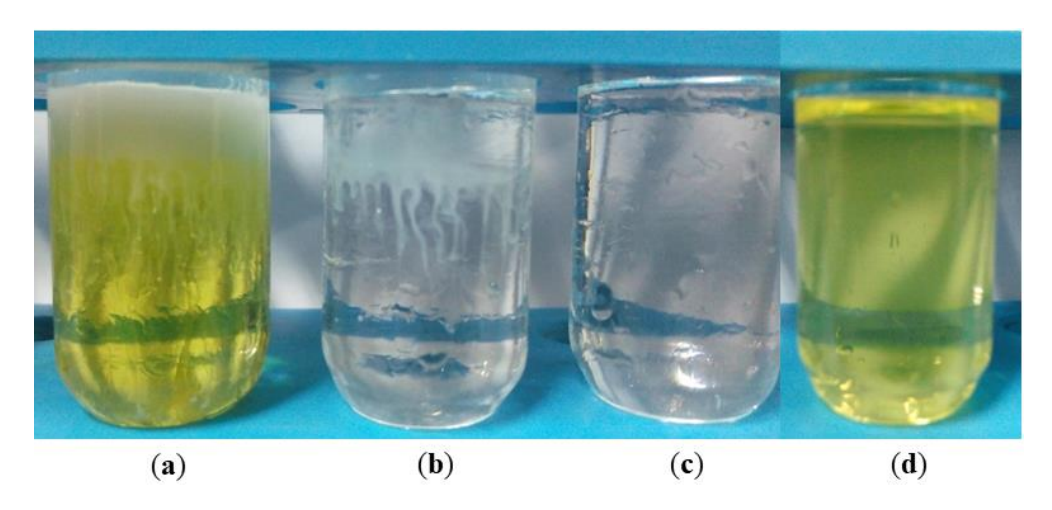


Figure 3.1. Silver nitrate test of (a) compound 1. (b) sodium chloride solution in DMSO (c) pure DMSO (d) compound 2.

The compound 1 was dissolved in DMSO, because of its poor solubility in other non-polar or less polar solvents, and to it was added few drops of 0.1M silver nitrate solution, where immediately a white precipitate was formed, but the precipitate disappeared soon, because AgCl is soluble in DMSO. Hence, in order to collect the precipitate formed, the test-tube where the test was done was rushed to suction, and the precipitate was collected. Figure 3.1 shows the silver nitrate test and the precipitate formed, in the DMSO solution of compound 1, sodium chloride, and pure DMSO, where no precipitate was found and also in DMSO solution of compound 2, where no changes were observed.

Nessler's Reagent Test

The DMSO solution of compound 1 was also tested for the presence of cationic ammonium ions using the Nessler's reagent, but since a brown precipitate $(HgO \cdot Hg(NH_2)I)^{11}$ was not formed in the test-tube (Figure 3.2), it confirmed the absence of the ammonium ions in the compound 1, but the brown precipitate in the test tube of DMSO solution of compound 2 confirms the presence of ammonium cations in the compound.

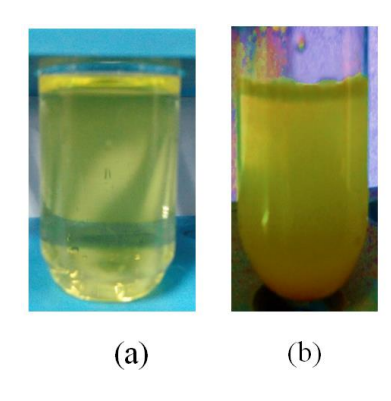


Figure 3.2. Nessler's reagent test (a) compound 1. (b) compound 2.

3.2.2 **Crystallography**

Table 3.1 Crystallographic Parameters of compound 1 and 2.

Compound	1	2
Formula	$C_{44}H_{78}Cl_{3}Mo_{12}N_{4}O_{58}P$	$C_{50}H_{78}N_6O_{56}SiMo_{12}$
Formula weight	2879.70	2838.52
Temperature (K)	273(2)	273(2)
Wavelength (Å)	0.71073	0.71073
Crystal system, space	Monoclinic	Triclinic
group	C2/m	P-1
a (Å)	25.354(3)	13.0629(4)
b (Å)	13.3940(12)	14.2146(5)
c (Å)	14.5145(13)	15.7083(5)
α (deg)	90	84.026(1)
β (deg)	116.607(7)	85.762(1)
γ (deg)	90	69.593(1)
Volume (Å ³)	4407.0(8)	2716.66(15)
$Z, \rho (g/cm^3)$	2, 2.170	1, 2.062
$\mu (\mathrm{mm}^{-1})$	1.859	1.455
F(000)	2808.0	1662.0, 1.094
goodness-of-fit on F2	1.253	0.0803
R1	0.0446	0.1745
wR2	0.1170	2.2

Crystal Structure of Compound [H₃PMo₁₂O₄₀{HCl(18-crown-6)}₃]·4CH₃CN (1)

Compound 1 crystallizes in C 2/m space group (*monoclinic*, Z=2). The asymmetric unit of compound 1 consists of a fragment of the polyoxometalate, { $P_{0.25}Mo_3O_{10}$ }, two

different fragments of the crown ether moieties, one of $\{C_3O_2\}$ and the other of $\{C_6O_4\}$ unit, two chloride ions, one of a half occupancy and the other of a quarter occupancy, therefore a chloride ion, $(Cl_{0.75})^-$, and two acetonitrile molecules each of $\{CN_{0.5}\}$ units. So, the full molecule of compound 1, can be formulated as $[(PMo_{12}O_{40})(Cl)_3(C_{12}O_6H_{24})_3(CH_3CN)_4H_6]$. Figure 3.3 shows the full molecule of compound 1, where we can see that the compound consists of one $PMo_{12}O_{40}$ unit, three crown ether units each encapsulating a chloride ion and four acetonitrile solvents.

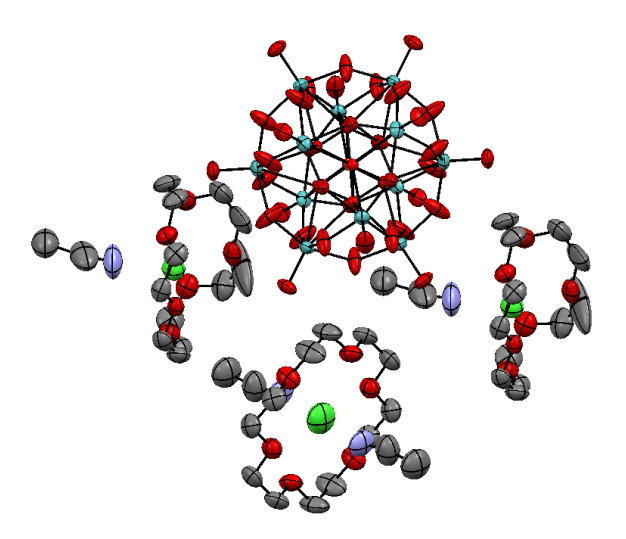


Figure 3.3. Full molecule of compound 1. (Colour Code: Cyan: molybdenum, Red: oxygen, white: carbon, blue: nitrogen, green: chloride ion)

The Keggin ion in compound 1 is $PMo_{12}O_{40}$. It has phosphorous atom as the central atom, which is coordinated tetrahedrally to four bridging oxygen atoms, O_c (O_c : central oxygen atoms) at a distance of 1.507-1.543 Å. The Mo- O_t (O_t : terminal oxygen; there are 12 such oxygen atoms) bond distances vary from 1.649-1.660 Å. The 24 bridging oxygen atoms (O_b) form Mo- O_b bonds, whose bond distances vary between 1.817-1.975 Å. All these values are in accordance to the earlier bond distance reports of Keggin ion. ¹²

The crown-ether that we have used here is the 18-crown-6. As can be seen from Figure 3.4 that the Cl1 ion is exactly at the centre of the cavity and also in the same plane of that of the crown ether. The distance between the Cl⁻ ion and the oxygen atoms in the crown ether moiety is 2.689 – 2.798 Å. The Cl2 ion encapsulated in the second crown-ether however makes the crown ether to bend and take a chair conformation (Figure 3.4(b)). This Cl⁻ ion also is placed at the centre of the cavity at a distance of 2.418 – 2.641 Å. There are two such bent crown-ether moieties encapsulating a chloride ion each. All the encapsulated chlorine ions face the nitrogen atoms of the acetonitrile solvents, at a distance of ~2.3 Å. The Cl1 however has two acetonitrile molecules interacting with it through the nitrogen atoms from both sides of the crown-ether (Figure 3.4(d)).

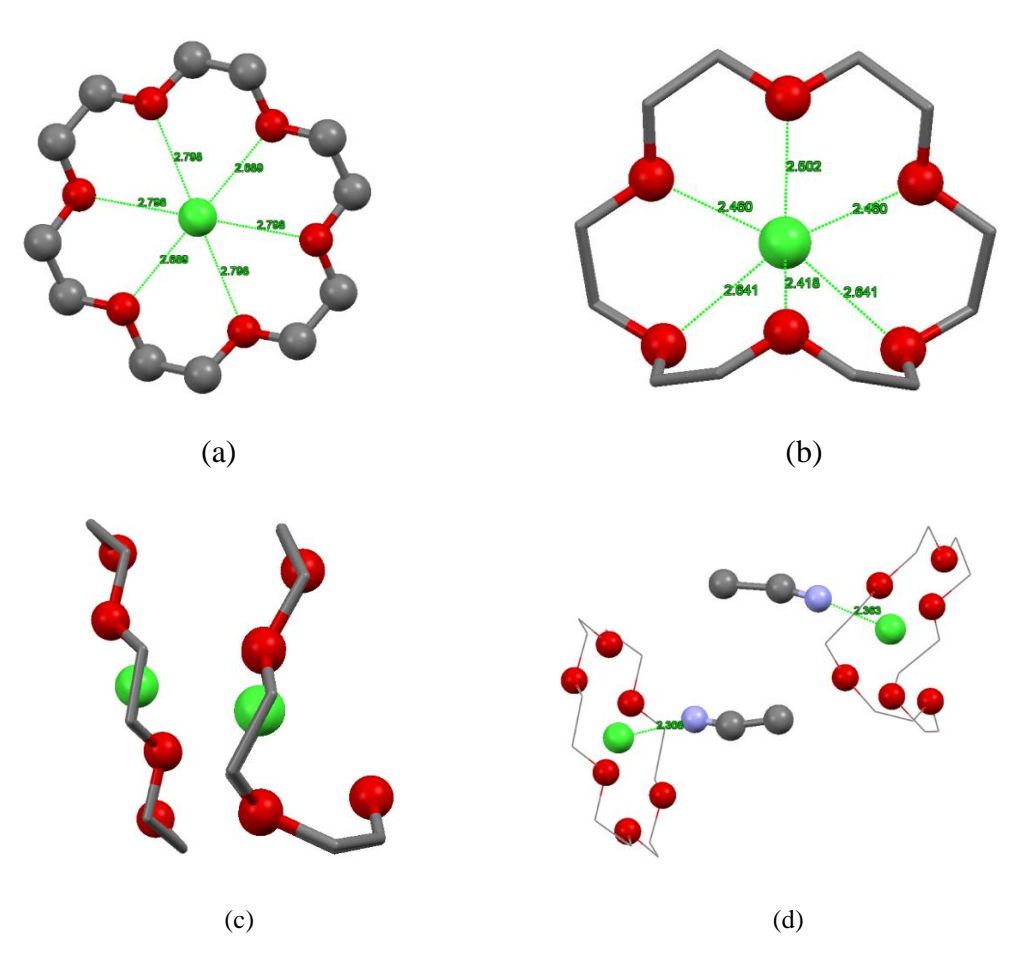


Figure 3.4 (a) The chloride ion encapsulated in the cavity of 18-crown-6 (b) The chloride ion encapsulated in the bent 18-crown-6. (c) Side-view of the chloride ion encapsulated crown ethers. (d) The interaction between the chloride anion encapsulated in the crown ether and the nitrogen atom of the solvent acetonitrile molecules.

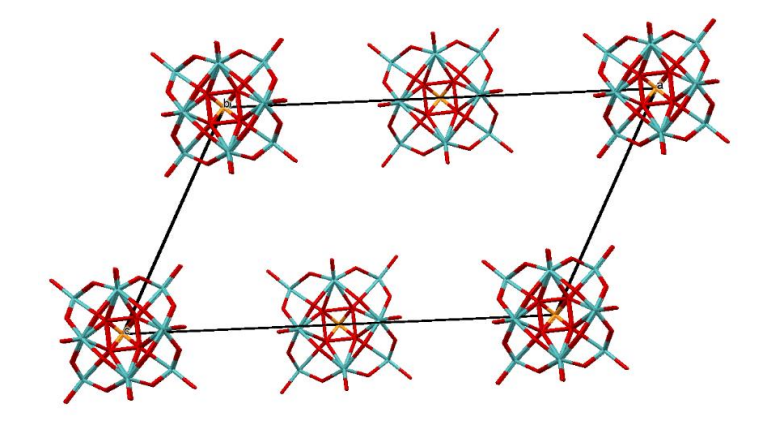


Figure 3.5 The arrangement of the Keggin ions in the unit cell in compound 1.

The packing diagram suggests that there are a total of two Keggin molecules in the unit cell, one each at the eight corners, contributing a total of one Keggin and two at the two opposite faces, contributing to the second Keggin molecule (Figure 3.5). There are also a total of six chloride ions encapsulated crown ether moieties; two whole inside the unit cell

and half each of eight chlorine encapsulated crown ether moieties at the faces. It also has eight acetonitrile solvent molecules per unit cell (Figure 3.6).

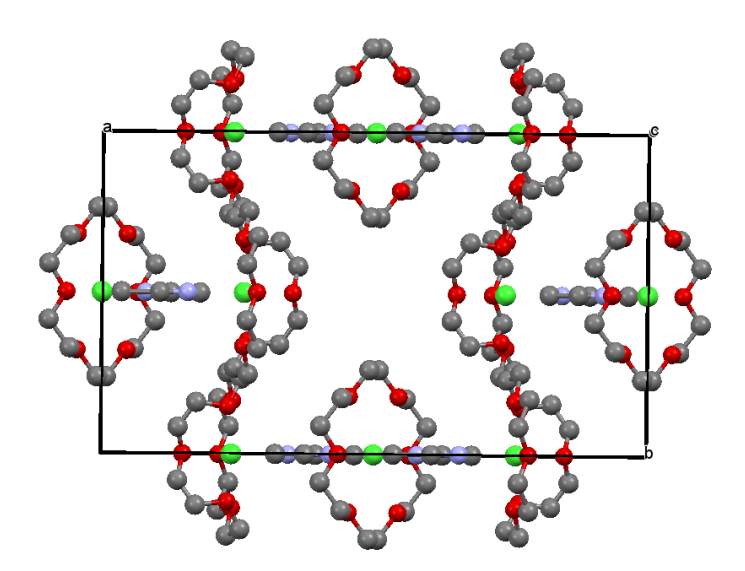


Figure 3.6. The arrangement of the chloride ion encapsulated crown ether and the acetonitrile molecules in the unit cell.

Crystal Structure of Compound $[SiMo_{12}O_{40}\{(NH_4)_2(dibenzo-24-crown-8)\}_2\{(CH_3CN)_2(dibenzo-24-crown-8)\}]\cdot 2CH_3CN$ (2)

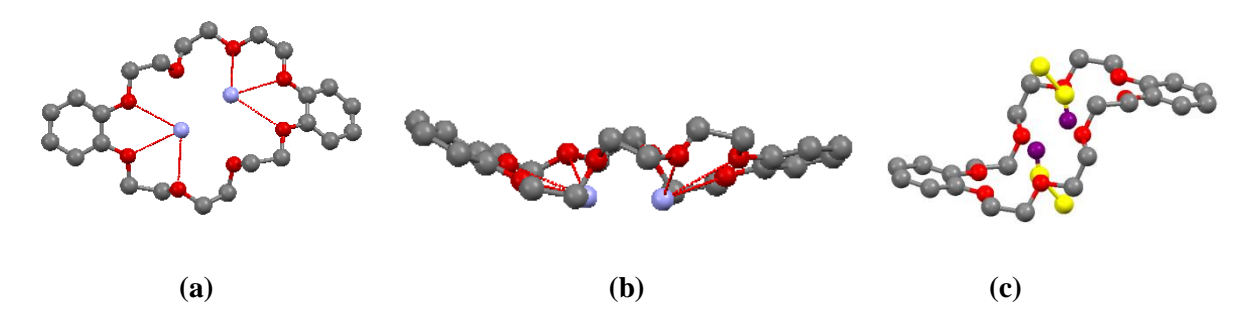


Figure 3.7 (a) Association of ammonium ion with the crown ether in Compound 2 (b) The boat shape crown ether after encapsulation of the ammonium ion (c) The chair conformation attained by another crown ether encapsulating acetonitrile in its cavity.

The compound **2** crystallizes in the P-1 space group. In its asymmetric unit, it contains half of the Keggin ion i.e., $Si_{0.5}Mo_6O_{40}$, one dibenzo-24-crown-8 encapsulating two ammonium ions, half of another dibenzo-24-crown-8, which has an acetonitrile encapsulated in it. The unit also contains an acetonitrile solvent, from which the species is crystallized. Thus the full molecule consists of a full Keggin ion $[SiMo_{12}O_{40}]^{4-}$, two dibenzo-24-crown-8 units each encapsulating two ammonium ions each, therefore contributing four positive charge hence, balancing the –4 charge of the Keggin anion, another dibenzo-24-crown-8 encapsulating two acetonitrile moieties and two acetonitrile solvent molecules, thus giving the formula of the compound $[SiMo_{12}O_{40}\{(NH_4)_2(dibenzo-24-crown-8)\}_2\{(CH_3CN)_2(dibenzo-24-crown-8)\}]\cdot 2CH_3CN$

In one of the crown ethers, which appears fully in the asymmetric unit, the two ammonium ions are connected to six of the eight oxygen atoms present in the crown ether. One of those three oxygen atoms is ethereal while the other two are catechol oxygen atoms (Figure 3.7a). Both of the nitrogen atoms of ammonium ions are present at a distance of ~2.9Å from the oxygen atoms. The crown ether also bends slightly from its normal position, bending away from the ammonium ions, thus forming a boat type structure (Figure 3.7b). A very interesting point here to be noted is that, as per our knowledge this is a very rare case, where two ammonium ions are included in the crown ether cavity. There have been reports where two cations like K⁺ and Na⁺ are present in the cavity, but the case of ammonia is not known till now. Even in a previous report from our group, 11 we used a flexible crown ether with still larger cavity i.e., dibenzo-30-crown-10, which could encapsulate only one ammonium ion. Here, although the cavity size is smaller than the reported one, still, it can encapsulate two ammonium ions. This may be attributed to the fact that, in the case of dibenzo-30-crown-10, the molecule is not rigid, hence it forms a bowl shape hence, the entry of the second crown ether is restricted, but the case is not the same with dibenzo-24-crown-8. Although dibenzo-24-crown-8 is also flexible, still it does not restrict the inclusion of the second ammonium ion, this may be attributed to the interaction between the polyoxometalate and the crown ether's hydrogen atoms.

The other crown ether present in the moiety, whose only half is involved in the asymmetric unit, when seen fully forms a chair-like structure, where, the two sides are bent from the normal position at angles of 109.20° and 112.75° (Figure 3.7c). Surprisingly, it encapsulates two acetonitrile moieties in it, such that the nitrogen atoms of the acetonitrile molecules are towards the cavity of the crown-ether. It is yet a very rare case since, although there are reports where the methyl carbon of the acetonitrile is reported to interact with crown-ether oxygen atoms through hydrogen bonds, ¹³ here the nitrogen atoms are associated with the crown-ether.

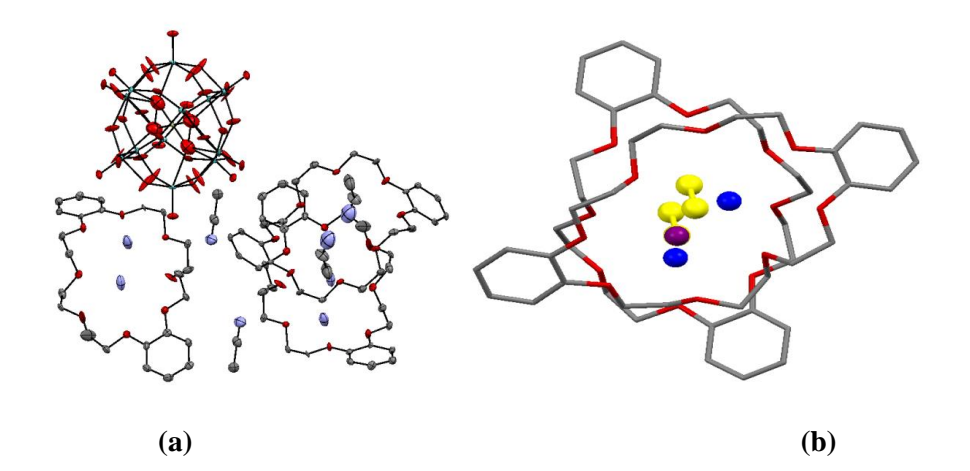


Figure 3.8 (a) The full molecule of compound 2. (b) The interactions between the ammonium ions in the crown ether and the oxygen atoms of the crown ether molecules.

The ammonium ions encapsulated crown ether adducts interact with the Keggin ion through hydrogen bonding interactions between the terminal oxygen of the POM and the hydrogen of the benzene ring in the crown ether. Similarly, the acetonitrile solvent present in

the crystal also is bonded through H-bonds with the host crown ether and the polyoxometalate, thus stabilizing the overall structure (Figure 3.8a). Similarly, the two crown ethers, which are at almost an angle of 90° to each other, are also connected through weak interactions between hydrogen atoms of one crown ether with the oxygen and carbon atoms of the other crown ether (Figure 3.8b). A point here to be noted is, due to the roatation of the crown ethers, the π - π stacking interactions between them are not possible, otherwise that would have been another factor of stabilization. The reason of rotation is not yet clear to us.

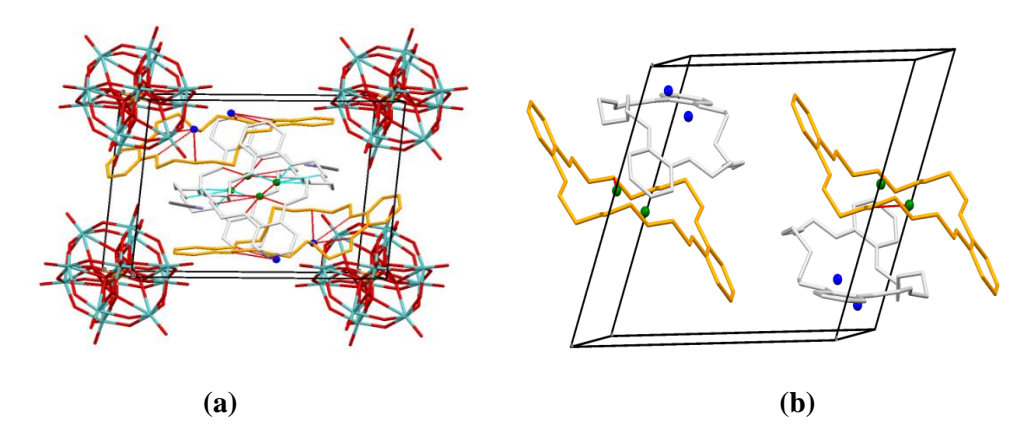


Figure 3.9 (a) The unit cell of compound 2. (b) The arrangement of ammonium ion encapsulated crown ether in the unit cell of compound 2. All the hydrogen atoms and the carbon atoms from the acetonitrile moieties have not been shown for clarity.

The compound in its unit cell arranges itself such that there are four Keggin ions in the four edges of the cell, therefore forming a total of one full Keggin in the unit cell (Figure 3.9). As we can see in the Figure 3.9b, in the unit cell there are four crown ether molecules too, but all of them are present partly in the crown ether. The unit cell also has four of the ammonium ions, which neutralize the tetraanionic Keggin ion. The overall packing pattern is also shown in the Figure 3.10.

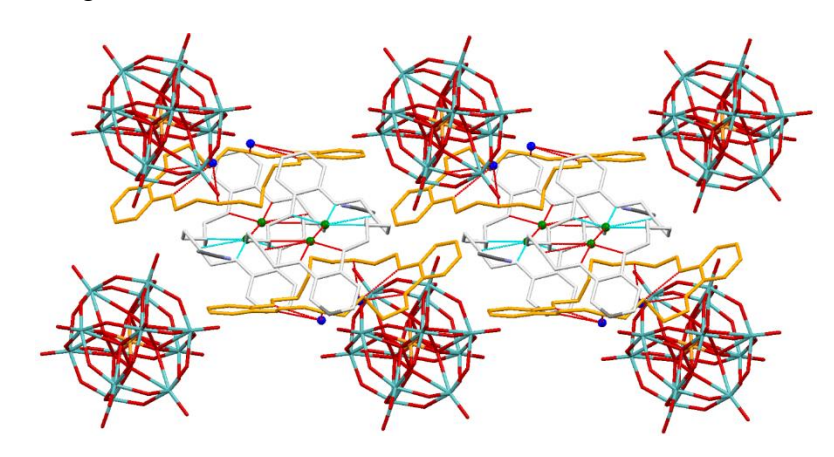


Figure 3.10. The packing in compound 2. All the hydrogen atoms and the carbon atoms from the acetonitrile moieties have not been shown for clarity.

3.2.3 Spectral Characterization.

FT-IR Spectroscopy

Detection of the presence of various functional groups can be done easily and effectively using Infrared spectroscopy.

The FT-IR spectra of compounds **1** and **2** are given in Figure 3.11 and 3.12 respectively. The various peaks around 780-800cm⁻¹, 860-890 cm⁻¹, 960-990 cm⁻¹ and 1060-1080 cm⁻¹, with few displacements due to various interactions can be attributed to the stretching frequencies of Mo–O_c–Mo, Mo–O_b–Mo, Mo=O_t and the P–O/ Si–O bonds. Peak at 2940 cm⁻¹ in the spectra is actually a multiplet centred at this point. These peaks can be attributed to the alkyl C-H stretch, which are present in the crown ethers. The peaks around 2300 cm⁻¹ is assigned to the nitrile C-N stretch originating from acetonitrile solvent present in the compound.

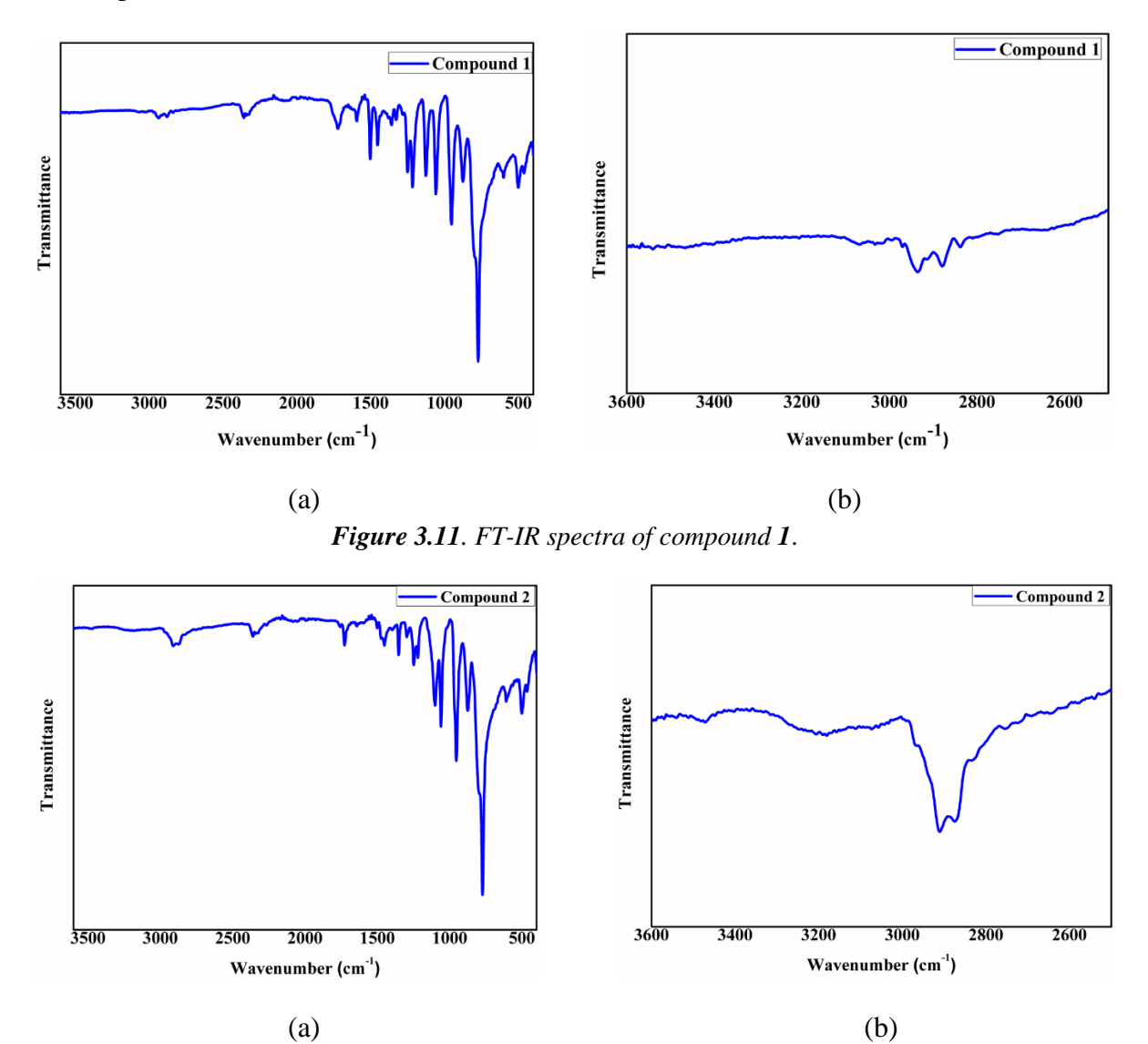


Figure 3.12. FT-IR spectra of compound 2.

Ammonium ion (NH₄⁺) in its free form has a tetrahedral symmetry, that shows a strong and broad absorption peak between 3300-3030 cm⁻¹. This peak is due to the N-H stretching vibrations. Yet another strong peak is seen around 1400 cm⁻¹, which can be accounted for the bending motions of the N-H bonds. Upon H-bonding of the relevant ion, these peaks tend to shift towards higher and lower wavelengths respectively. In Figure 3.12, the peak at around 3200 cm⁻¹ can be attributed to the stretching frequencies of the N-H bonds for the compound 2 (Figure 3.12b). Similarly, the bending motions of the N-H bonds in compounds 2 give their signature peaks around 1400 cm⁻¹ in the spectrum.

UV Spectroscopy

Compounds 1 and 2 consist of $[PMo_{12}O_{40}]^{3-}$ and $[SiMo_{12}O_{40}]^{4-}$ respectively, so they show the characteristic feature of the POM i.e., the broad shoulder 300-310 nm, which can be accredited as the ligand to metal charge transfer (LMCT), i.e., the oxygen to the molybdenum centres ($O^{2-} \rightarrow Mo^{6+}$) in the polyoxometalate. The peak around 256 nm also arises from the polyoxometalate anion (Figure 3.13). The compound 2 shows an extra peak around 270-280 nm can be attributed to the π to π^* transition in the benzo rings in the crown ether (Figure 3.13).

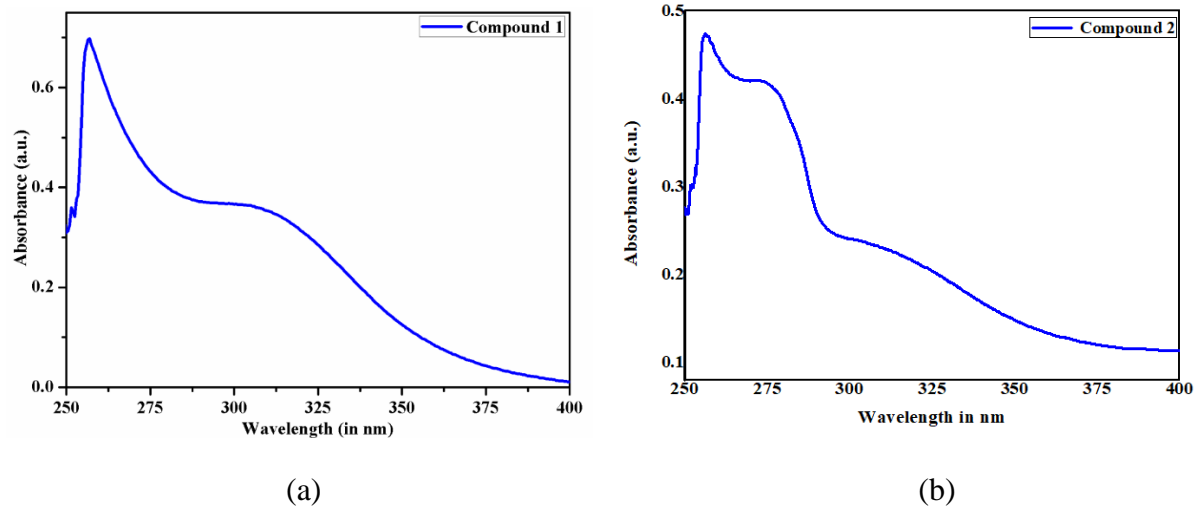


Figure 3.13. UV-visible spectra of compounds 1 and 2.

¹H NMR Spectroscopy

¹H NMR spectrum of compound **2** has been recorded in DMSO- d_6 at room temperature and is given in Figure 3.14. NH₄Cl exhibits a strong singlet at δ 7.49 in DMSO- d_6 , ¹⁰ although due to the coupling of ¹H to the ¹⁴N quadrupolar nucleus should give a triplet of equal intensity. ¹⁴ But, in practice, due to the tetrahedral structure of NH₄⁺ cation, we see only a narrow line for ¹⁴NH₄⁺. In compound **2**, due to hydrogen bonding interactions of the ammonium cations with the crown ether, the ammonium cations no more retain the tetrahedral structure and hence, by virtue of quadrupolar coupling, it shows triplets of equal intensity between δ 6.97 to 7.35. The peak is also shifted up-field, which is because of the shielding provided to the ion by the lone pairs on oxygen atoms inside the crown ether cavity.

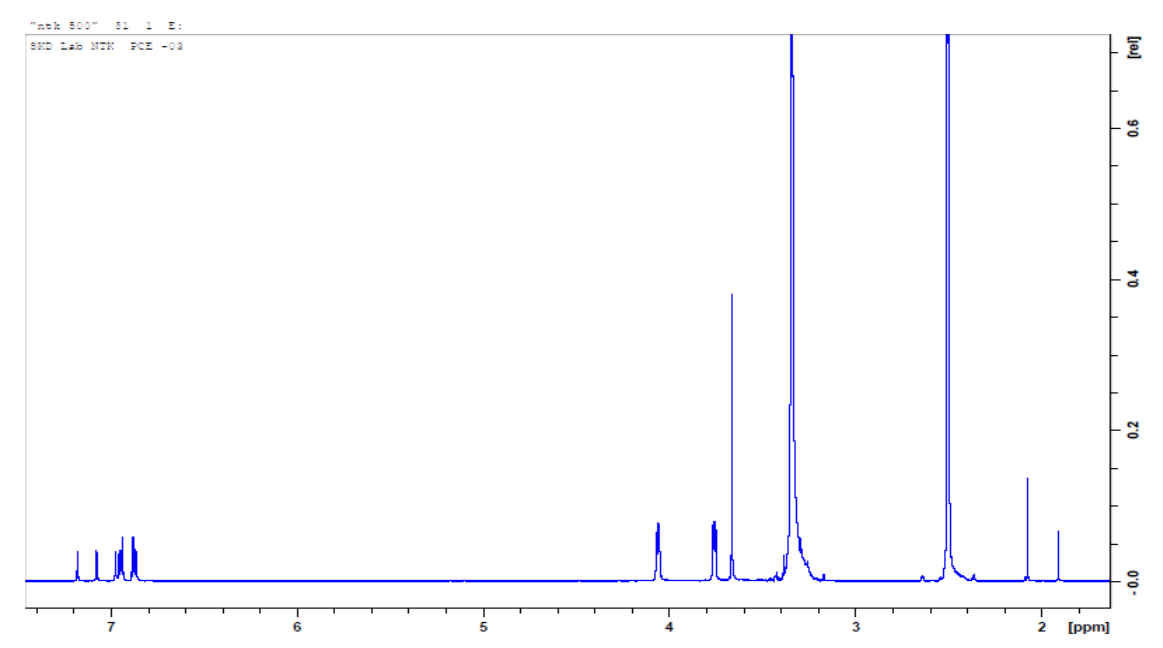


Figure 3.14. ¹H NMR spectrum of the compound 2

3.2.4. Thermogravimetric Analysis (TGA) and PXRD

Thermogravimetric analysis was used to study the thermal stability of the compounds. The TGA experiments were performed by increasing the temperature from 50 $^{\circ}$ C to 990 $^{\circ}$ C in the presence of N_2 gas.

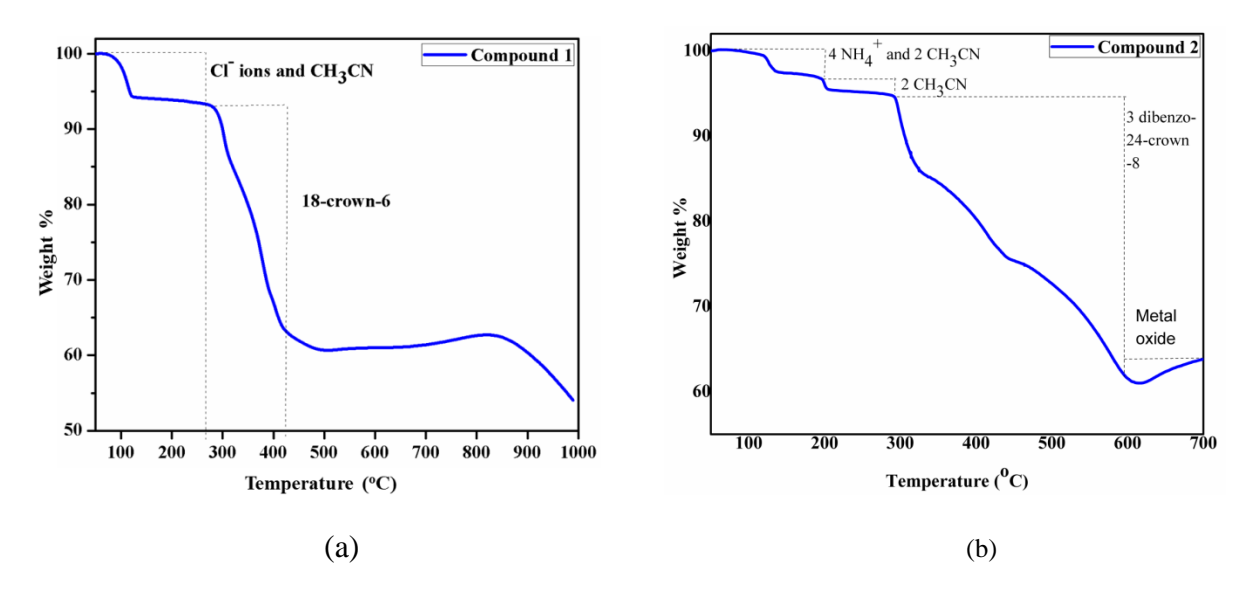


Figure 3.15. Thermogravimetric plot of (a) compound 1. (b) compound 2.

The thermogravimetric analysis of the compound **1** was done. As the temperature was increased from 50 °C to 990 °C, we see a three-step degradation of the compound. In the first step, the three chloride ions and the four acetonitrile solvent molecules are decomposed between 70 °C to 140 °C. Following this, the three crown ether molecules decompose between 200 to 400 °C, leaving therefore only the Keggin molecule, which also decomposes with the increase in temperature (Figure 3.15a).

The TGA plot of compound **2** is shown in Figure 3.15b. As can be seen, as the temperature rises from 70°C to150 °C, the ammonium ions and lattice acetonitrile solvent molecule are lost, followed by the loss of the acetonitrile moieties that are encapsulated in the cavity of the crown ether. In the temperature range of 300-700 °C, the compound exhibits a continuous weight loss, which is because of the loss of the crown ether moieties. Thereafter, only the polyoxometalate moiety is left.

TGA-MS Studies

The TGA-MS spectrum of compound **1** was also recorded, mainly to confirm the presence of the chloride ions. As can be seen in Figure 3.16, the recorded spectra when was made to inject the gas evolved after 60 °C into the mass spectrometer showed a strong peak at m/z value of 36, which can be attributed to the chloride ion.

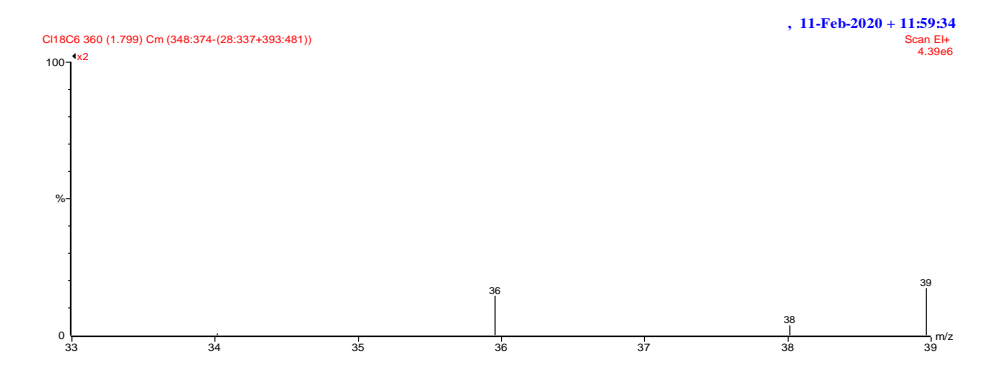


Figure 3.16. TGA-MS plot of compound 1.

Powder X-Ray Diffraction Studies

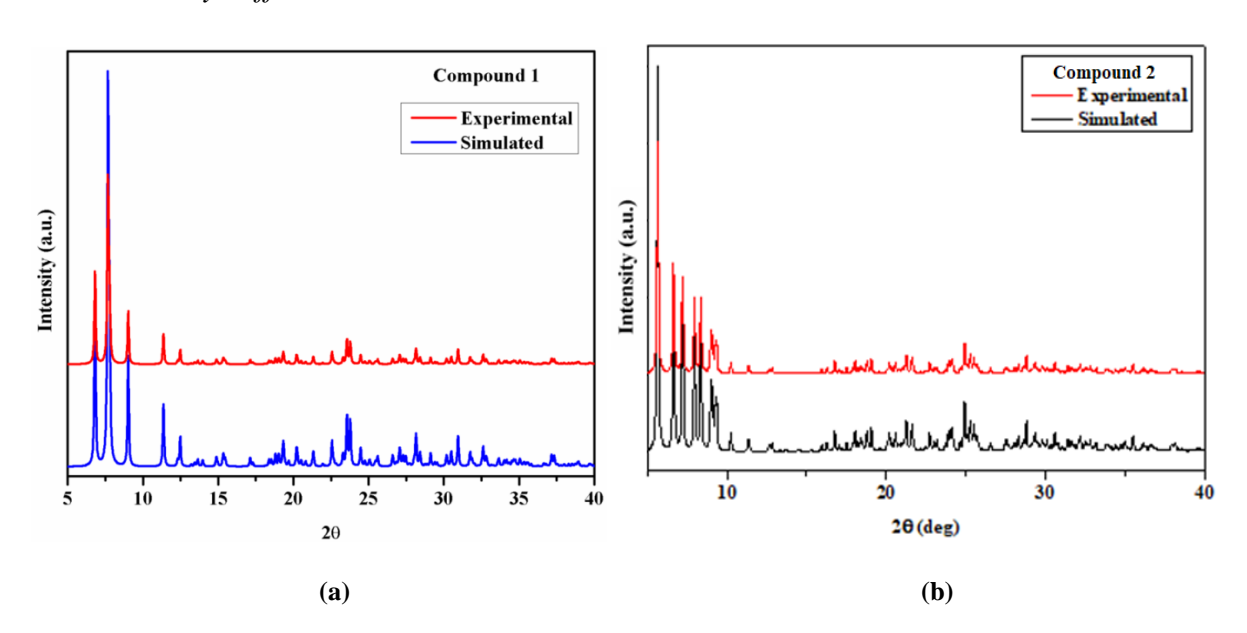


Figure 3.18. Powder X-ray diffraction plot of (a) compound 1. (b) compound 2.

The powder X-ray diffraction of compound 1 and 2 were performed and are compared with that of the simulated pattern generated from the CIF file of compound 1 and 2

respectively. It was found that almost all peaks were found concurrent with that of the simulated pattern, hence assuring the bulk homogeneity of both compounds (Figure 3.18).

3.2.5 EDAX Studies

The compound **1** was also tested for the elemental analysis using the EDAX technique, which also confirms the presence of the chloride ions in the compound (Figure 3.17, Table 3.2).

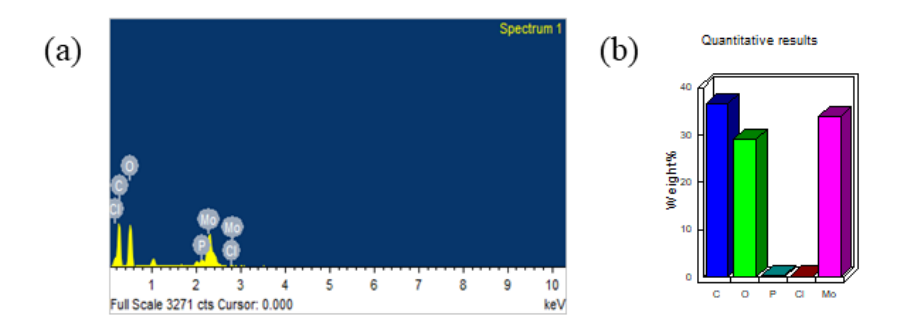


Figure 3.17. EDAX result of compound 1.

Table 3.2 . El	DAX report of	f compound $oldsymbol{1.}$
-----------------------	---------------	----------------------------

Element	Weight%	Atomic%
C K	36.54	58.15
ок	29.17	34.85
РК	0.33	0.21
Cl K	0.09	0.05
Mo L	33.87	6.75
Totals	100.00	

3.2.6 Discussion on the Type of Guest Molecule Encapsulated

In the present chapter we see that crown ethers encapsulate three types of guest molecules in their cavities, *viz.* chloride anions, ammonium cations and acetonitrile molecules. Whereas the inclusion of ammonium cations is well reported, the encapsulation of chloride anions in the crown-ether cavity, is reported for the first time. There are also reports on acetonitrile solvent complexation with crown-ether. Whereas there is a report based on crystal structure, where the methyl carbon of the acetonitrile molecule is encapsulated in the cavity, this is the first crystal structural proof of the nitrogen of the acetonitrile solvent being encapsulated in the cavity. As we know that both Cl⁻ and N of CH₃CN are borderline bases, so the encapsulation of these moieties in the hard-interactions preferring crown-ether cavities is not impossible.

The encapsulation of chloride ions in the 18-crown-6 cavity is serendipitous. Earlier we reported the encapsulation of ammonium ions in the crown-ether cavity¹⁰ and with the same aim we thought of proceeding using NH₄Cl as the ammonium source. But, 18-crown-6 picks up the chloride anions rather than the ammonium cations. There are reports earlier, where from an ammonium chloride solution, 18-crown-6 picks the ammonium ions, but in our case we see that it prefers hosting a chloride anion. Probably, the polyoxometalate anion plays the role of stabilizing this unusual host-guest entity. The same reaction was followed with a change of polyoxometalate and the crown-ether and we saw that not a chloride anion but ammonium cations were taken up by the crown-ether thus provided, dibenzo-24-crown-8, which has a larger cavity. In addition to this, this larger crown-ether also encapsulates two acetonitrile molecules in its cavity. Hence, we can infer that, apart from the hard-soft interactions between the host and guest molecules, the anion used, here a polyoxometalate anion, as well as the cavity size of crown-ether (which is obvious) plays major role in determining the guests to be encapsulated or included in the crown-ether cavity.

3.3 Conclusion

We have successfully synthesized two compounds, one where a chloride ion gets encapsulated in the crown ether cavity and the other, where ammonium ions and acetonitrile solvent molecules get encapsulated in the larger cavity of the larger crown ether. Both the compounds have been characterized using routine techniques and their structures have been elucidated using single crystal X-ray diffraction studies. Here we can see that the cavity size of the participating host crown ether plays a vital role in deciding the type of the guest molecules in the cavity of the host crown ether. This is the first ever report, to the best of our knowledge, where a chloride anion is encapsulated in the crown ether cavity in one case and an acetonitrile moiety is also encapsulated in yet another crown-ether cavity.

3.4 Experimental Section

3.4.1 Syntheses

Synthesis of $[H_3PMo_{12}O_{40}\{HCl(18\text{-crown-6})\}_3]\cdot 4CH_3CN$ (1)

18-crown-6 (0.03g, 0.13 mmol) was dissolved in 50 mL acetonitrile and $H_3[PMo_{12}O_{40}] \cdot xH_2O$ (0.16g, 0.09 mmol) was added to the reaction mixture. After all reactants got dissolved, 0.4g (0.79 mmol) ammonium chloride and 10 mL of glacial acetic acid (100%) were subsequently added into the reaction mixture and the reaction mixture was stirred for 18 hours under ambient conditions. Then the solution was filtered and allowed to evaporate slowly. Green crystals were obtained after one week. These were filtered from mother liquor thereafter and dried at room temperature. Yield: 0.148g (68.2% based on Mo).

Synthesis of [(NH₄)₂(DB24C8)]₂[(CH₃CN)₂DB24C8][SiMo₁₂O₄₀]·2CH₃CN (2)

Dibenzo-24-crown-8 (0.06g, 0.13mmol) was dissolved in 50 mL acetonitrile and H₃[SiMo₁₂O₄₀]·xH₂O (0.16g, 0.09mmol) was added to the reaction mixture. After all reactants got dissolved, 0.4g (0.79mmol) ammonium chloride followed by 10mL of glacial acetic acid (100%) were added to it. The yellow solution was stirred for 18 hours at room

temperature, filtered and allowed to evaporate slowly. Reddish brown crystals were obtained after one week. These were filtered from mother liquor thereafter. Yield: 0.122g (76.2% based on Mo).

3.4 References:

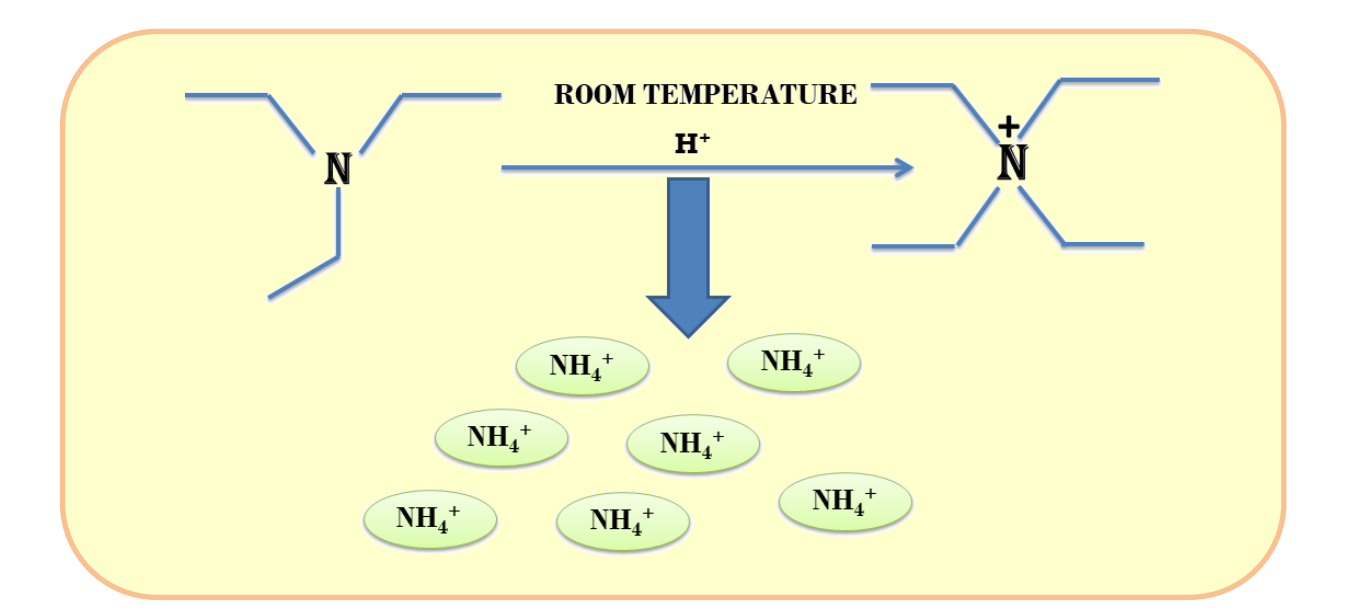
- 1. Pedersen, C. J. J. Am. Chem. Soc. 1967, 89 (10), 2495-2496.
- 2. Atwood, J. L.; Steed, J. W. In *Encyclopaedia of Supramolecular Chemistry*; Taylor & Francis: New York, **2004**.
- 3. Lehn, J. M. In Comprehensive Supramolecular Chemistry; Elsevier: Amsterdam, 1996.
- 4. Junk, P. C. New. J. Chem. 2008, 32, 762-773 and the references therein.
- 5. Pope, M. T. In *Heteropoly and Isopoly Oxometalates*; Springer-Verlag: Berlin, **1983**.
- 6. Muller, A.; Peters, F.; Pope, M. T.; Gatteschi, D. *Chem. Rev.***1998**, *98*, 239-272 and the references therein.
- 7. Udachin, K. A.; Alavi, S.; Ripmeester, J. A. J. Phys. Chem. C, **2013**, 117, 14176-14182.
- 8. Ochoa-Resendiz, D.; Batista-Romero, F. A.; Hernandez-Lamoneda, R. *J. Chem. Phy.*, **2016**, *145*, 161104.
- 9. Dureckova, H.; Woo, T. K.; Udachin, K. A.; Ripmeester, J. A.; Alavi, S. Faraday Discuss., 2017, 203, 61.
- 10. Chatterjee, T.; Sarma, M.; Das, S. K. Cryst. Growth Des. 2010, 10, 3149-3163.
- 11. Vogel, A. I.; Svehla, G. *Vogel's textbook of micro and semimicro qualitative inorganic analysis*, 5th Ed., **1979**, Longman Group Limited, London.
- 12. Xu, M.-X.; Lin, S.; Xu, L.-M.; Zhen, S.-L. Trans. Metal Chem. 2004, 29, 332-335.
- 13. Garrell, R. L.; Smyth, J. C.; Fronczek, F. R.; Gandour, R. D. *J. Incl. Phen.*, **1988**, *6*, 73-78.
- 14. Ebsworth, E. A. V.; Rankin, D. W. H.; Cradock, S. Structural methods in inorganic chemistry. 2nd Edn., 1991, p51-52.
- 15. Rudiger, V.; Schneider, H.-J.; Solov'ev, V. P.; Kazachenko, V. P.; Raevsky, O. A. *Eur. J. Org. Chem.* **1999**, *8*, 1847-1856.
- 16. Buschmann, H.-J.; Schollmeyer, E.; Mutihac, L. Supramol. Sci. 1998, 5, 139-142.
- 17. Chang, T.; Heiss, A. M.; cantrill, S. J.; Fyfe, M. C. T.; Pease, A. R.; Rowan, S. J.; Stoddart, J. F.; White, A. J. P.; Williams, D. J. *Org. Lett.* **2000**, *2*, 2947-2950.
- 18. Buschmann, H.-J.; Mutihac, R.-C.; Schollmeyer, E. J. Soln. Chem. 2009, 38, 209-217.
- 19. Buschmann, H.-J.; Mutihac, R.-C.; Schollmeyer, E. J. Soln. Chem. 2010, 39, 291-299.
- 20. Mosier-Boss, P. A.; Popov, A. I. J. Am. Chem. Soc. 1985, 107, 6168-6174.

CHAPTER

4

A New Rearrangement Reaction Resulting in Ammonium Ion at Room Temperature

Abstract. Triethylamine is a volatile liquid and is present in the atmosphere in the gas phase. It is a hazardous air pollutant and identified as a toxic air contaminant. Thus, producing ammonia (a vital chemical for fertilizer production) from the vapour state of this toxic substance is a challenging task. Diffusion of the vapour of triethylamine, (C₂H₅)₃N into an acidified aqueous solution of sodium molybdate results formation of single crystals compound $[(C_2H_5)_3NH]_2[(C_2H_5)_4N][NaMo_8O_{26}]$ (1). Notably, compound 1 includes a [(C₂H₅)₄N]⁺ cation, even though the concerned reaction mixture was not treated with any tetraethylammonium salt. The formation of the $[(C_2H_5)_4N]^+$ cation from (C₂H₅)₃N in an acidic aqueous medium is logically possible when an ammonium cation (NH₄⁺) is formed in the overall reaction: $4(C_2H_5)_3N + 4H^+ \rightarrow 3[(C_2H_5)_4N]^+ +$ [NH₄]⁺. We have thus demonstrated the room temperature ammonia synthesis from a polyoxometalate solution, to which (C₂H₅)₃N vapour is diffused — a gas-liquid interfacial reaction. Although the resulting NH₄⁺ cation (identified by Nessler's reagent test) is not included in the crystals of compound 1, it can be made associated with a crown ether in the isolation of single crystals of compound $[NH_4 \subset B15C5]_3[PMo_{12}O_{40}] \cdot B15C5$ (2), (B15C5 = benzo-15-crown-5). ¹H NMR studies on compound 2 have established the presence of H-bonded NH₄⁺ ion in 2.



4.1 Introduction

Ammonia is an essential inorganic chemical for fertilizer industry, and is the sixth largest chemical, produced in the world¹⁻⁴ and the key precursor of synthetic fertilizer.⁵⁻⁷ Till now Haber's process is the frequently used method for industrial production of ammonia, which involves molecular nitrogen and hydrogen requiring a drastic condition (500 °C at 150-200 atm).⁸⁻¹⁰ In Nature, nitrogenase enzymes containing iron and molybdenum cofactors (known as FeMoco) does the job of production of ammonia from atmospheric nitrogen at an ambient condition.¹¹⁻¹³ There are various reports where ammonia is generated using transition-metal catalysed reduction of nitrogen gas,¹⁴⁻²⁴ as well as through electrochemical²⁵⁻³³ and photo(electro)chemical methods.³⁴⁻³⁸ We have demonstrated, here, a unique inorganic rearrangement (not a redox reaction), occurring at room temperature, that involves diffusion of triethylamine vapour into an acidic aqueous polyoxomolybdate solution to generate ammonium ion (NH₄⁺) and tetraethylammonium ion, [(C₂H₅)₄N]⁺ as shown in equation 4.1. The relevant experiment is an example of gas-liquid interfacial reaction, we reported earlier.³⁹

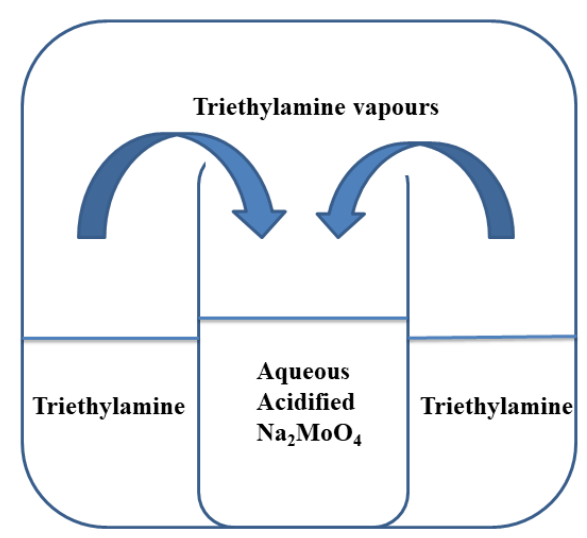
$$4(C_2H_5)_3N + 4H^+ \rightarrow 3[(C_2H_5)_4N]^+ + [NH_4]^+$$
 eqn. 4.1

There are quite a few inorganic rearrangement reactions reported. The Michaelis-Arbuzov rearrangement for the formation of C–P bonds,⁴⁰ intermolecular rearrangements in boron clusters,⁴¹ and rearrangement of polyamines⁴² are few of them. These rearrangement reactions have found immense applications in various fields. The rearrangement described here will be an addition to this family of inorganic rearrangement reactions as it demonstrates the rearrangement of triethylamine to tetraethylammonium ion and most importantly ammonium ions at room temperature.

Triethylamine is a colorless liquid (boiling point, 89.5°C), but it exists in the atmosphere in the gas phase. According to the United States Environmental Protection Agency (U.S. EPA), the concentration of triethylamine in an ambient air is as high as 4.2 µg/m³ or 1 part per billion from an unspecified location in the Northeast United States during 1983 (U.S. EPA, 1993a).⁴³ Thus, use of triethylamine in its vapour state to generate ammonia would be remarkable. In the present chapter, we have demonstrated the formation of ammonium ion from triethylamine vapour (eqn. 4.1) at room temperature; the work was initiated from a serendipitous observation (vide infra). We have characterized the resulting ammonium ion (NH₄⁺), formed in the rearrangement reaction (eqn. 4.1), by Nessler's reagent test, IR- and NMR-spectroscopy and TGA studies including elemental analysis. We have succeeded to manipulate the ammonium ion (NH₄⁺), formed in the rearrangement, to be associated with a crown-ether (benzo-15-crown-5 ≡ B15C5) in forming a ammonium-crownether supramolecular cation, is been crystallized with a Keggin type polyoxometalate anion $([PMo_{12}O_{40}]^{3-})$ resulting the single crystals compound in of $[NH_4 \subset B15C5]_3 [PMo_{12}O_{40}] \cdot B15C5$ (2).

4.2 Results and Discussion

4.2.1 Synthesis: Emergence of a Rearrangement Reaction



Scheme 4.1. A schematic representation of the experimental set-up for the synthesis of compound **1** in a gas-liquid interface reaction.

When we allowed the triethylamine vapours to diffuse slowly into an acidified aqueous solution of sodium molybdate (Scheme 4.1), it leads to the formation of single crystals of $[(C_2H_5)_3NH]_2[(C_2H_5)_4N][NaMo_8O_{26}]$ (1). Compound 1, as established from single crystal X-ray crystallography, includes triethylammonium cation, [(C₂H₅)₃NH]⁺ as expected and surprisingly, a tetraethylammonium cation [(C₂H₅)₄N]⁺, even though we have not used any tetraethylammonium salt in the concerned synthesis. In order to learn the source of $[(C_2H_5)_4N]^+$ cation, in the crystals of compound $[(C_2H_5)_3NH]_2[(C_2H_5)_4N][NaMo_8O_{26}]$ (1), we carefully investigated the whole experiment and relevant possible chemical reactions; we tetraethylammonium cation $[(C_2H_5)_4N]^+$ is formed from found out that, if the trimethylamine, (C₂H₅)₃N, then ammonium ion (NH₄⁺) has to be generated under an acidic condition as shown in equation 4.1. The presence of the ammonium ion in the concerned reaction mixture is confirmed using Nessler's reagent test (vide infra) and also by trapping the resulting ammonium ion with crown ether, forming a supramolecular adduct cation, which is stabilized and isolated with a polyoxometalate (POM) anion (vide infra).

As mentioned above, the diffusion of triethylamine vapours into the acidified solution of sodium molybdate gives compound 1. In the relevant reaction, we have used HNO₃ and HCl separately in two different experiments, to acidify the solution of sodium molybdate and the reaction mixture was set to a pH of 2.0-2.2. The presence of octamolydate isopolyanion, $[Mo_8O_{26}]^{4-}$ in compound 1 can be understood by the following reaction (eqn. 4.2) of protonation of molybdate anions followed by their condensation leading to the formation of octamolybdate POM anion.

$$8[MoO_4]^{2-} + 12H^+ \rightarrow [Mo_8O_{26}]^{4-} + 6H_2O$$
 eqn. 4.2

The coordination of this POM cluster anion with a sodium cation (Na⁺), readily available in the reaction mixture, resulting in [NaMo₈O₂₆]³⁻ anion. This needs three more cations to be isolated. This POM solution was exposed to triethylamine vapour, which on its diffusion to the acidified solution, gets protonated at the vapour-liquid interface forming $[(C_2H_5)_3NH]^+$ cation. We would not be surprised if the isolated compound 1 would have three $[(C_2H_5)_3NH]^+$ cations and have formula as $[(C_2H_5)_3NH]_3[NaMo_8O_{26}]$ (hypothetical); instead, compound 1 is characterized with two [(C₂H₅)₃NH]⁺ cations and one "unexpected" cation tertiaryammonium $[(C_2H_5)_4N]^+$ having the overall formula $[(C_2H_5)_3NH]_2[(C_2H_5)_4N][NaMo_8O_{26}]$ (1). The experiment clearly indicates that the tetraethylammonium cation, [(C₂H₅)₄N]⁺ has been generated from the triethylamine, $(C_2H_5)_3N$, which is only possible if we consider the following reaction:

$$4(C_2H_5)_3N + 4HA \rightarrow 3[(C_2H_5)_4N]A + NH_4A$$
 eqn. 4.3
(A= NO₃⁻ or Cl⁻; HA = HNO₃ or HCl).

Notably, one ammonium ion NH_4^+ is generated in this reaction (eqn. 4.3), which is not included in the crystals of compound $[(C_2H_5)_3NH]_2[(C_2H_5)_4N][NaMo_8O_{26}]$ (1).

In order to validate the above-described reaction (eqn. 4.1 or 4.3), thereby, to authenticate the crystal structure of compound $\mathbf{1}$ (or to prove the formation of tetraethylammonium cation from triethylamine), we need to prove the existence of ammonium cation, NH_4^+ (which is not picked up by compound $\mathbf{1}$ during its crystal formation) in the pertinent reaction mixture. The most classical and confirmative test for an ammonium ion (NH_4^+) in an aqueous solution is the Nessler's reagent test as described below for the NH_4^+ , formed in the rearrangement reaction (eqn. 4.1 or 4.3).

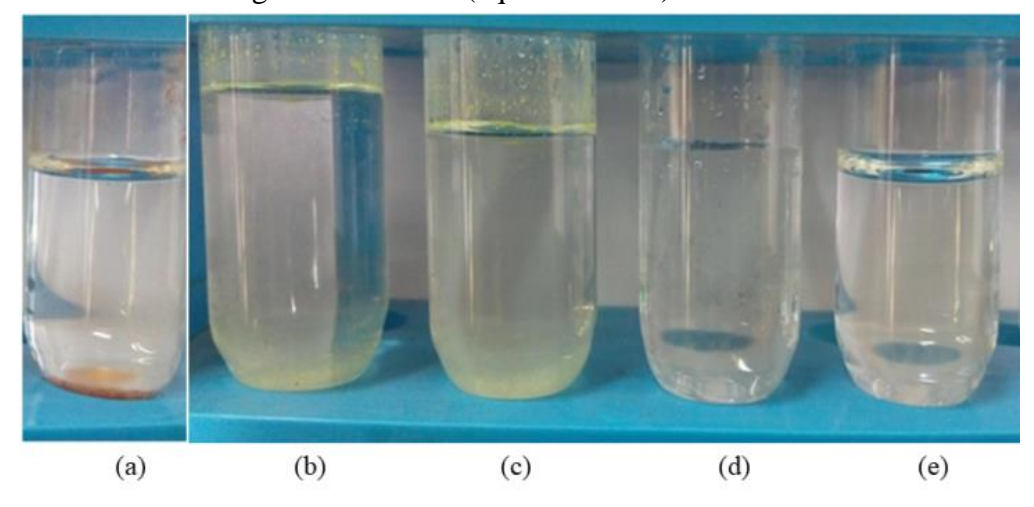


Figure 4. 1. Nessler's reagent test: (a) with ammonium chloride solution. (b) with filtrate containing HNO₃ acid, (c) with filtrate containing HCl acid, (d) with filtrate containing HNO₃ acid but without sodium molybdate, and (e) with sole water.

The Nessler's regent test was performed on different solutions in order to detect the presence of ammonium ions in the reaction mixture. First, as a reference, the reagent was added to an ammonium chloride aqueous solution, and as expected, a brown precipitate of $HgO\cdot Hg(NH_2)I$ was observed as shown in Figure 4.1(a). Then the filtrate, obtained after filtering the compound $[(C_2H_5)_3NH]_2[(C_2H_5)_4N][NaMo_8O_{26}]$ (1) crystals from the reaction

mixture (when the used acid was nitric acid), was treated with few drops of Nessler's reagent and an yellow coloration was observed in the test-tube as shown in Figure 4.1(b); similarly, the test was performed also with the filtrate, where HCl acid was used in the place of HNO₃ and there also an yellow coloration was observed (Figure 4.1(c)), as observed in the case of HNO₃ acid-molybdate reaction mixture. This yellow coloration instead of a brown precipitate (found in the case of Nessler's regent test with NH₄Cl solution) is a result of the brown coloration being affected by dilution. This is because, in the cases of diffusion of triethylamine vapour into the acidified sodium molybdate solution, a tiny amount of ammonium ions is formed.

The formation of compound 1 and ammonium ion (eqn. 4.3), irrespective of which acid (HNO3 and HCl acids) has been used, rules out the possibility of the formation of ammonium ions from nitrate ions, which again is a reaction, that occurs in drastic conditions. 44 To check the role of sodium molybdate in the reaction, a controlled reaction was performed, at similar conditions with HNO₃ / HCl, but sodium molybdate was not added into it; the resulting reaction yielded no crystals, as expected and also there was no coloration or precipitate observed upon addition of Nessler's reagent to the concerned reaction mixture (Figure 4.1(d)). Nessler's reagent was also added to pure water, to check the purity of the reagent, and no change was observed as can be seen in Figure 4.1(e). Thus, sodium molybdate plays a major role in the formation of the tetraethylammonium ion and in turn the ammonium ion (eqns. 4.1 and 4.3); although the exact role of sodium molybdate with mechanism is not clear.

A careful investigation on the eqn. 4.3, showing the formation of one equivalent of ammonium cation (NH₄⁺) and three equivalents of tetraethylammonium ((C₂H₅)₄N⁺) cations from four equivalents of triethylamine ($(C_2H_5)_3N$) under an acidic condition, clearly indicates that one equivalent of $(C_2H_5)_3N$ for every four equivalents of $(C_2H_5)_3N$ splits (or rearranges) into three equivalents ethyl cation $(3C_2H_5^+)$ and one equivalent nitride anion (N^{3-}) as shown in eqn. 4.4, showing breaking of three N–C bonds.

$$(C_2H_5)_3N: \rightarrow 3C_2H_5^+ + :N^{3-}$$
 eqn. 4.4

Then the rest three triethylamine molecules $\{3(C_2H_5)_3N:\}$, each having a lone pair of electrons on nitrogen, coordinates to the three ethyl cations (3C₂H₅⁺) formed in eqn. 4.4, resulting in three tetraethylammonium cations $3[(C_2H_5)_4N]^+$ as shown in eqn. 4.5 showing making of three N–C bonds.

$$3(C_2H_5)_3N: \rightarrow 3C_2H_5^+ = 3[(C_2H_5)_4N]^+$$
 eqn. 4.5

The nitride anion (N³⁻), formed in eqn. 4.4, accommodates four protons (the overall reaction is performed in an acidic condition) producing one ammonium (NH₄⁺) ion as shown in eqn. 4.6, showing making of four N-H bonds.

$$:N^{3-} + 4H^{+} = NH_{4}^{+}$$
 eqn. 4.6

So, the overall reaction of formation of one ammonium ion and three tetraethylammonium cations from four triethylamine molecules and four protons (eqn. 4.1 or eqn. 4.3) is the result of 4 N–H bonds formation (the number of N–C bond breaking is equal to number of N–C bond making). This is why eqn. 4.1 or 4.3 is probably thermodynamically feasible.

4.2.2 Serendipitous Observation: Crystal Structure Analysis

A gas-liquid interface reaction, wherein the vapours of a volatile organic amine is diffused into an acidified molybdate solution generating polyoxometalate (POM) cluster is a very simple synthetic approach to obtain a POM cluster containing compound, we developed recently.³⁹ Thus, diffusion of pyridine (py) and piperidine (pip) into an acidified aqueous solution of sodium molybdate results in the isolation of single crystals of pyridinium and piperidinium salts of octamolybdate, [pyH]₄[Mo₈O₂₆] and [pipH]₄[Mo₈O₂₆]·4H₂O, respectively. This synthetic strategy has been described as a "potential bag filter for volatile organic amines". This has an important implication in the sense that volatile amine vapours are serious threats to human health.³⁹ We wanted to rationalize this concept by taking other volatile amine and we used triethylamine vapours, in the present work, to diffuse into an acidified aqueous solution of Na₂MoO₄ and we obtained the single crystals of compound $[(C_2H_5)_3NH]_2[(C_2H_5)_4N][NaMo_8O_{26}]$ (1). We have made a serendipitous observation while analyzing the single crystal X-ray structure of compound 1. We found a tetraethylammonium cation [(C₂H₅)₄N]⁺ per formula unit of compound **1** in its crystal structure, even though we have not used any tetraethylammonium salt in the relevant synthesis.

Compound	1	2
Formula	$C_{20}H_{52}Mo_8N_3NaO_{26}$	$C_{56}H_{92}Mo_{12}N_3O_{60}P$
Formula weight	1541.14	2949.56
Temperature (K)	296	273(2)
Wavelength (Å)	0.71073	0.71073
Crystal system, space group	Monoclinic, C 2/c	Triclinic, P-1
a (Å)	24.9768(13)	13.6148(15)
<i>b</i> (Å)	11.1607(5)	14.8087(17)
<i>c</i> (Å)	18.0093(9)	25.588(3)
α (deg)	90	100.368(2)
β (deg)	120.271(2)	97.571(2)
γ (deg)	90	111.955(2)
Volume (ų)	4335.7(4)	4593.3(9)
$Z, \rho (g/cm^3)$	4, 2.358	1, 2.159
$\mu \ (\mathrm{mm}^{-1})$	2.332	1.707
F(000)	3900.0	2920.0
goodness-of-fit on F2	1.178	1.046
<i>R1</i>	0.0364	0.0755
wR2	0.1046	0.2033
Largest diff. peak/hole (e Å ⁻³)	3.65	7.29

Table 4.1. Crystal parameters of compounds 1 and 2.

Compound 1 crystallizes in a monoclinic C2/c space group. The asymmetric unit of the compound consists of half of an octamolybdate cluster, i.e., {Mo₄O₁₃}²⁻ unit, of which, four

surface oxygens being coordinated to a Na+ cation with half occupancy forming {Na_{0.5}Mo₄O₁₃}^{1.5} unit, a protonated triethylamine cation and half of a tetraethyl ammonium cation as shown in Figure 4.2(a).

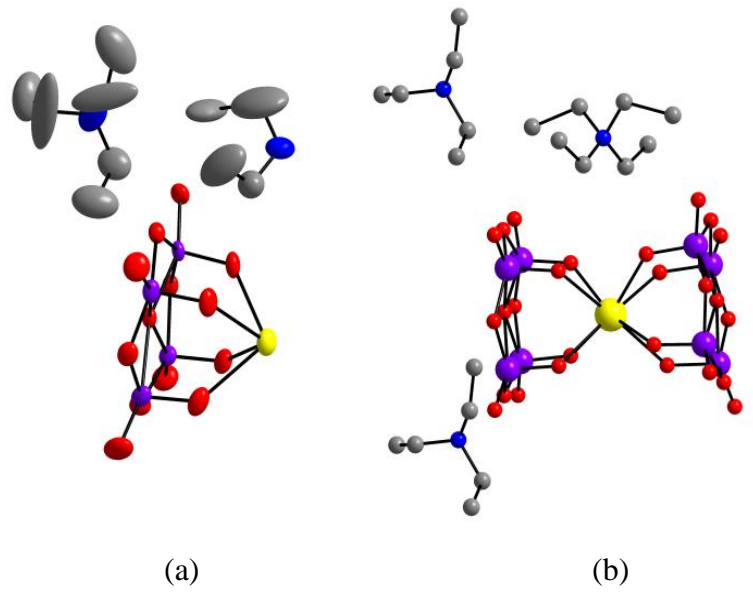


Figure 4.2. (a) The thermal ellipsoidal plot of the asymmetric unit in the crystal structure of compound 1 at the 50% probability level. (b) Full molecule of compound 1 showing that two different halves of two different $[Mo_8O_{26}]^4$ clusters are coordinated to a central Na^+ ion. Hydrogen atoms are not shown for clarity. Color code: Mo, purple; Na, yellow; O, red; N, blue; C, gray.

Accordingly, in the full molecule, two halves of the two different clusters coordinating to a common sodium ion, a tetraethylammonium cation and two protonated triethylamine cations are present as shown in Figure 4.2(b). Thus, in the crystal structure of compound 1, an octamolydate cluster anion coordinates to two Na⁺ ions from its opposite sides (each side, four surface terminal oxygen (O_t) atoms of the octamolybdacluster coordinate to sodium ion) resulting in the formation of a chain-like one-dimensional coordination polymer. Along this on-dimensional chain, each sodium ion is eight coordinated; the sodium ions are arranged in a zig-zag fashion throughout the molecular structure (Figure 4.3). The relevant Na⁺–O bond distances vary in between 2.545 to 2.666 Å.

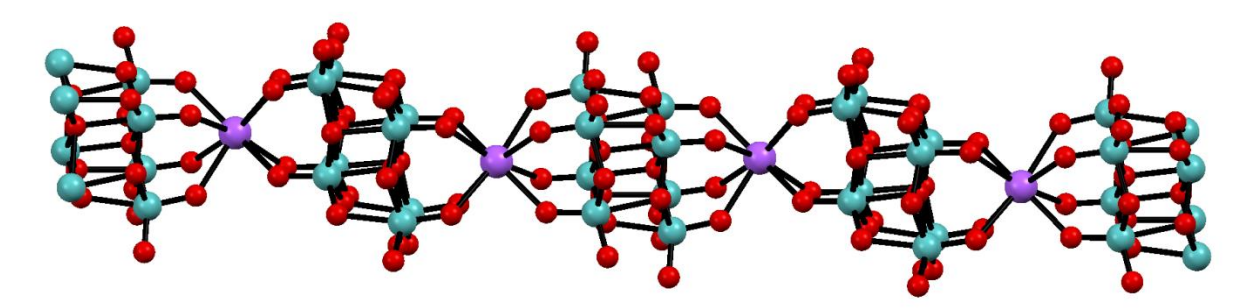


Figure 4.3. One-dimensional chain, formed by octamolybdate isopolyanions that coordinate to the Na⁺ ions.

The tetraethylammonium cation and some of the cluster oxygen atoms are hydrogen bonded to each other leading to a 3D supramolecular array in the crystal structure of compound 1. So, this serendipitous observation of a tetraethylammonium cation, $[(C_2H_5)_4N]^+$ in the crystals of compound 1 gives rise to the emergence of a new rearrangement reaction (eqn. 4.1), as already mentioned earlier.

$$4(C_2H_5)_3N + 4H^+ \rightarrow 3[(C_2H_5)_4N]^+ + [NH_4]^+$$
 eqn. 4.1

It is not surprising that the ammonium ion, produced in the rearrangement (eqns. 4.1) or 4.3), are not included in the crystals of compound 1, because the cations $[(C_2H_5)_3NH]^+$ and [(C₂H₅)₄N]⁺, present in the concerned reaction mixture with NH₄⁺ ion, are bulkier than NH₄⁺ ion. However, the ammonium ion in the mother liquor of compound 1 crystals can be associated with the crown ether, benzo-15-crown-5 (B15C5) when the mother liquor of compound 1 crystals is treated with B15C5 crown ether and a Keggin type polyoxometalate (POM) anion. More specifically, the $[NH_4^+ \subset B15C5]$ supramolecular cationic species forms a cation-anion adduct with [PMo₁₂O₄₀]³⁻ Keggin anion in an acidified organic medium leading to the isolation of single crystals of compound [NH₄⊂B15C5]₃[PMo₁₂O₄₀]⋅B15C5 (2). The asymmetric unit in the crystal structure of compound 2, which crystallizes in P-1 space group (triclinic, Z' = 1), consists of two halves of $[PMo_{12}O_{40}]^{3-}$ Keggin anion, three ammonium ion associated benzo-15-crown-5 crown ether supramolecular cations and one benzo-15 crown-5 as such, without any ammonium ion. Thus, the asymmetric unit represents the full molecular formula of compound [NH₄ \subset B15C5]₃[PMo₁₂O₄₀]·B15C5 (2) in this case (Figure 4.4). All the three ammonium ions (N1, N3 and N4 nitrogen atoms in the crystal structure, shown in Figure 4.5), are not present in the crown ether cavities, and have different hydrogen bonding environments. N4 ammonium ion interacts with Keggin POM anion (terminal oxygen atom) besides its hydrogen bonding interactions with the crown ether molecule. On the other hand, the N1 and N3 ammonium ions, besides their interactions with two different crown ether molecules, are hydrogen bonded to a common crown ether molecule as shown in Figure 4.5. Thus, we could characterize the NH₄⁺ ion, formed in the rearrangement reaction (eqn. 4.1 or 4.3), crystallographically in the crystals of compound [NH₄⊂B15C5]₃[PMo₁₂O₄₀]·B15C5 (2). It is surprising that compound 2 crystals include NH₄⁺ cation instead of [(C₂H₅)₃NH]⁺ and [(C₂H₅)₄N]⁺ cations, that are also present with NH₄⁺ ion in the concerned filtrate of compound 1 crystals. This can be understood by the fact that NH₄⁺ cation–crown ether association seems to be much stronger than [(C₂H₅)₃NH]⁺– and $[(C_2H_5)_4N]^+$ -crown ether associations because of the formation of N-H···O hydrogen bonds (NH₄⁺ can form four H-bonds, [(C₂H₅)₃NH]⁺ can form only one H-bond and [(C₂H₅)₄N]⁺ cannot form any N-H···O bond). The rearrangement reaction (eqn. 4.1 or 4.3) is not only characterized by Nessler's reagent test and single crystal X-ray crystallography, but also by various spectral studies (IR and ¹H NMR studies) including TGA analysis as described in the following sections.

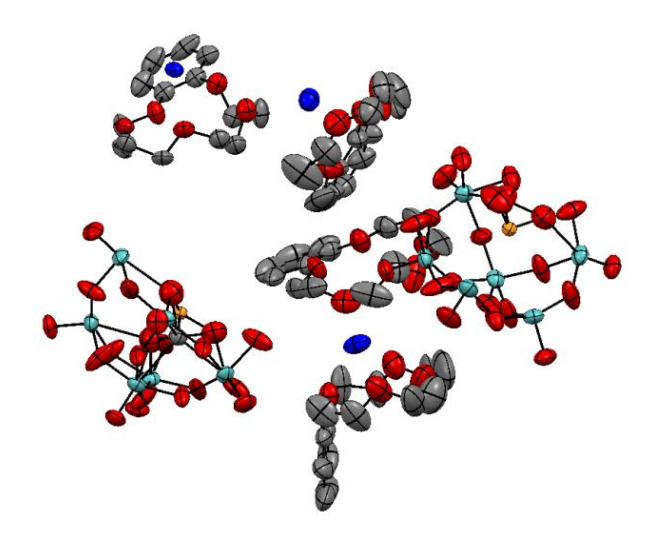


Figure 4.4. The thermal ellipsoidal plot of asymmetric unit in the crystal structure of compound 2 at the 50% probability level, representing the full molecule. Hydrogen atoms are omitted for clarity. Color code: Mo, cyan; O, red; C, gray; P, orange; N, blue.

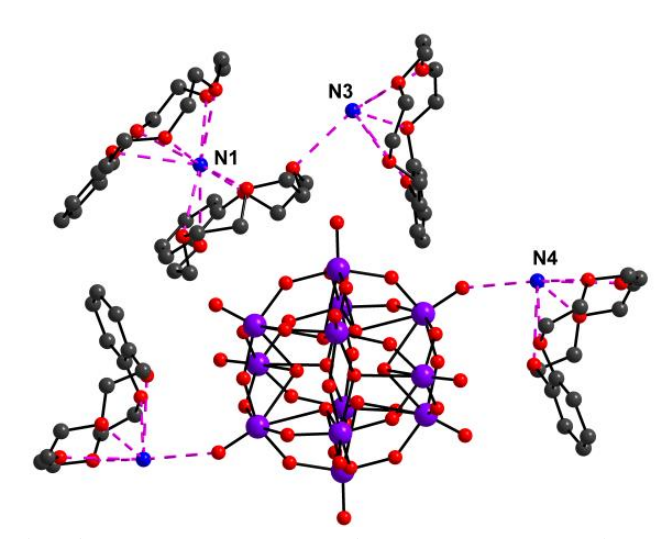


Figure 4.5. Hydrogen bonding interactions around ammonium ions in the crystal structure of compound $[NH_4 \subset B15C5]_3[PMo_{12}O_{40}] \cdot B15C5$ (2). Purple dotted lines represent $N-H\cdots O$ H-bonding interactions.

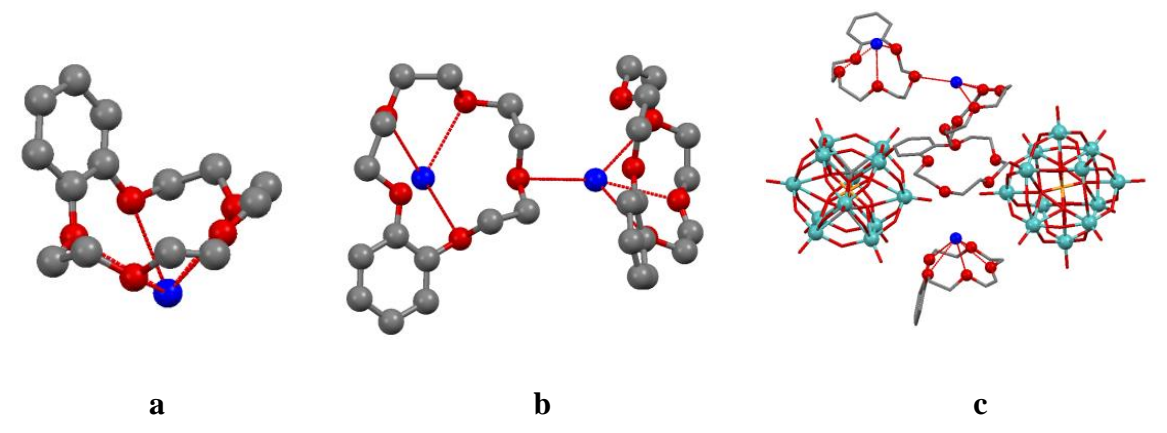


Figure 4.6. (a) The cradle shaped ammonium ion encapsulated benzo-15-crown-5 (b) H-bonding interactions between the ammonium ion and the crown ether oxygen atoms (c) The overall molecule and the weak interactions binding the molecule together. (Colour code: Cyan: molybdenum; red: oxygen; grey: carbon; blue: nitrogen).

The association of the ammonium ions in the three different benzo-15-crown-5 pockets is different (Figure 4.6). In one of the crown ethers, which acquire a chair conformation, the benzo group is raised as the back of the chair, forming an angle of ~101.44⁰. The ammonium ion is located in the pocket, and is connected through hydrogen bonding interactions, between the hydrogen atoms of the ammonium ion and the etheral oxygen atoms. The nitrogen atom of ammonium ion is not placed at the base of the crown ether plane; rather it is positioned below the basal plane of the oxygen atoms of the crown ether at a distance of ~2.9Å. The overall NH₄⊂ B15C5 looks like a cradle (Figure 4.6a). This crown ether, however, is not associated through hydrogen bonds with the Keggin anion through its methylene hydrogens. In a second crown ether-ammonium ion system, the ammonium ion is hydrogen bonded only to three ethereal oxygens of the crown ether from one side and is connected to a fourth oxygen atom of the neighbouring crown ether. The three hydrogen atoms which lie in a plane of the ammonium ion are connected to the three oxygen atoms of one crown ether at an angle of 56.48° and 58.18° (Figure 4.6b). Similarly the third ammonium ion is also connected through H-bonding interactions with the etheral oxygen atoms. All these hydrogen bonds are in the range of 2.5 to 3.1 Å. The crown ethers also interact with the oxygen atoms of the polyoxometalate anion through weak interactions between the hydrogen atoms of crown ether and the terminal as well as bridging oxygen atoms of the polyoxometalate, thus resulting in an overall stable structure (Figure 4.6c).

4.2.3 Spectroscopy

IR Spectroscopy. The FTIR spectrum of compound 1 is shown in Figure 4.7(a). The vibrational features of the octamolybdate isopolyanion are clearly seen in the IR spectrum of the compound (Figure 4.7b). The strong peak observed at 955 and 730 cm⁻¹ is accredited to the Mo-O_t asymmetric stretch and Mo-O_b-Mo bond asymmetric stretch respectively. The peaks at 730, 780, 838 and 898 cm⁻¹ can be attributed to the asymmetric stretch of Mo-O_b bond. All the above said features match with the reported values for the β-isomer of the octamolybdate. 45-46 The strong peak observed at 1214 cm⁻¹ is attributed to the C-N stretch. The two prominent peaks at 1380 and 1470 cm⁻¹ are assigned to CH₂ and CH₃ bending of the ethyl groups and the peaks at 2872 and 2968 cm⁻¹ are for C-H stretch. In the FTIR spectrum of compound 2 (Figure 4.7c), the peak at 3182 cm⁻¹ can be attributed to the stretching frequency of the N-H bonds of the NH₄⁺ions. Similarly, bending motions of the N-H bonds give their signature peaks at 1356 cm⁻¹. Peak at 2916 cm⁻¹ is actually a multiplet centred on this point. These peaks can be attributed to the alkyl C-H stretch, which are present in the crown ethers. The various peaks around 778, 892, 978, 1053, 1077 cm⁻¹ can be attributed to the stretching frequencies of Mo-O_c-Mo, Mo-O_b-Mo, Mo=O_t and the P-O bonds, respectively of the Keggin cluster anion (Figure 4.7d).⁴⁷

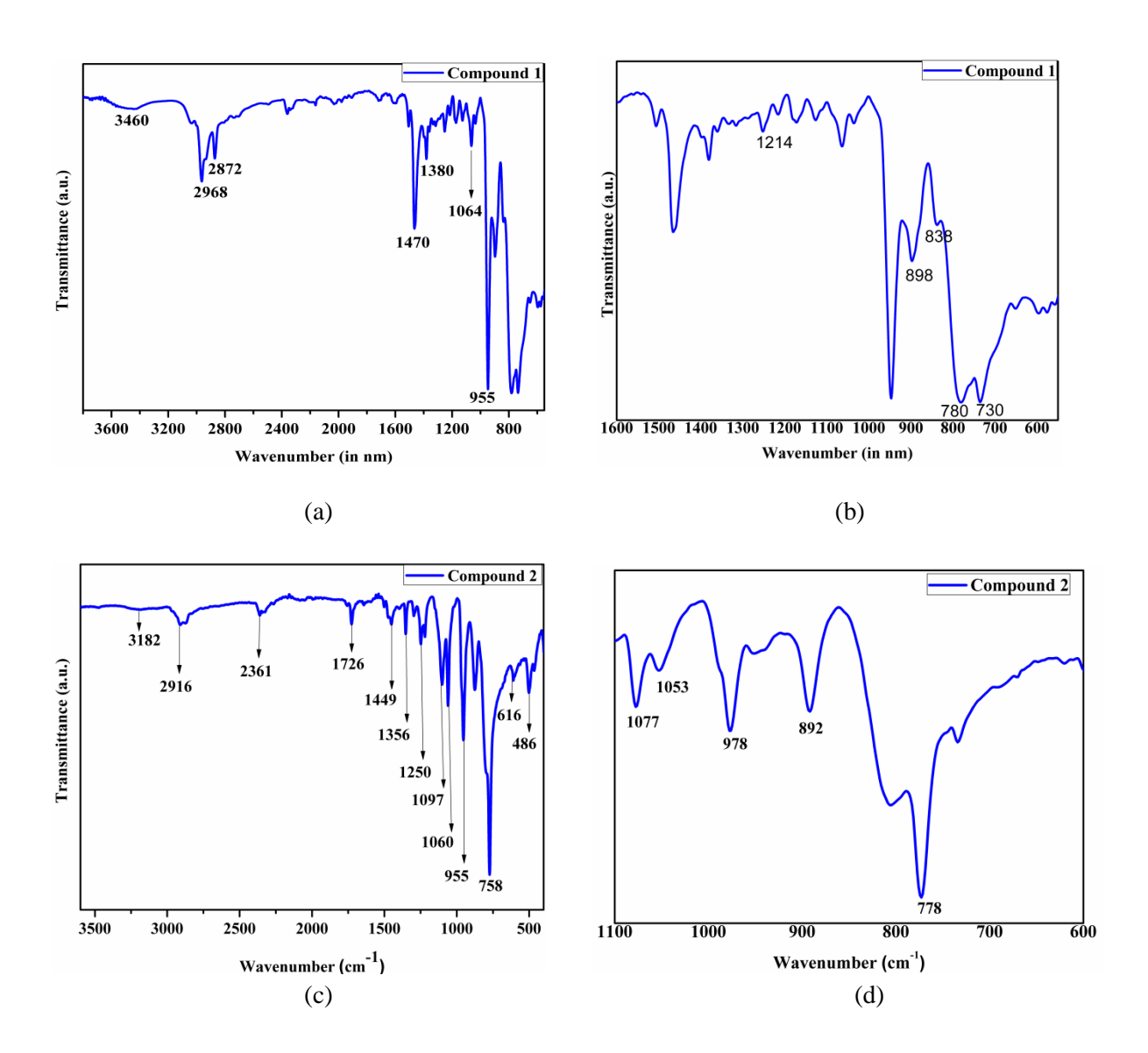


Figure 4.7. FT-IR spectra of compound 1 ((a) and (b)) and compound 2 ((c) and (d)).

 ^{1}H ^{1}H **NMR** Spectroscopy. The **NMR** of compound spectrum $[NH_4 \subset B15C5]_3[PMo_{12}O_{40}] \cdot B15C5$ (2), is recorded at room temperature in DMSO- d_6 and is given in Figure 4.8. NH₄Cl in DMSO- d_6 generally exhibits a strong singlet at δ 7.49 is seen, ⁴⁸ although, due to the coupling of ¹H to the ¹⁴N quadrupolar nucleus, it should give a triplet of equal intensity. 49 But, in practice, due to the tetrahedral structure of NH₄⁺ cation, we see only a narrow line for ¹⁴NH₄⁺. In the case of compound 2, due to H-bonding interactions of the NH₄⁺ cations with the crown ether as well as with the polyoxometalate anion, the NH₄⁺ does not retain its tetrahedral structure and hence, by virtue of quadrupolar coupling, it shows triplets of equal intensity between δ 6.97 to 7.35 as shown in Figure 4.8. The signal get shifted up-field probably due to the shielding created by lone pairs on oxygen atoms of the crown ether, around the ammonium cation inside the crown ether cavity. The full ¹H NMR spectrum of NH₄Cl and B15C5 in DMSO-D₆ are provided in Figures 4.9 and 4.10 respectively.

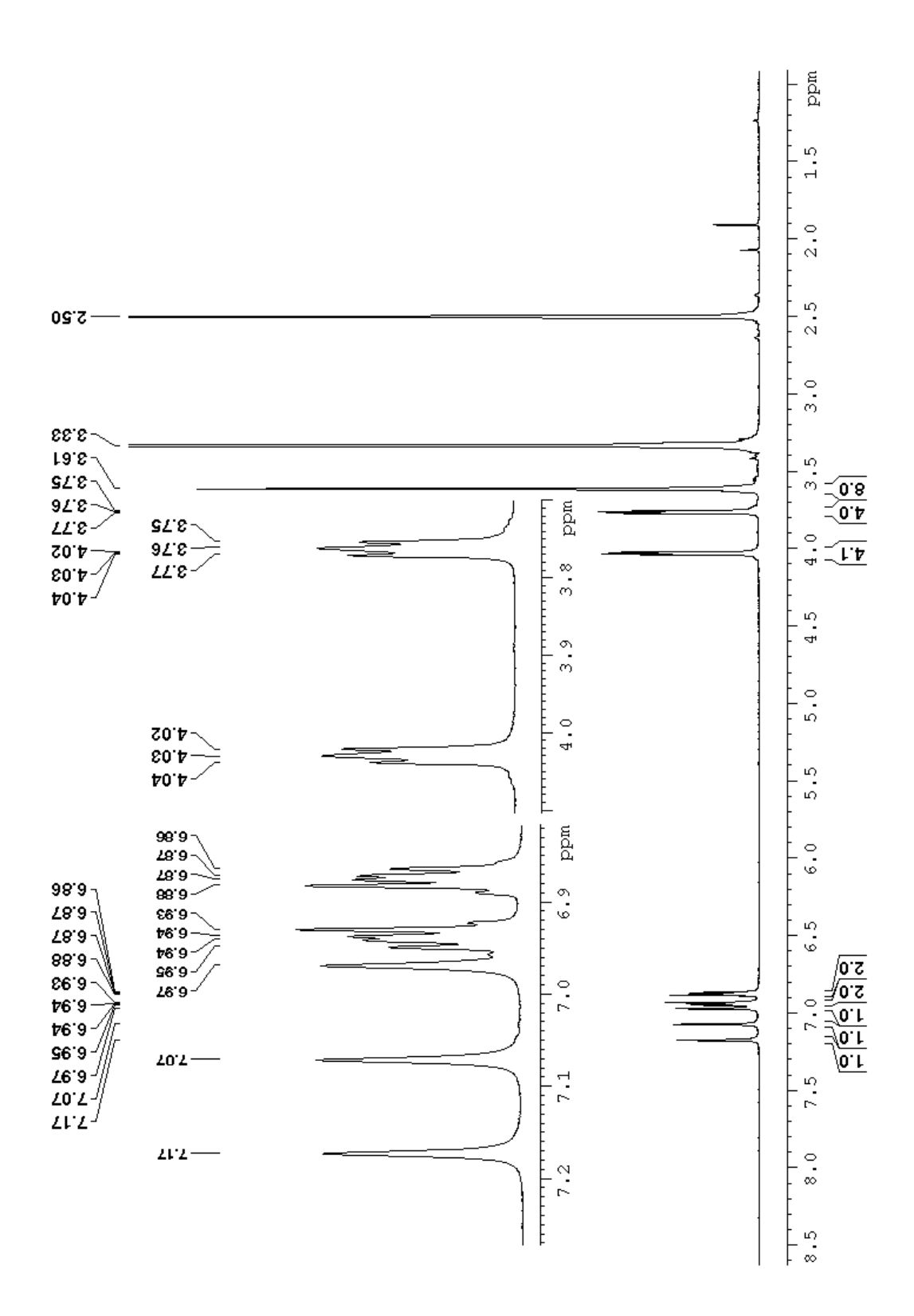


Figure 4.8. ¹H NMR spectrum of compound 2 in DMSO-D₆. The inset shows the region where the peaks of crown ether and the ammonium ion triplet appear.

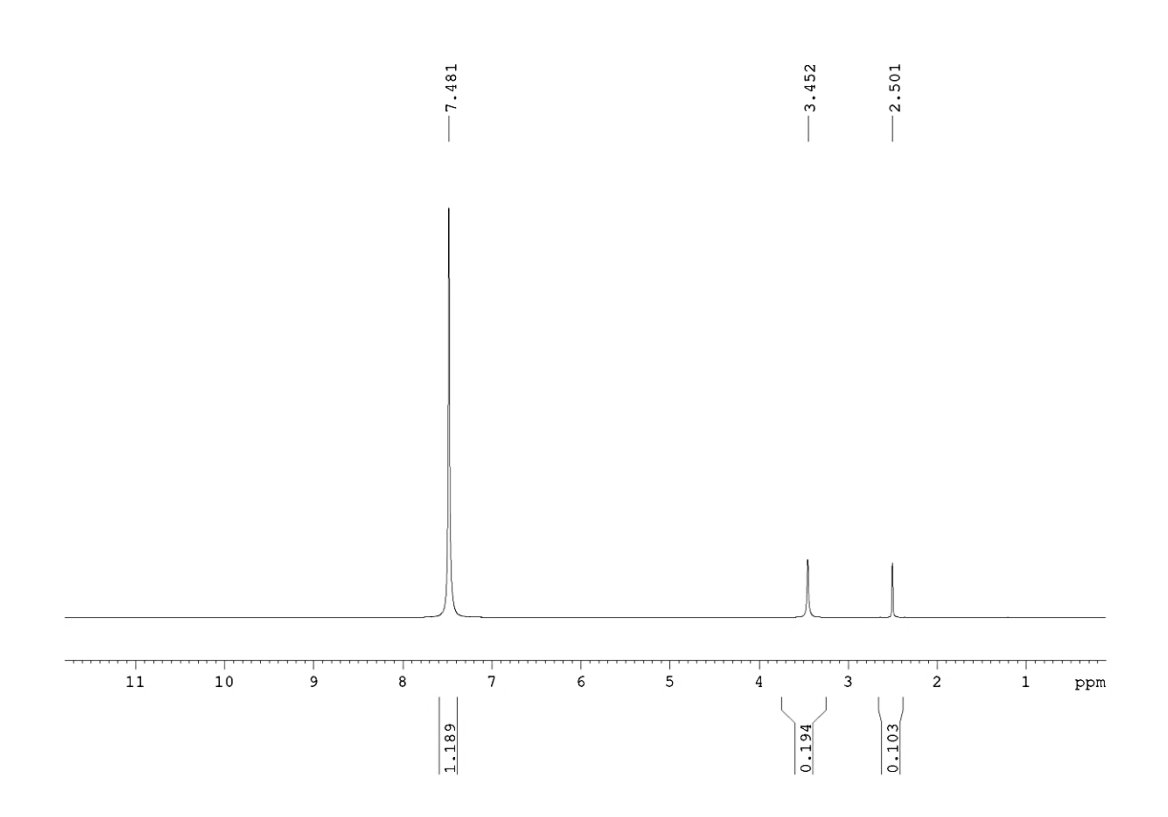


Figure 4.9. ¹H NMR spectrum of compound of NH₄Cl in DMSO-D₆.

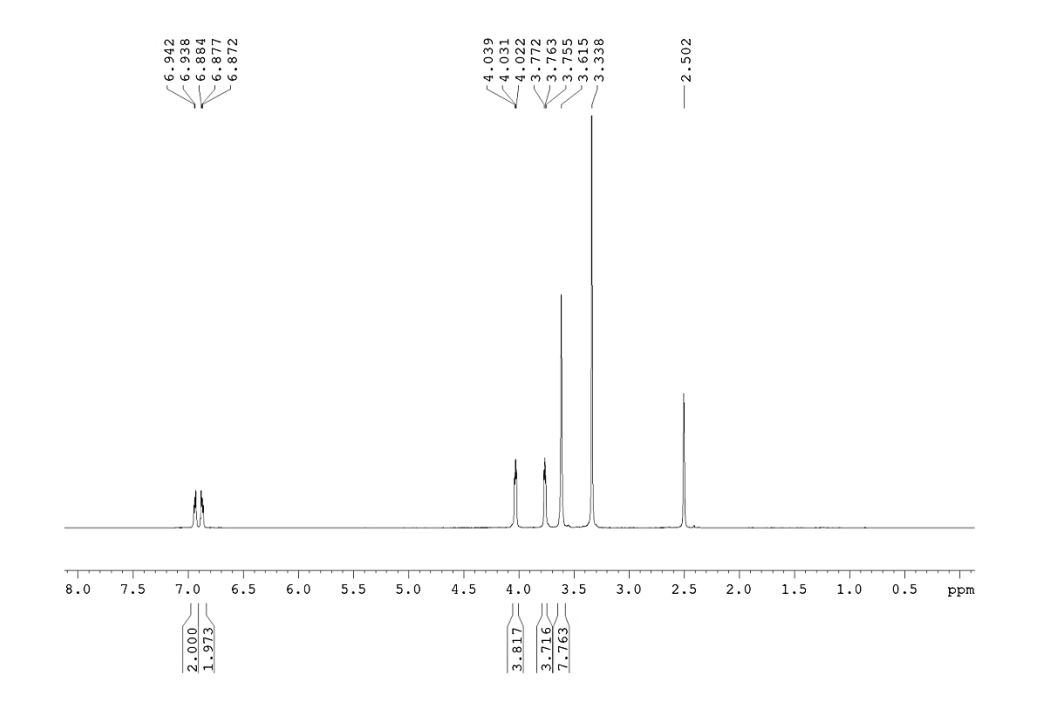


Figure 4.10. ¹H NMR spectrum of compound of benzo-15-crown-5 in DMSO-D₆.

4.2.4 Thermogravimetric Analysis and Powder X-Ray Diffraction Analysis

Thermal stability of both the compounds was evaluated using TG analysis and the relevant plots are shown in Figure 4.11. In compound **1**, the organic cations, *viz.*, the two protonated trimethylamine and the tetraethylamine are decomposed around 100 °C to around 370 °C, followed by the breaking up of the Na⁺–octamolybdate 1-D chain, hence leaving the metal oxides (sodium oxide and molybdenum oxide) in the further temperature range. The thermal stability of compound **2** was also checked and represented in Figure 4.11b. The ammonium ions that are arrested by the crown ether moieties are liberated first upon heating up to almost 150 °C, followed by the crown ether molecules in the temperature range of 280-580 °C. Then the Keggin polyoxometalate anion remains in the crucible and stable up to 700°C. After this temperature, the Keggin cluster starts decomposing.

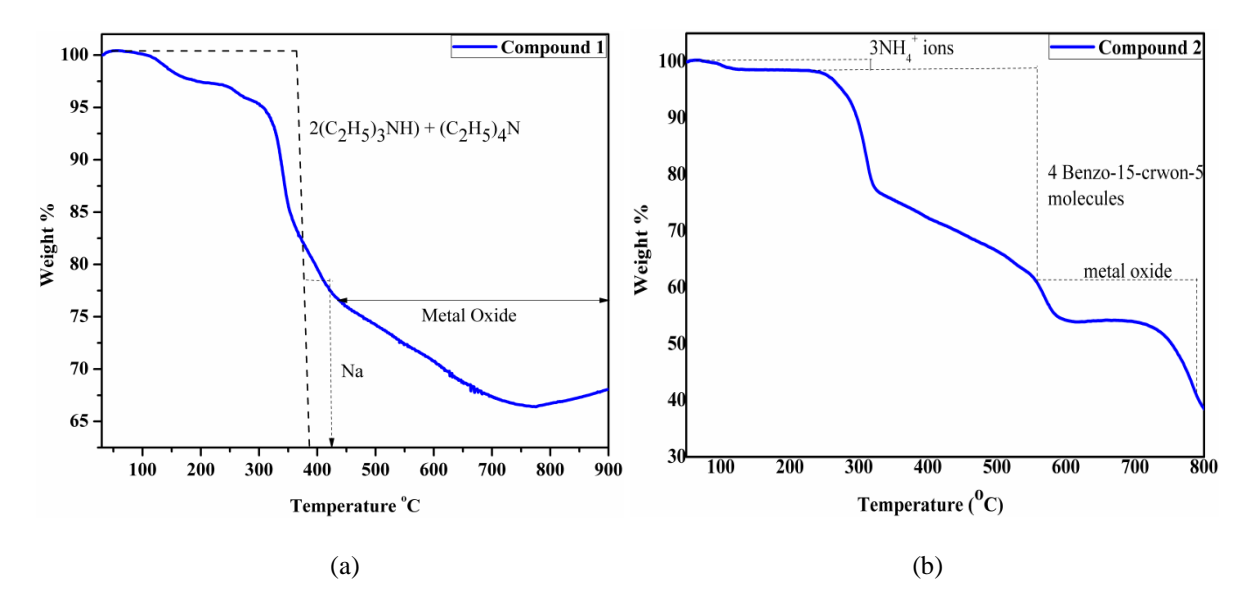


Figure 4.11. TGA Plots of (a) compound 1 and (b) compound 2.

The X-ray powder diffraction data for both compounds 1 and 2 have been recorded, to confirm the phase purity. The observed diffraction pattern and the simulated diffraction patterns were consistent, thus confirming the bulk purity of the crystalline solids, as shown in Figure 4.12.

4.2.4 EXAFS and CHN Analysis

The EXAFS and CHN analysis of compound **2** were recorded and are shown in Figure 4.13 and 4.14, which confirms the presence of ammonium cations by proving the presence of nitrogen atoms in the compound.

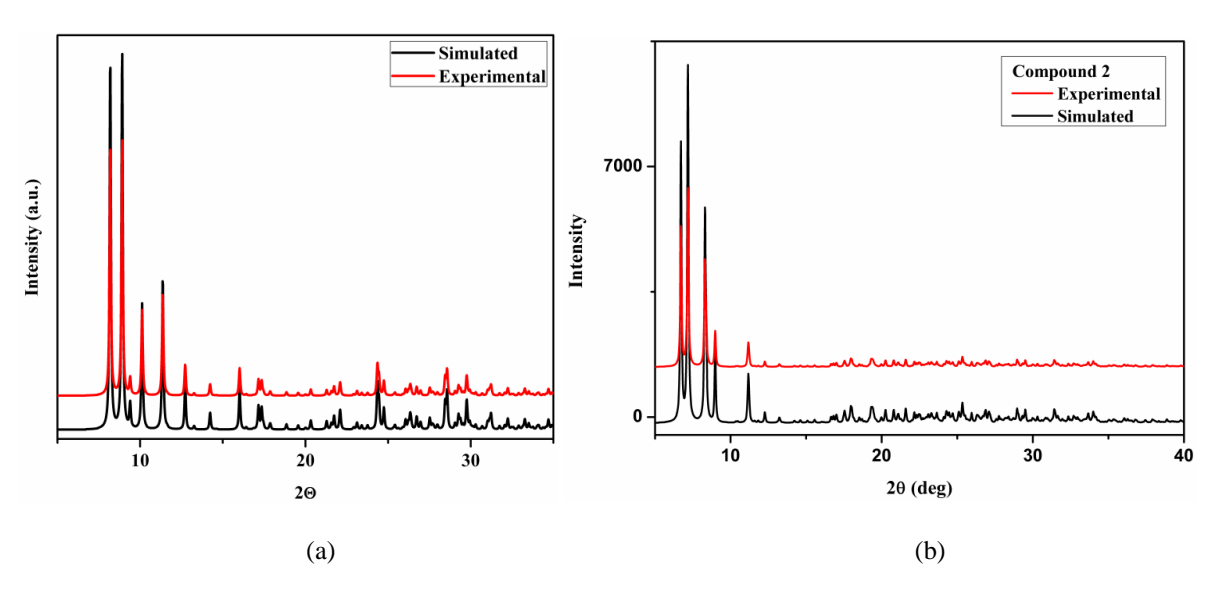


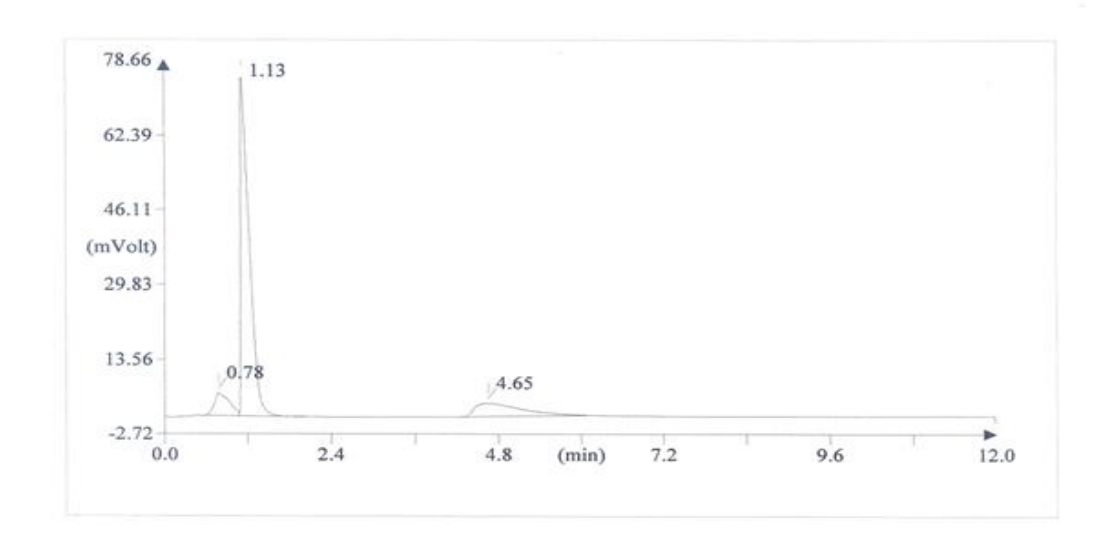
Figure 4.12. Observed and simulated PXRD patterns of (a) compound 1 and (b) compound 2.

FLASH EA 1112 SERIES CHN REPORT THERMO FINNIGAN

Method filename: Sample ID: Analysis type: Chromatogram filename: Sample weight: C:\Program Files\Thermo Finnigan\Eager 300 for EA1112\DATA\Sys_data_ex PL-1 (# 52)

PL-1 (# 52) UnkNown UNK-11042018-2.dat

2.011



Element Name	Element %	Ret. Time
Vitrogen	1. 36	0. 78
Carbon	23. 05	1. 13
Hydrogen	3. 18	4, 65

Figure 4.13. CHN Analysis Data of Compound 2.

The major finding of this work is that we have established a unique rearrangement reaction $4(C_2H_5)_3N + 4H^+ \rightarrow 3[(C_2H_5)_4N]^+ + [NH_4]^+$ (eqn. 4.1)

producing ammonium ions at room temperature from triethylamine in an acidic aqueous polyoxometalate solution. Thus the present system, where no ammonia has been used, but triethylamine is diffused, shows the abundance of ammonium ion which has been established not only by elemental analyses (Figure 4.13), Nessler's regent test, thermal analysis, *EDAX* analysis (Figure 4.14, Table 4.2), but also by ¹H NMR spectroscopy as well as single crystal X-ray crystallographic studies.

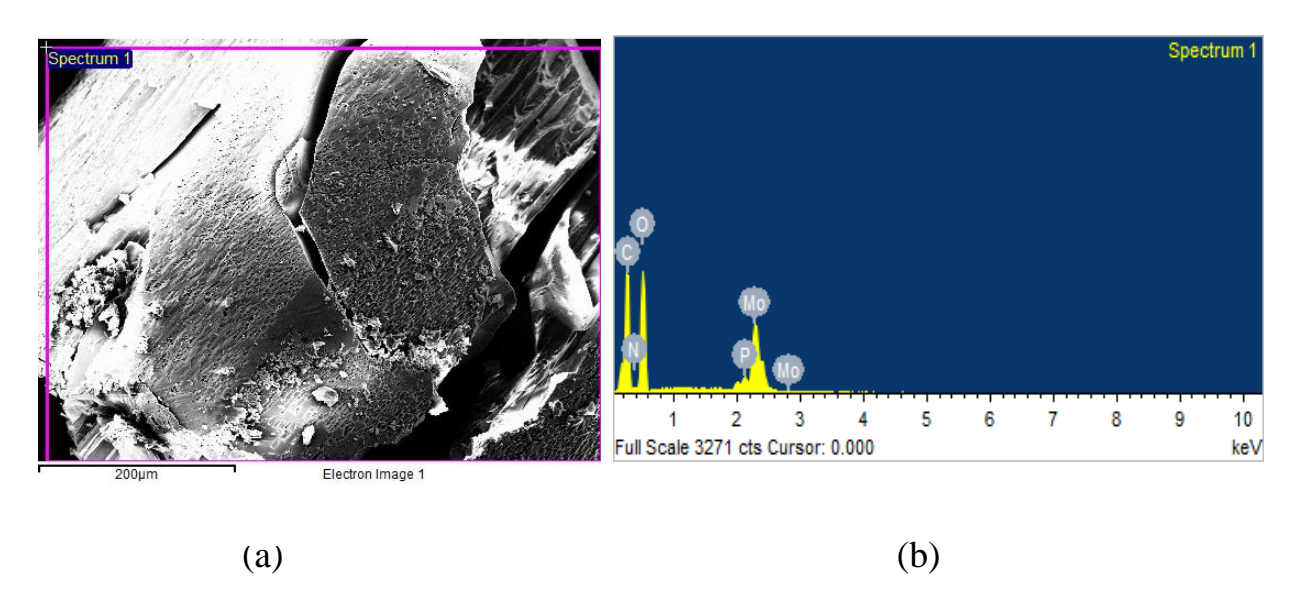


Figure 4.14. (a) The area under observation in EDAX analysis for compound $[NH_4 \subset B15C5]_3[PMo_{12}O_{40}] \cdot B15C5$ (2). (b) The EDAX plot of compound 2.

Element	Weight%	Atomic%		
СК	36.72	55.89		
NK	2.03	2.65		
ОК	31.15	35.59		
P K	0.33	0.20		
Mo L	29.77	5.67		
Totals	100.00			

Table 4.2. EDAX analysis of compound 2

4.3 Conclusion

Nature uses nitrogenase enzyme containing iron and molybdenum cofactors and produces ammonia from aerial nitrogen at an ambient condition. There are considerable numbers of efforts, reported to demonstrate ammonia from elemental nitrogen and hydrogen chemically, electrochemically and photo-chemically. We have demonstrated a hitherto unknown unique and fundamental rearrangement reaction that generates ammonium ion at room temperature from triethylamine simply by diffusion of the later into an acidified solution of sodium molybdate. The *in situ* formed polyoxometalate plays a vital role in the

generation of ammonium ions, which is serendipitous in nature. Although we could not establish yet the quantification of ammonia, generated in this reaction, still it provides a unique rearrangement reaction for the generation of ammonia from triethylamine at an ambient condition.

4.4 Experimental Section

4.4.1 Synthesis

Synthesis of [(C₂H₅)₃NH]₂[(C₂H₅)₄N][NaMo₈O₂₆] (1)

Sodium molybdate (3.5 g, 14.46 mmol) was dissolved in 50 mL of water. To this solution was added 10 mL of glacial acetic acid (100%) with stirring at room temperature. The reaction mixture was then acidified to pH 2 by the drop-wise addition of conc. HNO_3 , resulting in an almost clear solution. The resultant solution is filtered into a 100 mL beaker. This 100 mL beaker was then kept in a 250 mL beaker containing triethylamine liquid and closed by aluminium foil. The setup was then kept at room temperature for three days. The crystals of compound 1, that precipitated during this time, were filtered, washed with cold distilled water and dried at room temperature. Yield: 1.6 g (59% based on Mo). Anal. calcd. (in %) for $C_{20}H_{52}Mo_8N_3NaO_{26}$: C, 15.59; H, 3.40; N, 2.73. Found: C, 14.08; H, 2.95; N, 2.10.

Synthesis of [NH4⊂B15C5]3[PM012O40]-B15C5 (2)

To a solution of benzo-15-crown-5 (0.03g, 0.13 mmol) in 50 mL acetonitrile $H_3[PMo_{12}O_{40}]\cdot xH_2O$ (0.16g, 0.09 mmol) was added. After all reactants got dissolved, 20 mL of the filtrate of the compound **1** crystals was added to it. Then 10 mL of glacial acetic acid (100%) was added to the reaction mixture. The reaction mixture was then stirred for 18 hours at room temperature. Then the reaction solution was filtered and kept to evaporate slowly. Brown crystals of compound **2** were obtained after one week. These were filtered from mother liquor thereafter and dried at room temperature. Yield: 0.108g (67.5 % based on Mo). Anal. calcd. (in %) for $C_{56}H_{92}Mo_{12}N_3O_{60}P$: C, 22.80; H, 3.14; N, 1.42. Found C, 23.05; H, 3.18; N, 1.36.

4.5 References:

- 1. Modak, J. M. Resonance 2002, 69.
- 2. Schrock, R. R. Acc. Chem. Res. 2005, 38, 955-962.
- 3. Schrock, R. R. Proc. Natl. Acad. Sci. U.S.A. 2006, 103, 17087-17087.
- 4. Howard, J. B.; Rees, D. C. *Proc. Natl. Acad. Sci. U.S.A.*, **2006**, 103, 17088-17093.
- 5. Green, L. Int. J. Hydrogen Energy, **1982**, 7, 355-359.
- 6. Lan, R.; Irvine, J. T. S.; Tao, S. *Int. J. Hydrogen Energy*, **2012**, *3*, 1482-1494.
- 7. Fenwick, A. Q.; Gregoire, J. M.; Luca, O. R. *J. Photochem. Photobiol.*, *B*, **2015**, *152*, 47-57.
- 8. Aika, K.; Chiristiansen, L. J.; Dybkjacr, I.; Hansen, J. B.; Nielsen, A.; Stoltze, P.; Tamaru, K. *Ammonia*, Springer, Germany, **1995**.

- 9. Schlogl, R. Angew. Chem. Int. Ed., 2003, 42, 2004-2008.
- 10. Ertl, G. Angew. Chem. Int. Ed., 2008, 47, 3524-3535.
- 11. Rees, D. C.; Howard, J. B. *Curr. Opin. Chem. Biol.* **2000**, *4*, 559-566, and references therein.
- 12. Burgess, B. K. Chem. Rev. **1990**, 90, 1377-1406.
- 13. Burgess, B. K.; Lowe, D. J. Chem. Rev. 1996, 96, 2983-3011.
- 14. Ashida, Y.; Arashiba, K.; Nakajima, K.; Nishibayashi, Y. *Nature*, **2019**, *568*, 536-540.
- 15. Yandulov, D. V.; Schrock, R. R. Science, **2003**, *301*, 76-78.
- 16. Nishibayashi, Y. *Nirogen fixation (Topics in organometallic chemistry)* 1st edn, Vol. 60 **2017**, Springer, Heidelberg.
- 17. Arashiba, K.; Miyake, Y.; Nishibayashi, Y. Nat. Chem. 2011, 3, 120-125.
- 18. Anderson, J. S.; Rittle, J.; Peters, J. C. Nature, 2013, 501, 84-87.
- 19. Jr. Fajardo, J.; Peters, J. C. J. Am. Chem. Soc. 2017, 139, 16105-16108.
- 20. Arashiba, K. et al. Bull. Chem. Soc. Jpn. 2017, 90, 1111-1118.
- 21. Chatt, J.; Pearman, A. J.; Richards, R. L. *Nature*, **1975**, 253, 39-40.
- 22. Li, H.; Shang, J.; Ai, Z.; Zhang, L. J. Am. Chem. Soc. 2015, 137, 6393-6399.
- 23. Hirakawa, H.; Hashimoto, M.; Shiraishi, Y.; Hirai, T. *J. Am. Chem. Soc.* **2017**, *139*, 10929-10936.
- 24. Brown, K. A. et al. Science, 2016, 352, 448-450.
- 25. Guha, A.; Narayanaru, S.; Kaley, N. M.; Rao, D. K.; Mondal, J.; Narayanan, T. N. *Mat. Today Comm.*, **2019**, 100700.
- 26. Lan, R.; Irvine, J. T. S.; Tao, S. Sci. Rep. 2013, 3, 1145.
- 27. Cui, B.; Zhang, J.; Liu, S.; Xiang, W.; Liu, L.; Xin, H.; Lefler, M. J.; Licht, S. *Green Chem.*, **2017**, *19*, 298-304.
- 28. Manjunatha, R.; Karajic, A.; Goldstein, V.; Schechter, A. ACS Appl. Mater. Interfaces, 2019, 11, 8, 7981-7989.
- 29. Cong, L.; Yu, Z.; Liu, F.; Huang, W. Catal. Sci. Technol., 2019, 9, 1208-1214.
- 30. Giddey, S.; Badwal, S. P. S.; Kulkarni, A. *Int. J. Hydrog. Energy*, **2013**, *38*, 14576-14594.
- 31. Licht, S.; Cui, B.; Wang, B.; Li, F.-F.; Lau, J.; Liu, S. Science, **2014**, 345, 637-640.
- 32. Kyriakou, V.; Garagounis, I.; Vasileiou, E.; Vourros, A.; Stoukides, M. *Catal. Today*, **2017**, 286, 2-13.
- 33. Bao, D.; Zhang, Q.; Meng, F. L.; Zhong, H.; Shi, M.-M.; Zhang, Y.; Yan, J.-M.; Jiang, Q.; Zhang, X.-B. *Adv. Mater.* **2017**, *29*, 1604799.
- 34. Oshikiri, T.; Ueno, K.; Misawa, H. Angew. Chem. Int. ed. 2016, 55, 3942-3946.
- 35. Zheng, J.; Lyu, Y.; Qiao, M.; Wang, R.; Zhou, Y.; Li, H.; Chen, C.; Li, Y.; Zhou, H.; Jiang, S. P.; Wang, S. *Chem.* **2019**, *5*, 617-633.
- 36. Ali, M.; Zhou, F.; Chen, K.; Kotzur, C.; Xiao, C.; Bourgeois, L.; Zhang, X.; MacFarlane, D. R. *Nat. Commun.*, **2016**, 11335.
- 37. Oshikiri, T.; Ueno, K.; Misawa, H. *Green Chem.*, **2019**, *21*, 4443-4448.
- 38. Guo, C. X.; Ran, J. R.; Vasileff, A. et al. Energy Environ. Sci. 2018, 11, 45-56.
- 39. Shivaiah, V.; Kumar, N. T.; Das, S. K. J. Chem. Sci., 2018, 130, 37.
- 40. Bhattacharya, A. K.; Thyagarajan, G. Chem. Rev. 1981, 81, 415-430.

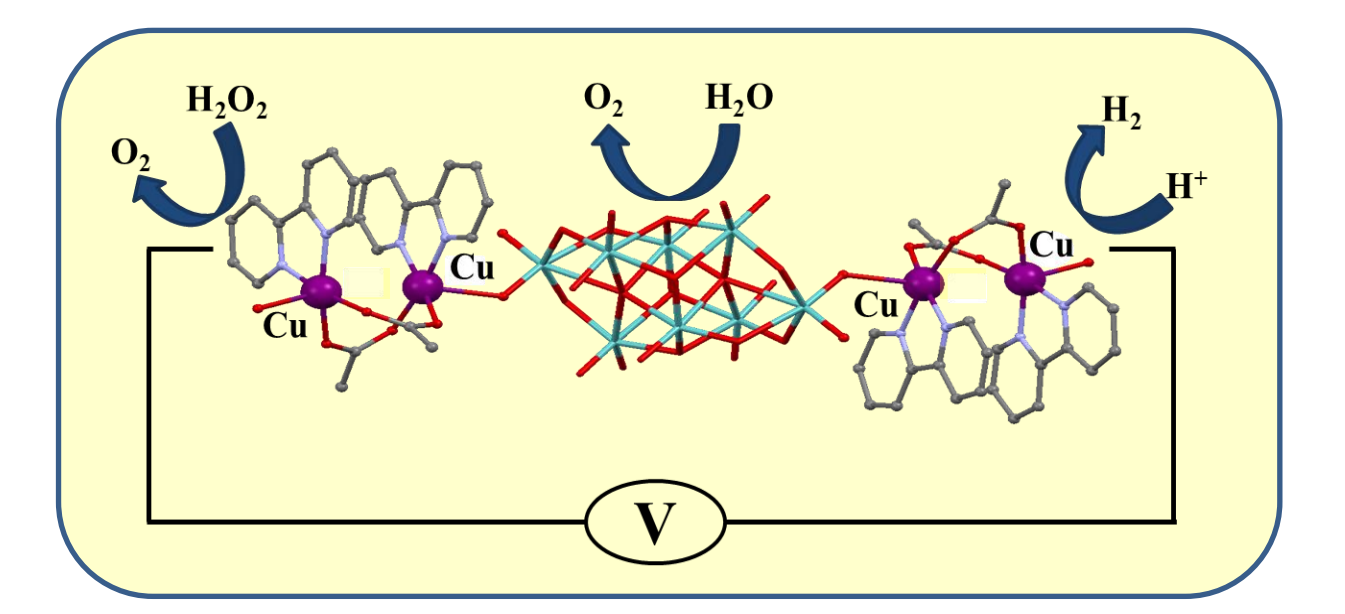
- 41. Muetterties, E. L.; Hoel, E. L.; Salentine, C. G.; Hawthone, M. F. Inorg. Chem. 1975, *14*, 950-951.
- 42. Satapathi, S. Inorg. Chem. Commun. 2015, 56, 89-101.
- 43. Triethylamine, US EPA, 1993a..
- 44. Summers, D. P. Orig. Life Evol. Biosph. 2005, 35, 299-312.
- 45. Rosnes, M. H.; Yvon, C.; Long, D.-L.; Cronin, L. Dalton Trans. 2012, 41, 10071-10079.
- 46. Zebiri, S.; Boufas, S.; Mosbah, L.; Bencharif, M.; Bencharif, J. Chem. Sci., 2015, 127, 1769-1775.
- 47. Aouissi, A.; Al-Othman, Z. A.; Al-Anezi, H. *Molecules*, **2010**, *15*, 3319-3328.
- 48. Chatterjee, T.; Sarma, M.; Das, S. K. Cryst. Growth Des., 2010, 10, 3149-3163.
- 49. Ebsworth, E. A. V.; Rankin, D. W. H.; Cradock, S. Structural methods in inorganic chemistry. 2nd Edn., **1991**, p51-52.

CHAPTER

5

A Polyoxometalate Supported Copper Dimeric Complex: Synthesis, Structure and Electrocatalysis

Abstract. A polyoxometalate (POM) supported copper dimeric $[Mo_8O_{26}\{Cu_2(2,2'-bpy)_2(CH_3COO)_2H_2O\}_2] \cdot H_4Mo_8O_{26}$ complex, ·16H₂O (1) has been synthesized using conventional wet synthesis. The compound has been characterized using routine spectral techniques and its molecular structure has been elucidated using single crystal X-ray crystallography. The two copper(II) ions are bridged by acetate ions and each copper ion is also coordinated to 2,2'-bipyridine molecule. In each dimer, one of the copper ions is bonded to the POM anion from one side, whereas the other copper ion is bonded to a water molecule, hence acquiring a penta-coordinated square pyramidal structure around each copper center. The lattice water molecules play an important role to stabilize the system, by forming a water pentamer, which binds both the polyoxometalate supported transition metal complex and the other POM anion [Mo₈O₂₆]⁴. Interestingly, compound 1 is found to function as a versatile heterogeneous electro-catalyst for water oxidation, proton reduction and hydrogen peroxide reduction.



5.1 Introduction

Polyoxometalates (POMs) are interesting transition metal oxide clusters, that have grabbed the attention of the contemporary scientists, because of their structural versatility and their applicability in a vivid range of areas ranging from catalysis, materials sciences, biology, magnetism, luminescence to molecular electronics through medicine. A recent modification to the polyoxometalates is the introduction of the coordination complexes into the framework by covalently grafting the complex through the terminal / bridging oxygen atom(s) of the polyoxometalates, taking into consideration the charge compensation or the structure direction, which are called polyoxometalate supported transition metal complexes (PSTMCs). This modification enhances the potential applications of these hybrid PSTMCs in many diverse fields.

Copper ions play a major role in biological processes. Among the copper containing metalloenzymes, hemocyanins (found in mollusks) are oxygen carriers. These hemocyanins contain a copper dimer, which is bridged by the oxygen atoms. Many modeling studies have been done, so far, in order to mimic the functional as well as the structural aspects of the copper dimeric complexes in copper metalloenzymes.⁴ Melnik and co-workers in the year 1997,⁵ published a review reporting more than nine hundred types of Cu(II) dimers, which evidences the importance and applicability of this family of compounds. According to this review, the earliest quotation to copper acetate was from the year 1594.⁵ The review⁵ also generalizes the fact that, as far as the stereochemistry of these dimeric compounds is concerned, they favor a square pyramidal geometry with different degrees of distortions about the Cu(II) ion. In the last two decades, there has been an extensive study on the reactivity of tetra- μ -acetatodicopper(II) towards the 2,2'-bipyridine (bpy). In 1992, Perlepes and co-workers reported the isolation of $[Cu_2(\mu-O_2CMe)_2(H_2O)_2(bpy)_2]$ (ClO₄)₂·H₂O from the reaction of $[Cu_2(OH)_2(bpy)_2]$ ClO₄ with an excess of MeCO₂H.⁶ Followed by this report, Chakravarty and Meenakumari reported the synthesis and crystal structure of [Cu₂(µ-O₂CMe)₂(H₂O)(bipy)₂](PF₆)₂, where the two Cu(II) ions exhibited two different coordination geometries.⁷

In the present chapter, we have synthesized the polyoxometalate supported dimeric transition metal complex $[Mo_8O_{26}\{Cu_2(2,2'-bpy)_2(CH_3COO)_2H_2O\}_2] \cdot H_4Mo_8O_{26} \cdot 16H_2O$ (1).

Prior to this work, there are few reports on copper dimeric complexes supported on diverse polyoxometalates (POMs). Gutiérrez-Zorrilla, Lezama and their co-workers have done enormous work in this field, i.e., POM supported dimeric copper complex. They reported a unique dinuclear copper complex, supported on a Keggin type of polyoxometalate $K_{14}[\{Cu_2(bpy)_2(\mu-ox)\}\{SiW_{11}O_{39} \quad Cu(H_2O)\}]_2[SiW_{11}O_{39}Cu(H_2O)] \cdot \sim 55H_2O.^8$ Subsequently, they depicted a full account of this work describing variable temperature magnetic studies. 9 In yet another report, they also reported reaction of a monosubstituted Keggin polyoxometalate (POM) generated in situ with copper–phenanthroline complexes, where the two Keggin cluster anions connected through terminal oxygen atom yielding $A_7[Cu_2(ac)_2(phen)_2(H_2O)_2][Cu_3(ac)_3(phen)_3(H_2O)_3]$ [Si₂W₂₂Cu₂O₇₈(H₂O)]:~18H₂O, where A= NH₄⁺ or Rb⁺. ¹⁰ A little later, the same groups described two interesting POM supported copper dimeric compounds, where the second one is the condensed dimer of the first one. 11 In the next year, they also reported the reaction of in situ generated copper(II)-monosubstituted Keggin

polyoxometalates and copper(II)-phenanthroline-oxalato complexes in ammonium or rubidium acetate buffers leading to the formation of two new hybrid POMs, where the dinuclear copperoxalato complex sandwiched by two copper-monosubstituted **POMs** $E_4[Cu(phen)(H_2O)_4]_2[Cu_4(phen)_4(H_2O)_4(ox)_3]_{0.6}[Cu_2(phen)_2(H_2O)_4(ox)]_{0.4}[Cu(phen)_4(H_2O)_4(ox)_3]_{0.6}[Cu_2(phen)_2(H_2O)_4(ox)_4(o$ $(ox)]_{0.8}$ $[\{SiW_{11}O_{39}Cu(H_2O)\}_2\{Cu_2(phen)_2(ox)\}] \cdot 20H_2O \ [E:\ Rb^+\ or\ NH_4^+].^{12}\ Ma\ and\ coworkers$ reported a one dimensional polyoxometalate-based chain, constructed from Keggin anions of [SiMo₁₂O₄₀]⁴⁻ weakly connected by dinuclear [Cu(ppy)₂] groups. The two copper atoms are connected to two terminal oxygen atoms of two different Keggin atoms, forming a planar rhombic copper dimer. 13 Wang and group reported reduced tungsten Keggin supported chlorobridged copper dimers including related supramolecular chemistry.¹⁴ Ma, Liu and co-workers reported the hydrothermal synthesis of a hybrid POM complex, [Cu₂(bipy)₃(µ₁-H₂O)₂(µ₂- $H_2O(\mu_2OH)(H_2BW_{12}O_{40})$] $\cdot 4H_2O$ (bipy =4,4'-bipy) having a Cu dimer connected to 4, 4'bipyridine from one side and the terminal oxygen of the cluster from the other side. The two copper ions are bridged by water molecules and showed the existence of weak antiferromagnetic interactions. 15 A similar complex was also reported by Ma and Pang, where the POM was [PW₁₂O₄₀]^{n-.16} Zhao and group have described (hydroxo)(chloro) bridged copper dimer, supported by the silicotungsten Keggin in compound $[Cu_2(phen)_2Cl(H_2O)(OH)]_2[\alpha-P(H_2O)(OH)]_2$ SiW₁₂O₄₀] *8H₂O.¹⁷ Ma, Pang and their co-workers reported two copper dimeric-POM $complexes \quad \{[Cu_2(en)_2(ox)][HPW_{12}O_{40}]\} \cdot (en)_2 \quad \cdot 2H_2O \quad and \quad \{[Cu_2(en)_2(ox)] \quad [H_3BW_{12}O_{40}]\} \cdot (en)_2 \cdot (e$ ·(en)₂·2H₂O.¹⁸ Xu and co-workers,¹⁹ have reported a similar PSTMC [Cu(bpy)(µ₂-OH)] $_4$ [(H₂O)-(bpy)₂HPW₁₁Cu₂O₃₉] $_2$ ·2C₂H₅OH·10H₂O, where the Cu(II) ions are located in the lacunary sites of the monolacunary anion [PW₁₁O₃₉]⁷ forming a dumbbell type structure.

Even though these impactful reports have brought about structural aesthetics and interesting magnetism on these polyoxometalate supported copper dimeric complexes, their use as electro-catalysts is scarcely reported. Ma, Pang and co-workers have reported the role of copper dimer, supported on polyoxometalates as electrocatalysts for the reductions of hydrogen peroxide, potassium iodate and nitrite. There are not many reports on electrocatalytic water oxidation and electrocatalytic proton reduction, catalyzed by POM supported copper dimers, that are enormously important today because the water splitting (WS) process using an inexpensive POM-based catalyst is a powerful alternative to curb the energy crisis on the earth surface. Water oxidation (WO) is considered to be the bottleneck process of water splitting because it advances in a thermodynamically uphill manner with the involvement of 4e⁻ and 4H⁺, ²⁰ according to the equation:

$$2H_2O \rightarrow 4H^+ + O_2 + 4e^- \qquad E^o = -1.23 \text{ V}$$
 (eqn. 1)

where E° is the standard Nernst potential for water oxidation; here a negative potential signifies the thermodynamic uphill nature of the process. Our group has reported a nickel coordination complex, attached to a polyoxometalate cluster anion, to be a robust electrocatalyst for water oxidation process.²¹

The present years have also seen an ample interest to design new molecular catalysts, containing earth-abundant 3d-transition metals as the active site for electrocatalytic hydrogen evolution reactions. Nickel,²² cobalt²³ and iron²⁴ based complexes are few popular molecular catalysts, which have been employed in electrocatalytic hydrogen evolution reactions (HER).

In 2014, Wang and co-workers, for the first time, reported a Cu-complex that can electrochemically catalyze water reduction 25a with a very high catalytic activity with 96% Faradic efficiency and 420 mV onset overpotential in pH 2.5 under buffer conditions. After this report, many Cu-based complexes were discovered, which showcased activity in catalyzing HER electrochemically. Recently, our group has described two Anderson-POM supported copper complexes acting as electrocatalysts for hydrogen evolution reaction in neutral medium. The electrocatalytic proton reduction to molecular hydrogen has attracted immense attention because the molecular hydrogen (H₂) is a clean and highly efficient fuel. Likewise, since hydrogen peroxide is commonly used as an oxidant in chemical mechanical planarization slurries leading to the metallization of copper for microelectronics applications, the electrocatalytic reduction of H_2O_2 by copper-containing catalyst is utmost demanding. In this chapter, we have demonstrated that the synthesized polyoxometalate supported dimeric copper complex $[Mo_8O_{26}\{Cu_2(2,2'-bpy)_2(CH_3COO)_2H_2O\}_2]\cdot H_4Mo_8O_{26}\cdot 16H_2O$ (1) can be used as a versatile heterogeneous catalyst for electrochemical water oxidation, proton reduction, and hydrogen peroxide reduction in acidic medium.

5.2. Results and Discussion

5.2.1 Synthesis

Compound 1 was synthesized following a one-pot conventional wet synthesis protocol at 70 °C. The blue-colored filtrate yielded 0.8 g (20.3% based on Mo) blue block crystals within four days. The relevant synthesis includes the reaction of sodium molybdate, 2, 2'-bipyridine, $Cu(NO_3)_2 \cdot 6H_2O$ and CH_3COONa in an aqueous acidic medium. The sodium molybdate solution, when acidified with glacial acetic acid immediately gives a white precipitate of $[Mo_8O_{26}]^{4-}$, which upon addition of $Cu(NO_3)_2 \cdot 6H_2O$ and CH_3COONa coordinates to Cu(II) through its terminal oxygen atom. Looking at the formula of 1, the following reactions can be proposed during the synthesis of compound 1:

$$\begin{split} &8[\text{MoO}_4]^{2-} + 12\text{H}^+ \rightarrow \{\text{Mo}_8\text{O}_{26}\}^{4-} + 6\text{H}_2\text{O} \\ &2\{\text{Mo}_8\text{O}_{26}\}^{4-} + 4\text{Cu}^{2+} + 4\text{CH}_3\text{COOH} + 4(2,2\text{'-bpy}) + 18\text{H}_2\text{O} \rightarrow [\text{Mo}_8\text{O}_{26}\{\text{Cu}_2(2,2\text{'-bpy})_2 + 18\text{COO}_{26}\}^{2}\} \cdot \text{H}_4\text{Mo}_8\text{O}_{26} \cdot 16\text{H}_2\text{O} \text{ (1)} \\ &(\text{eqn. 3)} \end{split}$$

The tetrahedral molybdate $[MoO_4]^{2-}$ in an acidic aqueous solution undergoes protonation followed by coordination expansion around molybdenum and subsequent condensation reaction results in the formation of the isopolyanion $\{Mo_8O_{26}\}^{4-}$, as shown in eqn. 1. Subsequently, the *in-situ* formed $\{Mo_8O_{26}\}^{4-}$ acts as the ligand through its terminal oxo donor to coordinate to one of the copper centres of each copper dimer (there are two such copper dimers per one POM cluster anion, formed *in situ* from the copper(II) salt, acetate anion and 2,2'-bipyridine (eqn. 2)).

The detailed synthetic procedure is provided in the Experimental Section.

5.5.2 Crystallography

The asymmetric unit of compound 1 consists of two halves of the octamolybdate anions, one copper acetate dimer, and eight lattice water molecules (Figure 1a). Thus the full

molecule contains two POM clusters, two copper dimers, and sixteen solvent water molecules as shown in Figure 1b. An octamolybdate anion, $[Mo_8O_{26}]^{4-}$ consists of eight edge-sharing octahedral $\{MoO_6\}$ units. The Mo–O bond distances can be grouped into four categories: 14 Mo–O_t (O_t = terminal oxygen) with the bond lengths in the range of 1.686-1.706 Å; six μ_2 -type bridged Mo–O_b (O_b = bridging oxygen) with bond distances in the range of 1.740- 2.295 Å; four μ_3 -type bridged Mo–O_b bonds in the range of 1.984-2.329 Å and two μ_5 -type Mo–O_b bonds (2.155 and 2.402 Å). The polyhedral representation of the POM clusters is shown in Figure 1c.

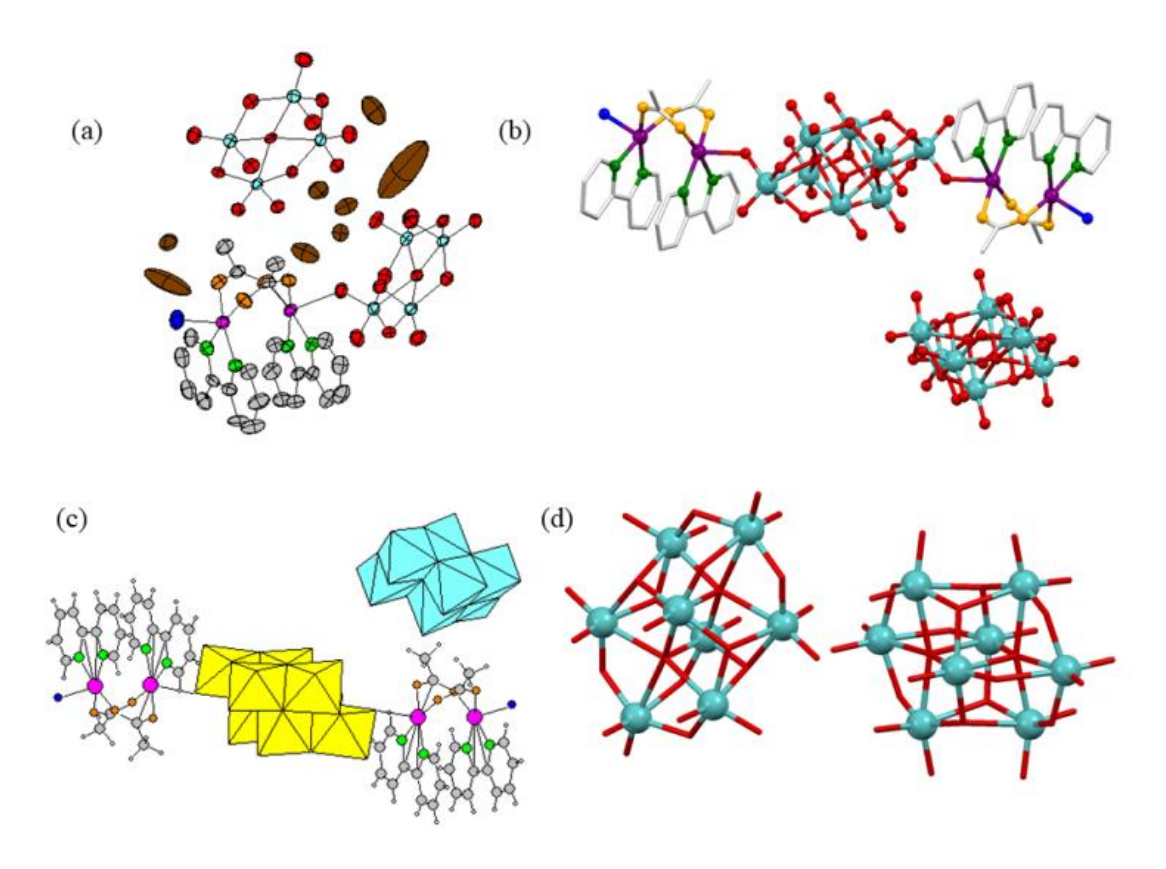


Figure 5.1. (a) The thermal ellipsoidal plot of compound 1 at the 50% probability level. Hydrogen atoms are omitted for clarity. (b) The full molecule of 1 excluding the lattice water molecules. (c) Polyhedral representation of the POM clusters in compound 1 excluding the water molecules. (d) Two independent cluster anions of [Mo₈O₂₆]⁴⁻ polyoxometalate, showing their β conformation. Color code: Cyan: molybdenum; Red: oxygen atoms of the octamolybdate cluster anion; violet: copper; grey: carbon; orange: oxygen atoms of acetate ions; green: nitrogen; blue: water molecule attached to the copper dimer; brown: lattice water molecules; white: hydrogen.

In the crystal structure, there are two independent POM cluster $[Mo_8O_{26}]^{4-}$ anions. One of these, supports two copper dimers *via* terminal Mo=O coordination resulting in the formation of POM supported copper dimeric complexes, $[Mo_8O_{26}\{Cu_2(CH_3COO)_2(bpy)_2(H_2O)\}_2]$ and other POM cluster remains as a lattice component as a proton salt along with sixteen lattice water molecules per formula unit, thereby giving the overall formula of the title compound as $[Mo_8O_{26}\{Cu_2(2,2'-bpy)_2(CH_3COO)_2H_2O\}_2]H_4Mo_8O_{26} \cdot 16H_2O$ (1). Each copper (Cu^{II}) dimeric complex is connected to the $[Mo_8O_{26}]^{4-}$ cluster through

an apical position of the copper complex. The copper dimeric complex comprises of two square-pyramidal Cu(II) atoms bridged by two acetic acid ligands in a *syn-syn* fashion with a Cu–Cu distance of 3.007 Å. The basal plane is occupied by two bipyridine N atoms and O atoms from the acetate ions with the apical position being coordinated to one of the terminal oxygen atoms of the octamolybdate for one Cu(II) ion and water to another Cu(II) ion. Overall, in the POM supported copper dimer complex system, [Mo₈O₂₆{Cu₂(CH₃COO)₂(bpy)₂(H₂O)}₂], the isopolyanion is covalently bonded to two copper dimeric complexes [Cu₂(CH₃COO)₂(bpy)₂(H₂O)]⁴⁺ from opposite sides. The β conformation of the POM clusters, stabilized in compound 1, is shown in Figure 1d that shows octahedral coordination of each molybdenum centre in {Mo₈O₂₆}⁴⁻.²⁷

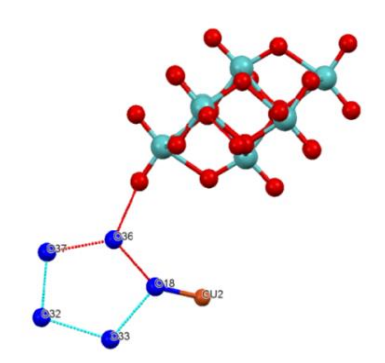


Figure 5.2. The water pentameric cluster and its association with the free octamolybdate cluster.

The detailed crystal structure analysis of compound **1** shows that the POM anion, coordinating copper dimers, interacts with a crystallographically independent POM cluster, remaining as a lattice component as an acid salt $H_4Mo_8O_{26}$, *via* a supramolecular cyclic water pentamer (H_2O_{5} . The water pentamer is an open envelope-shaped, as determined crystallographically in compound **1**. The five water molecules, involved, are the four lattice water molecules and the water, coordinated to the copper atom (Figure 5.2). The relevant $O \cdots O$ separations in the water pentamer, (H_2O_{5} are: $O18 \cdots O36$: 2.731 Å; $O36 \cdots O37$: 2.809 Å; $O37 \cdots O32$: 2.792 Å; $O32 \cdots O33$: 2.978 Å; $O33 \cdots O18$: 2.871 Å.

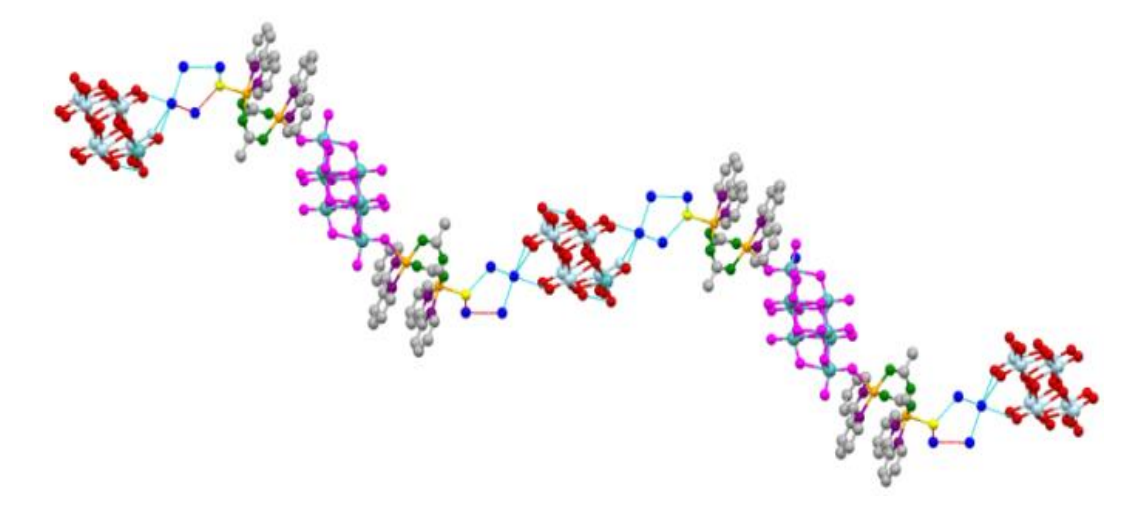


Figure 5.3. The chain-like structure formed through hydrogen bonds between the dimeric complex, the lattice octamolybdate cluster, and the water pentamers, (hydrogen atoms are not shown for clarity).

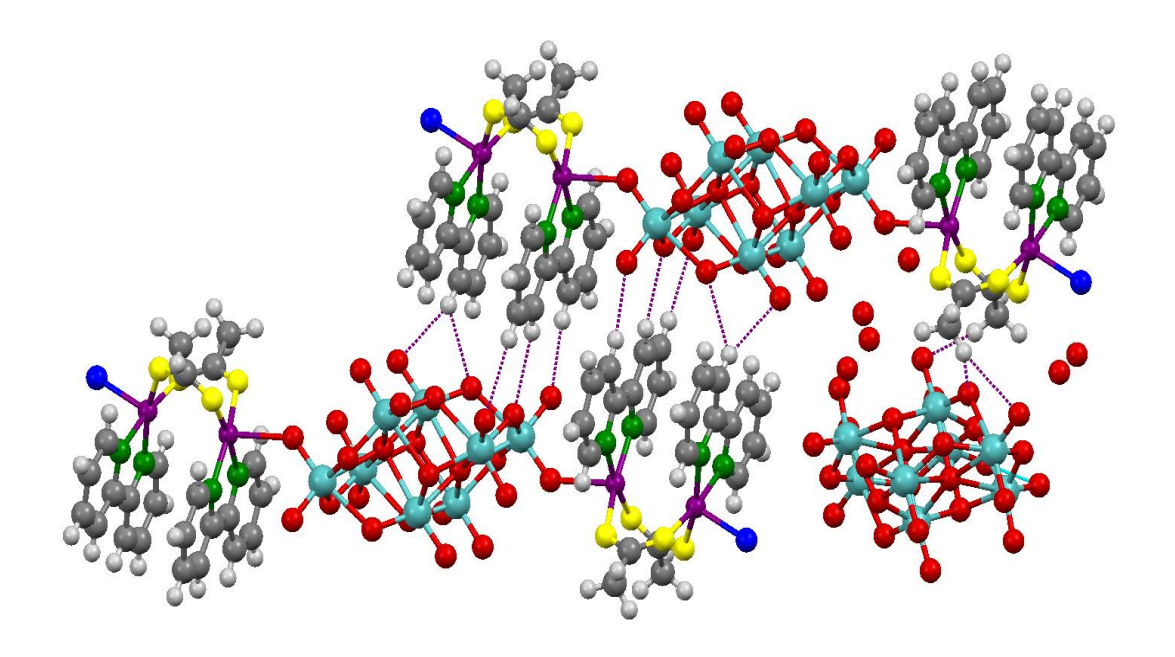


Figure 5.4. Hydrogen bonding Interactions between the –CH– groups and the terminal and bridging oxygen atoms of the octamolybdate cluster

Besides the stabilization of a water pentamer, there also exist the C–H···O hydrogen bonding interactions which contribute to stabilizing the supramolecular chainlike arrangement in the crystal structure of compound **1**, as shown in Figure 5.3. The –CH– groups of the carbon atoms C1, C2, C3, C4, C9, C10, C11, C12, C14, C19, C20, C22 and C24 donate their hydrogens to the surrounding available possible surface sites of the octamolybdate cluster anion (that include bridging and terminal oxygen atoms), (Figure 5.4).

The π - π stacking interactions in the compound **1** is also studied. Since there are four bipyridine ligands connected to the four copper(II) centres, each bipyridine ligand faces the other one, in a dimeric pair. As can be seen in Figure 5.5, the centroids of each pyridine ring pair are at a distance of 3.615 and 3.677 Å. These pyridine rings are slip-stacked to each other and not completely sandwiched, as the later leads to less stable compound, on account of high electronic repulsion of the electrons in the π -orbitals of the pyridine rings.

Bond Valence Sum Calculations

The BVS calculations suggest the following central atom valencies

Mo1	+6	Mo6	+6
Mo2	+6	Mo7	+6
Mo3	+6	Mo8	+6
Mo4	+6	Cu1	+2
Mo5	+6	Cu2	+2

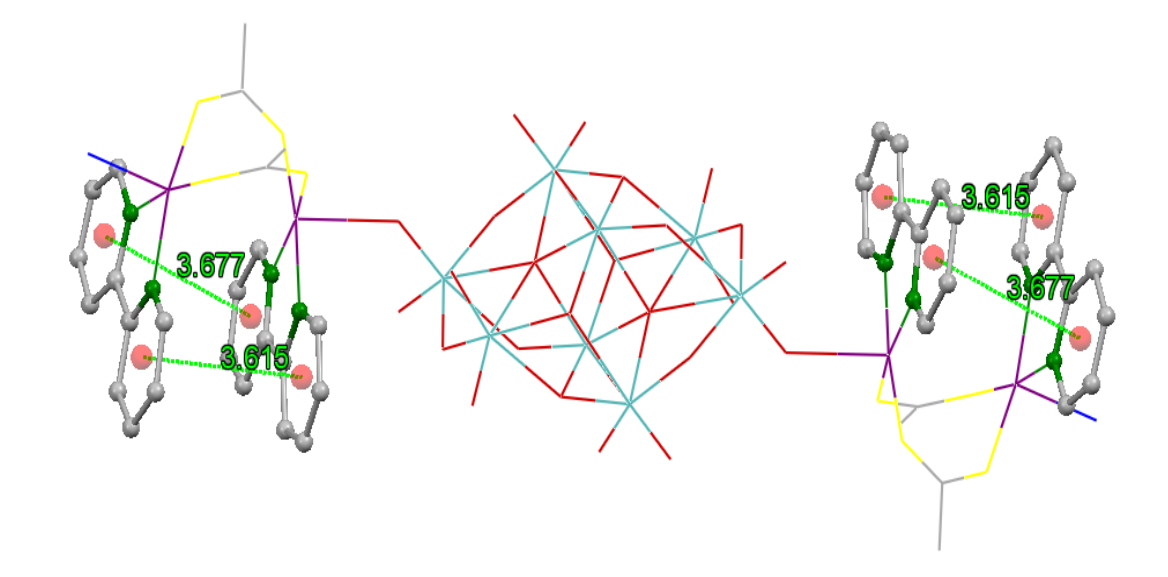


Figure 5.5. π – π stacking of the bipyridine molecules in compound 1.

Table 5.1 Crystal data and structure refinement for compound 1

	0 11
	Compound 1
Empirical formula	C48H44Cu4M016N8O78
fw	3770.16
$T(\mathrm{K}),\lambda(\mathrm{\AA})$	273(2), 0.71073
Crystal system	Triclinic
Space group	P-1
a (Å)	12.135(3)
b (Å)	12.766(3)
c (Å)	19.016(5)
α (°)	104.490(8)
β (°)	98.770(9)
γ (°)	111.063(8)
$V(\mathring{A}^3)$	2564.0(11)
$ m Z, d_{calcd}~(g~cm^3)$	1, 2.442
μ (mm ⁻¹), F(000)	2.808, 2139.0
${f goodness-of-fit}$ on $F2$	1.407
R1	0.0728
wR2	0.3005
Largest diff. peak/hole (e Å ⁻³)	2.6

D–H···A	d(D-H)	D(H···A)	$D(D\cdots A)$	<(DHA)
C(1) -H(1) ···O(14)	0.93	2.55	3.049(13)	114
$C(2) - H(2) \cdots O(20)$	0.93	2.50	3.259(16)	139
$C(3) - H(3) \cdots O(38)$	0.93	2.59	3.498(15)	167
C(4) -H(4) ···O(21)	0.93	2.41	3.309(16)	162
$C(9) - H(9) \cdots O(4)$	0.93	2.57	3.381(13)	146
$C(10) - H(10) \cdots O(15)$	0.93	2.51	3.022(13)	115
C(11) –H(11) ···O(16)	0.93	2.54	3.035(13)	114
$C(11) - H(11) \cdots O(22)$	0.93	2.49	3.255(15)	139
$C(12) - H(12) \cdots O(25)$	0.93	2.59	3.339(17)	138
C(14) -H(14) ···O(27)	0.93	2.47	3.282(15)	146
C(19) -H(19) ···O(9)	0.93	2.55	3.387(14)	150
C(20) -H(20) ···O(17)	0.93	2.57	3.057(14)	113
C(22) -H(22B) ··O(12)	0.96	2.54	3.284(14)	135
$C(22) -H(22C) \cdots O(7)$	0.96	2.59	3.545(15)	171
$C(24) = H(24C) \cdots O(26)$	0.96	2 38	3 297(13)	160

Table 5.2. Geometrical parameters of hydrogen bonds (Å, o), observed in the crystal structure of compound I (D = donor, A = acceptor)

5.2.3 Spectroscopy

The Fourier transformed infrared spectrum of the compound **1** was recorded. (Figure 5.6) The strong peak at 938 cm⁻¹ can be attributed to the asymmetric stretch of the Mo–O_t bond. Similarly, the asymmetric stretch of Mo–O_b–Mo bond is found to be seen at 724 cm⁻¹. The peaks at 724, 766, 838 and 893 cm⁻¹ are the characteristic peaks for Mo–O_b asymmetric stretch. All these values almost match with the vibrational features, reported for the β-isomer of the octamolybdate in the literature.²⁸ The vibrational features of compound **1** in two different ranges are given in Figures 5.6 and 5.7, which clearly show the characteristics of the β-isomer of the octamolybdate. The presence of the water molecules in the compound is evident from the broad peak around 3000 cm⁻¹. The peaks at 3520 and 3460 cm⁻¹ are attributed to the symmetric stretch corresponding to the water molecules bonded to the Cu(II) ions. Similarly, the broad peak at 2950 cm⁻¹ is for the symmetric stretch of the CH₃ groups of the acetate ions. The bands at 1600 and 1577 cm⁻¹ can be attributed to the asymmetric stretch of the COO⁻ group and at 1441 and 1428 cm⁻¹ for its symmetric stretch (Figure 5.7). The peak at 1636 cm⁻¹ is for the C=C bond of the bipyridine ligand. Other peaks at 1577, 1428, 1312, 1254, 1035 and 1020 cm⁻¹ can be attributed to the various vibrational features of the bipyridine ligands.²⁹

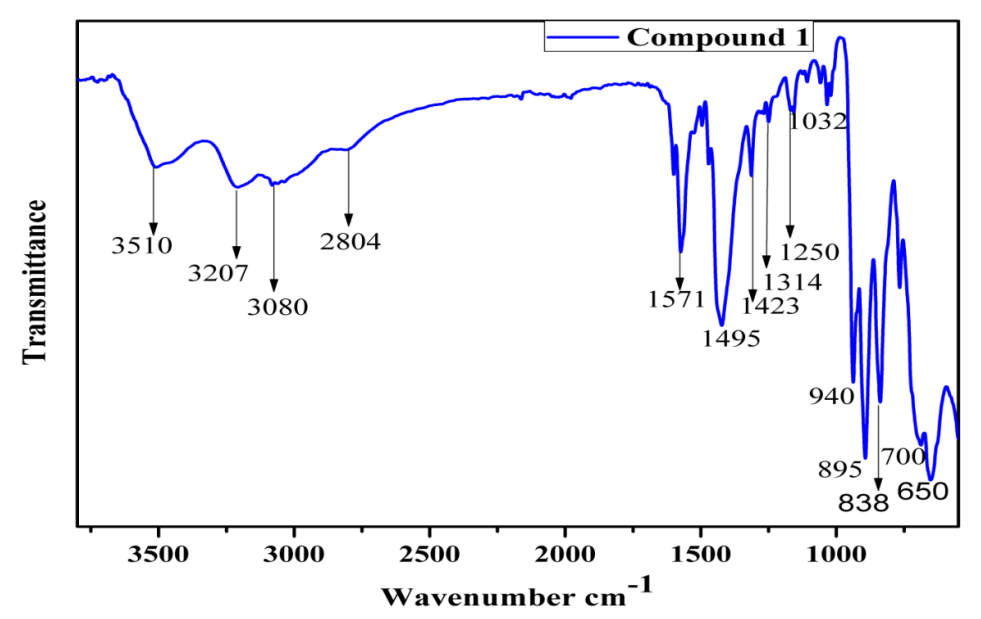


Figure 5.6. FT-IR spectrum of compound 1.

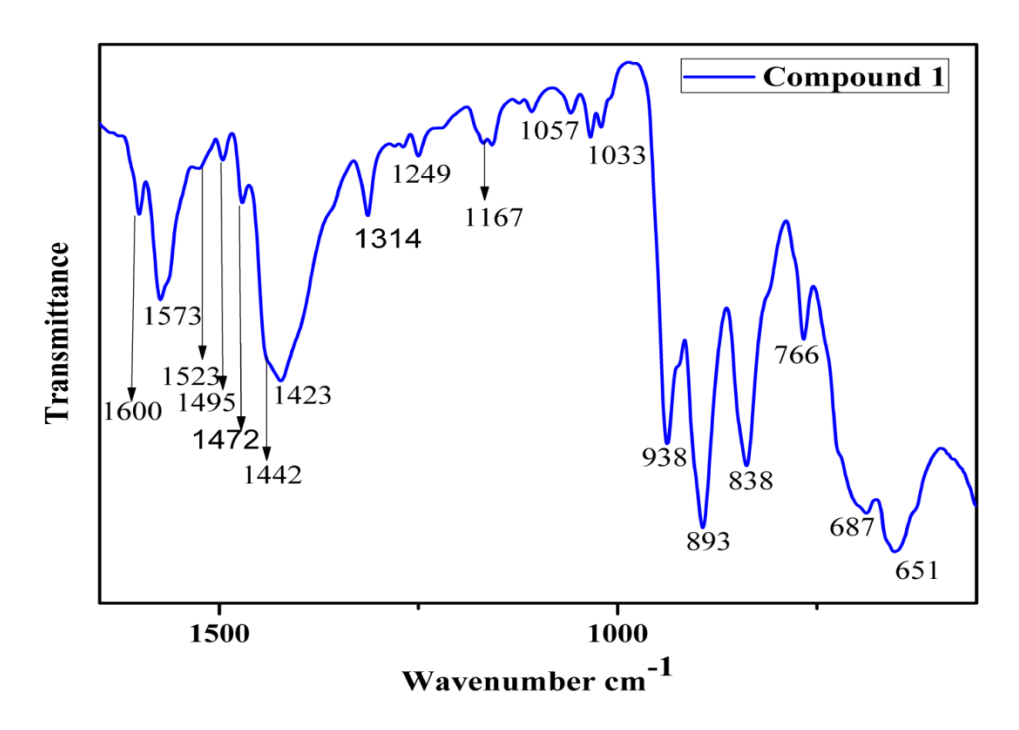


Figure 5.7. FT-IR spectrum of compound 1 in range $500 - 1600 \text{ cm}^{-1}$.

The electronic absorption spectrum of compound 1 is transformed into a Kubelka-Munk (K-M) derived plot as shown in Figure 5.8a. The sharp peak at 226 nm can be ascribed to the ligand to metal charge transfer from the oxygen 2p to the molybdenum d orbital.³⁰ The shoulder at 271 nm can be attributed to the intra-ligand bipyridine π - π * transitions. The broad peak centred around 467 nm can be attributed to the d to π * transitions.³¹ A diffused broad peak is also seen at around 350 nm, which can be attributed to the acetate to copper LMCT.³² A broad and weak peak is also seen around 600 nm, which is due to d-d transitions of the d9 Cu(II) centre in the title compound.

The thermal stability of the title compound has been studied by thermogravimetric analysis. The compound was taken for thermal studies without prior activation in a high-temperature vacuum. With an increase in temperature from 30 °C to nearly 240 °C, as shown in Figure 5.8b, there is a weight loss, which can be attributed to the loss of lattice water molecules as well as the water molecules coordinated to the Cu(II) ion. Followed by this, there is a weight loss of up to nearly 62% of the weight when the temperature increases from 240 °C to 380 °C. In this temperature range, the four acetate ligands and four bipyridine ligands of the copper dimers are lost leaving the octamolybdate clusters and the copper contents. Then after 750 °C, the polyoxometalate clusters and the copper content start to degrade into their oxides.

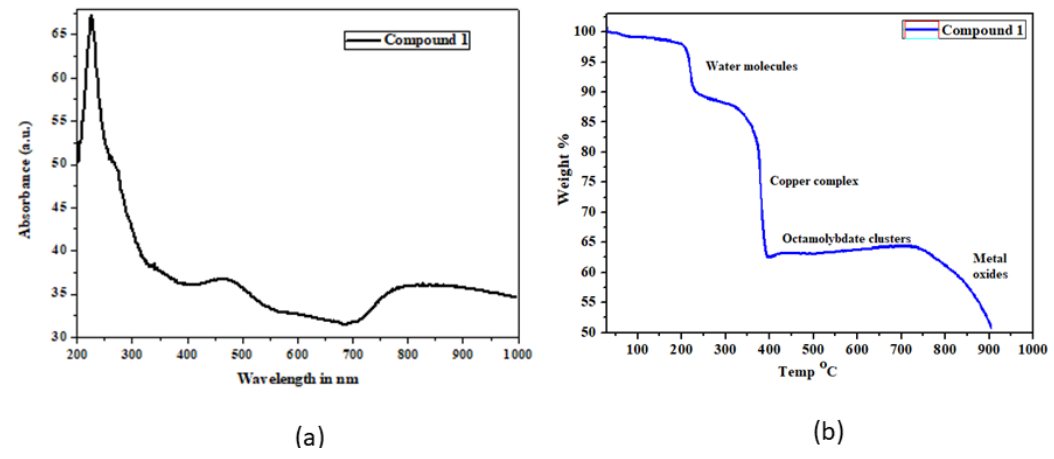


Figure 5.8. (a) The solid-state UV-Visible diffuse reflectance spectrum of compound 1. (b) The thermogravimetric plot of compound 1.

The powder X-ray diffraction (PXRD) pattern, generated from CIF file of single-crystal data of compound 1 (simulated PXRD pattern), matches well with that, obtained from the bulk PXRD measurement of the sample (Figure 5.9). This confirms the purity in the bulk sample.

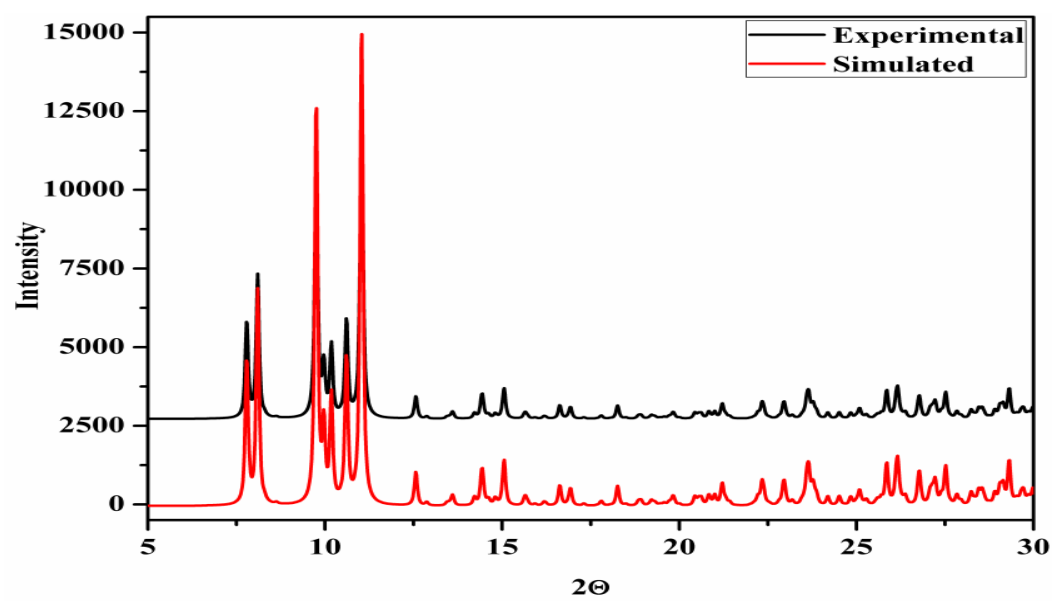


Figure 5.9. PXRD plots of compound 1.

5.2.4 Electrochemical Studies

The electrochemical responses of compound 1 were studied in various electrolytes. The responses in different electrolytes, as expected, were different. As we know that the $[Mo_8O_{26}]^{4-}$ cluster is stable in aqueous solution in pH less than 5.5 and is transformed to paramolybdic anions in pH 5.5 to 8^{33} hence all the electrochemical studies were performed in pH less than 5.5. The cyclic voltammetric studies were done in various electrolytes and at various pH values.

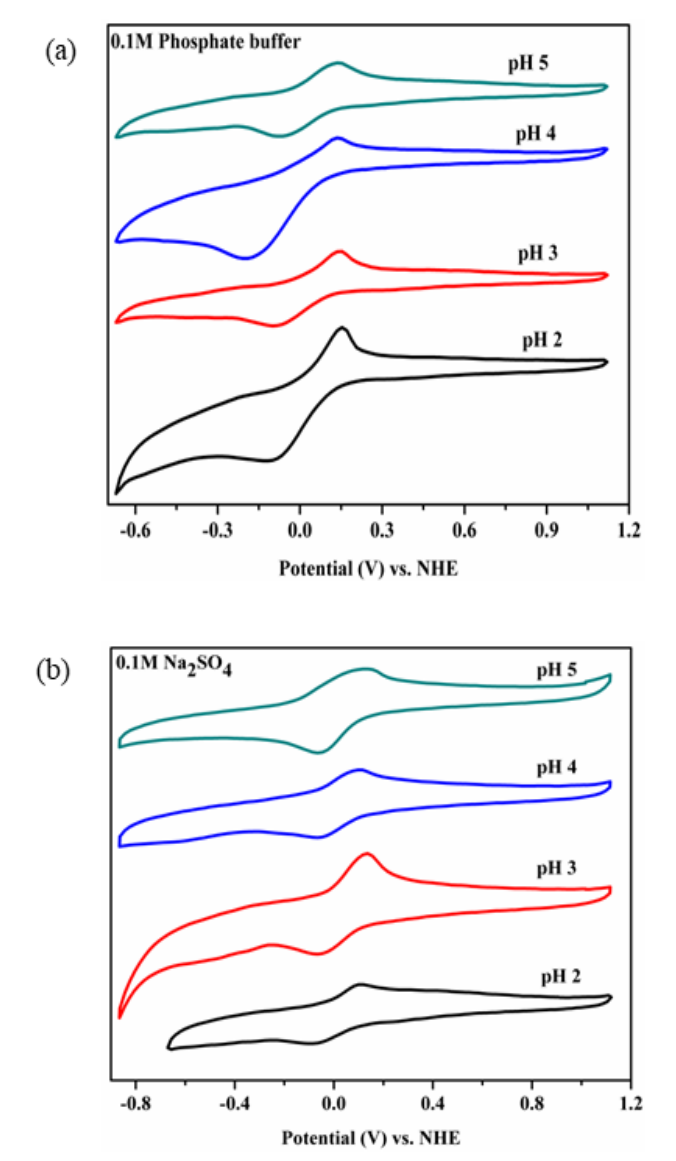


Figure 5.10. Cyclic Voltammograms of compound 1 at various pH values in (a) 0.1M phosphate buffer and (b) 0.1M Na₂SO₄, at a scan rate of 100 mVsec⁻¹.

The cyclic voltammograms of compound 1 in 0.1M phosphate buffer and 0.1M Na₂SO₄ solution at different pH values are shown in Figure 5.10. The compound shows similar redox responses at different pH values (except at pH 4 in 0.1M phosphate buffer) in both the electrolytes. A quasi-reversible redox couple, that has appeared as a major redox response in all the cases (except at pH 4 in 0.1M phosphate buffer), can be attributed to the Cu^{II}/Cu^I couple. In Na₂SO₄ solution, at pH 3, a careful observation reveals a weak reduction feature at -0.4V,

which can be attributed to the reduction of Mo^{VI} to Mo^{V} of the cluster, based on the weak redox responses appeared for the precursor compound $[Bu_4N]_4[Mo_8O_{26}]$ in $0.1M\ Na_2SO_4$ at pH 5 as shown in Figure 5.11. The voltammograms at varied scan rates in different electrolytes (at different pH values) are given in Figure 5.12. Table 5.3 gives the $E_{1/2}$ values of the compound at different pH values.

Table 5.3. $E_{1/2}$ values of the major A1/C1 peaks in the cyclic voltammograms of compound 1 in different electrolytes at different pH values (Figure 5.10)

Electrolyte	pН	E _{1/2} (in Volts)
0.1M Phosphate buffer	pH 2	0.030
0.1M Phosphate buffer	рН 3	0.035
0.1M Phosphate buffer	pH 4	-0.029
0.1M Phosphate buffer	pH 5	0.032
0.1M Na ₂ SO ₄	pH 2	0.013
0.1M Na ₂ SO ₄	рН 3	0.040
0.1M Na ₂ SO ₄	pH 4	0.022
0.1M Na ₂ SO ₄	рН 5	0.029

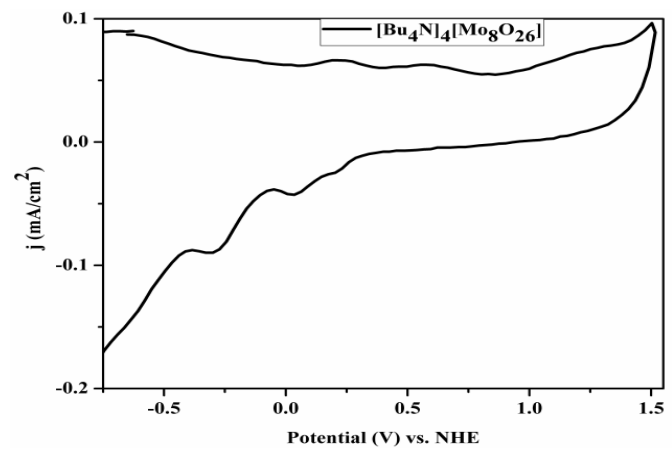
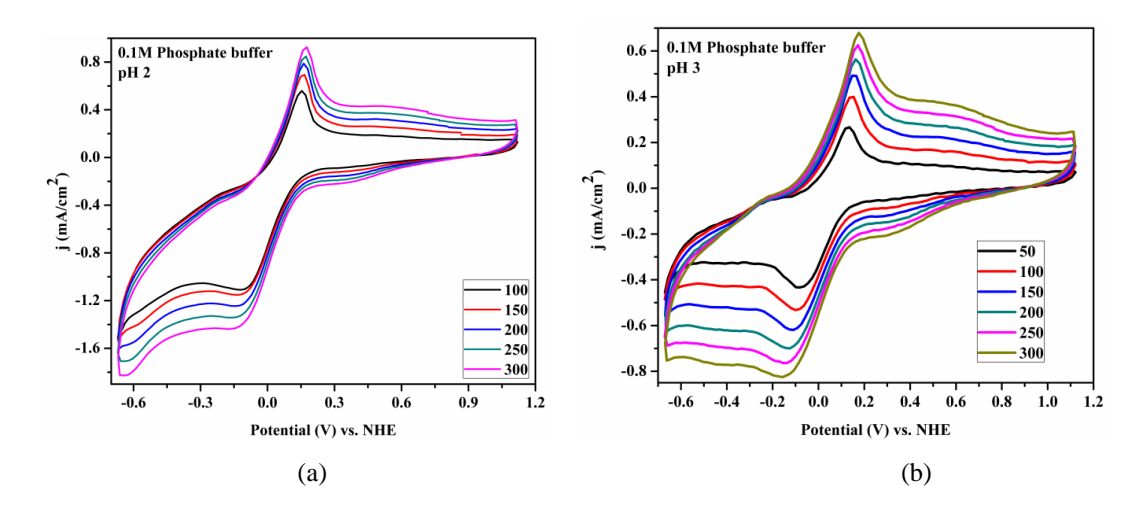


Figure 5.11. Cyclic Voltammetric plot of [Bu₄N]₄[Mo₈O₂₆] in 0.1M Na₂SO₄ at pH 5 at a scan rate of 100 mVsec⁻¹.



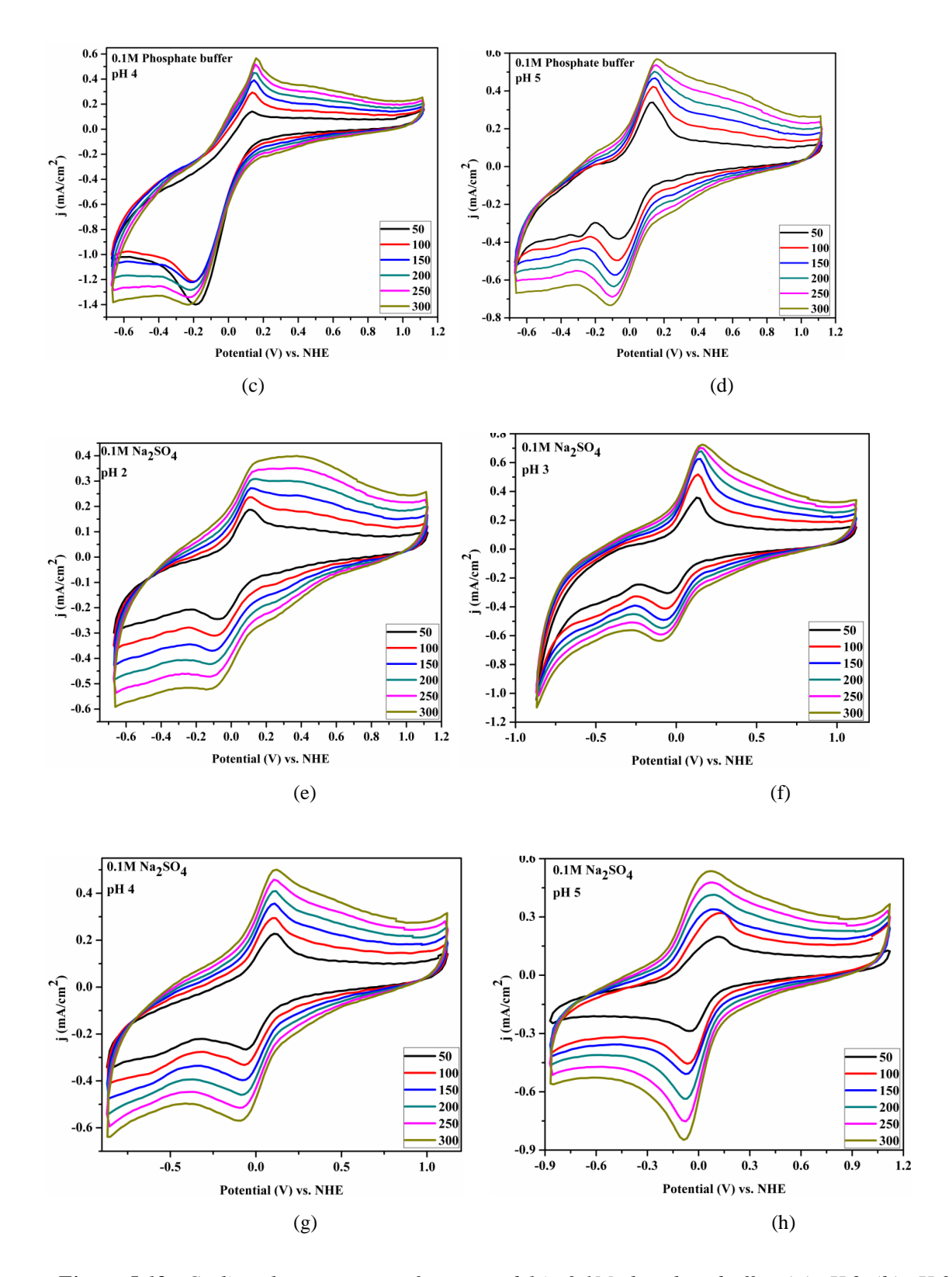


Figure 5.12. Cyclic voltammograms of compound 1 in 0.1M phosphate buffer: (a) pH 2, (b) pH 3, (c) pH 4 and (d) pH 5. Cyclic voltammograms of compound 1 in 0.1M Na₂SO₄: (e) pH 2, (f) pH 3, (g) pH 4 and (h) pH 5. The cyclic voltammograms were measured at different scan rates (in mV/sec), as mentioned in the respective graphs.

5.2.5 Electrocatalytic Water Oxidation

We tested the activity of compound **1** in 0.1M KCl solution and the results, so obtained, are given in Figure 5.13.

As can be seen from Figure 5.13a, the increase in the current at around 1.27 V signifies the electrocatalytic water oxidation process. The reversible couple A1/C1 (E_{A1} = 0.063 V; E_{C1} = 0.05; $E_{1/2}$ = 0.0065 V vs. NHE) can be attributed to the Cu^{II}/Cu^{I} couple. The activity of the compound is almost retained up to ten cycles as can be seen in Figure 5.13b.

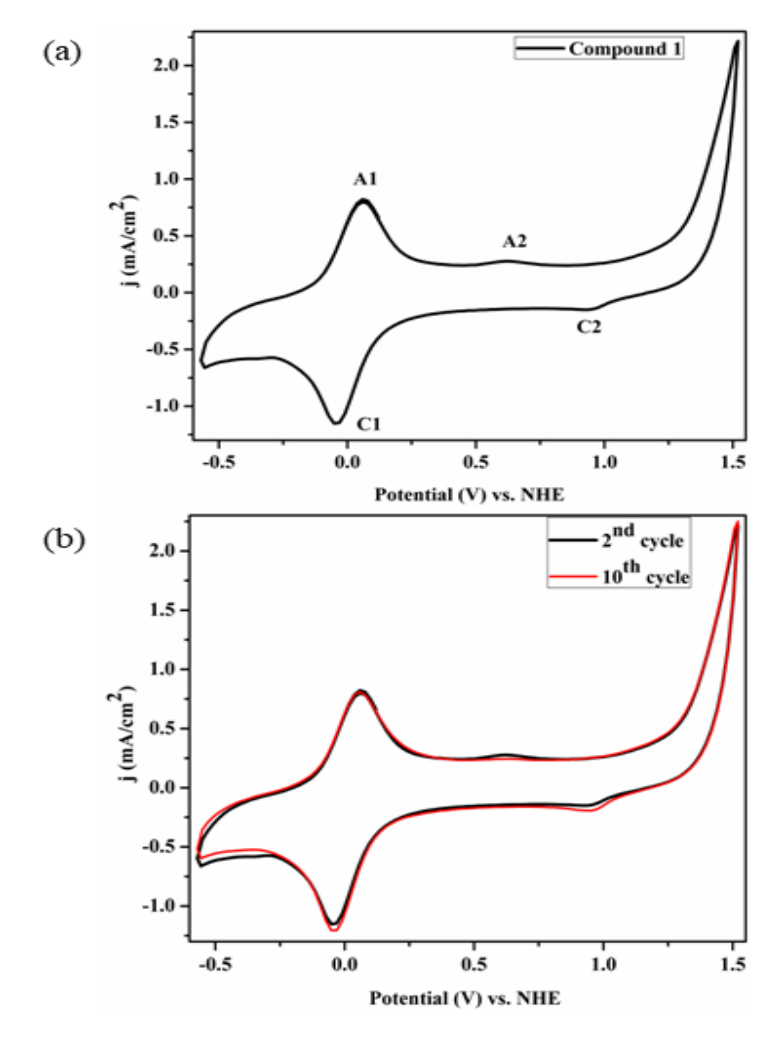


Figure 5.13. (a) Cyclic voltammogram of compound 1 in 0.1M KCl. (b) The water oxidation activity of compound 1 after 10 cycles.

In order to assess the electrocatalytic water oxidation activity of the title compound, cyclic voltammograms of compound 1 coated glassy carbon electrode were obtained in THF, a non-aqueous solvent, with [Bu₄N][BF₄] as the supporting electrolyte. This is because; we can add water sequentially (in the scale of micro-liters) to the non-aqueous reaction mixture in the electrochemical cell to investigate, whether the added water gets oxidized electrocatalytically.

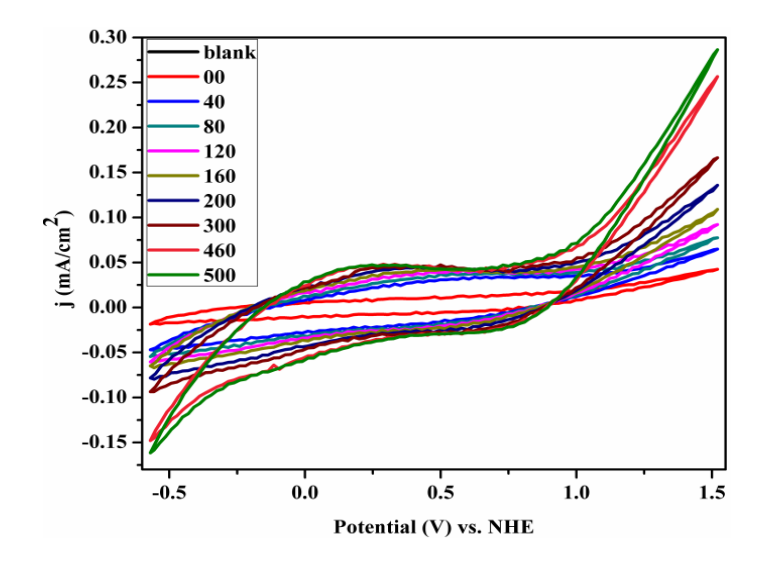


Figure 5.14. Cyclic voltammogram of compound 1 in THF with $[Bu_4N][BF_4]$ as supporting electrolyte and sequential addition of water. The values in the box indicate the amount of water added to the cell in μL .

The relevant voltammograms are represented in Figure 5.14. As can be seen from Figure 5.14, there is an increase in current in the anodic side with the sequential addition of water, with onset potential at around 0.9 V versus NHE. Thus compound 1 shows a significant electrocatalytic water oxidation response that the current intensity at around 0.9 V gradually increases with increasing amount of water. This is characteristic of electrocatalytic water oxidation. The small features, marked with A2 and C2 (Figure 5.13a), can be considered as Cu^{III}/Cu^{II} couple. It can be believed that the Cu(III) of this couple oxidizes water and comes back to its resting state, Cu(II), after water oxidation. The reason for the small feature of this Cu^{III}/Cu^{II} couple can be explained by the fact that Cu(II) center with {Cu^{II}N₂O₃} coordination with two soft donors would not be stable at its Cu(III) oxidation state, referring soft and hard acid-base principle.

5.2.6 Electrocatalytic Proton Reduction

The electrocatalytic proton reducing activity of the complex **1** was studied in 0.1M phosphate buffer, in 0.1M Na₂SO₄ at various pH values, in 0.1M KPF₆, in 0.1M KNO₃, in 0.1M H₂SO₄ as well as in 0.1M [Bu₄N][PF₆] in acetonitrile, with acetic acid addition, in the last case. As can be seen in Figure 5.15a, in 0.1M phosphate buffer, at pH 2, we get an onset at around – 0.5V for electrocatalytic proton reduction and the onset goes farther towards –1V, in pH 5. As shown in Figure 5.15a, the current height of electrocatalytic proton reduction increases enormously, as we go from pH 5 to pH 2. This proves that more is the number of protons (lesser the pH), more is the production of molecular hydrogen (H₂). The formation of hydrogen molecules was also evident from the visual observation of gas bubbles, found at the surface of the (working) glassy carbon electrode. In the case of 0.1M Na₂SO₄ (Figure 5.15b), a similar trend

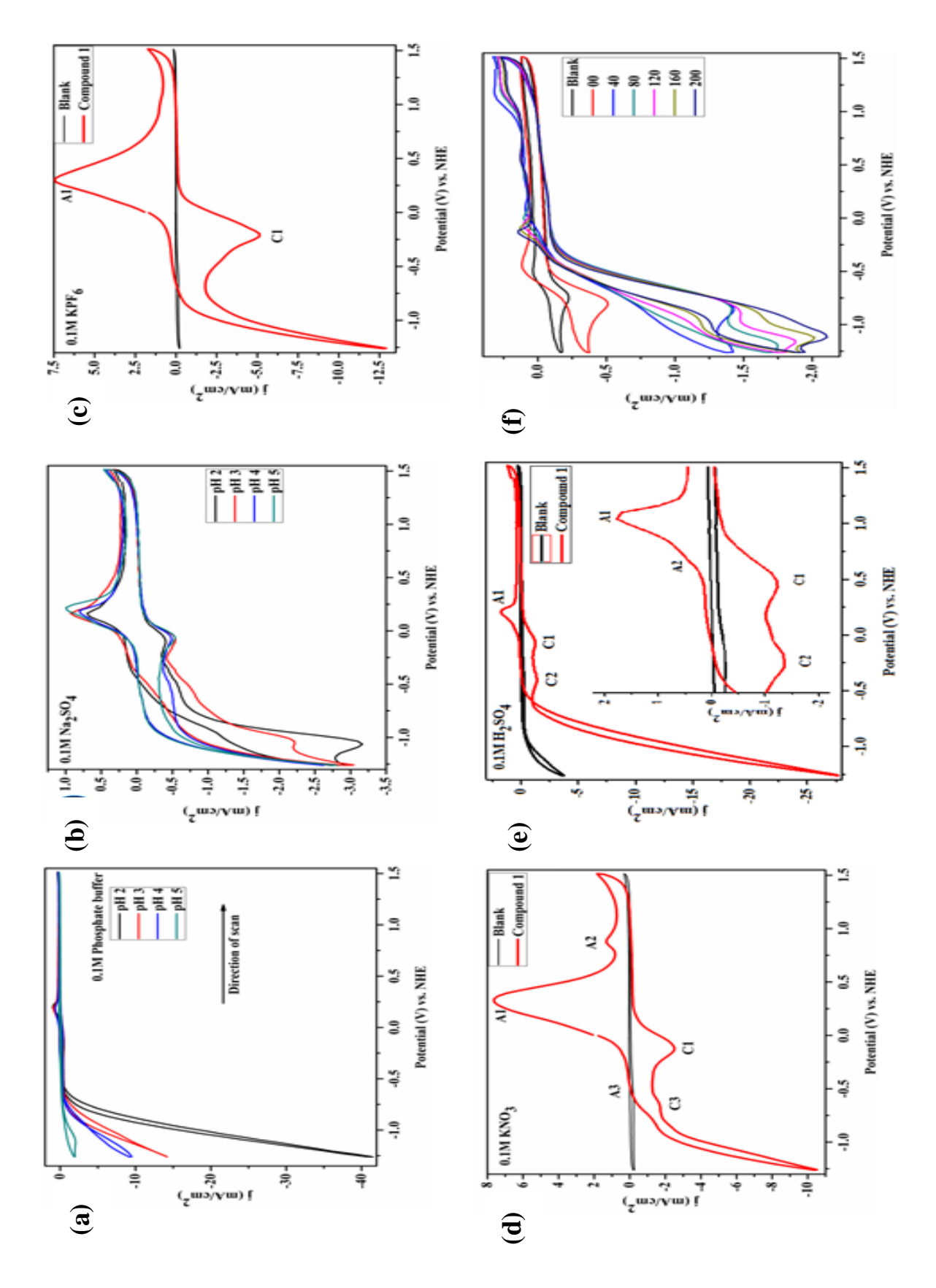


Figure 5.15. Proton reduction in (a) 0.1M phosphate buffer at different pH (b) 0.1M Na₂SO₄ (c) 0.1M KPF₆ (d) 0.1M KNO₃ (e) 0.1M H₂SO₄. In Figure 7e the inset shows a closer view of the redox behaviour of compound I(f) 0.1M $[Bu_4N][PF_6]$ in acetonitrile with sequential addition of acetic acid in μL .

is observed, i.e., with the decrease of pH, there is an increase in the amount of H_2 production. Notably, in this case, the Cu^{II}/Cu^{I} couple is visible (Figure 5.15b), unlike the case, where we have used phosphate buffer. Similarly, in 0.1M KPF₆ aqueous solution, along with the distinct A1/C1 couple (which can be assigned to the Cu^{II}/Cu^{I} couple), we see an onset at -0.75V (Figure 5.15c), which can be attributed to the electrocatalytic proton reduction to molecular hydrogen, catalyzed by compound **1**. A similar surge of current is also seen when the electrochemical reaction in carried out in 0.1M KNO₃ (Figure 5.15d). The huge reduction current can be attributed to the same fact that the concerned experiment of electrocatalytic proton reduction has been performed at pH = 1.3. This is also evident from the hydrogen bubbles that evolved in the cell, observed visually. Cyclic voltammograms of compound **1** in 0.1M H_2SO_4 at different scan rates (in mV/sec) are given in Figure 5.16.

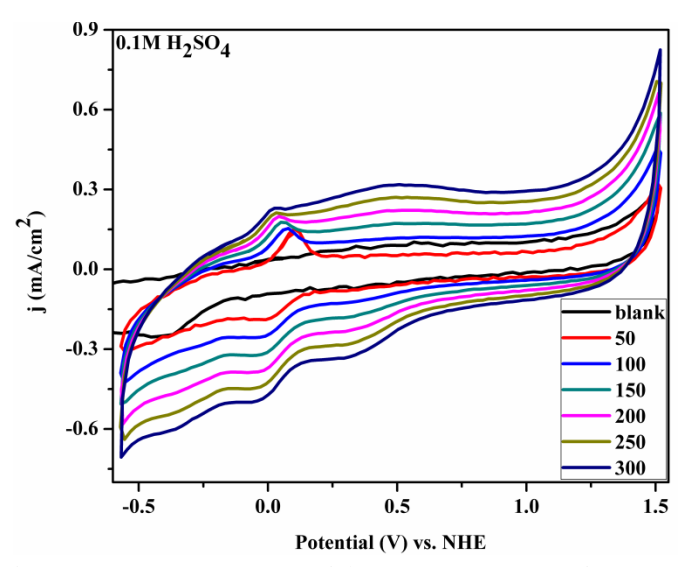


Figure 5.16. Cyclic voltammograms of compound 1 in $0.1M~H_2SO_4$ at different scan rates (in mV/sec), as mentioned in the above figure.

The behaviour of electrocatalytic proton reduction, catalyzed by compound 1 was also performed in dry acetonitrile with continuous nitrogen gas purging with 0.1M [Bu₄N][PF₆] as the supporting electrolyte (shown in Figure 5.15f). In this case, we found that with the addition of acetic acid to the cell, the current intensity of the reduction at -0.6V increased and the height of this reduction peak continuously increased as acetic acid concentration was increased in the cell through sequential addition from 40 μ L to 200 μ L. This continuous growth of the reduction peak is characteristic of the electrocatalytic reduction of acetic acid protons to hydrogen.

5.2.7 Electrocatalytic H₂O₂ Reduction

The electrocatalytic reduction of hydrogen peroxide was also assessed for compound 1. As we know that hydrogen peroxide undergoes thermal decomposition at room temperature, hence the electrocatalytic experiments were performed keeping the cell in an ice bath. The voltammograms corresponding to the reduction of hydrogen peroxide in 0.1M Na₂SO₄ at pH 5 with and without the catalyst are shown in Figure 5.16a and Figure 5.16b respectively. As we

can see, in both cases, the reduction peak increases with an increase in the concentration of H_2O_2 . But, the role of the catalyst is clear if we see the current produced in both cases. There is a substantial increase in the reduction current in the presence of compound 1, which proves that the compound plays the role of an electro-catalyst, which readily catalyzes the reduction of hydrogen peroxide.

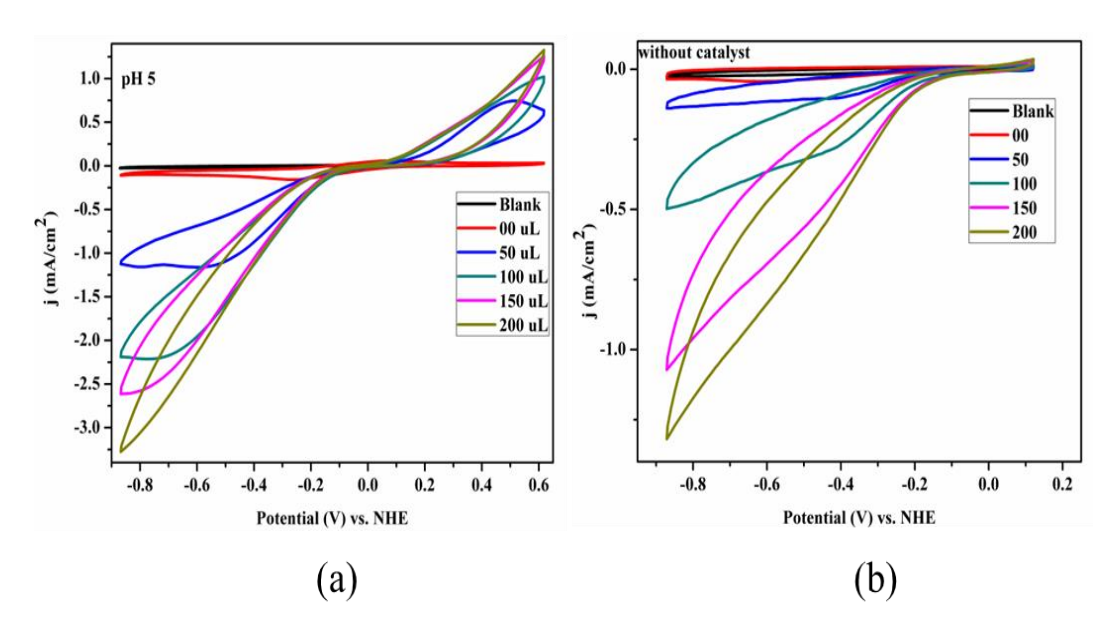


Figure 5.17. The electrocatalytic hydrogen peroxide reduction (a) without and (b) with compound 1 as a catalyst in 0.1M Na₂SO₄ at pH 5.

5.3 Conclusion

Polyoxometalate (POM) supported transition metal coordination complexes are a huge group of heterogeneous compounds in the POM family. And POM supported copper dimers belong to a very small class of compounds in this family; very few members of this class exhibit electrocatalytic applications. To our knowledge, there is no report, so far, on electrocatalytic water oxidation and proton reduction, catalyzed by a POM supported copper dimer complex. In the present article, we, not only, have demonstrated the successful synthesis and characterization of a copper dimeric complex, supported on a octamolybdate POM cluster anion, but also we have shown the electrocatalytic water oxidation to molecular oxygen, proton reduction to molecular hydrogen and electrocatalytic reduction of hydrogen peroxide using the synthesized POM supported copper dimeric complex.

5.4. Experimental Section

5.4.1 Synthesis

0.1037g (0.64 mmol) of 2, 2'-bipyridine was dissolved in 2 mL methanol followed by the addition of 50 mL water. To this solution, 15 mL glacial acetic acid was added and was stirred for 1 minute. To the stirred mixture, 1.4g (5.85 mmol) sodium molybdate was added and the resulting solution was kept for stirring. After 5 minutes, 0.5g (2.06 mmol) Cu(NO₃)₂·6H₂O was added followed by the addition of 1g (12.97 mmol) ammonium acetate. The resulting

solution was then stirred for 1 hour at 70 °C. The reaction mixture was then filtered and the blue color filtrate was kept at room temperature to yield blue block crystals after four days. Yield: 0.8 g (20.3% based on Mo). FT-IR (cm⁻¹): 650, 700, 838, 895, 940, 1032, 1250, 1314, 1423, 1495, 1571, 2804, 3080, 3207, 3510. Elemental analysis (in %): Calculated: C: 15.29; H: 1.18; N: 2.97; Found: C: 14.89; H 1.2; N: 2.68.

5.5 References

- 1. (a) Pope, M. T.; Muller, A. Angew. Chem. Int. Ed. 1991, 30, 34.
 - (b) Mizuno, N.; Misono, M. Chem. Rev. 1998, 98, 199.
 - (c) Kortz, U.; Savelieff, M. G.; Ghali, F. Y. A.; Khalil, L. M.; Maalouf, S. A.; Sinno, D. I. *Angew. Chem., Int. Ed.*, **2002**, *41*, 4070.
 - (d) Long, D. L.; Burkholder, E.; Cronin, L. Chem. Soc. Rev., 2007, 36, 105.
 - (e) Sun, C. Y.; Liu, S. X.; Liang, D. D.; Shao, K. Z.; Ren, Y. H.; Su, Z. M. J. Am. Chem. Soc. **2009**, *131*, 1883.
 - (f) Long, D. L.; Tsunashima, R.; Cronin, L. Angew. Chem., Int. Ed., 2010, 49, 1736.
- 2. (a) Singh, C.; Mukhopadhyay, S.; Das, S. K. Inorg. Chem. 2018, 57, 6479.
 - (b) Li, X.-M.; Chen, Y.-G.; Shi, T. Solid State Sci., 2016, 52, 112.
 - (c) Li, M.-T.; Sha, J.-Q.; Zong, X.-M.; Sun, J.-W.; Yan, P.-F.; Li, L.; Yang, X.-N. *Cryst. Growth Des.* **2014**, *14*, 2794.
 - (d) Liu, C.-M.; Huang, Y.-H.; Zhang, D.-Q.; Jiang, F.-C.; Zhu, D.-B. J. Coord. Chem. 2003, 56, 953.
 - (e) Wang, H.; Cheng, C.; Tian, Y. Chin. J. Chem. 2009, 27, 1099.
 - (f) Li, Y.-F.; Hubble, D. G.; Miller, R. G.; Zhao, H.-Y.; Pan, W.-P.; Parkin, S.; Yan, B. *Polyhedron* **2010**, *29*, 3324.
 - (g) Yi, Z.; Zhang, X.; Yu, X.; Liu, L.; Xu, X.; Cui, X.; Xu, J. J. Coord. Chem. 2013, 66, 1876.
- 3. (a) Xu, Y.; Xu, J.-Q.; Zhang, K.-L.; Zhang, Y.; You, X.-Y. Chem. Commun. 2000, 153.
 - (b) Wang, Y.; Zou, B.; Xiao, L.-N.; Jin, N.; Peng, Y.; Wu, F.-Q.; Ding, H.; Wang, T.-G.; Gao, Z.-M.; Zheng, D.-F.; Cui, X.-B.; Xu, J.-Q. *J. Solid State Chem.* **2011**, *184*, 557.
 - (c) Cui, J.-W.; Cui, X.-B.; Yu, H.-H.; Xu, J.-Q.; Yi, Z.-H.; Duan, W.-J. *Inorg. Chim. Acta* **2008**, *361*, 2641.
 - (d) Devi, R. N.; Burkholder, E.; Zubieta, J. Inorg. Chim. Acta 2003, 348, 150.
 - (e) Dolbecq, A.; Dumas, E.; Mayer, C. R.; Mialane, P. Chem. Rev. 2010, 110, 6009.
 - (f) Kumar, A.; Gupta, A. K.; Devi, M.; Gonsalves, K. E.; Pradeep, C. P. *Inorg. Chem.* **2017**, *56*, 10325.
- 4. (a) McKee, V.; Zvagulis, M.; Dagdigian, J. V.; Patch, M. G.; Reed, C. A. *J. Am. Chem. Soc.*, **1984**, *106*, 4675.
 - (b) Sorrell, T. N.; Garrity, M. L.; Ellis, D. J. Inorg. Chim. Acta, 1989, 166, 71.
 - (c) Mukherjee, R. N. Proc. Indian Natn. Sci. Acad. 2004, 70, 329.
 - (d) Novotna, R.; Travnicek, Z.; Herchel, Bioinorg. Chem. Appl. 2012, 704329.
- 5. Melink, M.; Kabesova, M.; Koman, M.; Macaskova, L.; Garaj, J.; Holloway, C. E.; Valent, A. *J. Coord. Chem.* **1998**, *45*, 147.
- 6. Perlepes, S. P.; Huffman, J. C.; Christou, G. Polyhedron 1992, 11, 1471.
- 7. Meenakumari, S.; Chakravarty, A. R. Polyhedron 1993, 12, 347.

- 8. Reinoso, S.; Vitoria, P.; Lezama, L.; Luque, A.; Gutierrez-Zorilla, J. M. *Inorg. Chem.* **2003**, 42, 3709.
- 9. Reinoso, S.; Vitoria, P.; Gutierrez-Zorilla, J. M.; Lezama, L.; Felices, L. S.; Beitia, J. I. *Inorg. Chem.* **2005**, *44*, 9731.
- 10. Reinoso, S.; Vitoria, P.; Felices, L. S.; Lezama, L.; Gutierrez-Zorilla, J. M. Chem. Eur. J. 2005, 11, 1538.
- 11. Reinoso, S.; Vitoria, P.; Felices, L. S.; Lezama, L.; Gutierrez-Zorilla, J. M. *Inorg. Chem.* **2006**, *45*, 108.
- 12. Reinoso, S.; Vitoria, P.; Gutierrez-Zorilla, J. M.; Lezama, L.; Madariaga, J. M.; Felices, L. S.; Iturrospe, A. *Inorg. Chem.* **2007**, *46*, 4010.
- 13. Ma, H.; Gong, L.; Wang, F.; Wang, X. Struct. Chem. 2008, 19, 435.
- 14. Han, Q. X.; Cheng, Y. M.; Li, J.; Wang, J. P. Russ. J. Coord. Chem. 2011, 37, 547.
- 15. Pang, H.; Yang, M.; Kang, L.; Ma, H.; Liu, B.; Li, S.; Liu, H. J. Solid State Chem. **2013**, 198, 440.
- 16. Li, S.; Ma, H.; Pang, H.; Zhang, L.; Zhang, Z. J. Mol. Struct. 2014, 1063, 351.
- 17. Luo, J.; Cheng, P.; Zhao, J.; Chen, L. Syn. React. Inorg. Metal-Org. Nano-metal Chem. **2015**, 45, 682-687.
- 18. Hou, Y.; Niu, Y.; Zhang, C.; Pang, H.; Ma, H. J. Chem. Sci. 2017, 129, 1639.
- 19. Miao, H.; Xu, X.; Ju, W.; Wan, W. H. X.; Zhang, Y.; Zhu, D. R.; Xu, Y. *Inorg. Chem.* **2014**, *53*, 2757-2759.
- 20. (a) Kudo, A.; Miseki, Y. Chem. Soc. Rev. 2009, 38, 253.
 - (b) Karkas, M. D.; Verho, O.; Johnston, E. V.; Akermark, B. Chem. Rev. 2014, 114, 11863.
 - (c) O'Regan, B.; Gratzel, M. *Nature* **1991**, *353*, 737.
 - (d) Kanan, M. W.; Nocera, D. G. Science. 2008, 321, 1072.
 - (e) Smith, R. D. L.; Prevot, M. S.; Fagan, R. D.; Zhang, Z. P.; Sedach, P. A.; Siu, M. K. J.; Trudel, S.; Berlinguette, C. P. *Science* **2013**, *340*, 60.
 - (f) Anantharaj, S.; Karthick, K.; Kundu, S. *Inorg. Chem.* **2018**, *57*, 3082.
- 21. Singh, C.; Mukhopadhyay, S.; Das, S. K. Inorg. Chem. 2018, 57, 6479.
- 22. (a) Cao, P.; Fang, T.; Fu, L. Z.; Zhou, L. L.; Zhan, S. Z. Int. J. Hyd. Energy 2014, 39, 10980.
 - (b) Zhang, P.; Wang, M.; Yong, Y.; Zheng, D.; Han, K.; Sun, L. Chem. Commun. 2014, 50, 14153.
 - (c) Aimoto, Y.; Koshiba, K.; Yamauchi, K.; Sakai, K. Chem. Commun. 2018, 54, 12820.
 - (d) Koshiba, K.; Yamauchi, K.; Sakai, K. Dalton Trans. 2018, 48, 635.
 - (e) Kilgore, U. J.; Roberts, J. A. S.; Pool, D. H.; Appel, A. M.; Stewart, M. P.; DuBois, M. R.; Dougherty, W. G.; Kassel, W. S.; Bullock, R. M.; DuBois, D. L. *J. Am. Chem. Soc.* **2011**, *133*, 5861.
 - (f) Inoue, S.; Mitsuhashi, M.; Ono, T.; Yan, Y.-N.; Kataoka, Y.; Handa, M.; Kawamoto, T. *Inorg. Chem.* **2017**, *56*, 12129.
 - (g) Han, Y.; Fang, H.; Jing, H.; Sun, H.; Lei, H.; Lai, W.; Cao, R. Angew. Chem. Int. Ed. 2017, 55, 5457.
- 23. (a) Liu, Y.; Fu, L.-Z.; Yang, L.-M.; Liu, X.-P.; Zhan, S.-Z.; Ni, C.-L. *J. Mol. Catal. A: Chem.* **2016**, *417*,101.
 - (b) Sun, H.; Han, Y.; Lei, H.; Chen, M.; Cao, R. Chem. Commun. 2017, 53, 6195.

- (c) Wang, J.; Li, C.; Zhou, Q.; Wang, W.; Zhou, Y.; Zhang, B.; Wang, X. Catal. Sci. Technol. **2016,** 6, 8482.
- (d) Li, X.; Lei, H.; Guo, X.; Zhao, X.; Ding, S.; Gao, X.; Zhang, W.; Cao, R. ChemSusChem **2017,** 10, 4632.
- (e) Lei, H.; Han, A.; Li, F.; Zhang, M.; Han, Y.; Du, P.; Lai, W.; Cao, R. Phys. Chem. Chem. Phys. 2014, 16, 1883.
- (f) Li, X.; Lei, H.; Liu, J.; Zhao, X.; Ding, S.; Zhang, Z.; Tao, X.; Zhang, W.; Wang, W.; Zheng X.; Cao, R. Angew. Chem. Int. Ed. 2018, 57, 15070.
- 24. (a) Mondal, B.; Dey, A. Chem. Commun. 2017, 53, 7707.
 - (b) Du, P.; Eisenberg, R. *Energy Environ. Sci.* **2012**, *5*, 6012.
 - (c) Rana, A.; Mondal, B.; Sen, P.; Dey, S.; Dey, A. *Inorg. Chem.* **2017**, *56*,1783.
- 25. (a) Zhang, P.; Wang, M.; Yong, Y.; Yao, T.; Sun, L. Angew Chem Int. Ed. 2014, 53, 13803.
 - (b) Fang, T.; Fu, L.-Z.; Zhou, L.-L.; Zhan, S.-Z. *Electrochim. Acta* **2015**, *161*, 388.
 - (c) Zhou, L.-L.; Fang, T.; Cao, J.-P.; Z., Z.-H.; Su, X.-T.; Zhan, S.-Z. J. Power Sour. 2015, 273, 298.
 - (d) Lei, H.; Fang, H.; Han, Y.; Lai, W.; Fu, X.; Cao, R. ACS Catal. 2015, 5, 5145.
- 26. Singh, C.; Das, S. K. Polyhedron (2019) DOI: 10.1016/j.poly.2019.03.026.
- 27. Bridgeman, A. J.; Cavigliasso, G. Inorg. Chem. 2002, 41, 3500.
- 28. (a) Rosnes, M. H.; Yvon, C.; Long, D.-L.; Cronin, L. Dalton Trans. 2012, 41, 10071.
 - (b) Zebiri, I.; Boufas, S.; Mosbah, S.; Bencharif, L.; Bencharif, M. J. Chem. Sci., 2015, 127, 1769.
- 29. (a) Kuz'mina, N. E.; Palkina, K. K.; Polyakova, N. V.; Strashnova, S. B.; Koval'chukova, O. V.; Zaitsev, B. E.; Levov, A. N. Russ. J. Coord. Chem. 2001, 27, 711.
 - (b) Bedowr, N. S.; Yahya, R. B.; Farhan, N. J. Saudi Chem. Soc. 2018, 22, (255.
- 30. (a) Yamase, T. Chem. Rev. 1998, 98, (307.
 - (b) Zhang, X. M.; Shen, B. Z.; You, X. Z.; Fun, H. K. Polyhedron 1997, 16, (95.
 - (c) Gong, Y.; Hu, C.; Li, H.; Tang, W.; Huang, K.; Hou, W. J. Mol. Struct. 2006, 784,228.
- 31. Coe, B. J.; Peers, M. K.; Scrutton, N. S. Polyhedron, 2015, 96, 57.
- 32. (a) Koo, B. W. Bull. Korean Chem. Soc. **2001**, 22, 113.
 - (b) Lever, A. B. P. *Inorganic Electronic Spectroscopy*, 2nd Ed.; Elsevier, Amsterdam, **1984**, 553-572, 636-638.
- 33. Wang, P.; Wang, X.; Zhu, G. *Electrochim. Acta*, **2000**, *46*, 637.

Summary and Future Scope

Summary

This thesis demonstrates the importance of the supramolecular interactions in polyoxometalates and their applications in various fields. Mainly we have studied the supramolecular interactions of polyoxometalates with other moieties. Using these supramolecular interactions of polyoxometalates, we have used them for molecular recognition. Apart from this, we have used them for a new rearrangement reaction and, also as electrocatalysts.

All the compounds in these chapters have been synthesized using conventional synthetic procedures, yielding single crystals of respective compounds. They are characterized using routine techniques, thermogravimetric analysis and ¹H NMR of some compounds have also been recorded. PXRD technique has been extensively used to ensure the bulk purity of all the compounds. The structures of all the compounds have been determined using single crystal X-ray diffraction technique.

Chapter 1 gives a general introduction about polyoxometalates, their history and properties along with their applications. It also gives an account of the motivation of the present thesis work.

Chapter 2 describes the role of polyoxometalates in isolating the transition metal aqua complexes in their preferred coordination number. Co(II), NI(II) and Zn(II)-aqua complexes were the focussed transition metal ions. The reactions yielded the metal-aqua complexes sandwiched between two crown ether moieties, which was stabilized by a hexamolybdte anion, through hydrogen bonding interactions. The chapter infers from the experimental results, that Ni(II) prefers a hexa-aqua coordination, hence forming an octahedron, while Zn(II) prefers a penta-aqua coordination forming a trigonal bipyramidal structure. Interestingly Co(II) exhibits a simultaneous co-existence of both penta-as well as hexa-aqua complex. The compounds have been characterized using routine techniques and its structure has been elucidated using single-crystal X-ray diffraction technique.

Chapter 3 portrays another example of molecular recognition by crown ether moieties where again the polyoxometalates a vital role. Here, the cavities of the crown ether moieties

determine the type of guest molecule that are encapsulated through host-guest interactions. In an attempt to get ammonium cation inclusion complexes in crown ether, we used NH4Cl as the ammonium source. While in the case of the first compound, where 18-crown-6 was used as the host, there instead of an ammonium cation, a chloride anion is encapsulated, exactly at the centre of the cavity. In the second compound, where dibenzo-24-crown-8, a crown ether with a larger cavity was used, two ammonium cations were encapsulated in the cavity. In a similar, but a novel way, two acetonitrile molecules are also encapsulated in the cavity, such that the N atoms of the CH3CN molecule is towards the cavity, hence giving space to N-O interactions, between the acetonitrile N atom and the O atoms of the crown ether. In both cases, Keggin type polyoxometalates were used, $[PMo_{12}O_{40}]^{3-}$ and $[SiMo_{12}O_{40}]^{4-}$ in compounds 1 and 2 respectively.

Chapter 4 introduces us with a new inorganic rearrangement reaction, where triethylamine vapours when allowed to diffuse into acidified aqueous solution of sodium molybdate leads to the generation of tetraethylammonium cation and ammonium cations. The tetraethylammonium cations are a part of crystal of compound 1, but the ammonium ions, which stays back in the mother liquor of compound 1 is included in the crown ether cavity by its association with a polyoxometalate, giving us compound 2. Thus, we have been successful in demonstrating a unique reaction, where a triethylamine rearranges itself to form an ammonium cation, at ambient conditions. In his rearrangement reaction, sodium molybdate plays a major role, absence of which the reaction doesn't proceed.

Chapter 5 describes the synthesis and characterization of a copper dimeric complex, that is supported on a polyoxometalate. It is synthesized using a conventional synthesis protocol. The compound described in this chapter has two dimeric units connected to the polyoxometalate unit in two opposite sides. The compound is shown to act as an electrocatalyst for water oxidation, proton reduction and hydrogen peroxide reduction.

Future Scope

Polyoxometalates for Molecular Recognition

Transition metals, which are used every now and then, on account of their vivid range of applications, need to be studied. As we have seen about the coordination umbers of Co, Ni, Cu and Zn, there are other transition metals of importance like Mg, Mn and Cr, whose coordination chemistry, especially a detailed study of their coordination number is to be done soon. These transition metals-aqua complexes, in their +2 oxidation states can be studied by sandwiching them between two crown ethers and stabilizing the compounds by polyoxometalates.

The chloride encapsulation in the crown ether cavity opens a new window for visualizing this rare phenomenon. Apart from chloride, bromide and iodide encapsulation in the crown ether cavity can also be studied taking crown ethers of different cavity sizes. This will help us in using these halogen encapsulated crown ether for sensing studies.

Polyoxometalate supported transition metal dimeric complexes for Catalysis

Polyoxometalates can act as good ligands, which can form bonds with transition metals through their terminal oxygen atom(s). There are many reports where such transition metal complexes have been used as electrocatalysts.

In **Chapter 5**, we have shown a copper dimeric complex supported on a polyoxometalate that has been shown to act as electrocatalyst for water oxidation, proton reduction and hydrogen peroxide reduction. We can synthesize more such dimeric complexes supported on polyoxometalates and use them as electrocatalysts and photocatalysts and catalysts for organic transformation reactions.

Appendix

A1. General Experimental Procedures

A1.1 Materials and Methods

All the starting materials were purchased as analytical grade and were used as received. IR spectra of the compounds were obtained on a JASCO-5300 FTIR spectrophotometer. UV-visible DRS electronic absorption spectra were recorded using a Shimadzu-2600 spectrophotometer. TGA was carried out on an STA 409 PC Analyzer. PXRD plots were recorded on a Bruker D8-Advance diffractometer using graphite-monochromated Cu $K\alpha_1$ (1.5406 Å) and $K\alpha_2$ (1.55439 Å) radiation.

A1.2 Crystal Data Collection

X-ray reflections were collected on Bruker D8 QUEST, CCD diffractometer equipped with a graphite monochromator and Mo-K α fine-focus sealed tube (λ = 0.71073 Å), and the reduction was performed using APEX-II Software.¹ Intensities were corrected for absorption using SADABS, and the structure was solved and refined using SHELX97.² All non-hydrogen atoms were refined anisotropically. Hydrogen atoms on atoms were located from difference electron-density maps, and all C-H H atoms were fixed geometrically. Hydrogen-bond geometries were determined in PLATON.^{3,4}

A1.3 Electrochemical Studies

All electrochemical experiments were conducted using a Zahner Zannium electrochemical workstation operated by *Thales* software. Complete electrochemical experiments were accomplished using a three-electrode electrochemical cell with compound A (A represents the compound studied) modified glassy carbon as the working electrode, homemade Ag/AgCl (1 M) as the reference electrode and a Pt flag as the counter electrode in acidic pH in an aqueous medium. For the preparation of the A-modified electrode, 4 mg of A and 1 mg of acetylene carbon black were placed in a 1 mL of 3:2 mixture of ethanol/water and to it, was added 10 µL of 5 wt % Nafion (aqueous). The mixture was sonicated for 30 minutes to make it a homogeneous suspension. Then 5 µL of this mixture was coated on a 3-mm-diameter glassy carbon electrode (geometrical area = 0.0706 cm^2), resulting in 10 µg of the sample (compound A) in each coating on the glassy carbon electrode. The same amount on the electrode surface was maintained for all electrochemical experiments. The coating mixture on the electrode was dried under an IR lamp (temperature approx. 70 °C) prior to the experiment. All the experiments were conducted under ambient temperature. Electrode potentials were converted to the normal hydrogen electrode (NHE) scale using the relationship E(NHE) = E(Ag/AgCl) +0.1263 V as Ag/AgCl was used as the reference electrode. CV scans were initiated at the open-circuit potential and the anodic side was scanned first, followed by the cathodic side scan. Five cycles were taken consecutively for each set of CV measurements in the solution. Cyclic voltammograms were also recorded at various scan rates. For experiments in a non-aqueous medium, nitrogen gas was purged into the cell throughout the experiment.

A1.4 References

- Bruker SMART, Version 5.625, SHELXTL, Version 6.12; Bruker AXS Inc.: Madison, 1. Wisconsin, USA, 2000.
- 2. Sheldrick, G. M. Program for Refinement of Crystal Structures; University of Göttingen, Germany, 1997.
- 3. Sheldrick, G. M. Acta Crystallogr., Sect. A: Found. Crystallogr. 2008, 64, 112–122.
- Sheldrick, G. M. Acta Crystallogr., Sect. C: Struct. Chem. 2015, 71, 3-8. 4.

A2. Chapter 2 Transition Metal-Aqua-Complexes: Six or Five Fold Coordination or **Together**

Table A2.1 Bond lengths [Å] and angles [deg] for compound [{Co(H₂O)₅([18]-crown-6)₂} ${Co(H_2O)_6([18]-crown-6)_2}][Mo_6O_{19}]_2$ (1)

C12 O25	1.327(14)	Mo4 O12D	1.928(3)
C12 C12	1.37(3)	Mo4 O6E	1.929(3)
C12 H12A	0.9700	Mo4 O2G	1.937(3)
C12 H12B	0.9700	Mo4 O7C	2.3335(6)
Mo3 O4M	1.683(5)	Mo2 O1S	1.674(6)
Mo3 O5	1.925(4)	Mo2 O3B	1.920(5)
Mo3 O6E	1.931(3)	Mo2 O8K	1.921(5)
Mo3 O6E	1.931(3)	Mo2 O2G	1.928(4)
Mo3 O3B	1.931(5)	Mo2 O2G	1.928(4)
Mo3 O7C	2.318(4)	Mo2 O7C	2.316(4)
Mo5 O11N	1.676(5)	Mo1 O9U	1.673(6)
Mo5 O14F	1.906(5)	Mo1 O8K	1.932(5)
Mo5 O5	1.921(5)	Mo1 O14F	1.940(6)
Mo5 O12D	1.933(4)	Mo1 O10H	1.943(4)
Mo5 O12D	1.933(4)	Mo1 O10H	1.943(4)
Mo5 O7C	2.322(4)	Mo1 O7C	2.302(4)
Mo4 O13R	1.688(4)	Co2 O32J	1.987(5)
Mo4 O10H	1.920(4)	Co2 O32J	1.987(5)

Co2 O33Q	1.994(7)	C5Z C6	1.491(9)
Co2 O30	2.073(4)	C5Z H5Z1	0.9700
Co2 O30	2.073(4)	C5Z H5Z2	0.9700
Co1 O35T	2.065(6)	C6 H6A	0.9700
Co1 O35T	2.065(6)	C6 H6B	0.9700
Co1 O34V	2.067(6)	C2 C1	1.499(9)
Co1 O34V	2.067(6)	C2 H2A	0.9700
Co1 O31A	2.085(4)	C2 H2B	0.9700
Co1 O31A	2.085(4)	O25 C7	1.342(12)
O7C Mo4	2.3334(6)	C1 H1A	0.9700
O22I C3X	1.415(7)	C1 H1B	0.9700
O22I C2	1.440(7)	O27 C11	1.295(12)
O23L C5Z	1.399(7)	O27 C10	1.352(12)
O23L C4W	1.431(7)	C7 C8	1.610(15)
O21O C1	1.403(6)	C7 H7A	0.9700
O21O C1	1.403(6)	C7 H7B	0.9700
O24P C6	1.410(6)	C8 H8A	0.9700
O24P C6	1.410(6)	C8 H8B	0.9700
C4W C3X	1.474(9)	C9 C10	1.568(13)
C4W H4W1	0.9700	C9 H9A	0.9700
C4W H4W2	0.9700	C9 H9B	0.9700
C3X H3X1	0.9700	C10 H10A	0.9700
C3X H3X2	0.9700	C10 H10B	0.9700
O26Y C8	1.344(10)	C11 H11A	0.9700
O26Y C9	1.375(10)	C11 H11B	0.9700

O25 C12 C12	124.6(7)	O11N Mo5 O12D	103.17(10)
O25 C12 H12A	106.2	O14F Mo5 O12D	87.51(11)
C12 C12 H12A	106.2	O5 Mo5 O12D	86.45(11)
O25 C12 H12B	106.2	O12D Mo5 O12D	153.6(2)
C12 C12 H12B	106.2	O11N Mo5 O7C	179.1(2)
H12A C12 H12B	106.4	O14F Mo5 O7C	76.80(18)
O4M Mo3 O5	102.7(3)	O5 Mo5 O7C	76.48(16)
O4M Mo3 O6E	103.00(10)	O12D Mo5 O7C	76.82(10)
O5 Mo3 O6E	87.20(10)	O12D Mo5 O7C	76.82(10)
O4M Mo3 O6E	103.00(10)	O13R Mo4 O10H	103.29(19)
O5 Mo3 O6E	87.20(10)	O13R Mo4 O12D	103.08(18)
O6E Mo3 O6E	154.0(2)	O10H Mo4 O12D	86.90(15)
O4M Mo3 O3B	103.9(3)	O13R Mo4 O6E	103.57(18)
O5 Mo3 O3B	153.4(2)	O10H Mo4 O6E	153.14(16)
O6E Mo3 O3B	86.88(10)	O12D Mo4 O6E	86.96(14)
O6E Mo3 O3B	86.88(10)	O13R Mo4 O2G	104.09(18)
O4M Mo3 O7C	179.2(2)	O10H Mo4 O2G	86.95(15)
O5 Mo3 O7C	76.51(17)	O12D Mo4 O2G	152.84(16)
O6E Mo3 O7C	77.00(10)	O6E Mo4 O2G	86.69(14)
O6E Mo3 O7C	77.00(10)	O13R Mo4 O7C	179.64(19)
O3B Mo3 O7C	76.93(16)	O10H Mo4 O7C	76.51(15)
O11N Mo5 O14F	104.1(3)	O12D Mo4 O7C	76.63(15)
O11N Mo5 O5	102.6(3)	O6E Mo4 O7C	76.64(13)
O14F Mo5 O5	153.3(2)	O2G Mo4 O7C	76.21(15)
O11N Mo5 O12D	103.17(10)	O1S Mo2 O3B	102.4(3)
O14F Mo5 O12D	87.51(11)	O1S Mo2 O8K	103.8(3)
O5 Mo5 O12D	86.45(11)	O3B Mo2 O8K	153.8(2)

O1S Mo2 O2G	103.21(10)	O32J Co2 O32J	117.8(4)
O3B Mo2 O2G	87.36(11)	O32J Co2 O33Q	121.11(18)
O8K Mo2 O2G	86.71(11)	O32J Co2 O33Q	121.11(18)
O1S Mo2 O2G	103.21(10)	O32J Co2 O30	90.24(6)
O3B Mo2 O2G	87.36(11)	O32J Co2 O30	90.24(6)
O8K Mo2 O2G	86.71(11)	O33Q Co2 O30	89.53(12)
O2G Mo2 O2G	153.6(2)	O32J Co2 O30	90.25(6)
O1S Mo2 O7C	179.6(2)	O32J Co2 O30	90.24(6)
O3B Mo2 O7C	77.17(16)	O33Q Co2 O30	89.53(12)
O8K Mo2 O7C	76.66(18)	O30 Co2 O30	179.1(2)
O2G Mo2 O7C	76.79(10)	O35T Co1 O35T	91.6(5)
O2G Mo2 O7C	76.79(10)	O35T Co1 O34V	89.5(4)
O9U Mo1 O8K	102.9(3)	O35T Co1 O34V	178.9(4)
O9U Mo1 O14F	103.6(3)	O35T Co1 O34V	178.9(4)
O8K Mo1 O14F	153.5(2)	O35T Co1 O34V	89.5(4)
O9U Mo1 O10H	103.13(10)	O34V Co1 O34V	89.4(6)
O8K Mo1 O10H	87.53(11)	O35T Co1 O31A	89.64(8)
O14F Mo1 O10H	86.50(11)	O35T Co1 O31A	89.64(8)
O9U Mo1 O10H	103.13(10)	O34V Co1 O31A	90.37(9)
O8K Mo1 O10H	87.53(11)	O34V Co1 O31A	90.37(9)
O14F Mo1 O10H	86.50(11)	O35T Co1 O31A	89.63(8)
O10H Mo1 O10H	153.7(2)	O35T Co1 O31A	89.64(8)
O9U Mo1 O7C	179.7(3)	O34V Co1 O31A	90.37(9)
O8K Mo1 O7C	76.82(18)	O34V Co1 O31A	90.37(9)
O14F Mo1 O7C	76.68(17)	O31A Co1 O31A	179.0(2)
O10H Mo1 O7C	76.88(10)	Mo5 O5 Mo3	117.0(2)
O10H Mo1 O7C	76.87(10)	Mo2 O3B Mo3	116.2(2)

Mo1 O7C Mo2	90.25(14)	C3X C4W H4W1	109.7
Mo1 O7C Mo3	179.98(19)	O23L C4W H4W2	109.7
Mo2 O7C Mo3	89.73(13)	C3X C4W H4W2	109.7
Mo1 O7C Mo5	90.05(13)	H4W1 C4W H4W2	108.2
Mo2 O7C Mo5	179.70(18)	O22I C3X C4W	109.0(5)
Mo3 O7C Mo5	89.97(13)	O22I C3X H3X1	109.9
Mo1 O7C Mo4	90.20(9)	C4W C3X H3X1	109.9
Mo2 O7C Mo4	90.16(9)	O22I C3X H3X2	109.9
Mo3 O7C Mo4	89.80(9)	C4W C3X H3X2	109.9
Mo5 O7C Mo4	89.84(9)	H3X1 C3X H3X2	108.3
Mo1 O7C Mo4	90.20(9)	C8 O26Y C9	109.0(9)
Mo2 O7C Mo4	90.16(9)	O23L C5Z C6	109.8(5)
Mo3 O7C Mo4	89.80(9)	O23L C5Z H5Z1	109.7
Mo5 O7C Mo4	89.84(9)	C6 C5Z H5Z1	109.7
Mo4 O7C Mo4	179.5(2)	O23L C5Z H5Z2	109.7
Mo4 O12D Mo5	116.71(17)	C6 C5Z H5Z2	109.7
Mo4 O6E Mo3	116.56(16)	H5Z1 C5Z H5Z2	108.2
Mo5 O14F Mo1	116.5(2)	O24P C6 C5Z	111.1(5)
Mo2 O2G Mo4	116.84(18)	O24P C6 H6A	109.4
Mo4 O10H Mo1	116.42(18)	C5Z C6 H6A	109.4
C3X O22I C2	111.6(5)	O24P C6 H6B	109.4
Mo2 O8K Mo1	116.3(2)	C5Z C6 H6B	109.4
C5Z O23L C4W	113.0(5)	H6A C6 H6B	108.0
C1 O21O C1	112.1(6)	O22I C2 C1	109.7(5)
C6 O24P C6	114.8(6)	O22I C2 H2A	109.7
O23L C4W C3X	109.9(5)	C1 C2 H2A	109.7
O23L C4W H4W1	109.7	O22I C2 H2B	109.7

C1 C2 H2B	109.7	C7 C8 H8B	109.7
H2A C2 H2B	108.2	H8A C8 H8B	108.2
C12 O25 C7	107.2(9)	O26Y C9 C10	110.3(7)
O21O C1 C2	110.8(5)	O26Y C9 H9A	109.6
O21O C1 H1A	109.5	C10 C9 H9A	109.6
C2 C1 H1A	109.5	O26Y C9 H9B	109.6
O21O C1 H1B	109.5	C10 C9 H9B	109.6
C2 C1 H1B	109.5	H9A C9 H9B	108.1
H1A C1 H1B	108.1	O27 C10 C9	108.5(8)
C11 O27 C10	109.8(9)	O27 C10 H10A	110.0
O25 C7 C8	108.2(8)	C9 C10 H10A	110.0
O25 C7 H7A	110.1	O27 C10 H10B	110.0
C8 C7 H7A	110.1	C9 C10 H10B	110.0
O25 C7 H7B	110.1	H10A C10 H10B	108.4
C8 C7 H7B	110.1	O27 C11 C11	124.7(6)
H7A C7 H7B	108.4	O27 C11 H11A	106.1
O26Y C8 C7	109.8(8)	C11 C11 H11A	106.1
O26Y C8 H8A	109.7	O27 C11 H11B	106.1
C7 C8 H8A	109.7	C11 C11 H11B	106.1
O26Y C8 H8B	109.7	H11A C11 H11B	106.3

Table A2.2 Bond lengths $[\mathring{A}]$ and angles [deg] for compound $[Ni(H_2O)_6([18]-crown-6)_2]$ [Mo₆O₁₉] (2)

O21 C3W	1.163(17)	C13 H13A	0.9700
O21 C2U	1.66(3)	C13 H13B	0.9700
C13 O17J	1.165(19)	Mo3 O9G	1.673(5)
C13 C8S	1.370(18)	Mo3 O7C	1.896(5)

Mo3 O6	1.916(6)	O7C Mo2	1.955(5)
Mo3 O8A	1.929(6)	O16I C5V	1.179(16)
Mo3 O10	1.965(5)	O16I C4L	1.598(17)
Mo3 O5	2.3119(6)	O17J C6O	1.381(13)
Mo2 O4F	1.673(5)	O19K C9T	1.152(16)
Mo2 O10	1.885(5)	O19K C8S	1.65(2)
Mo2 O3	1.923(6)	C4L C3W	1.72(2)
Mo2 O2B	1.929(6)	C4L H4L1	0.9700
Mo2 O7C	1.955(5)	C4L H4L2	0.9700
Mo2 O5	2.3185(6)	O18N C10R	1.360(15)
Mo1 O1H	1.681(6)	O18N C11Y	1.405(16)
Mo1 O8A	1.924(5)	C6O C5V	1.65(2)
Mo1 O2B	1.931(5)	C6O H6O1	0.9700
Mo1 O3	1.933(5)	C6O H6O2	0.9700
Mo1 O6	1.942(5)	O14P C1	1.247(17)
Mo1 O5	2.3225(6)	O14P C12Q	1.373(15)
Ni1 O11	2.037(4)	C12Q C11Y	1.44(2)
Ni1 O11	2.037(4)	C12Q H12A	0.9700
Ni1 O13E	2.059(6)	C12Q H12B	0.9700
Ni1 O13E	2.059(6)	C10R C9T	1.70(2)
Ni1 O12D	2.064(5)	C10R H10A	0.9700
Ni1 O12D	2.064(5)	C10R H10B	0.9700
O5 Mo3	2.3119(6)	C8S H8S1	0.9700
O5 Mo2	2.3186(6)	C8S H8S2	0.9700
O5 Mo1	2.3225(6)	C9T H9T1	0.9700
O8A Mo1	1.924(5)	С9Т Н9Т2	0.9700
O2B Mo1	1.931(5)	C2U C1	1.35(2)

C2U H2U1	0.9700	O8A Mo3 O10	85.1(2)
C2U H2U2	0.9700	O9G Mo3 O5	179.2(2)
C5V H5V1	0.9700	O7C Mo3 O5	77.29(15)
C5V H5V2	0.9700	O6 Mo3 O5	77.11(15)
C3W H3W1	0.9700	O8A Mo3 O5	76.89(15)
C3W H3W2	0.9700	O10 Mo3 O5	76.19(14)
C11Y H11A	0.9700	O4F Mo2 O10	103.5(3)
C11Y H11B	0.9700	O4F Mo2 O3	103.4(3)
C1 H1A	0.9700	O10 Mo2 O3	88.4(2)
C1 H1B	0.9700	O4F Mo2 O2B	103.0(3)
		O10 Mo2 O2B	88.4(2)
C3W O21 C2U	96.9(13)	O3 Mo2 O2B	153.5(2)
O17J C13 C8S	136(3)	O4F Mo2 O7C	102.9(3)
O17J C13 H13A	103.1	O10 Mo2 O7C	153.5(2)
C8S C13 H13A	103.1	O3 Mo2 O7C	85.0(2)
O17J C13 H13B	103.1	O2B Mo2 O7C	86.2(2)
C8S C13 H13B	103.1	O4F Mo2 O5	178.9(2)
H13A C13 H13B	105.1	O10 Mo2 O5	77.50(15)
O9G Mo3 O7C	103.4(3)	O3 Mo2 O5	76.81(15)
O9G Mo3 O6	103.2(3)	O2B Mo2 O5	76.80(15)
O7C Mo3 O6	89.0(2)	O7C Mo2 O5	76.05(15)
O9G Mo3 O8A	102.8(3)	O1H Mo1 O8A	102.7(3)
O7C Mo3 O8A	87.9(2)	O1H Mo1 O2B	102.3(3)
O6 Mo3 O8A	153.9(2)	O8A Mo1 O2B	86.8(2)
O9G Mo3 O10	103.1(3)	O1H Mo1 O3	104.5(3)
O7C Mo3 O10	153.5(2)	O8A Mo1 O3	87.6(2)
O6 Mo3 O10	86.1(2)	O2B Mo1 O3	153.2(2)

O1H Mo1 O6	104.2(3)	Mo3 O5 Mo2	89.93(2)
O8A Mo1 O6	153.1(2)	Mo3 O5 Mo2	90.07(2)
O2B Mo1 O6	86.5(2)	Mo2 O5 Mo2	180.00(3)
O3 Mo1 O6	86.7(2)	Mo3 O5 Mo1	90.08(2)
O1H Mo1 O5	178.8(3)	Mo3 O5 Mo1	89.92(2)
O8A Mo1 O5	76.72(16)	Mo2 O5 Mo1	90.01(2)
O2B Mo1 O5	76.66(16)	Mo2 O5 Mo1	89.99(2)
O3 Mo1 O5	76.53(16)	Mo3 O5 Mo1	89.92(2)
O6 Mo1 O5	76.37(16)	Mo3 O5 Mo1	90.08(2)
O11 Ni1 O11	180.0	Mo2 O5 Mo1	89.99(2)
O11 Ni1 O13E	89.7(2)	Mo2 O5 Mo1	90.01(2)
O11 Ni1 O13E	90.3(2)	Mo1 O5 Mo1	180.0
O11 Ni1 O13E	90.3(2)	Mo2 O10 Mo3	116.4(2)
O11 Ni1 O13E	89.7(2)	Mo3 O6 Mo1	116.4(2)
O13E Ni1 O13E	179.999(1)	Mo2 O3 Mo1	116.6(3)
O11 Ni1 O12D	90.1(2)	Mo1 O8A Mo3	116.4(3)
O11 Ni1 O12D	89.9(2)	Mo2 O2B Mo1	116.5(3)
O13E Ni1 O12D	90.3(3)	Mo3 O7C Mo2	116.6(2)
O13E Ni1 O12D	89.7(3)	C5V O16I C4L	101.2(14)
O11 Ni1 O12D	89.9(2)	C13 O17J C6O	129.9(17)
O11 Ni1 O12D	90.1(2)	C9T O19K C8S	99.5(13)
O13E Ni1 O12D	89.7(3)	O16I C4L C3W	110.1(7)
O13E Ni1 O12D	90.3(3)	O16I C4L H4L1	109.7
O12D Ni1 O12D	179.999(2)	C3W C4L H4L1	109.7
Mo3 O5 Mo3	180.0	O16I C4L H4L2	109.7
Mo3 O5 Mo2	90.07(2)	C3W C4L H4L2	109.7
Mo3 O5 Mo2	89.93(2)	H4L1 C4L H4L2	108.2

C10R O18N C11Y	112.8(12)	O19K C9T H9T1	112.5
O17J C6O C5V	114.2(9)	C10R C9T H9T1	112.5
O17J C6O H6O1	108.7	O19K C9T H9T2	112.5
C5V C6O H6O1	108.7	C10R C9T H9T2	112.5
O17J C6O H6O2	108.7	H9T1 C9T H9T2	110.1
C5V C6O H6O2	108.7	C1 C2U O21	106.9(14)
H6O1 C6O H6O2	107.6	C1 C2U H2U1	110.3
C1 O14P C12Q	124.5(14)	O21 C2U H2U1	110.3
O14P C12Q C11Y	107.0(15)	C1 C2U H2U2	110.3
O14P C12Q H12A	110.3	O21 C2U H2U2	110.3
C11Y C12Q H12A	110.3	H2U1 C2U H2U2	108.6
O14P C12Q H12B	110.3	O16I C5V C6O	99.6(15)
C11Y C12Q H12B	110.3	O16I C5V H5V1	111.9
H12A C12Q H12B	108.6	C6O C5V H5V1	111.9
O18N C10R C9T	108.2(8)	O16I C5V H5V2	111.9
O18N C10R H10A	110.1	C6O C5V H5V2	111.9
C9T C10R H10A	110.1	H5V1 C5V H5V2	109.6
O18N C10R H10B	110.1	O21 C3W C4L	94.3(14)
C9T C10R H10B	110.1	O21 C3W H3W1	112.9
H10A C10R H10B	108.4	C4L C3W H3W1	112.9
C13 C8S O19K	110.0(11)	O21 C3W H3W2	112.9
C13 C8S H8S1	109.7	C4L C3W H3W2	112.9
O19K C8S H8S1	109.7	H3W1 C3W H3W2	110.3
C13 C8S H8S2	109.7	O18N C11Y C12Q	109.8(12)
O19K C8S H8S2	109.7	O18N C11Y H11A	109.7
H8S1 C8S H8S2	108.2	C12Q C11Y H11A	109.7
O19K C9T C10R	96.1(14)	O18N C11Y H11B	109.7

C12Q C11Y H11B	109.7	C2U C1 H1A	105.3
H11A C11Y H11B	108.2	O14P C1 H1B	105.3
O14P C1 C2U	128.2(15)	C2U C1 H1B	105.3
O14P C1 H1A	105.3	H1A C1 H1B	106.0
Table A2.3 Bond lengths [Mo ₆ O ₁₉] (3)	[Å] and angles [deg]	for compound [Zn(H ₂ O) ₅ ([1	8]-crown-6)2]
Mo(1)O(1)	1.677(14)	Mo(2)O(10)#2	1.916(19)
Mo(1)O(2)	1.878(15)	Mo(2)O(10)	1.916(19)
Mo(1)O(8)	1.915(10)	Mo(2)O(9)	2.284(19)
Mo(1)O(8)#1	1.915(10)	Zn(1)O(13)	1.89(3)
Mo(1)O(4)	1.913(13)	Zn(1)O(12)#4	2.030(19)
Mo(1)O(9)	2.3222(18)	Zn(1)O(12)	2.030(19)
Mo(4)O(5)	1.69(2)	Zn(1)O(11)	2.033(13)
Mo(4)O(4)#2	1.910(14)	Zn(1)O(11)#4	2.033(13)
Mo(4)O(4)	1.910(14)	O(9)Mo(3)#2	2.323(2)
Mo(4)O(6)	1.901(13)	O(9)Mo(1)#2	2.3222(18)
Mo(4)O(6)#2	1.901(13)	C(5)C(4)	1.49(5)
Mo(4)O(9)	2.312(19)	C(5)O(32)	1.36(3)
Mo(3)O(7)	1.676(17)	O(35)C(20)	1.23(3)
Mo(3)O(10)	1.908(17)	O(35)C(20)#5	1.23(3)
Mo(3)O(6)	1.915(14)	C(2)O(30)	1.29(4)
Mo(3)O(8)	1.934(10)	C(2)C(3)	1.43(5)
Mo(3)O(8)#3	1.934(10)	O(31)C(4)	1.28(3)
Mo(3)O(9)	2.323(2)	O(31)C(3)	1.35(3)
Mo(2)O(3)	1.69(2)	O(32)C(5)#5	1.36(3)
Mo(2)O(2)#2	1.958(16)	O(30)C(22)	1.37(4)
Mo(2)O(2)	1.958(16)	C(20)C(22)	1.75(5)

		O(4)#2Mo(4)O(9)	76.7(4)
O(1)Mo(1)O(2)	102.8(7)	O(4)Mo(4)O(9)	76.7(4)
O(1)Mo(1)O(8)	103.4(3)	O(6)Mo(4)O(9)	76.8(4)
O(2)Mo(1)O(8)	87.0(3)	O(6)#2Mo(4)O(9)	76.8(4)
O(1)Mo(1)O(8)#1	103.4(3)	O(7)Mo(3)O(10)	105.0(9)
O(2)Mo(1)O(8)#1	87.0(3)	O(7)Mo(3)O(6)	103.3(9)
O(8)Mo(1)O(8)#1	153.2(6)	O(10)Mo(3)O(6)	151.7(6)
O(1)Mo(1)O(4)	104.2(6)	O(7)Mo(3)O(8)	103.7(3)
O(2)Mo(1)O(4)	153.0(6)	O(10)Mo(3)O(8)	86.5(3)
O(8)Mo(1)O(4)	86.8(3)	O(6)Mo(3)O(8)	86.8(3)
O(8)#1Mo(1)O(4)	86.8(3)	O(7)Mo(3)O(8)#3	103.7(3)
O(1)Mo(1)O(9)	179.4(7)	O(10)Mo(3)O(8)#3	86.5(3)
O(2)Mo(1)O(9)	76.6(7)	O(6)Mo(3)O(8)#3	86.8(3)
O(8)Mo(1)O(9)	76.6(3)	O(8)Mo(3)O(8)#3	152.5(6)
O(8)#1Mo(1)O(9)	76.6(3)	O(7)Mo(3)O(9)	179.6(9)
O(4)Mo(1)O(9)	76.4(6)	O(10)Mo(3)O(9)	75.4(7)
O(5)Mo(4)O(4)#2	103.3(4)	O(6)Mo(3)O(9)	76.3(6)
O(5)Mo(4)O(4)	103.3(4)	O(8)Mo(3)O(9)	76.3(3)
O(4)#2Mo(4)O(4)	153.4(7)	O(8)#3Mo(3)O(9)	76.3(3)
O(5)Mo(4)O(6)	103.2(4)	O(3)Mo(2)O(2)#2	103.9(4)
O(4)#2Mo(4)O(6)	87.00(13)	O(3)Mo(2)O(2)	103.9(4)
O(4)Mo(4)O(6)	87.00(13)	O(2)#2Mo(2)O(2)	152.2(8)
O(5)Mo(4)O(6)#2	103.2(4)	O(3)Mo(2)O(10)#2	103.7(4)
O(4)#2Mo(4)O(6)#2	87.00(13)	O(2)#2Mo(2)O(10)#2	86.73(15)
O(4)Mo(4)O(6)#2	87.00(13)	O(2)Mo(2)O(10)#2	86.73(15)
O(6)Mo(4)O(6)#2	153.7(8)	O(3)Mo(2)O(10)	103.7(4)
O(5)Mo(4)O(9)	180.000(6)	O(2)#2Mo(2)O(10)	86.73(15)

O(2)Mo(2)O(10)	86.73(15)	Mo(2)O(9)Mo(1)	90.4(5)
O(10)#2Mo(2)O(10)	152.5(9)	Mo(3)#2O(9)Mo(1)	89.996(8)
O(3)Mo(2)O(9)	180.000(9)	Mo(3)O(9)Mo(1)	89.996(8)
O(2)#2Mo(2)O(9)	76.1(4)	Mo(4)O(9)Mo(1)#2	89.6(5)
O(2)Mo(2)O(9)	76.1(4)	Mo(2)O(9)Mo(1)#2	90.4(5)
O(10)#2Mo(2)O(9)	76.3(4)	Mo(3)#2O(9)Mo(1)#2	89.996(8)
O(10)Mo(2)O(9)	76.3(4)	Mo(3)O(9)Mo(1)#2	89.996(8)
O(13)Zn(1)O(12)#4	121.5(8)	Mo(1)O(9)Mo(1)#2	179.2(9)
O(13)Zn(1)O(12)	121.5(8)	Mo(4)O(6)Mo(3)	117.4(7)
O(12)#4Zn(1)O(12)	117.1(16)	Mo(1)O(8)Mo(3)	117.1(5)
O(13)Zn(1)O(11)	89.5(4)	Mo(4)O(4)Mo(1)	117.3(7)
O(12)#4Zn(1)O(11)	90.27(19)	Mo(1)O(2)Mo(2)	116.8(7)
O(12)Zn(1)O(11)	90.27(19)	Mo(3)O(10)Mo(2)	117.7(8)
O(13)Zn(1)O(11)#4	89.5(4)	C(4)C(5)O(32)	113(2)
O(12)#4Zn(1)O(11)#4	90.27(19)	C(20)O(35)C(20)#5	95(4)
O(12)Zn(1)O(11)#4	90.27(19)	O(30)C(2)C(3)	102(3)
O(11)Zn(1)O(11)#4	179.0(7)	C(4)O(31)C(3)	133(4)
Mo(4)O(9)Mo(2)	180.000(1)	C(5)#5O(32)C(5)	110(4)
Mo(4)O(9)Mo(3)#2	89.4(5)	C(2)O(30)C(22)	112(3)
Mo(2)O(9)Mo(3)#2	90.6(5)	C(2)C(3)O(31)	129(4)
Mo(4)O(9)Mo(3)	89.4(5)	O(31)C(4)C(5)	123(3)
Mo(2)O(9)Mo(3)	90.6(5)	O(35)C(20)C(22)	108(2)
Mo(3)#2O(9)Mo(3)	178.9(9)	C(20)C(22)O(30)	115(3)
Mo(4)O(9)Mo(1)	89.6(5)		

A3. Chapter 3 Polyoxometalates Stabilized Ammonium Cation and Unusual Chloride Anion Inclusion Crown Ether Complexes: Synthesis, Characterization Crystallography

Table A2.1 Bond lengths [Å] and angles [deg] for compound [H₃PMo₁₂O₄₀{HCl (18-crown-6)}₃]·4CH₃CN (1)

C4 C5	1.298(19)	Mo4 O17	2.457(6)
C4 O3	1.318(17)	Mo4 O100	2.493(7)
C4 H4A	0.9700	Mo2 O10	1.649(4)
C4 H4B	0.9700	Mo2 O16	1.810(5)
Mo1 O7	1.643(6)	Mo2 O15	1.825(5)
Mo1 O9	1.817(5)	Mo2 O11	1.970(5)
Mo1 O9	1.817(5)	Mo2 O9	1.981(5)
Mol O8	1.975(5)	Mo2 O17	2.452(7)
Mol O8	1.975(5)	Mo2 O100	2.498(7)
Mo1 O100	2.465(7)	P1 O100	1.507(7)
Mo1 O100	2.465(7)	P1 O100	1.507(7)
Mo3 O12	1.657(6)	P1 O100	1.507(7)
Mo3 O11	1.829(5)	P1 O100	1.507(7)
Mo3 O11	1.829(5)	P1 O17	1.543(6)
Mo3 O13	1.963(5)	P1 O17	1.543(6)
Mo3 O13	1.963(5)	P1 O17	1.543(6)
Mo3 O17	2.476(6)	P1 O17	1.543(6)
Mo3 O17	2.476(6)	O6 C9	1.408(9)
Mo4 O14	1.660(4)	O6 C9	1.408(9)
Mo4 O8	1.831(5)	O8 Mo4	1.831(5)
Mo4 O13	1.835(5)	O9 Mo2	1.981(5)
Mo4 O15	1.966(4)	O15 Mo2	1.825(5)
Mo4 O16	1.982(5)	O5 C7	1.415(11)

O5 C8	1.420(10)	C2 H2B	0.9700
O3 C4	1.318(17)	C6 C7	1.481(14)
O2 C3	1.412(10)	C6 H6A	0.9700
O2 C3	1.412(10)	С6 Н6В	0.9700
O1 C2	1.386(10)	C7 H7A	0.9700
O1 C1	1.415(11)	C7 H7B	0.9700
O16 Mo2	1.810(5)	C1 C1	1.451(19)
O4 C5	1.401(12)	C1 H1A	0.9700
O4 C6	1.427(13)	C1 H1B	0.9700
C9 C8	1.467(13)	C5 H5A	0.9700
C9 H9A	0.9700	C5 H5B	0.9700
С9 Н9В	0.9700	O100 O100	1.694(13)
O17 O100	1.764(9)	O100 O17	1.764(9)
O17 O100	1.767(9)	O100 Mo4	2.493(7)
O17 O17	1.814(13)	O100 Mo2	2.498(7)
O17 Mo2	2.452(7)	N1 C100	1.10(2)
C8 H8A	0.9700	C100 C101	1.43(3)
C8 H8B	0.9700	C101 H10A	0.9600
C3 C2	1.480(13)	C101 H10B	0.9600
СЗ НЗА	0.9700	C101 H10C	0.9600
C3 H3B	0.9700	N2 C102	1.17(3)
C2 H2A	0.9700	C102 C103	1.71(3)
C5 C4 O3	131.5(12)	O3 C4 H4B	104.4
C5 C4 H4A	104.4	H4A C4 H4B	105.6
O3 C4 H4A	104.4	O7 Mo1 O9	103.3(3)
C5 C4 H4B	104.4	O7 Mo1 O9	103.3(3)

O9 Mo1 O9	96.3(3)	O11 Mo3 O13	155.9(3)
O7 Mo1 O8	100.0(3)	O13 Mo3 O13	81.8(4)
O9 Mo1 O8	155.1(3)	O12 Mo3 O17	158.09(16)
O9 Mo1 O8	86.6(2)	O11 Mo3 O17	64.5(2)
O7 Mo1 O8	100.0(3)	O11 Mo3 O17	96.3(3)
O9 Mo1 O8	86.6(2)	O13 Mo3 O17	91.4(3)
O9 Mo1 O8	155.1(3)	O13 Mo3 O17	63.0(2)
O8 Mo1 O8	81.0(3)	O12 Mo3 O17	158.09(16)
O7 Mo1 O100	159.38(17)	O11 Mo3 O17	96.3(3)
O9 Mo1 O100	95.0(3)	O11 Mo3 O17	64.5(2)
O9 Mo1 O100	64.9(2)	O13 Mo3 O17	63.0(2)
O8 Mo1 O100	63.7(2)	O13 Mo3 O17	91.4(3)
O8 Mo1 O100	90.2(3)	O17 Mo3 O17	43.0(3)
O7 Mo1 O100	159.38(17)	O14 Mo4 O8	102.6(3)
O9 Mo1 O100	64.9(2)	O14 Mo4 O13	102.6(3)
O9 Mo1 O100	95.0(3)	O8 Mo4 O13	95.1(3)
O8 Mo1 O100	90.2(3)	O14 Mo4 O15	100.9(3)
O8 Mo1 O100	63.7(2)	O8 Mo4 O15	87.7(2)
O100 Mo1 O100	40.2(3)	O13 Mo4 O15	155.0(3)
O12 Mo3 O11	102.9(3)	O14 Mo4 O16	100.4(3)
O12 Mo3 O11	102.9(3)	O8 Mo4 O16	156.0(3)
O11 Mo3 O11	95.0(4)	O13 Mo4 O16	86.5(2)
O12 Mo3 O13	100.1(3)	O15 Mo4 O16	81.3(2)
O11 Mo3 O13	155.9(3)	O14 Mo4 O17	158.4(2)
O11 Mo3 O13	87.0(2)	O8 Mo4 O17	96.2(3)
O12 Mo3 O13	100.1(3)	O13 Mo4 O17	64.8(3)
O11 Mo3 O13	87.0(2)	O15 Mo4 O17	90.2(2)

O16 Mo4 O17	62.8(3)	O17 Mo2 O100	41.8(2)
O14 Mo4 O100	159.2(2)	O100 P1 O100	68.4(5)
O8 Mo4 O100	64.7(2)	O100 P1 O100	111.6(5)
O13 Mo4 O100	95.2(3)	O100 P1 O100	180.000(3)
O15 Mo4 O100	63.7(2)	O100 P1 O100	180.000(3)
O16 Mo4 O100	91.3(3)	O100 P1 O100	111.6(5)
O17 Mo4 O100	41.7(2)	O100 P1 O100	68.4(5)
O10 Mo2 O16	104.0(3)	O100 P1 O17	109.2(3)
O10 Mo2 O15	102.9(3)	O100 P1 O17	70.7(3)
O16 Mo2 O15	95.3(3)	O100 P1 O17	109.3(3)
O10 Mo2 O11	100.3(3)	O100 P1 O17	70.8(3)
O16 Mo2 O11	87.2(2)	O100 P1 O17	70.8(3)
O15 Mo2 O11	155.3(3)	O100 P1 O17	109.3(3)
O10 Mo2 O9	99.0(3)	O100 P1 O17	70.7(3)
O16 Mo2 O9	155.9(3)	O100 P1 O17	109.2(3)
O15 Mo2 O9	86.5(2)	O17 P1 O17	180.000(1)
O11 Mo2 O9	81.6(2)	O100 P1 O17	70.7(3)
O10 Mo2 O17	159.6(2)	O100 P1 O17	109.2(3)
O16 Mo2 O17	64.9(3)	O100 P1 O17	70.8(3)
O15 Mo2 O17	95.4(3)	O100 P1 O17	109.3(3)
O11 Mo2 O17	63.4(2)	O17 P1 O17	72.0(5)
O9 Mo2 O17	91.0(2)	O17 P1 O17	108.0(5)
O10 Mo2 O100	157.2(2)	O100 P1 O17	109.3(3)
O16 Mo2 O100	96.6(3)	O100 P1 O17	70.8(3)
O15 Mo2 O100	65.1(2)	O100 P1 O17	109.2(3)
O11 Mo2 O100	90.2(3)	O100 P1 O17	70.7(3)
O9 Mo2 O100	62.4(2)	O17 P1 O17	108.0(5)

O17 P1 O17	72.0(5)	O100 O17 Mo2	129.5(4)
O17 P1 O17	180.000(3)	O100 O17 Mo2	70.5(3)
C9 O6 C9	112.1(8)	O17 O17 Mo2	134.73(15)
Mo4 O8 Mo1	139.0(3)	P1 O17 Mo4	123.8(3)
Mo3 O11 Mo2	139.1(4)	O100 O17 Mo4	70.2(3)
Mo1 O9 Mo2	140.2(3)	O100 O17 Mo4	136.8(4)
Mo2 O15 Mo4	139.7(3)	O17 O17 Mo4	127.29(16)
Mo4 O13 Mo3	139.4(4)	Mo2 O17 Mo4	92.8(2)
C7 O5 C8	113.1(7)	P1 O17 Mo3	122.4(4)
C4 O3 C4	114(2)	O100 O17 Mo3	133.7(4)
C3 O2 C3	111.8(9)	O100 O17 Mo3	126.6(4)
C2 O1 C1	110.7(7)	O17 O17 Mo3	68.51(15)
Mo2 O16 Mo4	139.1(4)	Mo2 O17 Mo3	92.5(2)
C5 O4 C6	115.3(9)	Mo4 O17 Mo3	92.5(2)
O6 C9 C8	107.8(6)	O5 C8 C9	108.4(7)
O6 C9 H9A	110.1	O5 C8 H8A	110.0
C8 C9 H9A	110.1	C9 C8 H8A	110.0
O6 C9 H9B	110.1	O5 C8 H8B	110.0
C8 C9 H9B	110.1	C9 C8 H8B	110.0
H9A C9 H9B	108.5	H8A C8 H8B	108.4
P1 O17 O100	53.7(3)	O2 C3 C2	108.2(7)
P1 O17 O100	53.7(3)	O2 C3 H3A	110.1
O100 O17 O100	89.8(4)	C2 C3 H3A	110.1
P1 O17 O17	54.0(2)	O2 C3 H3B	110.1
O100 O17 O17	88.1(3)	C2 C3 H3B	110.1
O100 O17 O17	88.1(3)	НЗА СЗ НЗВ	108.4
P1 O17 Mo2	124.0(3)	O1 C2 C3	108.8(7)

O1 C2 H2A	109.9	O4 C5 H5B	108.8
C3 C2 H2A	109.9	H5A C5 H5B	107.7
O1 C2 H2B	109.9	P1 O100 O100	55.8(3)
C3 C2 H2B	109.9	P1 O100 O17	55.6(3)
H2A C2 H2B	108.3	O100 O100 O17	91.9(3)
O4 C6 C7	113.5(8)	P1 O100 O17	55.6(3)
O4 C6 H6A	108.9	O100 O100 O17	91.9(3)
C7 C6 H6A	108.9	O17 O100 O17	90.0(4)
O4 C6 H6B	108.9	P1 O100 Mo1	125.6(4)
C7 C6 H6B	108.9	O100 O100 Mo1	69.90(16)
H6A C6 H6B	107.7	O17 O100 Mo1	136.1(4)
O5 C7 C6	107.5(8)	O17 O100 Mo1	128.7(4)
O5 C7 H7A	110.2	P1 O100 Mo4	123.5(4)
C6 C7 H7A	110.2	O100 O100 Mo4	128.40(15)
O5 C7 H7B	110.2	O17 O100 Mo4	68.0(3)
C6 C7 H7B	110.2	O17 O100 Mo4	132.7(4)
H7A C7 H7B	108.5	Mo1 O100 Mo4	91.9(2)
O1 C1 C1	109.9(9)	P1 O100 Mo2	123.1(4)
O1 C1 H1A	109.7	O100 O100 Mo2	135.61(15)
C1 C1 H1A	109.7	O17 O100 Mo2	125.3(4)
O1 C1 H1B	109.7	O17 O100 Mo2	67.7(3)
C1 C1 H1B	109.7	Mo1 O100 Mo2	92.0(2)
H1A C1 H1B	108.2	Mo4 O100 Mo2	91.0(2)
C4 C5 O4	113.6(11)	N1 C100 C101	163(2)
C4 C5 H5A	108.8	C100 C101 H10A	109.5
O4 C5 H5A	108.8	C100 C101 H10B	109.5
C4 C5 H5B	108.8	H10A C101 H10B	109.5

C100 C101 H10C	109.5	H10B C101 H10C	109.5
H10A C101 H10C	109.5	N2 C102 C103	170(3)

Table A3.2 Bond lengths $[\mathring{A}]$ and angles [deg] for compound $[SiMo_{12}O_{40}\{(NH_4)_2(dibenzo-24-crown-8)\}_2\{(CH_3CN)_2(dibenzo-24-crown-8)\}] \cdot 2CH_3C$ N (2)

Mo12 O00Y	1.669(9)	Mo2 O28	1.979(9)
Mo12 O00P	1.797(9)	Mo2 O34	2.017(9)
Mo12 O00X	1.812(9)	Mo2 O35	2.424(9)
Mo12 O40	2.007(10)	Mo1 O25	1.670(9)
Mo12 O015	2.010(9)	Mo1 O28	1.825(9)
Mo12 O00I	2.446(9)	Mo1 O30	1.869(9)
Mo6 O023	1.667(9)	Mo1 O29	1.971(9)
Mo6 O00N	1.837(9)	Mo1 O31	1.999(9)
Mo6 O00T	1.843(9)	Mo1 O42	2.425(9)
Mo6 O011	1.978(9)	Mo3 O26	1.694(9)
Mo6 O016	2.005(9)	Mo3 O011	1.837(9)
Mo6 O00J	2.481(9)	Mo3 O29	1.841(9)
Mo8 O39	1.667(9)	Mo3 O01T	2.000(9)
Mo8 O40	1.819(10)	Mo3 O32	2.009(9)
Mo8 O38	1.855(9)	Mo3 O00J	2.449(9)
Mo8 O33	1.984(9)	Mo4 O01G	1.665(9)
Mo8 O01Y	1.981(10)	Mo4 O44	1.829(9)
Mo8 O35	2.430(9)	Mo4 O010	1.828(9)
Mo2 O27	1.688(9)	Mo4 O30	1.959(9)
Mo2 O32	1.812(9)	Mo4 O36	2.001(9)
Mo2 O33	1.860(8)	Mo4 O42	2.444(9)

O24 C66	1.371(16)	C10 H10A	0.9700
O24 C67	1.463(17)	C10 H10B	0.9700
O15 C040	1.41(2)	O8 C043	1.46(2)
O15 C039	1.41(2)	O8 C300	1.41(2)
O3 C13	1.390(18)	C43 C44	1.50(2)
O3 C12	1.443(17)	C43 H43A	0.9700
O22 C02I	1.420(17)	C43 H43B	0.9700
O22 C03P	1.449(19)	C49 C54	1.380(19)
O18 C56	1.403(18)	C49 C50	1.40(2)
O18 C57	1.47(2)	C1 C2	1.34(2)
O21 C032	1.404(18)	C1 C6	1.40(2)
O21 C68	1.435(18)	C54 C53	1.37(2)
O12 C37	1.381(17)	O7 C20	1.32(4)
O12 C36	1.447(19)	O7 C76	1.40(4)
O1 C6	1.373(17)	C44 H44A	0.9700
O1 C7	1.428(19)	C44 H44B	0.9700
O19 C59	1.41(2)	C40 C39	1.33(2)
O19 C58	1.45(2)	C40 C41	1.35(2)
O2 C9	1.382(16)	C40 H40	0.9300
O2 C8	1.435(19)	C02H C043	1.50(2)
O9 C30	1.31(2)	C02H H02A	0.9700
O9 C31	1.440(19)	C02H H02B	0.9700
O4 C18	1.36(2)	C02I C02S	1.55(2)
O4 C75	1.41(3)	C02I H02C	0.9700
C42 C37	1.39(2)	C02I H02D	0.9700
C42 C41	1.38(2)	C6 C5	1.37(2)
C10 C9	1.52(2)	C65 C66	1.34(2)

C38 H38

0.9300

C039 C03N

1.53(2)

C039 H03C	0.9700	C03N H03E	0.9700
C039 H03D	0.9700	C03N H03F	0.9700
C31 H31A	0.9700	C56 H56A	0.9700
C31 H31B	0.9700	C56 H56B	0.9700
C18 C17	1.42(3)	C03P H03G	0.9700
C11 H11A	0.9700	С03Р Н03Н	0.9700
C11 H11B	0.9700	C58 H58A	0.9700
C62 H62	0.9300	C58 H58B	0.9700
C33 H33A	0.9700	C53 C52	1.49(2)
С33 Н33В	0.9700	C53 H53	0.9300
C68 H68A	0.9700	C28 C27	1.36(3)
C68 H68B	0.9700	C28 H28	0.9300
C57 C58	1.53(2)	C15 C16	1.34(3)
C57 H57A	0.9700	C15 H15	0.9300
C57 H57B	0.9700	C26 C27	1.37(3)
C29 C28	1.38(3)	C26 H26	0.9300
C29 H29	0.9300	C7 H7A	0.9700
C2 C3	1.39(2)	C7 H7B	0.9700
C2 H2	0.9300	C3 H3	0.9300
C8 C7	1.48(2)	C16 H16	0.9300
C8 H8A	0.9700	C36 H36A	0.9700
C8 H8B	0.9700	C36 H36B	0.9700
C17 C16	1.34(3)	C040 C041	1.45(3)
C17 H17	0.9300	C040 H04A	0.9700
C59 H59A	0.9700	C040 H04B	0.9700
C59 H59B	0.9700	C041 H04C	0.9700
С39 Н39	0.9300	C041 H04D	0.9700

C043 H04G	0.9700	O00Y Mo12 O40	100.9(4)
C043 H04H	0.9700	O00P Mo12 O40	154.0(4)
C20 C300	1.52(4)	O00X Mo12 O40	85.1(4)
C20 H20A	0.9700	O00Y Mo12 O015	98.5(4)
C20 H20B	0.9700	O00P Mo12 O015	86.1(4)
C27 H27	0.9300	O00X Mo12 O015	154.3(4)
C51 C52	1.34(2)	O40 Mo12 O015	80.0(4)
C51 H51	0.9300	O00Y Mo12 O00I	168.7(4)
C52 H52	0.9300	O00P Mo12 O00I	73.8(4)
C75 C76	1.45(4)	O00X Mo12 O00I	86.4(4)
C75 H75A	0.9700	O40 Mo12 O00I	80.9(3)
C75 H75B	0.9700	O015 Mo12 O00I	70.7(3)
C76 H76A	0.9700	O023 Mo6 O00N	101.9(5)
C76 H76B	0.9700	O023 Mo6 O00T	104.1(5)
C300 H30A	0.9700	O00N Mo6 O00T	96.3(4)
C300 H30B	0.9700	O023 Mo6 O011	99.8(4)
C300 H20C	0.9600	O00N Mo6 O011	87.0(4)
C300 H20D	0.9600	O00T Mo6 O011	154.6(4)
C300 H20E	0.9600	O023 Mo6 O016	103.0(5)
C220 C221	0.99(3)	O00N Mo6 O016	154.0(4)
C221 N8	1.65(4)	O00T Mo6 O016	84.8(4)
N10 C225	1.95(5)	O011 Mo6 O016	81.6(4)
		O023 Mo6 O00J	168.6(4)
		O00N Mo6 O00J	72.9(3)
O00Y Mo12 O00P	102.8(5)	O00T Mo6 O00J	86.7(4)
O00Y Mo12 O00X	104.9(5)	O011 Mo6 O00J	70.1(3)
O00P Mo12 O00X	98.8(4)	O016 Mo6 O00J	81.2(3)

O39 Mo8 O40	103.4(4)	O33 Mo2 O35	72.8(4)
O39 Mo8 O38	102.2(4)	O28 Mo2 O35	82.4(3)
O40 Mo8 O38	96.9(4)	O34 Mo2 O35	71.2(3)
O39 Mo8 O33	99.9(4)	O25 Mo1 O28	103.9(5)
O40 Mo8 O33	155.0(4)	O25 Mo1 O30	102.2(4)
O38 Mo8 O33	86.8(4)	O28 Mo1 O30	96.2(4)
O39 Mo8 O01Y	101.2(4)	O25 Mo1 O29	101.4(4)
O40 Mo8 O01Y	85.0(4)	O28 Mo1 O29	85.7(4)
O38 Mo8 O01Y	155.3(4)	O30 Mo1 O29	155.1(4)
O33 Mo8 O01Y	81.8(4)	O25 Mo1 O31	98.5(4)
O39 Mo8 O35	169.6(4)	O28 Mo1 O31	156.3(4)
O40 Mo8 O35	86.6(4)	O30 Mo1 O31	86.3(4)
O38 Mo8 O35	73.2(3)	O29 Mo1 O31	82.5(4)
O33 Mo8 O35	70.8(3)	O25 Mo1 O42	168.7(4)
O01Y Mo8 O35	82.4(4)	O28 Mo1 O42	86.8(4)
O27 Mo2 O32	104.3(5)	O30 Mo1 O42	72.7(3)
O27 Mo2 O33	101.7(4)	O29 Mo1 O42	82.6(3)
O32 Mo2 O33	97.8(4)	O31 Mo1 O42	71.4(3)
O27 Mo2 O28	101.7(4)	O26 Mo3 O011	102.2(4)
O32 Mo2 O28	85.6(4)	O26 Mo3 O29	104.0(4)
O33 Mo2 O28	154.7(4)	O011 Mo3 O29	97.8(4)
O27 Mo2 O34	97.5(4)	O26 Mo3 O01T	100.0(4)
O32 Mo2 O34	156.5(4)	O011 Mo3 O01T	85.6(4)
O33 Mo2 O34	86.2(4)	O29 Mo3 O01T	154.4(4)
O28 Mo2 O34	81.4(4)	O26 Mo3 O32	103.0(4)
O27 Mo2 O35	167.5(4)	O011 Mo3 O32	153.5(4)
O32 Mo2 O35	87.7(4)	O29 Mo3 O32	84.1(4)

O01T Mo3 O32	82.0(4)	O00W Mo11 O00P	99.4(4)
O26 Mo3 O00J	169.0(4)	O01B Mo11 O00P	155.4(4)
O011 Mo3 O00J	72.9(3)	O017 Mo11 O00P	84.5(4)
O29 Mo3 O00J	86.5(4)	O00T Mo11 O00P	82.0(4)
O01T Mo3 O00J	70.1(3)	O00W Mo11 O00I	167.5(4)
O32 Mo3 O00J	80.8(3)	O01B Mo11 O00I	87.2(4)
O01G Mo4 O44	102.9(5)	O017 Mo11 O00I	71.9(4)
O01G Mo4 O010	103.2(5)	O00T Mo11 O00I	82.3(3)
O44 Mo4 O010	97.1(4)	O00P Mo11 O00I	69.6(3)
O01G Mo4 O30	100.2(4)	O012 Mo10 O41	103.5(4)
O44 Mo4 O30	87.8(4)	O012 Mo10 O015	102.3(4)
O010 Mo4 O30	154.4(4)	O41 Mo10 O015	95.9(4)
O01G Mo4 O36	101.4(4)	O012 Mo10 O010	101.6(4)
O44 Mo4 O36	154.7(4)	O41 Mo10 O010	84.7(4)
O010 Mo4 O36	84.3(4)	O015 Mo10 O010	155.3(4)
O30 Mo4 O36	80.9(4)	O012 Mo10 O017	99.7(4)
O01G Mo4 O42	170.1(4)	O41 Mo10 O017	155.3(4)
O44 Mo4 O42	73.2(4)	O015 Mo10 O017	87.3(4)
O010 Mo4 O42	86.4(4)	O010 Mo10 O017	82.4(4)
O30 Mo4 O42	70.9(3)	O012 Mo10 O00I	169.6(4)
O36 Mo4 O42	81.7(3)	O41 Mo10 O00I	86.5(4)
O00W Mo11 O01B	104.4(4)	O015 Mo10 O00I	73.2(4)
O00W Mo11 O017	101.8(4)	O010 Mo10 O00I	82.1(3)
O01B Mo11 O017	96.2(4)	O017 Mo10 O00I	71.0(4)
O00W Mo11 O00T	102.5(4)	O018 Mo7 O01T	102.5(4)
O01B Mo11 O00T	87.1(4)	O018 Mo7 O01Y	104.7(5)
O017 Mo11 O00T	153.8(4)	O01T Mo7 O01Y	98.8(4)

O018 Mo7 O00X	102.2(4)	O43 Mo5 O016	104.5(5)
O01T Mo7 O00X	153.3(4)	O43 Mo5 O31	102.0(5)
	, ,		
O01Y Mo7 O00X	84.6(4)	O016 Mo5 O31	99.6(4)
O018 Mo7 O00N	98.6(4)	O43 Mo5 O01B	101.1(4)
O01T Mo7 O00N	85.7(4)	O016 Mo5 O01B	84.4(4)
O01Y Mo7 O00N	154.6(4)	O31 Mo5 O01B	154.7(4)
O00X Mo7 O00N	80.7(4)	O43 Mo5 O44	99.2(5)
O018 Mo7 O00J	168.6(4)	O016 Mo5 O44	154.1(4)
O01T Mo7 O00J	72.5(4)	O31 Mo5 O44	85.6(4)
O01Y Mo7 O00J	86.4(4)	O01B Mo5 O44	80.7(4)
O00X Mo7 O00J	81.4(3)	O43 Mo5 O42	168.3(4)
O00N Mo7 O00J	71.1(3)	O016 Mo5 O42	87.0(4)
O37 Mo9 O36	104.7(4)	O31 Mo5 O42	73.1(4)
O37 Mo9 O34	101.9(5)	O01B Mo5 O42	82.2(3)
O36 Mo9 O34	96.9(4)	O44 Mo5 O42	70.1(3)
O37 Mo9 O41	101.5(4)	O00J P1 O00I	110.6(6)
O36 Mo9 O41	86.1(4)	O00J P1 O42	109.7(5)
O34 Mo9 O41	154.8(4)	O00I P1 O42	110.1(5)
O37 Mo9 O38	98.1(4)	O00J P1 O35	108.9(5)
O36 Mo9 O38	155.7(4)	O00I P1 O35	108.8(5)
O34 Mo9 O38	86.3(4)	O42 P1 O35	108.7(5)
O41 Mo9 O38	81.2(4)	P1 O35 Mo2	124.9(5)
O37 Mo9 O35	167.9(4)	P1 O35 Mo8	125.4(5)
O36 Mo9 O35	87.1(4)	Mo2 O35 Mo8	90.0(3)
O34 Mo9 O35	73.3(4)	P1 O35 Mo9	125.4(5)
O41 Mo9 O35	81.9(3)	Mo2 O35 Mo9	90.2(3)
O38 Mo9 O35	70.8(3)	Mo8 O35 Mo9	90.0(3)

P1 O00I Mo10	126.5(6)	Mo12 O00X Mo7	152.1(5)
P1 O00I Mo12	126.1(5)	Mo5 O31 Mo1	126.2(5)
Mo10 O00I Mo12	89.7(3)	Mo4 O010 Mo10	152.5(5)
P1 O00I Mo11	124.7(5)	Mo3 O011 Mo6	128.5(5)
Mo10 O00I Mo11	89.4(3)	Mo10 O41 Mo9	150.3(5)
Mo12 O00I Mo11	88.8(3)	Mo10 O015 Mo12	126.1(5)
P1 O00J Mo3	127.2(5)	Mo5 O016 Mo6	152.7(5)
P1 O00J Mo7	126.2(5)	Mo11 O017 Mo10	127.7(5)
Mo3 O00J Mo7	89.2(3)	Mo3 O29 Mo1	151.3(5)
P1 O00J Mo6	125.1(5)	Mo1 O30 Mo4	126.9(5)
Mo3 O00J Mo6	88.4(3)	Mo11 O01B Mo5	149.6(5)
Mo7 O00J Mo6	88.6(3)	Mo8 O40 Mo12	150.9(5)
P1 O42 Mo1	126.1(5)	Mo2 O33 Mo8	126.4(5)
P1 O42 Mo4	126.0(5)	Mo9 O36 Mo4	150.9(5)
Mo1 O42 Mo4	89.4(3)	C61 O20 C60	114.1(11)
P1 O42 Mo5	124.9(5)	C1 O6 C02H	115.4(12)
Mo1 O42 Mo5	89.3(3)	C25 O16 C03N	115.6(14)
Mo4 O42 Mo5	89.7(3)	C49 O23 C02S	113.3(12)
Mo6 O00N Mo7	127.3(4)	Mo9 O34 Mo2	125.2(5)
Mo8 O38 Mo9	126.1(5)	C041 O14 C44	114.4(14)
Mo12 O00P Mo11	127.8(5)	C34 O11 C35	112.8(14)
Mo1 O28 Mo2	150.2(5)	C54 O17 C55	118.0(12)
C32 O10 C33	116.5(13)	C10 O5 C11	114.6(13)
Mo4 O44 Mo5	126.9(5)	C66 O24 C67	116.7(11)
Mo6 O00T Mo11	150.1(5)	C040 O15 C039	117.0(16)
Mo2 O32 Mo3	151.2(5)	Mo7 O01T Mo3	128.1(5)
C42 O13 C43	117.5(12)	C13 O3 C12	115.2(13)

C02I O22 C03P	111.3(14)	O23 C49 C50	120.4(14)
C56 O18 C57	113.5(14)	C54 C49 C50	122.1(15)
C032 O21 C68	115.4(14)	C2 C1 O6	124.4(16)
Mo7 O01Y Mo8	151.5(5)	C2 C1 C6	120.0(17)
C37 O12 C36	116.0(13)	O6 C1 C6	115.2(14)
C6 O1 C7	114.2(14)	O17 C54 C53	123.8(14)
C59 O19 C58	111.0(14)	O17 C54 C49	118.8(14)
C9 O2 C8	112.8(14)	C53 C54 C49	117.1(15)
C30 O9 C31	116.4(15)	C20 O7 C76	110(3)
C18 O4 C75	119.3(17)	O14 C44 C43	110.1(12)
C37 C42 C41	121.7(16)	O14 C44 H44A	109.6
C37 C42 O13	115.5(14)	C43 C44 H44A	109.6
C41 C42 O13	122.8(16)	O14 C44 H44B	109.6
O5 C10 C9	107.2(13)	C43 C44 H44B	109.6
O5 C10 H10A	110.3	H44A C44 H44B	108.2
C9 C10 H10A	110.3	C39 C40 C41	122.2(17)
O5 C10 H10B	110.3	C39 C40 H40	118.9
C9 C10 H10B	110.3	C41 C40 H40	118.9
H10A C10 H10B	108.5	O6 C02H C043	105.1(14)
C043 O8 C300	118.8(17)	O6 C02H H02A	110.7
O13 C43 C44	108.5(13)	C043 C02H H02A	110.7
O13 C43 H43A	110.0	O6 C02H H02B	110.7
C44 C43 H43A	110.0	C043 C02H H02B	110.7
O13 C43 H43B	110.0	H02A C02H H02B	108.8
C44 C43 H43B	110.0	O22 C02I C02S	105.5(14)
H43A C43 H43B	108.4	O22 C02I H02C	110.6
O23 C49 C54	117.3(13)	C02S C02I H02C	110.6

O22 C02I H02D	110.6	C38 C37 C42	116.9(15)
C02S C02I H02D	110.6	C38 C37 O12	124.5(14)
H02C C02I H02D	108.8	C42 C37 O12	118.5(14)
C5 C6 O1	122.0(16)	C14 C13 O3	124.8(16)
C5 C6 C1	120.4(16)	C14 C13 C18	120.3(18)
O1 C6 C1	116.3(15)	O3 C13 C18	114.9(16)
C66 C65 C64	118.2(16)	O11 C34 C33	107.5(14)
C66 C65 H65	120.9	O11 C34 H34A	110.2
C64 C65 H65	120.9	C33 C34 H34A	110.2
C40 C41 C42	118.5(16)	O11 C34 H34B	110.2
C40 C41 H41	120.7	C33 C34 H34B	110.2
C42 C41 H41	120.7	H34A C34 H34B	108.5
O2 C9 C10	107.8(13)	O23 C02S C02I	108.1(14)
O2 C9 H9A	110.1	O23 C02S H02E	110.1
C10 C9 H9A	110.1	C02I C02S H02E	110.1
O2 C9 H9B	110.1	O23 C02S H02F	110.1
C10 C9 H9B	110.1	C02I C02S H02F	110.1
H9A C9 H9B	108.5	H02E C02S H02F	108.4
C62 C63 C64	119.2(16)	C13 C14 C15	120.2(18)
C62 C63 H63	120.4	C13 C14 H14	119.9
C64 C63 H63	120.4	C15 C14 H14	119.9
O20 C60 C59	110.1(13)	O9 C30 C25	118.2(15)
O20 C60 H60A	109.6	O9 C30 C29	126.8(18)
C59 C60 H60A	109.6	C25 C30 C29	115.0(19)
O20 C60 H60B	109.6	O20 C61 C62	123.3(14)
C59 C60 H60B	109.6	O20 C61 C66	119.2(13)
H60A C60 H60B	108.2	C62 C61 C66	117.4(14)

C37 C38 C39	122.6(15)	O21 C032 C03P	107.7(15)
C37 C38 H38	118.7	O21 C032 H03A	110.2
C39 C38 H38	118.7	C03P C032 H03A	110.2
O11 C35 C36	113.1(16)	O21 C032 H03B	110.2
O11 C35 H35A	109.0	C03P C032 H03B	110.2
C36 C35 H35A	109.0	H03A C032 H03B	108.5
O11 C35 H35B	109.0	C26 C25 O16	117.6(17)
C36 C35 H35B	109.0	C26 C25 C30	123.9(17)
H35A C35 H35B	107.8	O16 C25 C30	118.3(16)
O3 C12 C11	105.2(13)	O17 C55 C56	105.9(13)
O3 C12 H12A	110.7	O17 C55 H55A	110.6
C11 C12 H12A	110.7	C56 C55 H55A	110.6
O3 C12 H12B	110.7	O17 C55 H55B	110.6
C11 C12 H12B	110.7	C56 C55 H55B	110.6
H12A C12 H12B	108.8	H55A C55 H55B	108.7
C68 C67 O24	112.4(13)	C65 C66 O24	125.5(14)
C68 C67 H67A	109.1	C65 C66 C61	121.6(15)
O24 C67 H67A	109.1	O24 C66 C61	112.9(12)
C68 C67 H67B	109.1	O10 C32 C31	112.4(14)
O24 C67 H67B	109.1	O10 C32 H32A	109.1
H67A C67 H67B	107.8	C31 C32 H32A	109.1
C6 C5 C4	120.4(18)	O10 C32 H32B	109.1
C6 C5 H5	119.8	C31 C32 H32B	109.1
C4 C5 H5	119.8	H32A C32 H32B	107.9
C5 C4 C3	117.6(19)	C51 C50 C49	121.2(17)
C5 C4 H4	121.2	C51 C50 H50	119.4
C3 C4 H4	121.2	C49 C50 H50	119.4

C63 C64 C65	123.4(17)	O10 C33 C34	109.5(14)
C63 C64 H64	118.3	O10 C33 H33A	109.8
C65 C64 H64	118.3	C34 C33 H33A	109.8
O15 C039 C03N	107.6(16)	O10 C33 H33B	109.8
O15 C039 H03C	110.2	C34 C33 H33B	109.8
C03N C039 H03C	110.2	H33A C33 H33B	108.2
O15 C039 H03D	110.2	O21 C68 C67	112.5(14)
C03N C039 H03D	110.2	O21 C68 H68A	109.1
H03C C039 H03D	108.5	C67 C68 H68A	109.1
O9 C31 C32	104.4(15)	O21 C68 H68B	109.1
O9 C31 H31A	110.9	C67 C68 H68B	109.1
C32 C31 H31A	110.9	H68A C68 H68B	107.8
O9 C31 H31B	110.9	O18 C57 C58	105.3(14)
C32 C31 H31B	110.9	O18 C57 H57A	110.7
H31A C31 H31B	108.9	C58 C57 H57A	110.7
O4 C18 C13	119.2(17)	O18 C57 H57B	110.7
O4 C18 C17	123.7(17)	C58 C57 H57B	110.7
C13 C18 C17	116.5(19)	H57A C57 H57B	108.8
O5 C11 C12	111.6(14)	C28 C29 C30	121(2)
O5 C11 H11A	109.3	C28 C29 H29	119.7
C12 C11 H11A	109.3	C30 C29 H29	119.7
O5 C11 H11B	109.3	C1 C2 C3	119.0(19)
C12 C11 H11B	109.3	C1 C2 H2	120.5
H11A C11 H11B	108.0	C3 C2 H2	120.5
C63 C62 C61	120.2(16)	O2 C8 C7	110.3(16)
C63 C62 H62	119.9	O2 C8 H8A	109.6
C61 C62 H62	119.9	C7 C8 H8A	109.6

O2 C8 H8B	109.6	O22 C03P C032	105.0(14)
C7 C8 H8B	109.6	O22 C03P H03G	110.7
H8A C8 H8B	108.1	C032 C03P H03G	110.7
C16 C17 C18	121.2(19)	O22 C03P H03H	110.7
C16 C17 H17	119.4	C032 C03P H03H	110.7
C18 C17 H17	119.4	H03G C03P H03H	108.8
O19 C59 C60	107.0(15)	O19 C58 C57	106.7(14)
O19 C59 H59A	110.3	O19 C58 H58A	110.4
C60 C59 H59A	110.3	C57 C58 H58A	110.4
O19 C59 H59B	110.3	O19 C58 H58B	110.4
C60 C59 H59B	110.3	C57 C58 H58B	110.4
H59A C59 H59B	108.6	H58A C58 H58B	108.6
C40 C39 C38	117.8(17)	C54 C53 C52	120.7(17)
C40 C39 H39	121.1	C54 C53 H53	119.6
C38 C39 H39	121.1	C52 C53 H53	119.6
O16 C03N C039	110.0(14)	C29 C28 C27	122(2)
O16 C03N H03E	109.7	C29 C28 H28	119.0
C039 C03N H03E	109.7	C27 C28 H28	119.0
O16 C03N H03F	109.7	C16 C15 C14	120(2)
C039 C03N H03F	109.7	C16 C15 H15	119.8
H03E C03N H03F	108.2	C14 C15 H15	119.8
O18 C56 C55	113.7(15)	C25 C26 C27	118(2)
O18 C56 H56A	108.8	C25 C26 H26	121.1
C55 C56 H56A	108.8	C27 C26 H26	121.1
O18 C56 H56B	108.8	O1 C7 C8	110.8(14)
C55 C56 H56B	108.8	O1 C7 H7A	109.5
H56A C56 H56B	107.7	C8 C7 H7A	109.5

O1 C7 H7B	109.5	O8 C043 C02H	112.5(16)
C8 C7 H7B	109.5	O8 C043 H04G	109.1
H7A C7 H7B	108.1	C02H C043 H04G	109.1
C2 C3 C4	122.2(19)	O8 C043 H04H	109.1
C2 C3 H3	118.9	C02H C043 H04H	109.1
C4 C3 H3	118.9	H04G C043 H04H	107.8
C15 C16 C17	121(2)	O7 C20 C300	111(3)
C15 C16 H16	119.5	O7 C20 H20A	109.4
C17 C16 H16	119.5	C300 C20 H20A	109.4
O12 C36 C35	108.2(14)	O7 C20 H20B	109.4
O12 C36 H36A	110.1	C300 C20 H20B	109.4
C35 C36 H36A	110.1	H20A C20 H20B	108.0
O12 C36 H36B	110.1	C26 C27 C28	120(2)
C35 C36 H36B	110.1	C26 C27 H27	120.0
H36A C36 H36B	108.4	C28 C27 H27	120.0
O15 C040 C041	110.6(16)	C52 C51 C50	119.3(18)
O15 C040 H04A	109.5	C52 C51 H51	120.3
C041 C040 H04A	109.5	C50 C51 H51	120.3
O15 C040 H04B	109.5	C51 C52 C53	119.4(18)
C041 C040 H04B	109.5	C51 C52 H52	120.3
H04A C040 H04B	108.1	C53 C52 H52	120.3
O14 C041 C040	108.4(19)	O4 C75 C76	111(3)
O14 C041 H04C	110.0	O4 C75 H75A	109.4
C040 C041 H04C	110.0	C76 C75 H75A	109.4
O14 C041 H04D	110.0	O4 C75 H75B	109.4
C040 C041 H04D	110.0	C76 C75 H75B	109.4
H04C C041 H04D	108.4	H75A C75 H75B	108.0

O7 C76 C75	103(3)	H30B C300 H20C	126.0
O7 C76 H76A	111.1	O8 C300 H20D	109.5
C75 C76 H76A	111.1	C20 C300 H20D	91.2
O7 C76 H76B	111.1	H30A C300 H20D	123.7
C75 C76 H76B	111.1	H30B C300 H20D	19.8
H76A C76 H76B	109.1	H20C C300 H20D	109.5
O8 C300 C20	114(2)	O8 C300 H20E	109.5
O8 C300 H30A	108.6	C20 C300 H20E	120.8
C20 C300 H30A	108.6	H30A C300 H20E	16.8
O8 C300 H30B	108.6	H30B C300 H20E	91.9
C20 C300 H30B	108.6	H20C C300 H20E	109.5
H30A C300 H30B	107.6	H20D C300 H20E	109.5
O8 C300 H20C	109.5	C220 C221 N8	138(5)
C20 C300 H20C	18.6		
H30A C300 H20C	94.8		

A4. Chapter 4 A New Rearrangement Reaction Resulting in Ammonium Ion at Room Temperature

Table A4.1 Bond lengths [Å] and angles [deg] for compound $[(C_2H_5)_3NH]_2[(C_2H_5)_4N][NaMo_8O_{26}]\ (1)$

C5 N1	1.57(2)	Mo1 O5	1.742(3)
C5 C6	1.73(3)	Mol O6	1.947(3)
C4 C13	1.501(14)	Mo1 O12	1.952(3)
C4 N1	1.508(9)	Mo1 O13	2.178(3)
N1 C5	1.57(2)	Mo1 O13	2.290(3)
N1 C4	1.508(9)	Mo2 O7G	1.690(4)
Mol OlD	1.687(3)	Mo2 O2C	1.702(3)

Mo2 O8B	1.903(3)	Na1 O4F	2.667(4)
Mo2 O6	2.003(3)	N2 C11	1.447(15)
Mo2 O12	2.301(3)	N2 C9	1.521(15)
Mo2 O13	2.323(3)	N2 C8	1.548(11)
Mo4 O11E	1.691(4)	C8 C7	1.469(14)
Mo4 O4F	1.700(3)	C9 C10	1.398(18)
Mo4 O10A	1.898(4)	C12 C11	1.306(19)
Mo4 O12	2.005(3)		
Mo4 O6	2.306(3)	N1 C5 C6	116.8(12)
Mo4 O13	2.342(3)	C13 C4 N1	113.6(9)
Mo3 O3H	1.699(4)	C5 N1 C5	98(2)
Mo3 O9I	1.707(4)	C5 N1 C4	118.1(9)
Mo3 O10A	1.912(4)	C5 N1 C4	107.7(7)
Mo3 O8B	1.929(3)	C5 N1 C4	107.7(7)
Mo3 O5	2.307(3)	C5 N1 C4	118.1(9)
Mo3 O13	2.406(3)	C4 N1 C4	107.8(8)
O12 Mo2	2.301(3)	O1D Mo1 O5	105.78(17)
O5 Mo3	2.308(3)	O1D Mo1 O6	100.19(16)
O13 Mo1	2.290(3)	O5 Mo1 O6	96.87(15)
O6 Mo4	2.306(3)	O1D Mo1 O12	100.29(15)
O2C Na1	2.542(4)	O5 Mo1 O12	97.82(15)
O1D Na1	2.569(4)	O6 Mo1 O12	150.43(12)
O4F Na1	2.667(4)	O1D Mo1 O13	95.71(15)
O3H Na1	2.660(5)	O5 Mo1 O13	158.50(13)
Na1 O2C	2.542(4)	O6 Mo1 O13	78.42(11)
Na1 O1D	2.569(4)	O12 Mo1 O13	78.52(12)
Na1 O3H	2.660(5)	O1D Mo1 O13	171.40(15)

O5 Mo1 O13	82.82(13)	O10A Mo4 O6	83.66(13)
O6 Mo1 O13	78.24(11)	O12 Mo4 O6	71.61(11)
O12 Mo1 O13	78.32(11)	O11E Mo4 O13	162.85(16)
O13 Mo1 O13	75.69(12)	O4F Mo4 O13	91.20(15)
O7G Mo2 O2C	105.89(19)	O10A Mo4 O13	76.99(12)
O7G Mo2 O8B	101.89(19)	O12 Mo4 O13	73.64(11)
O2C Mo2 O8B	101.06(17)	O6 Mo4 O13	70.62(10)
O7G Mo2 O6	100.76(17)	O3H Mo3 O9I	106.0(2)
O2C Mo2 O6	96.26(16)	O3H Mo3 O10A	99.19(18)
O8B Mo2 O6	146.34(13)	O9I Mo3 O10A	101.87(18)
O7G Mo2 O12	91.29(16)	O3H Mo3 O8B	98.07(17)
O2C Mo2 O12	160.85(15)	O9I Mo3 O8B	101.8(2)
O8B Mo2 O12	83.14(13)	O10A Mo3 O8B	145.43(14)
O6 Mo2 O12	71.76(11)	O3H Mo3 O5	161.74(17)
O7G Mo2 O13	162.49(16)	O9I Mo3 O5	92.22(18)
O2C Mo2 O13	91.38(14)	O10A Mo3 O5	77.49(13)
O8B Mo2 O13	77.03(12)	O8B Mo3 O5	76.77(13)
O6 Mo2 O13	73.90(11)	O3H Mo3 O13	91.94(16)
O12 Mo2 O13	71.20(10)	O9I Mo3 O13	162.04(18)
O11E Mo4 O4F	105.8(2)	O10A Mo3 O13	75.15(12)
O11E Mo4 O10A	101.89(19)	O8B Mo3 O13	74.55(12)
O4F Mo4 O10A	100.29(18)	O5 Mo3 O13	69.83(10)
O11E Mo4 O12	101.40(18)	Mo1 O12 Mo4	109.69(15)
O4F Mo4 O12	96.23(16)	Mo1 O12 Mo2	109.72(13)
O10A Mo4 O12	146.44(13)	Mo4 O12 Mo2	103.83(12)
O11E Mo4 O6	92.23(16)	Mo1 O5 Mo3	114.16(15)
O4F Mo4 O6	160.18(14)	Mo1 O13 Mo1	104.31(12)

Mo1 O13 Mo2	91.46(10)	O1D Na1 O3H	108.30(11)
Mo1 O13 Mo2	98.03(10)	O2C Na1 O3H	78.34(13)
Mo1 O13 Mo4	91.32(10)	O2C Na1 O3H	70.26(13)
Mo1 O13 Mo4	98.06(10)	O1D Na1 O3H	108.30(11)
Mo2 O13 Mo4	162.44(14)	O1D Na1 O3H	122.14(12)
Mo1 O13 Mo3	162.49(14)	O3H Na1 O3H	105.1(2)
Mo1 O13 Mo3	93.20(10)	O2C Na1 O4F	99.00(11)
Mo2 O13 Mo3	86.39(10)	O2C Na1 O4F	107.49(11)
Mo4 O13 Mo3	85.75(9)	O1D Na1 O4F	68.91(13)
Mo1 O6 Mo2	109.40(13)	O1D Na1 O4F	69.13(13)
Mo1 O6 Mo4	110.36(13)	O3H Na1 O4F	168.95(14)
Mo2 O6 Mo4	103.66(13)	O3H Na1 O4F	69.19(13)
Mo4 O10A Mo3	115.99(15)	O2C Na1 O4F	107.49(11)
Mo2 O8B Mo3	115.35(18)	O2C Na1 O4F	99.00(11)
Mo2 O2C Na1	134.07(18)	O1D Na1 O4F	69.13(13)
Mol OlD Nal	130.08(19)	O1D Na1 O4F	68.91(13)
Mo4 O4F Na1	132.2(2)	O3H Na1 O4F	69.19(13)
Mo3 O3H Na1	131.4(2)	O3H Na1 O4F	168.95(14)
O2C Na1 O2C	127.3(2)	O4F Na1 O4F	118.0(2)
O2C Na1 O1D	161.72(17)	C11 N2 C9	113.0(13)
O2C Na1 O1D	70.60(12)	C11 N2 C8	116.9(13)
O2C Na1 O1D	70.60(12)	C9 N2 C8	108.9(7)
O2C Na1 O1D	161.72(17)	C7 C8 N2	113.0(8)
O1D Na1 O1D	91.9(2)	C10 C9 N2	121.0(8)
O2C Na1 O3H	70.26(13)	C12 C11 N2	125.7(11)
O2C Na1 O3H	78.34(13)		
O1D Na1 O3H	122.14(12)		

Table A4.2 Bond [NH4⊂B15C5]3[PM012O40]	0	and angles [deg]	for compound
C62 C35	1.27(4)	C17 O52	1.427(14)
C62 C34	1.41(3)	C17 C18	1.519(16)
C55 O76	1.294(18)	C16 O54	1.411(12)
C55 C31	1.48(2)	C18 O53	1.413(14)
O59 P1	1.566(10)	C23 C12	1.370(14)
O59 O200	1.749(14)	C23 C24	1.426(19)
O59 O32	1.783(15)	C26 C25	1.33(2)
O59 Mo3	2.430(10)	C26 C11	1.411(15)
O59 Mo5	2.445(11)	C24 C25	1.35(2)
O59 Mo2	2.475(10)	Mol O9	1.650(6)
O60 P1	1.554(9)	Mo1 O25	1.872(7)
O60 O200	1.755(14)	Mol Ol5	1.874(7)
O60 O32	1.800(14)	Mo1 O29	1.912(7)
O60 Mo1	2.428(10)	Mo1 O26	1.925(7)
O60 Mo6	2.453(10)	Mo1 O200	2.492(10)
O60 Mo2	2.486(10)	Mo2 O13	1.646(6)
O80 C20	1.369(13)	Mo2 O29	1.881(7)
O80 C42	1.436(15)	Mo2 O14	1.898(7)
O79 C21	1.367(15)	Mo2 O56	1.903(8)
O79 C48	1.462(15)	Mo2 O33	1.906(7)
C15 O51	1.428(12)	Mo3 O10	1.635(6)
C15 C16	1.514(17)	Mo3 O33	1.875(7)
C21 C47	1.387(18)	Mo3 O27	1.877(7)
C21 C20	1.418(17)	Mo3 O23	1.900(7)
C20 C44	1.315(19)	Mo3 O15	1.920(7)

Mo3 O200	2.481(10)	Mo8 O4	1.658(7)
Mo4 O22	1.653(6)	Mo8 O35	1.843(8)
Mo4 O28	1.873(7)	Mo8 O18	1.854(7)
Mo4 O23	1.887(7)	Mo8 O30	1.955(7)
Mo4 O34	1.896(7)	Mo8 O17	1.960(8)
Mo4 O25	1.928(7)	Mo8 O202	2.436(11)
Mo4 O32	2.462(10)	Mo8 O72	2.458(11)
Mo4 O200	2.494(10)	Mo9 O1	1.643(7)
Mo5 O11	1.638(6)	Mo9 O6	1.837(8)
Mo5 O14	1.878(7)	Mo9 O16	1.852(8)
Mo5 O34	1.894(8)	Mo9 O2	1.937(8)
Mo5 O55	1.900(7)	Mo9 O18	1.941(8)
Mo5 O27	1.925(7)	Mo9 O71	2.423(12)
Mo5 O32	2.474(11)	Mo9 O72	2.514(10)
Mo6 O12	1.659(6)	Mo10 O24	1.666(7)
Mo6 O26	1.874(7)	Mo10 O39	1.826(9)
Mo6 O55	1.882(7)	Mo10 O38	1.833(7)
Mo6 O56	1.896(7)	Mo10 O35	1.954(8)
Mo6 O28	1.921(7)	Mo10 O36	1.970(8)
Mo6 O32	2.492(11)	Mo10 O73	2.470(10)
Mo7 O5	1.656(7)	Mo10 O202	2.522(11)
Mo7 O19	1.840(7)	Mo11 O7	1.663(6)
Mo7 O30	1.852(8)	Mo11 O36	1.846(8)
Mo7 O6	1.951(8)	Mo11 O2	1.862(9)
Mo7 O38	1.953(7)	Mo11 O8	1.919(8)
Mo7 O71	2.436(11)	Mo11 O19	1.967(7)
Mo7 O202	2.503(12)	Mo11 O73	2.465(11)

Mo11 O71	2.521(12)	C6 O31	1.417(14)
Mo12 O20	1.656(7)	O31 C30	1.387(16)
Mo12 O17	1.826(8)	O37 C31	1.406(16)
Mo12 O8	1.870(8)	O32 O200	1.714(14)
Mo12 O16	1.940(8)	O51 C7	1.446(13)
Mo12 O39	1.959(8)	O53 C12	1.394(12)
Mo12 O73	2.446(10)	O54 C11	1.360(13)
Mo12 O72	2.472(11)	O50 C8	1.423(12)
P1 O200	1.505(9)	O50 C9	1.428(13)
P1 O200	1.505(9)	O52 C10	1.496(14)
P1 O32	1.527(11)	O57 C13	1.369(14)
P1 O32	1.527(11)	O57 C28	1.402(13)
P2 O72	1.509(10)	O58 C32	1.400(14)
P2 O72	1.509(10)	O58 C14	1.406(14)
P2 O202	1.514(11)	C12 C11	1.379(15)
P2 O202	1.514(11)	C8 C7	1.517(16)
P2 O73	1.549(10)	C9 C10	1.422(17)
P2 O73	1.549(10)	C14 C13	1.344(17)
P2 O71	1.561(10)	C14 C51	1.419(17)
P2 O71	1.561(10)	C13 C34	1.392(17)
C3 C27	1.32(2)	O73 O72	1.763(15)
C3 C4	1.41(2)	O73 O202	1.793(16)
C1 C6	1.358(17)	O72 O202	1.680(14)
C1 C27	1.373(19)	O72 O71	1.770(15)
C5 C4	1.349(16)	O71 O202	1.757(15)
C5 O37	1.360(14)	O77 C38	1.39(2)
C5 C6	1.401(15)	O77 C37	1.409(19)

O74 C29	1.431(19)	C50 C58	1.35(4)
O74 C52	1.49(2)	C60 C59	1.17(5)
C28 C29	1.42(2)	C206 C205	1.15(4)
O75 C206	1.29(3)		
O75 C33	1.41(2)	C35 C62 C34	126(2)
C32 C33	1.47(2)	O76 C55 C31	114.4(14)
C30 C57	1.46(2)	P1 O59 O200	53.7(4)
O76 C56	1.394(19)	P1 O59 O32	53.8(5)
C35 C51	1.34(3)	O200 O59 O32	90.2(7)
O82 C50	1.43(2)	P1 O59 Mo3	124.4(5)
O82 C43	1.445(18)	O200 O59 Mo3	70.7(5)
O78 C57	1.18(2)	O32 O59 Mo3	134.1(7)
O78 C36	1.369(18)	P1 O59 Mo5	123.4(6)
C42 C43	1.36(2)	O200 O59 Mo5	134.1(7)
C36 C37	1.40(2)	O32 O59 Mo5	69.6(5)
C38 C56	1.40(3)	Mo3 O59 Mo5	93.9(4)
O83 C49	1.38(2)	P1 O59 Mo2	121.4(6)
O83 C60	1.43(3)	O200 O59 Mo2	129.8(7)
O85 C53	1.35(2)	O32 O59 Mo2	129.3(6)
O85 C205	1.48(3)	Mo3 O59 Mo2	92.6(3)
O84 C58	1.19(3)	Mo5 O59 Mo2	92.6(3)
O84 C59	1.44(4)	P1 O60 O200	53.7(4)
C44 C45	1.43(3)	P1 O60 O32	53.6(5)
C47 C46	1.35(3)	O200 O60 O32	89.4(6)
C49 C48	1.43(2)	P1 O60 Mo1	124.7(5)
C52 C53	1.43(3)	O200 O60 Mo1	71.1(5)
C45 C46	1.45(3)	O32 O60 Mo1	134.4(6)

P1 O60 Mo6	123.4(5)	O25 Mo1 O15	88.9(3)
O200 O60 Mo6	133.3(6)	O9 Mo1 O29	101.7(4)
O32 O60 Mo6	69.8(5)	O25 Mo1 O29	88.4(3)
Mo1 O60 Mo6	93.9(3)	O15 Mo1 O29	156.7(4)
P1 O60 Mo2	121.4(5)	O9 Mo1 O26	100.9(4)
O200 O60 Mo2	131.5(6)	O25 Mo1 O26	156.8(4)
O32 O60 Mo2	128.6(6)	O15 Mo1 O26	87.4(4)
Mo1 O60 Mo2	92.9(3)	O29 Mo1 O26	86.0(3)
Mo6 O60 Mo2	91.9(3)	O9 Mo1 O60	157.9(4)
C20 O80 C42	117.5(12)	O25 Mo1 O60	94.4(4)
C21 O79 C48	119.0(13)	O15 Mo1 O60	93.1(4)
O51 C15 C16	107.2(9)	O29 Mo1 O60	64.0(4)
O79 C21 C47	124.1(16)	O26 Mo1 O60	63.0(4)
O79 C21 C20	116.1(10)	O9 Mo1 O200	160.3(4)
C47 C21 C20	119.7(16)	O25 Mo1 O200	65.0(3)
C44 C20 O80	125.4(13)	O15 Mo1 O200	64.7(3)
C44 C20 C21	123.0(13)	O29 Mo1 O200	93.3(4)
O80 C20 C21	111.6(11)	O26 Mo1 O200	92.8(4)
O52 C17 C18	112.4(9)	O60 Mo1 O200	41.8(3)
O54 C16 C15	105.0(9)	O13 Mo2 O29	101.3(4)
O53 C18 C17	105.6(11)	O13 Mo2 O14	102.0(4)
C12 C23 C24	118.0(13)	O29 Mo2 O14	88.5(4)
C25 C26 C11	121.0(14)	O13 Mo2 O56	101.6(4)
C25 C24 C23	119.7(13)	O29 Mo2 O56	87.7(3)
C26 C25 C24	121.6(12)	O14 Mo2 O56	156.5(5)
O9 Mo1 O25	102.3(4)	O13 Mo2 O33	102.2(4)
O9 Mo1 O15	101.6(4)	O29 Mo2 O33	156.5(4)

O14 Mo2 O33	86.2(3)	O15 Mo3 O59	93.1(4)
O56 Mo2 O33	88.1(4)	O10 Mo3 O200	158.7(4)
O13 Mo2 O59	158.0(4)	O33 Mo3 O200	92.5(4)
O29 Mo2 O59	94.3(4)	O27 Mo3 O200	93.1(4)
O14 Mo2 O59	62.7(4)	O23 Mo3 O200	63.6(4)
O56 Mo2 O59	94.5(4)	O15 Mo3 O200	64.4(3)
O33 Mo2 O59	63.1(4)	O59 Mo3 O200	41.7(3)
O13 Mo2 O60	157.9(4)	O22 Mo4 O28	103.9(4)
O29 Mo2 O60	63.1(4)	O22 Mo4 O23	102.2(4)
O14 Mo2 O60	93.5(4)	O28 Mo4 O23	89.0(4)
O56 Mo2 O60	64.2(4)	O22 Mo4 O34	102.4(4)
O33 Mo2 O60	94.4(4)	O28 Mo4 O34	87.8(3)
O59 Mo2 O60	44.0(3)	O23 Mo4 O34	155.3(4)
O10 Mo3 O33	103.1(4)	O22 Mo4 O25	100.1(4)
O10 Mo3 O27	101.7(4)	O28 Mo4 O25	156.0(4)
O33 Mo3 O27	88.4(3)	O23 Mo4 O25	86.9(3)
O10 Mo3 O23	102.1(4)	O34 Mo4 O25	86.1(3)
O33 Mo3 O23	87.8(3)	O22 Mo4 O32	161.3(4)
O27 Mo3 O23	156.1(4)	O28 Mo4 O32	64.8(4)
O10 Mo3 O15	100.6(4)	O23 Mo4 O32	92.8(4)
O33 Mo3 O15	156.3(4)	O34 Mo4 O32	63.8(4)
O27 Mo3 O15	87.6(3)	O25 Mo4 O32	91.7(4)
O23 Mo3 O15	86.5(3)	O22 Mo4 O200	158.1(4)
O10 Mo3 O59	159.6(4)	O28 Mo4 O200	92.8(4)
O33 Mo3 O59	64.4(4)	O23 Mo4 O200	63.4(4)
O27 Mo3 O59	63.4(4)	O34 Mo4 O200	92.2(4)
O23 Mo3 O59	93.8(4)	O25 Mo4 O200	64.3(3)

O32 Mo4 O200	40.5(3)	O55 Mo6 O56	156.7(4)
O11 Mo5 O14	101.9(4)	O12 Mo6 O28	100.3(4)
O11 Mo5 O34	102.6(4)	O26 Mo6 O28	156.8(5)
O14 Mo5 O34	89.5(4)	O55 Mo6 O28	87.0(3)
O11 Mo5 O55	102.3(4)	O56 Mo6 O28	87.2(4)
O14 Mo5 O55	155.7(4)	O12 Mo6 O60	159.7(4)
O34 Mo5 O55	87.4(3)	O26 Mo6 O60	63.0(4)
O11 Mo5 O27	101.4(4)	O55 Mo6 O60	92.9(4)
O14 Mo5 O27	86.3(3)	O56 Mo6 O60	65.0(4)
O34 Mo5 O27	156.0(4)	O28 Mo6 O60	94.5(4)
O55 Mo5 O27	86.8(4)	O12 Mo6 O32	157.6(4)
O11 Mo5 O59	157.7(4)	O26 Mo6 O32	94.2(4)
O14 Mo5 O59	63.6(4)	O55 Mo6 O32	63.9(4)
O34 Mo5 O59	94.5(4)	O56 Mo6 O32	93.3(4)
O55 Mo5 O59	92.6(4)	O28 Mo6 O32	63.6(4)
O27 Mo5 O59	62.6(4)	O60 Mo6 O32	42.7(3)
O11 Mo5 O32	159.8(4)	O5 Mo7 O19	103.1(4)
O14 Mo5 O32	93.0(4)	O5 Mo7 O30	103.3(4)
O34 Mo5 O32	63.5(4)	O19 Mo7 O30	93.6(4)
O55 Mo5 O32	64.1(4)	O5 Mo7 O6	100.7(5)
O27 Mo5 O32	93.1(4)	O19 Mo7 O6	87.5(3)
O59 Mo5 O32	42.5(3)	O30 Mo7 O6	155.1(5)
O12 Mo6 O26	102.9(4)	O5 Mo7 O38	101.2(4)
O12 Mo6 O55	101.6(4)	O19 Mo7 O38	154.8(4)
O26 Mo6 O55	88.8(4)	O30 Mo7 O38	86.8(3)
O12 Mo6 O56	101.7(4)	O6 Mo7 O38	81.9(4)
O26 Mo6 O56	87.7(3)	O5 Mo7 O71	158.5(4)

O19 Mo7 O71	65.5(4)	O18 Mo8 O72	64.6(4)
O30 Mo7 O71	95.9(4)	O30 Mo8 O72	90.9(4)
O6 Mo7 O71	62.0(4)	O17 Mo8 O72	62.6(4)
O38 Mo7 O71	89.4(4)	O202 Mo8 O72	40.2(3)
O5 Mo7 O202	159.1(4)	O1 Mo9 O6	102.6(5)
O19 Mo7 O202	94.3(4)	O1 Mo9 O16	102.1(5)
O30 Mo7 O202	63.8(4)	O6 Mo9 O16	91.4(4)
O6 Mo7 O202	91.3(5)	O1 Mo9 O2	101.7(5)
O38 Mo7 O202	63.4(4)	O6 Mo9 O2	88.4(3)
O71 Mo7 O202	41.6(3)	O16 Mo9 O2	155.7(5)
O4 Mo8 O35	103.3(5)	O1 Mo9 O18	101.7(4)
O4 Mo8 O18	102.9(4)	O6 Mo9 O18	155.4(5)
O35 Mo8 O18	92.7(4)	O16 Mo9 O18	87.2(4)
O4 Mo8 O30	100.6(4)	O2 Mo9 O18	83.0(4)
O35 Mo8 O30	88.5(3)	O1 Mo9 O71	159.5(4)
O18 Mo8 O30	155.5(4)	O6 Mo9 O71	63.5(4)
O4 Mo8 O17	100.6(5)	O16 Mo9 O71	93.6(4)
O35 Mo8 O17	155.7(4)	O2 Mo9 O71	64.7(4)
O18 Mo8 O17	86.4(3)	O18 Mo9 O71	92.0(4)
O30 Mo8 O17	82.6(3)	O1 Mo9 O72	158.4(4)
O4 Mo8 O202	160.6(4)	O6 Mo9 O72	94.9(5)
O35 Mo8 O202	66.2(4)	O16 Mo9 O72	64.5(4)
O18 Mo8 O202	94.1(4)	O2 Mo9 O72	91.3(4)
O30 Mo8 O202	64.1(4)	O18 Mo9 O72	62.4(4)
O17 Mo8 O202	89.6(4)	O71 Mo9 O72	42.0(3)
O4 Mo8 O72	158.4(4)	O24 Mo10 O39	103.5(5)
O35 Mo8 O72	95.1(4)	O24 Mo10 O38	103.7(4)

O39 Mo10 O38	92.7(4)	O2 Mo11 O19	85.7(3)
O24 Mo10 O35	100.7(4)	O8 Mo11 O19	83.9(4)
O39 Mo10 O35	154.8(5)	O7 Mo11 O73	158.7(4)
O38 Mo10 O35	87.9(3)	O36 Mo11 O73	65.6(4)
O24 Mo10 O36	100.2(4)	O2 Mo11 O73	95.6(4)
O39 Mo10 O36	87.5(3)	O8 Mo11 O73	63.4(4)
O38 Mo10 O36	155.4(4)	O19 Mo11 O73	92.1(4)
O35 Mo10 O36	81.8(4)	O7 Mo11 O71	157.0(4)
O24 Mo10 O73	158.6(4)	O36 Mo11 O71	97.2(4)
O39 Mo10 O73	63.3(4)	O2 Mo11 O71	63.3(4)
O38 Mo10 O73	94.1(4)	O8 Mo11 O71	92.8(4)
O35 Mo10 O73	91.5(4)	O19 Mo11 O71	62.2(4)
O36 Mo10 O73	64.0(4)	O73 Mo11 O71	43.9(3)
O24 Mo10 O202	158.8(4)	O20 Mo12 O17	102.9(5)
O39 Mo10 O202	94.7(5)	O20 Mo12 O8	103.0(5)
O38 Mo10 O202	64.2(4)	O17 Mo12 O8	93.1(4)
O35 Mo10 O202	63.0(4)	O20 Mo12 O16	100.3(5)
O36 Mo10 O202	91.2(4)	O17 Mo12 O16	88.0(4)
O73 Mo10 O202	42.1(3)	O8 Mo12 O16	155.8(5)
O7 Mo11 O36	101.9(4)	O20 Mo12 O39	101.4(5)
O7 Mo11 O2	102.5(4)	O17 Mo12 O39	155.2(5)
O36 Mo11 O2	93.1(4)	O8 Mo12 O39	86.3(3)
O7 Mo11 O8	100.6(5)	O16 Mo12 O39	82.7(4)
O36 Mo11 O8	88.4(3)	O20 Mo12 O73	158.8(4)
O2 Mo11 O8	156.1(5)	O17 Mo12 O73	95.0(4)
O7 Mo11 O19	100.4(4)	O8 Mo12 O73	64.3(4)
O36 Mo11 O19	157.4(5)	O16 Mo12 O73	91.4(4)

O39 Mo12 O73	62.4(4)	O60 P1 O59	106.8(5)
O20 Mo12 O72	158.8(4)	O200 P1 O59	110.6(5)
O17 Mo12 O72	63.7(4)	O200 P1 O59	69.4(5)
O8 Mo12 O72	94.5(4)	O32 P1 O59	70.4(6)
O16 Mo12 O72	64.5(4)	O32 P1 O59	109.6(6)
O39 Mo12 O72	91.6(5)	O60 P1 O59	106.8(5)
O73 Mo12 O72	42.0(3)	O60 P1 O59	73.2(5)
O200 P1 O200	180.0	O59 P1 O59	180.0(4)
O200 P1 O32	68.9(5)	O72 P2 O72	180.0(8)
O200 P1 O32	111.1(5)	O72 P2 O202	112.4(6)
O200 P1 O32	111.1(5)	O72 P2 O202	67.6(6)
O200 P1 O32	68.9(5)	O72 P2 O202	67.6(6)
O32 P1 O32	180.0(8)	O72 P2 O202	112.4(6)
O200 P1 O60	110.0(5)	O202 P2 O202	180.0(7)
O200 P1 O60	70.0(5)	O72 P2 O73	70.4(6)
O32 P1 O60	71.5(5)	O72 P2 O73	109.6(6)
O32 P1 O60	108.5(5)	O202 P2 O73	71.7(6)
O200 P1 O60	70.0(5)	O202 P2 O73	108.3(6)
O200 P1 O60	110.0(5)	O72 P2 O73	109.6(6)
O32 P1 O60	108.5(5)	O72 P2 O73	70.4(6)
O32 P1 O60	71.5(5)	O202 P2 O73	108.3(6)
O60 P1 O60	180.0	O202 P2 O73	71.7(6)
O200 P1 O59	69.4(5)	O73 P2 O73	180.0
O200 P1 O59	110.6(5)	O72 P2 O71	109.6(6)
O32 P1 O59	109.6(6)	O72 P2 O71	70.4(6)
O32 P1 O59	70.4(6)	O202 P2 O71	110.3(6)
O60 P1 O59	73.2(5)	O202 P2 O71	69.7(6)

O73 P2 O71	73.6(6)	Mo4 O23 Mo3	140.9(5)
O73 P2 O71	106.4(6)	Mo7 O19 Mo11	139.8(5)
O72 P2 O71	70.4(6)	Mo4 O28 Mo6	139.3(5)
O72 P2 O71	109.6(6)	Mo3 O27 Mo5	139.2(5)
O202 P2 O71	69.7(6)	C30 O31 C6	116.3(10)
O202 P2 O71	110.3(6)	Mo6 O26 Mo1	139.7(6)
O73 P2 O71	106.4(6)	Mo2 O29 Mo1	139.7(5)
O73 P2 O71	73.6(6)	Mo1 O25 Mo4	138.8(4)
O71 P2 O71	180.0	Mo7 O30 Mo8	139.0(5)
Mo1 O15 Mo3	139.0(4)	Mo10 O38 Mo7	141.2(5)
Mo9 O16 Mo12	139.5(5)	C5 O37 C31	119.4(10)
Mo9 O6 Mo7	139.4(6)	Mo5 O34 Mo4	139.7(5)
Mo5 O14 Mo2	140.9(5)	Mo11 O36 Mo10	137.6(5)
C27 C3 C4	121.1(13)	Mo8 O35 Mo10	138.5(5)
Mo11 O2 Mo9	139.5(5)	P1 O32 O200	55.0(5)
C6 C1 C27	119.2(13)	P1 O32 O59	55.8(5)
Mo12 O8 Mo11	139.3(6)	O200 O32 O59	92.4(7)
C4 C5 O37	126.3(11)	P1 O32 O60	55.0(4)
C4 C5 C6	117.8(12)	O200 O32 O60	90.9(7)
O37 C5 C6	115.9(10)	O59 O32 O60	88.7(7)
C1 C6 C5	121.7(11)	P1 O32 Mo4	125.7(6)
C1 C6 O31	122.2(11)	O200 O32 Mo4	70.8(5)
C5 C6 O31	116.1(11)	O59 O32 Mo4	133.9(6)
C5 C4 C3	119.7(12)	O60 O32 Mo4	132.4(7)
Mo8 O18 Mo9	140.6(5)	P1 O32 Mo5	123.7(6)
Mo3 O33 Mo2	139.4(5)	O200 O32 Mo5	132.9(7)
Mo12 O17 Mo8	140.4(5)	O59 O32 Mo5	67.9(5)

O60 O32 Mo5	128.7(6)	C13 C14 O58	114.1(10)
Mo4 O32 Mo5	92.2(3)	C13 C14 C51	120.6(13)
P1 O32 Mo6	122.5(6)	O58 C14 C51	125.2(14)
O200 O32 Mo6	131.2(7)	C14 C13 O57	115.5(9)
O59 O32 Mo6	128.1(6)	C14 C13 C34	119.1(13)
O60 O32 Mo6	67.5(4)	O57 C13 C34	125.3(13)
Mo4 O32 Mo6	91.7(4)	C9 C10 O52	108.5(10)
Mo5 O32 Mo6	91.4(4)	P2 O73 O72	53.7(5)
Mo10 O39 Mo12	140.8(6)	P2 O73 O202	53.3(5)
C15 O51 C7	113.9(8)	O72 O73 O202	89.9(7)
C12 O53 C18	116.0(9)	P2 O73 Mo12	123.5(6)
C11 O54 C16	118.2(9)	O72 O73 Mo12	69.8(5)
C8 O50 C9	112.8(8)	O202 O73 Mo12	135.7(7)
C17 O52 C10	112.0(10)	P2 O73 Mo11	123.0(5)
C13 O57 C28	118.2(11)	O72 O73 Mo11	132.9(7)
C32 O58 C14	117.4(11)	O202 O73 Mo11	127.6(6)
Mo6 O56 Mo2	138.4(5)	Mo12 O73 Mo11	92.6(3)
Mo6 O55 Mo5	140.1(5)	P2 O73 Mo10	123.6(6)
C23 C12 C11	121.9(10)	O72 O73 Mo10	130.6(6)
C23 C12 O53	118.9(10)	O202 O73 Mo10	70.5(5)
C11 C12 O53	119.1(9)	Mo12 O73 Mo10	93.0(3)
O54 C11 C12	115.7(9)	Mo11 O73 Mo10	92.2(3)
O54 C11 C26	126.6(11)	P2 O72 O202	56.4(5)
C12 C11 C26	117.7(11)	P2 O72 O73	55.9(5)
O50 C8 C7	107.2(8)	O202 O72 O73	92.3(7)
O51 C7 C8	111.3(9)	P2 O72 O71	56.2(5)
C10 C9 O50	112.0(10)	O202 O72 O71	94.0(8)

O73 O72 O71	89.6(7)	O202 O71 Mo11	130.4(7)
P2 O72 Mo8	125.4(6)	O72 O71 Mo11	125.9(7)
O202 O72 Mo8	69.2(5)	Mo9 O71 Mo11	92.2(4)
O73 O72 Mo8	135.6(7)	Mo7 O71 Mo11	92.3(4)
O71 O72 Mo8	130.1(7)	C3 C27 C1	120.4(13)
P2 O72 Mo12	124.0(6)	C38 O77 C37	113.5(14)
O202 O72 Mo12	129.6(7)	C29 O74 C52	122.3(14)
O73 O72 Mo12	68.2(5)	O57 C28 C29	108.1(12)
O71 O72 Mo12	129.9(7)	C28 C29 O74	113.8(11)
Mo8 O72 Mo12	92.5(4)	C206 O75 C33	118(2)
P2 O72 Mo9	122.4(6)	O37 C31 C55	111.9(13)
O202 O72 Mo9	134.2(7)	O58 C32 C33	105.2(12)
O73 O72 Mo9	126.4(7)	O75 C33 C32	113.1(13)
O71 O72 Mo9	66.3(5)	O31 C30 C57	111.3(13)
Mo8 O72 Mo9	91.9(3)	C55 O76 C56	110.5(18)
Mo12 O72 Mo9	91.0(3)	C13 C34 C62	115.8(19)
P2 O71 O202	53.9(5)	C62 C35 C51	119(2)
P2 O71 O72	53.4(5)	C50 O82 C43	113.3(15)
O202 O71 O72	90.8(7)	C57 O78 C36	131.1(16)
P2 O71 Mo9	125.2(6)	C43 C42 O80	115.7(15)
O202 O71 Mo9	134.0(7)	O78 C36 C37	119.5(18)
O72 O71 Mo9	71.8(5)	C42 C43 O82	113.3(14)
P2 O71 Mo7	125.0(6)	O77 C38 C56	114.9(15)
O202 O71 Mo7	71.2(5)	C36 C37 O77	111.4(14)
O72 O71 Mo7	138.6(7)	C49 O83 C60	107.0(19)
Mo9 O71 Mo7	94.0(4)	C53 O85 C205	110(2)
P2 O71 Mo11	119.3(6)	C58 O84 C59	130(3)

C35 C51 C14	119.6(19)	O59 O200 Mo1	129.8(6)
C20 C44 C45	119.5(19)	O60 O200 Mo1	67.2(5)
C46 C47 C21	118(2)	Mo3 O200 Mo1	91.2(3)
O83 C49 C48	114.7(19)	P1 O200 Mo4	124.9(6)
C49 C48 O79	110.3(12)	O32 O200 Mo4	68.8(5)
C53 C52 O74	114.1(13)	O59 O200 Mo4	132.3(7)
C44 C45 C46	117(2)	O60 O200 Mo4	131.7(6)
C47 C46 C45	122.5(19)	Mo3 O200 Mo4	91.6(3)
C58 C50 O82	117(2)	Mo1 O200 Mo4	91.1(3)
O85 C53 C52	109.1(17)	P2 O202 O72	56.1(5)
O76 C56 C38	120.1(18)	P2 O202 O71	56.4(5)
C59 C60 O83	121(3)	O72 O202 O71	93.7(7)
C60 C59 O84	112(3)	P2 O202 O73	55.1(5)
O78 C57 C30	127.6(17)	O72 O202 O73	91.9(7)
O84 C58 C50	130(3)	O71 O202 O73	89.1(7)
P1 O200 O32	56.2(5)	P2 O202 Mo8	126.6(6)
P1 O200 O59	57.0(4)	O72 O202 Mo8	70.6(5)
O32 O200 O59	93.8(7)	O71 O202 Mo8	137.5(8)
P1 O200 O60	56.3(4)	O73 O202 Mo8	129.3(7)
O32 O200 O60	92.3(7)	P2 O202 Mo7	123.5(6)
O59 O200 O60	91.3(7)	O72 O202 Mo7	129.9(8)
P1 O200 Mo3	124.6(6)	O71 O202 Mo7	67.1(5)
O32 O200 Mo3	132.7(7)	O73 O202 Mo7	131.1(7)
O59 O200 Mo3	67.6(5)	Mo8 O202 Mo7	92.4(4)
O60 O200 Mo3	129.4(6)	P2 O202 Mo10	122.4(7)
P1 O200 Mo1	123.5(6)	O72 O202 Mo10	134.8(7)
O32 O200 Mo1	129.9(7)	O71 O202 Mo10	124.0(7)

O73 O202 Mo10	67.4(5)	C205 C206 O75	131(3)
Mo8 O202 Mo10	91.5(4)	C206 C205 O85	119(2)
Mo7 O202 Mo10	90.6(3)		

A5. Chapter 5 A Polyoxometalate Supported Copper Dimeric Complex: Synthesis, Structure and Electrocatalysis

Table A5.1 Complete list of bond lengths and bond angles of compound $[Mo_8O_{26}\{Cu_2(2,2'-bpy)_2\ (CH_3COO)_2H_2O\}_2]\cdot H_4Mo_8O_{26}\cdot 16H_2O\ 1$

Mo4 O12	1.701(6)	Mo3 O6	1.993(6)
Mo4 O11	1.749(7)	Mo3 O8	2.334(5)
Mo4 O10	1.953(6)	Mo3 O10	2.331(6)
Mo4 O6	1.969(6)	Mo5 O22	1.691(8)
Mo4 O8	2.159(6)	Mo5 O31	1.695(6)
Mo4 O8	2.359(6)	Mo5 O29	1.922(8)
Mo6 O27	1.688(6)	Mo5 O23	1.991(7)
Mo6 O24	1.739(6)	Mo5 O28	2.319(6)
Mo6 O25	1.947(7)	Mo5 O25	2.337(6)
Mo6 O23	1.962(6)	Mo7 O26	1.689(8)
Mo6 O28	2.151(6)	Mo7 O20	1.713(6)
Mo6 O28	2.349(6)	Mo7 O30	1.905(7)
Mo6 Mo5	3.2170(13)	Mo7 O25	1.994(6)
Mol Ol	1.697(6)	Mo7 O23	2.332(6)
Mo1 O13	1.697(7)	Mo7 O28	2.331(6)
Mo1 O2	1.902(7)	Mo8 O21	1.704(8)
Mo1 O10	2.004(6)	Mo8 O19	1.718(6)
Mol O6	2.323(6)	Mo8 O29	1.901(8)
Mo1 O8	2.345(5)	Mo8 O30	1.928(7)
Mo3 O7	1.701(7)	Mo8 O24	2.286(6)
Mo3 O5	1.704(6)	Mo8 O28	2.485(6)
Mo3 O4	1.895(8)	Mo2 O3	1.686(8)
			` /

Mo2 O9	1.700(7)	N1 C1	1.330(12)
Mo2 O4	1.912(6)	O17 C016	1.269(12)
Mo2 O2	1.929(6)	C8 C9	1.356(17)
Mo2 O11	2.288(6)	C8 C7	1.404(16)
Mo2 O8	2.423(6)	C8 H8	0.9300
Cu09 O15	1.942(6)	C016 O15	1.252(11)
Cu09 O14	1.955(6)	C016 C025	1.476(14)
Cu09 N1	2.001(8)	O16 C01R	1.259(11)
Cu09 N2	2.015(8)	C15 C14	1.401(14)
Cu09 O19	2.343(7)	C15 C16	1.455(13)
Cu09 Cu0A	3.0060(17)	O23 Mo7	2.332(6)
Cu0A O16	1.948(7)	C7 C6	1.384(14)
Cu0A O17	1.981(8)	C7 H7	0.9300
Cu0A N3	1.998(9)	N2 C10	1.319(12)
Cu0A N4	2.002(8)	N2 C6	1.320(13)
Cu0A O18	2.189(7)	C5 C4	1.386(16)
O25 Mo5	2.337(6)	C5 C6	1.485(13)
O28 Mo6	2.349(6)	N4 C20	1.343(13)
O6 Mo1	2.323(6)	N4 C16	1.386(13)
N3 C11	1.336(12)	C18 C17	1.387(16)
N3 C15	1.349(12)	C18 C19	1.386(19)
O8 Mo4	2.359(6)	C18 H18	0.9300
O10 Mo3	2.331(6)	C17 C16	1.375(14)
O11 Mo2	2.288(6)	C17 H17	0.9300
O14 C01R	1.264(11)	C19 C20	1.370(16)
O24 Mo8	2.286(6)	C19 H19	0.9300
N1 C5	1.356(13)	C1 C2	1.368(17)

C1 H1	0.9300	O11 Mo4 O10	96.8(3)
C01R C01S	1.507(12)	O12 Mo4 O6	102.6(3)
C01S H01A	0.9600	O11 Mo4 O6	96.4(3)
C01S H01B	0.9600	O10 Mo4 O6	149.7(2)
C01S H01C	0.9600	O12 Mo4 O8	98.7(3)
C11 C12	1.362(16)	O11 Mo4 O8	156.7(3)
C11 H11	0.9300	O10 Mo4 O8	78.7(2)
C20 H20	0.9300	O6 Mo4 O8	78.4(2)
C9 C10	1.396(15)	O12 Mo4 O8	174.2(3)
С9 Н9	0.9300	O11 Mo4 O8	81.0(3)
C14 C13	1.340(16)	O10 Mo4 O8	77.4(2)
C14 H14	0.9300	O6 Mo4 O8	77.9(2)
C10 H10	0.9300	O8 Mo4 O8	75.7(2)
C3 C2	1.353(19)	O27 Mo6 O24	104.4(3)
C3 C4	1.376(17)	O27 Mo6 O25	101.7(3)
C3 H3	0.9300	O24 Mo6 O25	97.2(3)
C025 H02A	0.9600	O27 Mo6 O23	100.5(3)
C025 H02B	0.9600	O24 Mo6 O23	97.0(3)
C025 H02C	0.9600	O25 Mo6 O23	149.8(3)
C12 C13	1.406(18)	O27 Mo6 O28	98.2(3)
C12 H12	0.9300	O24 Mo6 O28	157.4(2)
C4 H4	0.9300	O25 Mo6 O28	78.3(3)
C13 H13	0.9300	O23 Mo6 O28	78.3(3)
C2 H2	0.9300	O27 Mo6 O28	174.0(3)
		O24 Mo6 O28	81.6(2)
O12 Mo4 O11	104.6(3)	O25 Mo6 O28	77.6(2)
O12 Mo4 O10	100.3(3)	O23 Mo6 O28	78.2(2)

O28 Mo6 O28	75.8(2)	O4 Mo3 O6	146.1(2)
O27 Mo6 Mo5	89.3(2)	O7 Mo3 O8	94.8(3)
O24 Mo6 Mo5	132.8(2)	O5 Mo3 O8	160.0(3)
O25 Mo6 Mo5	124.40(18)	O4 Mo3 O8	77.0(2)
O23 Mo6 Mo5	35.83(19)	O6 Mo3 O8	73.8(2)
O28 Mo6 Mo5	46.10(17)	O7 Mo3 O10	164.2(3)
O28 Mo6 Mo5	86.28(15)	O5 Mo3 O10	88.8(3)
O1 Mo1 O13	105.0(4)	O4 Mo3 O10	83.1(2)
O1 Mo1 O2	101.9(4)	O6 Mo3 O10	71.6(2)
O13 Mo1 O2	102.2(3)	O8 Mo3 O10	71.18(19)
O1 Mo1 O10	100.9(3)	O22 Mo5 O31	104.7(4)
O13 Mo1 O10	96.3(3)	O22 Mo5 O29	101.5(4)
O2 Mo1 O10	145.7(2)	O31 Mo5 O29	101.2(3)
O1 Mo1 O6	89.3(3)	O22 Mo5 O23	100.6(3)
O13 Mo1 O6	163.0(3)	O31 Mo5 O23	97.0(3)
O2 Mo1 O6	83.3(2)	O29 Mo5 O23	146.6(3)
O10 Mo1 O6	71.6(2)	O22 Mo5 O28	160.3(3)
O1 Mo1 O8	161.0(3)	O31 Mo5 O28	94.7(3)
O13 Mo1 O8	93.6(3)	O29 Mo5 O28	77.0(3)
O2 Mo1 O8	76.7(2)	O23 Mo5 O28	73.8(2)
O10 Mo1 O8	73.4(2)	O22 Mo5 O25	89.1(3)
O6 Mo1 O8	71.8(2)	O31 Mo5 O25	163.5(3)
O7 Mo3 O5	105.1(3)	O29 Mo5 O25	84.5(3)
O7 Mo3 O4	101.2(3)	O23 Mo5 O25	71.2(2)
O5 Mo3 O4	100.4(3)	O28 Mo5 O25	71.2(2)
O7 Mo3 O6	98.0(3)	O22 Mo5 Mo6	135.8(3)
O5 Mo3 O6	101.2(3)	O31 Mo5 Mo6	85.4(2)

O29 Mo5 Mo6	118.9(2)	O29 Mo8 O24	78.2(3)
O23 Mo5 Mo6	35.24(18)	O30 Mo8 O24	77.4(3)
O28 Mo5 Mo6	41.93(15)	O21 Mo8 O28	158.1(3)
O25 Mo5 Mo6	78.32(14)	O19 Mo8 O28	97.8(3)
O26 Mo7 O20	105.3(4)	O29 Mo8 O28	73.2(3)
O26 Mo7 O30	101.3(4)	O30 Mo8 O28	73.8(3)
O20 Mo7 O30	101.2(3)	O24 Mo8 O28	69.1(2)
O26 Mo7 O25	100.8(4)	O3 Mo2 O9	105.6(4)
O20 Mo7 O25	97.2(3)	O3 Mo2 O4	102.5(4)
O30 Mo7 O25	146.3(3)	O9 Mo2 O4	98.8(3)
O26 Mo7 O23	90.1(3)	O3 Mo2 O2	101.7(4)
O20 Mo7 O23	162.5(3)	O9 Mo2 O2	98.6(3)
O30 Mo7 O23	83.5(3)	O4 Mo2 O2	145.0(3)
O25 Mo7 O23	71.2(2)	O3 Mo2 O11	90.6(3)
O26 Mo7 O28	162.0(3)	O9 Mo2 O11	163.8(3)
O20 Mo7 O28	92.5(3)	O4 Mo2 O11	78.1(2)
O30 Mo7 O28	78.0(3)	O2 Mo2 O11	76.8(2)
O25 Mo7 O28	73.2(2)	O3 Mo2 O8	160.6(3)
O23 Mo7 O28	71.8(2)	O9 Mo2 O8	93.7(3)
O21 Mo8 O19	104.0(3)	O4 Mo2 O8	74.5(2)
O21 Mo8 O29	104.0(4)	O2 Mo2 O8	74.3(2)
O19 Mo8 O29	99.6(3)	O11 Mo2 O8	70.1(2)
O21 Mo8 O30	101.4(4)	O15 Cu09 O14	92.2(3)
O19 Mo8 O30	98.2(3)	O15 Cu09 N1	171.9(3)
O29 Mo8 O30	144.2(3)	O14 Cu09 N1	93.1(3)
O21 Mo8 O24	89.1(3)	O15 Cu09 N2	92.6(3)
O19 Mo8 O24	166.8(3)	O14 Cu09 N2	169.3(3)

N1 Cu09 N2	81.2(3)	Mo7 O25 Mo5	104.3(3)
O15 Cu09 O19	95.6(3)	Mo6 O28 Mo5	92.0(2)
O14 Cu09 O19	91.3(3)	Mo6 O28 Mo7	91.9(2)
N1 Cu09 O19	90.4(3)	Mo5 O28 Mo7	162.7(3)
N2 Cu09 O19	97.8(3)	Mo6 O28 Mo6	104.2(2)
O15 Cu09 Cu0A	78.6(2)	Mo5 O28 Mo6	97.9(2)
O14 Cu09 Cu0A	79.83(19)	Mo7 O28 Mo6	97.4(2)
N1 Cu09 Cu0A	96.4(2)	Mo6 O28 Mo8	164.4(3)
N2 Cu09 Cu0A	91.8(2)	Mo5 O28 Mo8	86.32(19)
O19 Cu09 Cu0A	169.05(19)	Mo7 O28 Mo8	85.5(2)
O16 Cu0A O17	91.4(3)	Mo6 O28 Mo8	91.4(2)
O16 Cu0A N3	93.1(3)	Mo4 O6 Mo3	109.1(3)
O17 Cu0A N3	165.6(3)	Mo4 O6 Mo1	110.4(2)
O16 Cu0A N4	171.8(3)	Mo3 O6 Mo1	104.2(3)
O17 Cu0A N4	92.3(3)	C11 N3 C15	120.0(9)
N3 Cu0A N4	81.6(3)	C11 N3 Cu0A	125.8(7)
O16 Cu0A O18	89.9(3)	C15 N3 Cu0A	114.2(7)
O17 Cu0A O18	97.8(3)	Mo4 O8 Mo3	91.7(2)
N3 Cu0A O18	95.9(3)	Mo4 O8 Mo1	91.5(2)
N4 Cu0A O18	96.8(3)	Mo3 O8 Mo1	163.3(3)
O16 Cu0A Cu09	75.2(2)	Mo4 O8 Mo4	104.3(2)
O17 Cu0A Cu09	76.5(2)	Mo3 O8 Mo4	97.79(19)
N3 Cu0A Cu09	91.4(2)	Mo1 O8 Mo4	97.2(2)
N4 Cu0A Cu09	98.6(2)	Mo4 O8 Mo2	163.4(3)
O18 Cu0A Cu09	163.8(2)	Mo3 O8 Mo2	85.93(18)
Mo6 O25 Mo7	109.7(3)	Mo1 O8 Mo2	86.33(19)
Mo6 O25 Mo5	110.2(3)	Mo4 O8 Mo2	92.3(2)

Mo4 O10 Mo1	109.4(3)	Mo5 O23 Mo7	104.6(3)
Mo4 O10 Mo3	111.0(2)	C8 C7 C6	118.3(10)
Mo1 O10 Mo3	103.5(3)	C8 C7 H7	120.9
Mo1 O2 Mo2	116.8(3)	C6 C7 H7	120.8
Mo4 O11 Mo2	116.7(3)	C10 N2 C6	119.7(9)
C01R O14 Cu09	123.7(6)	C10 N2 Cu09	126.0(7)
Mo7 O30 Mo8	117.1(3)	C6 N2 Cu09	114.2(6)
Mo6 O24 Mo8	117.9(3)	N1 C5 C4	120.0(9)
Mo3 O4 Mo2	116.8(3)	N1 C5 C6	113.8(8)
Mo5 O29 Mo8	118.7(3)	C4 C5 C6	126.1(10)
C5 N1 C1	118.9(9)	C20 N4 C16	118.8(9)
C5 N1 Cu09	114.6(6)	C20 N4 Cu0A	127.2(8)
C1 N1 Cu09	126.5(7)	C16 N4 Cu0A	114.0(6)
C016 O17 Cu0A	127.5(6)	N2 C6 C7	121.5(9)
Mo8 O19 Cu09	132.0(4)	N2 C6 C5	116.0(8)
C9 C8 C7	120.0(10)	C7 C6 C5	122.5(9)
C9 C8 H8	120.0	C17 C18 C19	119.6(11)
C7 C8 H8	120.0	C17 C18 H18	120.2
O15 C016 O17	124.1(9)	C19 C18 H18	120.2
O15 C016 C025	118.9(9)	C18 C17 C16	119.9(12)
O17 C016 C025	117.0(8)	C18 C17 H17	120.0
C01R O16 Cu0A	130.2(6)	C16 C17 H17	120.1
N3 C15 C14	120.0(9)	C20 C19 C18	118.6(11)
N3 C15 C16	116.2(9)	C20 C19 H19	120.8
C14 C15 C16	123.8(9)	C18 C19 H19	120.6
Mo6 O23 Mo5	108.9(3)	N1 C1 C2	123.3(11)
Mo6 O23 Mo7	109.7(3)	N1 C1 H1	118.3

118.3	C15 C14 H14	120.2
120.2(10)	N2 C10 C9	123.3(10)
113.9(8)	N2 C10 H10	118.3
125.9(10)	C9 C10 H10	118.4
124.8(8)	C2 C3 C4	120.4(11)
117.4(8)	C2 C3 H3	119.8
117.7(8)	C4 C3 H3	119.9
109.4	C016 C025 H02A	109.5
109.5	C016 C025 H02B	109.4
109.5	H02A C025 H02B	109.5
109.5	C016 C025 H02C	109.5
109.5	H02A C025 H02C	109.5
109.5	H02B C025 H02C	109.5
122.1(11)	C11 C12 C13	118.1(11)
118.9	C11 C12 H12	120.9
119.0	C13 C12 H12	121.0
122.8(12)	C3 C4 C5	119.3(12)
118.6	C3 C4 H4	120.4
118.6	C5 C4 H4	120.4
127.5(7)	C12 C13 C14	120.1(11)
117.2(10)	C12 C13 H13	119.9
121.5	C14 C13 H13	120.0
121.4	C3 C2 C1	118.1(10)
119.6(11)	C3 C2 H2	121.0
120.2	C1 C2 H2	120.9
	120.2(10) 113.9(8) 125.9(10) 124.8(8) 117.4(8) 117.7(8) 109.4 109.5 109.5 109.5 109.5 109.5 119.0 122.1(11) 118.9 119.0 122.8(12) 118.6 118.6 127.5(7) 117.2(10) 121.5 121.4 119.6(11)	120.2(10) N2 C10 C9 113.9(8) N2 C10 H10 125.9(10) C9 C10 H10 124.8(8) C2 C3 C4 117.4(8) C2 C3 H3 117.7(8) C4 C3 H3 109.4 C016 C025 H02A 109.5 C016 C025 H02B 109.5 H02A C025 H02C 109.5 H02B C025 H02C 109.5 H02B C025 H02C 122.1(11) C11 C12 C13 118.9 C11 C12 H12 119.0 C13 C12 H12 122.8(12) C3 C4 C5 118.6 C3 C4 H4 117.2(10) C12 C13 C14 117.2(10) C12 C13 H13 121.5 C14 C13 H13 121.4 C3 C2 C1 119.6(11) C3 C2 H2

Publications

- 1. A planar anthracene-imidazolium / anthracene-benzimidazolium cation system in a spherical polyoxometalate matrix: synthesis, crystallography and spectroscopy
 - Tanmay Chatterjee, N. Tanmaya Kumar, Samar K. Das*, *Polyhedron*, 2017, 127, 68-83.
- 2. A gas-liquid synthetic strategy in polyoxometalate chemistry: potential bag filter for volatile organic amines
 - Vadipally Shivaiah, N. Tanmaya Kumar, Samar K. Das* J. Chem. Sci., 2018, 130:37
- 3. A polyoxometalate supported copper dimeric complex: Synthesis, structure and electrocatalysis
 - N. Tanmaya Kumar, Umashis Bhoi, Pragya Naulakha, Samar K. Das* *Inorg. Chim. Acta.* 2020, *506*, 119554.
- 4. Transition Metal-Aqua-Complexes: Six or Five Fold Coordination or Together
 - N. Tanmaya Kumar, Shyam Sreedhar, Manju Sharma* and Samar K. Das* (Manuscript under preparation)
- 5. Polyoxometalates Stabilized Ammonium Cation and Unusual Chloride anion Inclusion Crown Ether Complexes: Synthesis, Characterization and Crystallography
 - N. Tanmaya Kumar and Samar K. Das* (Manuscript under preparation)
- 6. A New Rearrangement Reaction Resulting in Ammonium Ion at Room Temperature
 - N. Tanmaya Kumar and Samar K. Das* (Manuscript under preparation)
- 7. Polyoxometalate based crown-ether supramolecular assemblies (review article)
 - N. Tanmaya Kumar and Samar K. Das* (Manuscript under preparation)

Posters and Presentations

- 1. Presented a <u>poster</u> on "Crystallization of Lindqvist type iso-polyanions with anthracene-based counter cations: salts or coulombic co-crystals? synthesis, crystallography and spectroscopy" in **CRSI-National** Symposium in Chemistry, 2017, held in Gauhati University, Gauhati, 2nd to 5th February, 2017.
- 2. Presented a <u>poster</u> on "A planar anthracene-imidazolium / anthracene-benzimidazolium cation system in a spherical polyoxometalate matrix: synthesis, crystallography and spectroscopy" in International Conference on Recent Advances in Materials Chemistry 2017, held in Utkal University, Bhubaneswar, 24th to 26th February, 2017.
- 3. Presented a <u>poster</u> on "Structurally mismatched components, a spherical polyoxometalate anion and a planar anthracene-imidazolium / anthracene-benzimidazolium cation, in a coloumbic crystal: synthesis, crystallography and spectroscopy" in CHEMFEST 2017, held in School of Chemistry, University of Hyderabad, 3rd to 4th March, 2017.
- 4. Oral and poster presentation on "A gas-liquid synthetic strategy in polyoxometalate chemistry: potential bag filter for volatile organic amines" in Asian Meeting on Metal Oxide Assemblies (AMMOA 2017) held in IISER Kolkata, 9th-10th May, 2017.
- 5. Poster presentation on "Ionic crystals consisting of trinuclear macrocations and polyoxometalate anions exhibiting single crystal to single crystal transformation: breathing of crystals" in National Meeting of Synthetic and Theoretical Chemists (NMSTC 2017) held in University of Hyderabad, Hyderabad held from 13th to14th October, 2017.
- 6. Poster presentation on "A gas-liquid synthetic strategy in polyoxometalate chemistry: potential bag filter for volatile organic amines" in Modern Trends in Inorganic Chemistry (MTIC 2017) held in National Chemical Laboratory, Pune held from 11th to 14th December, 2017.
- 7. Oral and poster presentation on "Supramolecular sandwiches stabilized by a polyoxometalate: synthesis, structure and electrocatalytic water oxidation" in National Conference in New Perspective to Advanced and

- Functional Materials (NPAFM 2017) held in Ravenshaw University, Cuttack held from 15th to 17th December, 2017.
- 8. <u>Poster presentation</u> on "Gas-Liquid Interfacial Reaction of Triethylamine Vapour and Polyoxometalate Solution Leading to the Generation of Ammonium Ion" in CHEMFEST 2018 held in School of Chemistry, University of Hyderabad, from 9th-10th March, 2018.
- 9. <u>Poster presentation</u> on "Transition metal aqua-complexes: hexacoordination versus penta-coordination" in International symposium on solid state chemistry of transition metal oxides 2018, held in JNCASR, Bangalore, from 29-30th November, 2018.
- 10. Poster presentation on "Polyoxometalate supported copper dimer: synthesis, structure and electrochemistry" in International winter school: frontiers in materials science 2018, held in JNCASR, Bangalore, from 2nd-7th December, 2018.
- 11. Poster presentation on "Gas-liquid interfacial reaction of triethylamine vapour and polyoxometalate solution leading to the generation of ammonium ion" in Modern Trends in Inorganic Chemistry (MTIC 2019) held in Indian Institute of Technology, Guwahati, held from 11th to 14th December, 2019.
- 12. Oral and poster presentation on "Molecular recognition by crown-ether assisted by polyoxometalates: A supramolecular approach" in CHEMFEST 2020 held in School of Chemistry, University of Hyderabad, from 27th-28th February, 2020.

Supramolecular Chemistry of Polyoxometalates: Molecular Recognition, Inorganic Rearrangement and Electrocatalysis

by N Tanmaya Kumar

Submission date: 19-Oct-2020 02:39PM (UTC+0530)

Submission ID: 1419645828

File name: 15CHPH20_phd_thesis_for_plagiarism_check_1.pdf (6.59M)

Word count: 27236 Character count: 140013

Supramolecular Chemistry of Polyoxometalates : Molecular Recognition, Inorganic Rearrangement and Electrocatalysis

ORIGIN	ALITY REPORT			
2 SIMIL	5% ARITY INDEX	7% INTERNET SOURCES	25% PUBLICATIONS	2% STUDENT PAPERS
PRIMAR	RY SOURCES			
1	Naulakha supporte structure	aya Kumar, Uma a, Samar K. Das. d copper dimeric and electrocatal Acta, 2020	"A polyoxome complex: Syn	etalate thesis, ca SKDA ki. Das mistry derabad 20/10/20
2	Polyoxor	. Das. "Supramol netalates", Macro d Metal-Like Eler	molecules Co	ntaining
3	Das. "Sur Ammoniu in Polyox	Chatterjee, Monii pramolecular Arc um-Crown Ether I ometalate Assoc , and Spectrosco	hitectures fror nclusion Com iation: Synthe	n plexes sis,
	Internet Source	nangras wku uda		<1

5	Vaddypally Shivaiah, N Tanmaya Kumar, Samar K Das. "A gas–liquid interface synthesis in polyoxometalate chemistry: potential bag filter for volatile organic amines", Journal of Chemical Sciences, 2018 Publication	<1%
6	pubs.rsc.org Internet Source	<1%
7	hdl.handle.net Internet Source	<1%
8	Vaddypally Shivaiah, Samar K. Das. "Fivefold Coordination of a Cull-Aqua Ion: A Supramolecular Sandwich Consisting of Two Crown Ether Molecules and a Trigonal-Bipyramidal [Cu(H2O)5]2+ Complex", Angewandte Chemie International Edition, 2006 Publication	<1%
9	livrepository.liverpool.ac.uk Internet Source	<1%
10	www.freepatentsonline.com Internet Source	<1%
11	Srinivasa Rao Amanchi, Samar K. Das. "A Versatile Polyoxovanadate in Diverse Cation Matrices: A Supramolecular Perspective", Frontiers in Chemistry, 2018	<1%

Das. "Polyoxometalate Supported Transition Metal Complexes: Synthesis, Crystal Structures, and Supramolecular Chemistry", Crystal Growth & Design, 2010 Publication Vaddypally Shivaiah, Samar K. Das. " <1% 13 Polyoxometalate-Supported Transition Metal Complexes and Their Charge Complementarity: Synthesis and Characterization of [M(OH) Mo O {Cu(Phen)(H O) }][M(OH) Mo O {Cu(Phen)(H O) CI $\}$ 1.5H O (M = AI , Cr) ", Inorganic Chemistry, 2005 Publication Janik, M.J.. "A computational and experimental <1% study of anhydrous phosphotungstic acid and its interaction with water molecules", Applied Catalysis A, General, 20031230 Publication www.arb.ca.gov 15 Internet Source Tatiana R. Amarante, Patrícia Neves, Ana C. 16 Gomes, Mariela M. Nolasco et al. "Synthesis, Structural Elucidation, and Catalytic Properties in Olefin Epoxidation of the Polymeric Hybrid Material [Mo O (2-[3(5)-Pyrazolyl]pyridine)] ", Inorganic Chemistry, 2014

T. Arumuganathan, A. Srinivasa Rao, Samar K.

12

<1%

	Publication	
17	www.zora.uzh.ch Internet Source	<1%
18	Ivan V. Kozhevnikov. "Catalysis by Heteropoly Acids and Multicomponent Polyoxometalates in Liquid-Phase Reactions", Chemical Reviews, 1998 Publication	<1%
19	Willey, G.R "Crown ether complexation of p-block metal halides: synthesis and structural characterisation of [Inl"2(dibenzo-24-crown-8) (H"2O)][Inl"4], [(SnBr"4)"2(dibenzo-24-crown-8)].MeCN, [(SbCl"3)"2(dibenzo-24-crown-8)].MeCN, [(BiCl"3)"2(dibenzo-24-crown-8)].MeCN and [(SbBr"3)"2(dibenzo-24-crown-8)]", Inorganica Chimica Acta, 20000420 Publication	<1%
20	aquila.usm.edu Internet Source	<1%
21	Submitted to University of Central Lancashire Student Paper	<1%
22	ethesis.inp-toulouse.fr Internet Source	<1%
23	Suresh Bommakanti, Uppari Venkataramudu, Samar K. Das. "Functional Coordination Polymers from a Bifunctional Ligand: A	<1%

Quantitative Transmetalation via Single Crystal to Single Crystal Transformation", Crystal Growth & Design, 2018

<1%

<1%

Publication

Publication

28

- Jun Gao, Tiantian Yang, Xuejiao Wang, Qihang He et al. "Spherical phosphomolybdic acid immobilized on graphene oxide nanosheets as an efficient electrochemical sensor for detection of diphenylamine", Microchemical Journal, 2020
- Chandani Singh, Subhabrata Mukhopadhyay, Samar K. Das. "Polyoxometalate-Supported Bis(2,2'-bipyridine)mono(aqua)nickel(II) Coordination Complex: an Efficient Electrocatalyst for Water Oxidation", Inorganic Chemistry, 2018

worldwidescience.org

Sridevi Yerra, Sabbani Supriya, Samar K. Das.

"Reversible morphological transition between nano-rods to micro-flowers through micro-hexagonal crystals in a sonochemical synthesis based on a polyoxovanadate compound", Inorganic Chemistry Communications, 2013

Samar K. Das. "Supramolecular Structures and

	Polyoxometalates", Wiley, 2009 Publication	<1%
29	T. Arumuganathan. "Two different zinc(II)-aqua complexes held up by a metal-oxide based support: Synthesis, crystal structure and catalytic activity of [HMTAH]2[{Zn(H2O)5} {Zn(H2O)4}{Mo7O24}]·2H2O (HMTAH = protonated hexamethylenetetramine)", Journal of Chemical Sciences, 01/2008	<1%
30	etheses.bham.ac.uk Internet Source	<1%
31	ir.library.osaka-u.ac.jp Internet Source	<1%
32	Ravada Kishore, Samar K. Das. "Diversities of Coordination Geometry Around the Cu Center in Bis(maleonitriledithiolato)metalate Complex Anions: Geometry Controlled by Varying the Alkyl Chain Length of Imidazolium Cations ", Crystal Growth & Design, 2012	<1%
33	Ping Che. "Hydrothermal synthesis and crystal structure of a new two-dimensional zinc citrate complex", Journal of Coordination Chemistry, 11/1/2005 Publication	<1%

34	Ai-xiang Tian, Jun Ying, Jun Peng, Jing-quan Sha, Hai-jun Pang, Peng-peng Zhang, Yuan Chen, Min Zhu, Zhong-min Su. "Tuning the Dimensionality of the Coordination Polymer Based on Polyoxometalate by Changing the Spacer Length of Ligands", Crystal Growth & Design, 2008	<1%
35	www.mdpi.com Internet Source	<1%
36	fr.scribd.com Internet Source	<1%
37	Submitted to University of Science and Technology, Yemen Student Paper	<1%
38	H. Feinberg, I. Columbus, S. Cohen, M. Rabinovitz, H. Selig, G. Shoham. "Crystallographic evidence for different modes of interaction of BF3/BF4- species with water molecules and 18-crown-6", Polyhedron, 1993 Publication	<1%
39	macau.uni-kiel.de Internet Source	<1%
40	Doxsee, K.M "Hydration, Ion Pairing, and Sandwich Motifs in Ammonium Nitrate Complexes of Crown Ethers", Tetrahedron,	<1%

20000901

Publication

41	Gary D. Fallon, Vei-Lin Lau, Steven J. Langford. "Ammonium 2,5,8,11,21,24,27- octaoxatricyclo[26.4.0.0]dotriaconta- 1(32),12(17),13,15,28,30-hexaene hexafluorophosphate ", Acta Crystallographica Section E Structure Reports Online, 2002 Publication	<1%
42	Submitted to Chonnam National University	<1%

Submitted to Chonnam National University
Student Paper

<1 9

Santiago Reinoso, Pablo Vitoria, Leire San Felices, Ainara Montero, Luis Lezama, Juan M. Gutiérrez-Zorrilla. " Tetrahydroxy- - benzoquinone as a Source of Polydentate O-Donor Ligands. Synthesis, Crystal Structure, and Magnetic Properties of the [Cu(bpy)(dhmal)] Dimer and the Two-Dimensional [{SiW O }{Cu (bpy) (H O)(ox)}]·16H O Inorganic–Metalorganic Hybrid ", Inorganic Chemistry, 2007

www.hindawi.com
Internet Source

Encyclopedia of Polymeric Nanomaterials, 2015.
Publication

www.hindawi.com
<1%

eprints.kfupm.edu.sa

46	Internet Source	<1%
47	A. Pasquarello. "First Solvation Shell of the Cu(II) Aqua Ion: Evidence for Fivefold Coordination", Science, 2001	<1%
48	www.science.gov Internet Source	<1%
49	Submitted to Ewha Womans University Student Paper	<1%
50	Chatterjee, T "Polyoxometalate associated ion- pair solid based on a crown ether inclusion complex: Synthesis, structure and spectroscopy", Journal of Molecular Structure, 20100924 Publication	<1%
51	Submitted to Texas Christian University Student Paper	<1%
52	Chandani Singh, Samar K. Das. "Anderson polyoxometalate supported Cu(H2O)(phen) complex as an electrocatalyst for hydrogen evolution reaction in neutral medium", Polyhedron, 2019	<1%
53	patents.justia.com Internet Source	<1%

Exclude quotes

Exclude bibliography

On

On

Exclude matches

< 14 words

